



3 4456 0282912 5

ORNL/TM-10971

# ornl

## OAK RIDGE NATIONAL LABORATORY

### Proceedings of the Second Conference on **Radiation Protection and Dosimetry**

**MARTIN MARIETTA**

Edited by: **R. E. Swaja and C. S. Sims**

OAK RIDGE NATIONAL LABORATORY  
CENTRAL RESEARCH LIBRARY  
CIRCULATION SECTION  
4500N ROOM 271  
**LIBRARY LOAN COPY**  
DO NOT TRANSFER TO ANOTHER PERSON  
If you wish someone else to see this  
report, send in name with report and  
the library will arrange a loan.



**Holiday Inn – Crowne Plaza Hotel  
Orlando, Florida**

**October 31–November 3, 1988**

OPERATED BY  
MARTIN MARIETTA ENERGY SYSTEMS, INC.  
FOR THE UNITED STATES  
DEPARTMENT OF ENERGY

SECOND CONFERENCE ON RADIATION PROTECTION AND DOSIMETRY

October 31-November 3, 1988

CONFERENCE CHAIRMAN

Charles S. Sims  
Oak Ridge National Laboratory  
Oak Ridge, Tennessee

TECHNICAL PROGRAM

Richard E. Swaja  
Oak Ridge National Laboratory  
Oak Ridge, Tennessee

TECHNICAL EXHIBITS

John R. Frazier  
International Technology  
Oak Ridge, Tennessee

CONFERENCE COORDINATOR

Bonnie S. Reesor  
Oak Ridge National Laboratory  
Oak Ridge, Tennessee

SECRETARY/TREASURER

Linda R. Pyles  
Oak Ridge National Laboratory  
Oak Ridge, Tennessee

TECHNICAL PROGRAM COMMITTEE

Joe L. Alvarez  
Rockwell International-Rocky Flats  
Golden, Colorado

Donald E. Jones  
Lawrence Livermore National Laboratory  
Livermore, California

John P. Cusimano  
U. S. Department of Energy  
Idaho Falls, Idaho

John W. Poston  
Texas A&M University  
College Station, Texas

Keith F. Eckerman  
Oak Ridge National Laboratory  
Oak Ridge, Tennessee

Hans Schraube  
GSF - Neuherberg  
Federal Republic of Germany

Dale E. Hankins  
Lawrence Livermore National Laboratory  
Livermore, California

Leon E. West  
University of Arkansas  
Fayetteville, Arkansas

PROCEEDINGS OF THE SECOND CONFERENCE ON  
RADIATION PROTECTION AND DOSIMETRY

Edited by: R. E. Swaja and C. S. Sims

Holiday Inn - Crowne Plaza Hotel  
Orlando, Florida

October 31 - November 3, 1988

Date Published: November 1988

Prepared by the  
OAK RIDGE NATIONAL LABORATORY  
Oak Ridge, Tennessee 37831  
operated by  
MARTIN MARIETTA ENERGY SYSTEMS, INC.  
for the  
U.S. DEPARTMENT OF ENERGY  
under  
Contract No. DE-AC05-84OR21400

MARTIN MARIETTA ENERGY SYSTEMS LIBRARIES



3 4456 0282912 5

Printed in the United States of America. Available from  
National Technical Information Service  
U.S. Department of Commerce  
5285 Port Royal Road, Springfield, Virginia 22161  
NTIS price codes—Printed Copy:A11 Microfiche A01

This report was prepared as an account of work sponsored by an agency of the United States Government. Neither the United States Government nor any agency thereof, nor any of their employees, makes any warranty, express or implied, or assumes any legal liability or responsibility for the accuracy, completeness, or usefulness of any information, apparatus, product, or process disclosed, or represents that its use would not infringe privately owned rights. Reference herein to any specific commercial product, process, or service by trade name, trademark, manufacturer, or otherwise, does not necessarily constitute or imply its endorsement, recommendation, or favoring by the United States Government or any agency thereof. The views and opinions of authors expressed herein do not necessarily state or reflect those of the United States Government or any agency thereof.

## FOREWORD

The Second Conference on Radiation Protection and Dosimetry was held during October 31 - November 3, 1988, at the Holiday Inn - Crowne Plaza Hotel in Orlando, Florida. This meeting was designed with the objectives of promoting communication among applied, research, regulatory, and standards personnel involved in radiation protection and providing them with sufficient information to evaluate their programs. To facilitate meeting these objectives, a technical program consisting of more than 75 invited and contributed oral presentations encompassing all aspects of radiation protection was prepared. General topics considered in the technical sessions included external dosimetry, internal dosimetry, calibration, standards and regulations, instrumentation, accreditation and test programs, research advances, and applied program experience. In addition, special sessions were held to afford attendees the opportunity to make short presentations of recent work or to discuss topics of general interest.

This document provides a summary of the conference technical program and a partial collection of full papers for the oral presentations in order of delivery. Starred titles in the program summary indicate those presentations which have papers included in these proceedings. In the interest of attracting persons with a variety of experience and preparing a program which contains the most current information, full papers were not required of speakers. Thus, this collection does not contain papers for all presentations. A complete collection of abstracts for this meeting is available in the program and abstracts book which was distributed at registration.

The editors are grateful to the members of the Conference Coordination Committee and the Technical Program Committee for their efforts in making this conference a success. The technical program was informative and comprehensive, and we hope that these proceedings will be useful to all attendees.

Charles S. Sims  
General Chairman  
Oak Ridge National Laboratory

Richard E. Swaja  
Technical Program Chairman  
Oak Ridge National Laboratory



## TABLE OF CONTENTS

	Page
Conference Technical Program .....	v
R. J. Vetter, "Radiation Protection in the Hospital Environment" ...	1
R. C. Yoder, "Perspective from a Commercial Supplier of Dosimetry Services" .....	10
P. Neeson, "Implementation of the Department of Energy Laboratory Accreditation Program (DOELAP) and the New Exposure Reporting Requirements" .....	14
S. J. Cipolla, R. J. Powell, R. K. Stultz, G. Norris, M. Hawes, and B. Hearty, "Improved Performance of a Two-Element TLD Badge for Determining Gamma and Beta Doses Using Multiple Linear Regression" .....	23
P. S. Weng, P. C. Hsu, T. C. Chen, "The Angular Energy Response of Personnel Thermoluminescent Dosimeters" .....	33
J. Hoffman, B. B. Shachar, and G. L. Catchen, "Linearity of and Minimum Measurable Dose for Li <sub>2</sub> B <sub>4</sub> O <sub>7</sub> :Cu and CaSO <sub>4</sub> :Tm TL Elements used in a Personnel/Environmental Dosimeter .....	43
M. Moscovitch, J. Chamberlain, and K. J. Velbeck, "Dose Determination Algorithms for a Nearly Tissue-Equivalent Multi-Element Thermoluminescent Dosimeter" .....	48
N. M. Moghari and R. T. Devine, "Accident Level Dosimetry with TLD" .....	60
L. G. Faust, C. M. Stroud, and E. J. Vallario, "DOE Personnel Neutron Dosimetry Evaluation and Upgrade Program" .....	68
R. Jahr, R. Hollnagel, and B. R. L. Siebert, "Computational Individual Neutron Dosimetry at the PTB" .....	75
D. E. Hankins, S. G. Homann, and J. Westermark, "Personnel Neutron Dosimetry Applications of Track-Size Distributions on Electrochemically Etched CR-39 Foils" .....	85
R. P. Bradley and F. N. Ryan, "Development and Implementation of a Fast Neutron Monitoring System Based on Plastic Track Detectors .....	96
R. Strong, "A Review of Experience with Plutonium Exposure Assessment Methodologies at the Nuclear Fuel Reprocessing Site of British Nuclear Fuels PLC" .....	106

L. M. Hodgson, O. W. Cypret, and R. R. Culp, "Analysis of Particulate Contamination from a PWR" .....	117
K. J. Velbeck and M. Moscovitch, "A Time-Temperature Controlled Non-Contact Automatic TLD System Methodology for Performance Evaluation" .....	126
R. A. Tawil, G. Bencke, and M. Moscovitch, "Quality Assurance Package for Routine Thermoluminescence Dosimetry Program" .....	138
S. H. Benedict, J. H. Kleck, and J. E. McLaughlin, "Factors and Strategies in the Occupational Monitoring of Personnel in Medical Angiography" .....	147
P. T. Glennon, "Vinten Exposure Measurements of the Salem Unit I Lower Core Barrel" .....	157
M. Olin and W. T. Bartlett, "Dosimetry of an In-Core Detector Exposure Accident" .....	169
A. Jeffries and A. Mohseni, "Estimating Radiation Doses from Reactor Accidents" .....	179
H. Kluge, K. Weise, and J. B. Hunt, "The Calibration of Neutron Sensitive Spherical Devices with a D2O-Moderated Cf Source at Close Distances" .....	190
L. E. West, F. X. Masse, and K. L. Swinth, "Health Physics Society Program for Accreditation of Calibration Laboratories" .....	200
W. H. Casson and C. S. Sims, "A New Dosimeter Calibration Laboratory at ORNL" .....	206
C. H. Mao, "Portable Single Channel Analyzer Incorporated with a GM Counter for Radiation Protection" .....	211
C. S. Sims, "Review of ANSI N13.11: A Status Report" .....	219

SECOND CONFERENCE ON RADIATION  
PROTECTION AND DOSIMETRY

Orlando, Florida  
October 31-November 3, 1988

TECHNICAL PROGRAM

*All technical sessions will be held  
in the Plaza Grand Ballroom of the  
Holiday Inn Crowne Plaza Hotel.  
Presentations will last 10 - 30  
minutes, refreshment breaks will  
last 30 minutes, and about 1.5  
hours will be available for lunch.*

Monday, October 31

8:00 AM Registration

9:00 AM Welcome and Introduction to the Conference  
General Chairman: C. S. Sims (Oak Ridge National Laboratory)  
Technical Program Chairman: R. E. Swaja (Oak Ridge National  
Laboratory)

Welcome Address: S. V. Kaye (Oak Ridge National  
Laboratory)

Reflections on Radiation Protection  
J. P. Cusimano (DOE-Idaho)

9:50 AM Session I: Overview of Radiation Protection  
Chairman: J. W. Poston (Texas A&M University)

Radiation Protection Concepts and Quantities: Past and Present  
K. F. Eckerman (Oak Ridge National Laboratory)

The Status of External Radiation Dosimetry  
D. E. Jones (Lawrence Livermore National Laboratory)

\*Radiation Protection in the Hospital Environment  
R. J. Vetter (Mayo Clinic)

Military Radiation Protection Dosimetry  
G. H. Zeman and L. W. Lockett (AFRRI)

\*Perspective from a Commercial Supplier of Radiation Dosimetry  
Services  
R. C. Yoder (R. S. Landauer, Jr. and Co.)

11:30 AM Lunch

\*Indicates full paper included in proceedings.

1:00 PM Session II: Regulations and Standards for Radiation Protection  
Chairman: *J. P. Cusimano (DOE-Idaho)*

Proposed Changes to 10CFR20 and Their Impact on Radiation Protection  
*J. W. Poston (Texas A&M)*

\*Implementation of the DOE Laboratory Accreditation Program (DOELAP) and the New Exposure Reporting Requirements  
*P. Neeson (DOE-Chicago)*

Implications of the New ICRU Dose Equivalent Quantities for Radiation Protection Measurements  
*R. B. Schwartz (National Bureau of Standards)*

Limitation of Lifetime Doses- A New Approach to Limiting the Risk from Occupational Radiation Exposure  
*H. Eckerl, M. Zankl, and G. Drexler (GSF-FRG)*

Risks Associated with Radiation Protection and Environmental Radiation Standards for Members of the Public  
*D. C. Kocher (Oak Ridge National Laboratory)*

The Status of National Measurement Quality Assurance Programs  
*E. H. Eisenhower (National Bureau of Standards)*

The Status of Extremity Dosimetry  
*G. W. Campbell (Lawrence Livermore National Laboratory)*

Enforcing Radiological Health Regulations: A Perspective of the Pennsylvania Program  
*G. A. Karron and I. O. Shanbaky (Pennsylvania Department of Environmental Resources)*

3:30 PM Opening of Technical Exhibits

Tuesday, November 1

8:30 AM Session III: External Dosimetry  
Chairman: *D. E. Jones (Lawrence Livermore National Laboratory)*

The Status of Beta Dosimetry  
*J. L. Alvarez (Rockwell International-Rocky Flats)*

\*Improved Performance of a Two-Element TLD for Determining Gamma and Beta Doses Using Multiple Linear Regression  
*S. J. Cipolla (Creighton University)*  
*R. K. Stultz, C. Norris, and M. Hawes (OPPD)*

The Response of a Two Element Dosimeter for Several Beta Emitters and Low Energy Photons  
*C. W. King (Harshaw/Filtrol)*

\*The Angular Energy Response of Personnel Thermoluminescent Dosimeters

*P. S. Weng, P. C. Hsu, and T. C. Chen (NTHN-ROC)*

\*Linearity of and Minimum Measurable Dose for

$\text{Li}_2\text{B}_4\text{O}_7:\text{Cu}$  and  $\text{CaSO}_4:\text{Tm}$  TL Elements used in a Personnel/Environmental Dosimeter

*J. Hoffman, B. B. Shachar, and G. L. Catchen (PSU)*

\*Dose Determination Algorithms for a Nearly Tissue-Equivalent Multi-Element Thermoluminescent Dosimeter

*M. Moscovitch, J. Chamberlain, and K. J. Velbeck (Harshaw/Filtrol)*

New and Future Designs of Dosimeters For Use by the NRPB'S Personnel Monitoring Service

*T. O. Marshall, D. T. Bartlett, P. H. Burgess, J. C. Dutt, and T. M. Francis (NRPB-UK)*

A Six Element Dosimetry Badge for Beta and Photon Spectrometry  
*S. J. Waligora (TMA/Eberline)*

An Automated Area Dosimeter for Beta and Gamma Radiation

*L. L. Nichols and J. J. Fix (Battelle Pacific Northwest Laboratory)*

An Analysis of the Performance of the Italian Individual Dosimetry Services by Means of X and Gamma Ray Irradiation Tests

*A. Cavallini (ENEA-Italy)*

*S. Kaftal and V. Klamert (CESNEF-Italy)*

Preliminary Results of Some Tests on the Use of the Dose Equivalent Operational Quantities for Some Dosimetric Systems

*G. Busuoli and A. Cavallini (ENEA-Italy)*

*V. Klamert and F. Monteventi (CESNEF-Italy)*

\*Accident Level Photon Dosimetry with TLD

*N. M. Moghari, (Georgetown)*

*R. T. Devine (NNDC)*

11:30 AM Lunch

1:00 PM Session IV: Neutron Dosimetry

*Chairman: H. Schraube (GSF-FRG)*

\*The DOE Personnel Neutron Dosimetry Evaluation and Upgrade Program

*L. E. Faust and C. M. Stroud (Battelle Pacific Northwest Laboratories)*

*E. J. Vallario (DOE)*

The Status and Future of Personal Neutron Monitoring Around Particle Accelerators

*M. Hofert (CERN-Switzerland)*

\*Computational Individual Neutron Dosimetry at the PTB

*B. R. L. Siebert, R. Hollnagel, and R. Jahr (PTB-FRG)*

\*Personnel Neutron Dosimetry Applications of Track-Size  
Distributions on Electrochemically Etched CR-39 Foils  
*D. E. Hankins, S. G. Homann, and J. Westermarck (Lawrence  
Livermore National Laboratory)*

\*Development and Implementation of a Fast Neutron Monitoring  
System Based on Plastic Track Detectors  
*R. P. Bradley and F. N. Ryan (RPB-Canada)*

A Novel Area/Spectrum Monitor for Neutrons  
*R. E. Apfel and J. B. Morrell (Apfel Enterprises)*

Superheated Drop Neutron Area/Spectrum Monitor  
*G. K. Riel and N. Rao (NSWC)*  
*R. T. Devine and T. L. Johnson (NNMC)*  
*R. B. Schwartz (NBS)*

Stability, Repeatability, and Homogeneity of the Chalk River  
Bubble-Damage Neutron Detector  
*R. Jones (NAVSEA)*

Lower Limit of Detection and Linearity of the Chalk River  
Bubble-Damage Neutron Detector  
*R. B. Schwartz (National Bureau of Standards)*

The Effect of Temperature on the Response of the Chalk River  
Bubble-Damage Neutron Detector  
*G. K. Riel (NSWC)*

Wednesday, November 2

8:30 AM Session V: Internal Dosimetry and Contamination Dose Assessment  
Chairman: *K. F. Eckerman (Oak Ridge National Laboratory)*

What's New in the World of Whole Body Counting?  
*C. D. Berger (IT Corporation)*

Bioassay Standards and Requirements  
*A. N. Tschaeche (INEL)*

Bioassay Levels for Selected Radionuclides  
*T. K. Haider and G. G. Eichholz (Georgia Tech)*

\*A Review of Experience with Plutonium Exposure Assessment  
Methodologies at the Nuclear Fuel Reprocessing Site of British  
Nuclear Fuels, PLC  
*R. Strong (BNF-UK)*

Dose Estimation by Bioassay for Population Involved in an  
Accident with Plutonium Release  
*E. Iranzo, A. Espinosa, and E. Iranzo (Spain)*

Skeletal Pb-210 from Inhalation of Radon and Its Decay Products  
*A. T. Keane and R. A. Schlenker (ANL)*

Development of a Practical Internal Dose Evaluation Code  
*S. Iwai and Y. Rintsu (Mitsubishi- Japan)*

Assessing Skin Dose From Contamination  
*J. R. Flood (Tennessee Valley Authority)*

\*Analysis of Particulate Contamination from a PWR  
*L. M. Hodgson, O. W. Cypret, and R. R. Culp (ATU)*

Contaminated Coveralls - What Was the True Dose?  
*A. N. Tschaeche and C. W. Nielsen (INEL)*

11:30 AM Lunch

1:00 PM Session VI: Radiation Protection Programs and Experience  
Chairman: *J. L. Alvarez (Rockwell International-Rocky Flats)*

Operational Dosimetry Experience with the INEL Personnel  
Dosimetry System  
*J. P. Cusimano, G. A. Loftus, and T. F. Gesell (Department  
of Energy-Idaho)*

Implementation of the Panasonic TLD System for Personnel  
Monitoring at the Nevada Test Site  
*M. E. DeMarre, C. L. Teasdale, and L. S. Sygitowicz  
(REECO)*

\*A Time-Temperature Controlled Noncontact Automatic TLD System  
Methodology for Performance Evaluation  
*M. Moscovitch and K. L. Velbeck (Harshaw/Filtrol)*

\*Quality Assurance Package for Routine Thermoluminescent  
Dosimetry Programs  
*R. A. Tawil, G. Bencke, and M. Moscovitch (Harshaw)*

PREMS: Personnel Radiation Exposure Management System  
*H. Kahnhauser (Virginia Electric Power Company)*

\*Factors and Strategies in the Occupational Monitoring of  
Personnel in Medical Angiography Laboratories  
*S. H. Benedict, J. H. Kleck, and J. E. McLaughlin  
(University of California-Los Angeles)*

Radiation Monitoring in a Clinical PET Facility: Preliminary  
Exposure Data  
*C. M. Plott and K. F. Hubner (University of Tennessee)*

Advances in Environmental Monitoring Instrumentation  
*L. A. Rathbun (Battelle Pacific Northwest Laboratories)*

Personnel and Environmental Thermoluminescent Dosimetry at  
High Grade Uranium Mines Near the Grand Canyon National Park  
*J. W. McKlveen and G. W. Klingler (Arizona State  
University)*

Film Badge Dosimetry for Veterans of The U. S. Atmospheric Weapons Testing Program  
*F. X. Masse (Massachusetts Institute of Technology)*

\*Experimental Confirmation of Predicted Dose Rates of the Salem Lower Core Barrel  
*P. T. Glennon (PSEG)*

\*Dosimetry of an In-Core Detector Exposure Incident  
*M. R. Olin and W. T. Bartlett (Virginia Electric Power Company)*

\*Estimating Radiation Doses from Reactor Accidents  
*A. Jeffries (Washington DSHS)*

Use of American and Taiwanese Coins as Quick Sort Indicators of Neutron Accident Exposure  
*S. H. Yeh (INER-ROC)*  
*R. E. Swaja (Oak Ridge National Laboratory)*

6:30 PM - Conference Dinner (Holiday Inn- Crowne Plaza Hotel)

Thursday, November 3

8:30 AM Session VII: Calibration and Instrumentation  
Chairman: *D. E. Hankins (Lawrence Livermore National Laboratory)*

Recent Developments at the NBS Nearly Monoenergetic Electron Beam Facility  
*C. G. Soares (National Bureau of Standards)*

Performance Characteristics of Portable Radiation Survey Instruments  
*K. L. Swinth and J. M. Selby (Battelle Pacific Northwest Laboratories)*

Implementation of Dose Equivalent Meters Based on Microdosimetric Techniques in Radiation Protection  
*H. G. Menzel (US-FRG)*

\*The Calibration of Neutron Sensitive Spherical Devices with a D<sup>2</sup>O-Moderated Cf-252 Source at Close Distances  
*K. Kluge and K. Weise (PTB-FRG)*  
*J. B. Hunt (NPL-UK)*

Determination of the Source-to-Detector Effective Calibration Distance for a l/V Detector Mounted on a Water-filled Phantom  
*J. B. Hunt (NPL-UK)*

Review of Scattering Corrections for Calibration of Neutron Instruments  
*C. M. Eisenhauer and R. B. Schwartz (National Bureau of Standards)*

Calibration of Two Types of Albedo Dosimeters in the  
Neutron Radiation Field of a BWR  
*H. Schraube (GSF-FRG)*

Intercomparison of Calibrations Carried Out at NBS, NPL,  
PTB, and CEA Using Two Different Survey Meters as Transfer  
Devices  
*J. B. Hunt (NPL-UK) et. al.*

\*Health Physics Society Program for Accreditation of  
Calibration Laboratories  
*L. E. West (University of Arkansas)*  
*F. X. Masse (MIT)*  
*K. L. Swinth (BPNL)*

\*A New Dosimeter Calibration Laboratory at ORNL  
*W. H. Casson and C. S. Sims (Oak Ridge National  
Laboratory)*

\*Portable Single Channel Analyzer Incorporated with a GM  
Counter for Radiation Protection  
*C. H. Mao (NTHU-ROC)*

11:30 AM Lunch

1:00 PM Session VIII: Accreditation and Testing Programs  
*Chairman: L. E. West (University of Arkansas)*

\*Review of ANSI N13.11: A Status Report  
*C. S. Sims (Oak Ridge National Laboratory)*

Test Categories for NVLAP Whole Body Dosimetry  
Accreditation  
*D. O. Nellis (Nuclear Regulatory Commission)*

Operation of a Performance Testing Laboratory for  
Radiation Dosimetry  
*R. A. Fox and J. C. McDonald (BPNL)*

DOELAP Performance Testing  
*R. D. Carlson and T. F. Gesell (DOE-Idaho)*

Experience with NVLAP Dosimetry Assessments  
*C. G. Hudson (Tennessee Valley Authority)*

Preparing for the DOELAP Onsite Assessment  
*R. D. Carlson, T. F. Gesell, and E. J. Vallario (DOE)*

3:30 PM Closing Statements  
*Technical Program Committee*



# RADIATION PROTECTION IN THE HOSPITAL ENVIRONMENT

Richard J. Vetter  
Mayo Clinic/Foundation

## ABSTRACT

The hospital environment contains numerous sources of ionizing radiation that may contribute to public and occupational radiation exposure. Radiation exposure from x rays is minimized through engineering design, administrative controls, and quality control. Exposure from patients that contain therapeutic quantities is minimized by isolation in appropriately controlled private rooms. Administrative controls are relied on for controlling radiation exposure from diagnostic nuclear medicine patients. Hospital radiation installations must be planned and periodically reviewed to take advantage of the latest developments in radiation protection and to keep public and occupational exposure as low as reasonably achievable.

## INTRODUCTION

The largest source of population exposure from man-made radiation is medical use of x rays and radiopharmaceuticals. These two sources contribute approximately 80% of the man-made and 15% of the total average effective dose equivalent in the United States population (1). While nearly all the radiation exposure is received by the patient who derives a direct benefit, some of the radiation exposure is accrued to medical personnel associated with patient care. In recent years numerous dose reduction techniques have been recommended which reduce direct patient dose and scatter to medical personnel. This paper will describe general considerations in hospital radiation protection.

## PRINCIPLE OBJECTIVES OF A HOSPITAL RADIATION PROTECTION PROGRAM

The primary consideration in the use of radiation in medicine is its contribution to the welfare of the patient. If there is no contribution, both the patient and staff receive unnecessary radiation exposure that is avoidable. Secondly, the facilities and procedures should be designed to obtain the necessary clinical information or deliver a therapeutic dose to target tissue while delivering to patients and staff an effective dose equivalent that is as low as reasonably achievable (ALARA). This may be ensured by concomitant provision of modern clinical equipment, protective equipment and facilities, and adequate training in their use. While there is no regulation or recommendation that limits patient dose to a specific level other than

the general statement that the acceptable dose is directly related to the expected benefit to the patient, federal and state regulations specifically limit radiation exposure of medical staff and often require a documented ALARA program.

## PROTECTION OF THE PATIENT

Radiation is a principle tool of diagnostic and therapeutic medicine. Therefore, exposure of patients to radiation is deliberate with a goal of providing a benefit. Patients receive radiation exposure from diagnostic and therapeutic x rays, radiopharmaceuticals, and sealed radiation sources.

One aim of a radiation protection program is to limit patient radiation exposure to levels no higher than necessary to achieve the benefit. In diagnostic radiology, this is accomplished through the use of film-screen combinations that provide good image quality with minimal dose. The literature available on film-screen combinations is too vast to review here, but many radiology and radiologic physics textbooks provide an introduction to this technique. A good quality control program is imperative to low dose radiography and high quality images (2).

Until recently there was little that could be done to reduce fluoroscopic radiation exposure to patients except for limiting the beam diameter to that of the image intensifier and properly tuning the video display. However, a new technique in cardiac fluoroscopy allows pulsed progressive scanning of the image (3). This system reduces patient exposure by approximately 50% and can be added to any pulsed fluoroscopic or cine x-ray system.

Patient exposure reduction in diagnostic nuclear medicine depends primarily on a good camera quality control program that assures acceptable images with the lowest possible dosages of radiopharmaceuticals. The U.S. Nuclear Regulatory Commission (NRC) has been emphasizing patient exposure reduction through quality assurance steps that decrease the chance of misadministrations. In a recent advance notice of proposed rulemaking the NRC contemplated additional quality assurance requirements to further reduce the chance of a misadministration that could result in a therapeutic dose to certain organs of the body, e.g. the thyroid (4).

Computerized treatment planning is now used at most radiation oncology centers to maximize tumor dose and minimize dose to normal tissues. In brachytherapy Cs-137 and Ir-192 have largely replaced radium, which has resulted in a reduced patient normal tissue dose as well as occupational dose to oncology and nursing personnel.

Patients and control subjects may receive radiation exposure from x rays or radiopharmaceuticals by virtue of their participation in a research protocol. Institutional review boards and radiation safety committees must evaluate these protocols for appropriateness of the radiation exposure relative to the information sought by the investigator. Consideration must include the number of subjects in each protocol. More subjects than are required to obtain a statistically valid sample will result in wasted and unnecessary exposure of some subjects. Likewise, too few subjects to answer the protocol question will result in all subjects being exposed unnecessarily since no benefit from the exposures will be realized.

Finally, radiation protection of the patient is optimized by the skill of the operator or technologist. Patient dose is significantly reduced by adequate preplanning, selection of proper radiographic techniques, skillful administration of radiopharmaceuticals, use of minimum radiographic field size, minimizing fluoroscopic time through the use of video recording and display of the most recent projection, and elimination of repetitive filming. Excluding radiation oncology, the highest patient doses occur in the cardiac angiographic laboratory. The Society for Cardiac Angiography stresses the importance of adequate training, a solid understanding of the image modality being used, and logical thinking in maintaining radiation safety in the cardiac laboratory (5).

#### PROTECTION OF STAFF

The elements of a hospital radiation protection program vary widely according to the hazards associated with equipment and techniques. Consideration must always be given to appropriate facility design, proper operating procedures, adequate training of operators and patient care personnel, use of appropriate equipment, quality control, and radiation safety monitoring.

##### Facility Design

While space and protective requirements of radiation facilities should always be considered in the early planning stages of the new facility, such requirements are equally important in the remodeling of existing facilities. Early and frequent communications between facilities engineers and radiation safety staff are important in assuring adequate protection at a reasonable cost. It is advisable that a planning team be appointed to review equipment and technical considerations as well as radiation safety requirements. This planning team should consist of a representative from the hospital facilities group or administration, architect, radiologist or radiation oncologist or representative, and a radiation protection advisor. In some

cases it may be necessary to include outside consultants who have special expertise in the design of radiological facilities. This may be especially important in radiotherapy facilities where the amount of shielding and cost of construction are major considerations.

The design of the radiology department should take into consideration the possibility of changes within the next several years due to new developments in equipment and techniques or changes in patient needs. Provisions should be made to allow for such developments with minimal structural changes and wherever possible should include space for new modalities or future expansion. The general building construction needs to take into account protective shielding and ventilation requirements for radiology and diagnostic nuclear medicine as well as radiation oncology. Recommendations and technical information on structural shielding design and evaluation for most medical installations is provided in NCRP Report No. 49 (6).

Many of the considerations in the design of radiological facilities will depend upon the level of medical care. Centralization versus decentralization of radiation facilities and sophistication of equipment and techniques will largely depend upon size of the facility and whether or not it is oriented toward primary or tertiary care. The planning team needs to be aware of such considerations and for small facilities is advised to consult outside experts in the field.

Whenever possible, safety should be engineered into the facility. This is particularly important with respect to shielding design. NCRP Report No. 49 provides appropriate shielding design for most medical facilities. The walls of rooms used in radiology and radiation oncology should be shielded in accordance with the proposed use for the room. In diagnostic and therapeutic nuclear medicine radiation protection considerations must include the delivery of high intensity sources to the nuclear pharmacy laboratory which may be shielded, and treated patients which may be a significant source of radiation exposure. Dispensing of radiopharmaceuticals is normally carried out with the use of remote handling tools or shields which provide local shielding. Administration of the radiopharmaceutical usually involves the use of shielded syringes for protection of the technologist. Since the diagnostic nuclear medicine patient cannot be shielded, facility design considerations of an imaging room should include adequate distance between the patient and the technologist during the scanning procedure. If the imaging room is too small, the nuclear medicine technologist is not able to take advantage of adequate distance to sufficiently reduce occupational radiation exposure.

In addition to the use of appropriate local shielding, the nuclear pharmacy laboratory must contain appropriate local exhaust to carry away any radioiodine fumes produced during the dispensing of liquid radioiodine and noble gases exhaled from patients participating in lung ventilation studies.

It is often advantageous to designate specific hospital rooms for hospitalization of patients who have received therapeutic doses of radiopharmaceuticals or radiation implants. The designation of specific rooms for this purpose allows the addition of appropriate shielding in the walls to protect staff, members of the public, and other patients. In lieu of the availability of such rooms these patients must usually be located in a corner room and the adjacent room must be kept vacant to provide adequate distance between the patient and other persons. The cost of leaving the adjacent room vacant often justifies the additional expense associated with shielding the walls of the room. Portable bedside shielding should be provided to reduce radiation exposure to patient care staff.

#### Radiation Protection Procedures

The effectiveness of a radiation protection program is largely dependent upon composition of and compliance with standard operating procedures that directly or indirectly incorporate specific steps for minimizing radiation exposure. The radiation protection program must include special and routine surveys to determine radiation levels inside and outside radiological areas and audits of radiological programs to ensure compliance with radiation protection procedures.

Visual inspection during construction or remodeling of facilities is important to ensure the installation complies with specifications. The inspection should include determination or examination of shielding thickness and construction or installation technique, lead butting or lapping of appropriate joints and penetrations, location of interlocks and warning lights, wall thickness and location of primary barriers in radiation oncology installations, leaded glass specified in viewing windows, and location of control booths. After the installation is complete, diagnostic x-ray and nuclear medicine shielding should be examined for stray or unanticipated radiation fields. Radiation oncology facilities should be surveyed in accordance with the American Association of Physicists in Medicine procedure for conducting radiation surveys of therapy installations (7). Random transmission measurements of shielded walls and viewing windows in diagnostic facilities should be conducted to verify adequacy of shielding. Once operational these facilities and adjacent areas should be monitored with environmental or personnel dosimeters to establish operational radiation levels. Safety devices such as door interlocks, beam limiting switches and mechanical

stops should be checked before routine facility operation and as part of a regular quality control check. Radiation monitors which may have been specified, e.g. in a teletherapy room, must be calibrated before operation and regularly thereafter. The daily quality control program should include a monitor check with a sealed reference radiation source to confirm operational status. Appropriate warning signs should be posted in accordance with state or federal regulations.

A report of the facility radiation survey should be compiled to include all survey results and any anticipated occupational exposures that may exceed ALARA program goals or approach regulatory limits. The report should also indicate whether a resurvey is required after modifications or whether any limitations of occupancy or operational techniques are necessary.

Long-lived sealed sources for radiotherapy are usually kept in a shielded safe located within the radiation oncology department or near the hospital rooms where they are used in implants. Shorter lived sealed sources such as Ir-192 may be received and inventoried in the same area or in the radiation safety department. All sealed sources must be regularly inventoried to ensure a source does not become lost. Patients and patient rooms must be monitored following implants as a double check that all sources have been removed. The source storage room should be surveyed regularly to ensure that sources are stored in a shielded configuration and that radiation levels within the room are acceptable. Sealed sources should be wipe tested on a regular basis for early detection of a leaking source.

Nuclear medicine facilities should be surveyed regularly to detect unacceptable radiation fields and contamination of facilities and equipment. These surveys should include examination of waste handling procedures to assure that personnel are protected from the radiological as well as the infectious nature of the waste. Needles and syringes should be collected in a container separate from contaminated gloves and other disposable items to minimize accidental punctures and ensure proper disposal of the potentially infected needles. Since most nuclear medicine procedures utilize radionuclides with short half-lives, it is acceptable to store the needles and syringes for radioactive decay with subsequent incineration in the hospital incinerator.

#### TRAINING

It has been demonstrated that employee education and awareness significantly reduce occupational exposure to diagnostic (8) and therapeutic radiation (9). Training programs should include an initial orientation session that describes the radiological environment and safety procedures of the work area and discusses

the ALARA program. Annual in-service training seminars and occasional written communications are helpful in updating personnel in safety procedures and maintaining an awareness of the radiation safety program.

#### PERSONNEL MONITORING

Routine monitoring of staff for external and, where appropriate, internal radiation exposure is important to establish that occupational exposures are within regulatory limits. Personnel monitoring is also important to measure the effectiveness of facility design and operational procedures relative to ALARA program goals. While personnel monitoring is recommended (10) or required by state or federal regulations for individuals who could receive radiation exposures in excess of 25% of the maximum occupational exposure limits, monitoring of individuals who are likely to receive lower levels of radiation exposure can reveal developing trends or unusual practices, will assist in documenting such exposures for the ALARA program, and gives peace of mind to those radiation workers who expected to receive low exposures.

A special class of radiation worker that may require additional monitoring is the pregnant worker. Since the maximum recommended radiation exposure to the fetus is 5 mSv (500 mrem) (11), monitoring of such workers is often required in facilities where routine monitoring is normally not provided. Such monitoring may take the form of a routine personnel monitoring badge or a pocket ionization chamber or equivalent device that allows the pregnant worker to monitor her exposure on a frequent basis. If personnel monitoring badges are provided for this purpose, it should be recognized that the sensitivity of the badge may require a minimum monitoring period greater than one week due to the low anticipated exposure. In addition, the badge should be worn under the lead apron when one is required, which produces a condition of a nearly negligible radiation field at the abdomen of the pregnant worker. Therefore, the probability of detecting a dose during a short monitoring period is often negligible.

In addition to appropriate external monitoring, bioassay procedures are appropriate for medical personnel who handle radiopharmaceuticals. Technologists who dispense and administer radioiodine should have a thyroid count within three days of the procedure (12). All other nuclear medicine personnel who dispense or administer radiopharmaceuticals should receive a whole body count or urinalysis on a regular schedule or after any incident that could result in internal contamination.

## CONCLUSIONS

The ultimate goal of a hospital radiation protection program is to limit radiation exposures to levels that provide benefits of the radiologic technique without jeopardizing patient care. This goal is reached through proper facility design, utilization of carefully conceived standard operating procedures, adequate training of personnel and rigorous radiation monitoring. Whether a facility is small and treats a few thousand patients per year, or large and treats hundreds of thousands of patients, careful integration of each of these elements into a comprehensive radiation protection program will result in patient and personnel effective dose equivalents that are as low as reasonably achievable.

## REFERENCES

1. National Council on Radiation Protection and Measurements. Ionizing radiation exposure of the population of the United States. Bethesda, MD.: NCRP; NCRP Report No. 93; 1987.
2. Gray, J.E.; Winkler, N.T.; Stears, J.G.; Frank, E.D. Quality control in diagnostic imaging. Rockville, MD: Aspen Publications, Inc.; 1983.
3. Holmes, D.R.; Bove, A.A.; Wondrow, M.A.; Gray, J.E. Video x-ray progressive scanning: new technique for decreasing x-ray exposure without decreasing image quality during cardiac catheterization. Mayo Clinic Proc. 61:321-326; 1986.
4. U.S. Nuclear Regulatory Commission. Comprehensive quality assurance in medical use and a standard of care. Federal Register 52:36949-36953; 1987.
5. Society for Cardiac Angiography. Guidelines for radiation protection in the cardiac catheterization laboratory. Catheterization and Cardiovascular Diagnosis 10:87-92; 1984.
6. National Council on Radiation Protection and Measurements. Structural shielding design and evaluation for medical use of x rays and gamma rays of energies up to 10 MeV. Bethesda, M.D: NCRP; NCRP Report No. 49; 1976.
7. American Association of Physicists in Medicine. Code of practice for x-ray therapy linear accelerators. Part II: installation and performance measurements for x-ray linacs. Medical Phys. 2:110-121; (1975).
8. Vetter, R.J.; Gray, J.E. The impact of education on occupational radiation exposure reduction in a diagnostic radiology department. In: Proceedings of the Health Physics Society midyear topical symposium; Reno, NV. 1987: 28-34.
9. Braun, J.S.; Vetter, R.J.; Schray, M.F. Personnel exposures in interstitial brachytherapy and cost-benefit analysis of remote afterloading. Health Phys. 50:552; 1986.
10. National Council on Radiation Protection and Measurements. Operational radiation safety program. Bethesda, MD.: NCRP; NCRP Report No. 59; 1978.
11. National Council on Radiation Protection and Measurements. Recommendations on limits for exposure to ionizing radiation. Bethesda, MD: NCRP; NCRP Report No. 91; 1987.
12. U.S. Nuclear Regulatory Commission. Medical use of byproduct material; final rule; 35.315, safety precautions. Federal Register 51:36959; 1986.

PERSPECTIVE FROM A COMMERCIAL SUPPLIER  
OF DOSIMETRY SERVICES

R. Craig Yoder  
Tech/Ops Landauer, Inc.  
Glenwood, IL 60425

Abstract

The traditional radiation related industries in the United States have matured. The growth rates in the numbers of radiation workers have moderated and ALARA programs have favorably reduced many exposures. Dosimetry testing and accreditation by the National Bureau of Standards have identified those services possessing satisfactory dosimetry systems and technical competence. These developments have influenced the business perspectives. Combined with the overall renewed emphasis on competition and productivity in American business, many dosimetry services have become more aggressive in seeking new markets; residential radon measurements being most obvious. The potential size of these markets is making investments in technical research more attractive. In the past, most research funding was provided by the government. The renewed research interest by the private sector could stimulate the entry of new professionals into radiation measurement research. Research results have the potential for improving traditional services and expanding the applicability of certain measurement methods.

Introduction

Basic corporate performance indices such as sales, income, productivity and growth affect the investments made by commercial suppliers of dosimetry services. By their nature, commercial firms are motivated to provide cost efficient dosimetry that meet the needs and expectations of their clients. Investments in new or improved measurement methods are evaluated by their ability to add or create value. This value can be expressed in terms of quality, technical performance and/or economic results. The relative importance given to these distinguish commercial from in-house dosimetry processors; processors from users; and, scientists from businessmen.

The perspectives used to assess value are influenced by the growth characteristics of the industries and institutions using radiation. During periods of expansion, investments in technology development are easier to assess. Risks are more palatable when presented with the knowledge that more workers are going to be monitored.

Mature industries often exhibit very slow growth; special cases would be those that are highly cyclical. During slow growth, development programs are harder to assess. Approved efforts are likely to offer quick rewards.

There is evidence to suggest that the traditional radiation industries are maturing. Whether these industries are experiencing a short term lull is uncertain. A return to the growth rates experienced in the late 1970's is unlikely before the end of the decade. One might infer that technological developments could be minimal; however, the potential for new markets, renewed competitive spirit and entrepreneurship could promise increased investment by the private sector in improving or developing new technologies.

### The Past

During the 1970's and extending into the early 1980's the radiation related industries were expanding rapidly. There was a boom in nuclear power plant construction that was to lead to new radiation workers. Oil exploration and nondestructive testing also added workers. The medical industry experienced major advances in nuclear medicine, diagnostic imaging and radiation therapy. National research laboratories were examining nuclear fuel reprocessing and alternative reactor designs.

Concurrent with these events were the application of new dosimetry methods, some having only been used in the laboratory. Thermoluminescent dosimetry received greater acceptance and automated processing systems were introduced. In 1978, R. S. Landauer, Jr. & Co. introduced Neutrak I, a polycarbonate based solid state nuclear track detector. Within a few years, CR-39 neutron dosimetry was introduced. There was also some excitement in new electronic dosimeters as cadmium telluride and mercury iodide detectors became available.

Unfortunately, a series of events stopped the expansion: Three Mile Island, plentiful oil, high interest rates and inflation. The uncertain growth outlook changed the perspective for assessing dosimetry investments.

A new revolution began as the radiation industry matured: computers and microprocessor applications. The features of personal and mini computers in data manipulation and electronic communications offered new opportunities for easing the administrative burdens of personnel monitoring. Microprocessors found widespread use for controlling instruments.

With the ability of telephone systems to link computers and terminals, clients were offered new values that did not rely on new measurement technologies. On-line transactions of adding, deleting, or changing badges made new instructions quicker to execute. Dosimetry information could be reported on tape and diskette; or, data could be directly transferred from one computer to another.

Computers also increased the efficiency of dosimeter processing. Many processes and quality control parameters could be monitored. More advanced, automated processing systems were introduced. These systems provided large amounts of information for the analysts and computers became necessary for intelligently displaying the data.

Not receiving much attention were measurement technologies. Government funding supported feasibility studies of some technologies, but these efforts were focused on special problems. Whether the results of these programs could be broadly applied at affordable costs were too uncertain. Without a vigorously growing market, the risks become perceived differently. Investments that translate laboratory, experimental methods into a large scale, reliable commercial product can be large. A new stimulus was needed if new technologies were to reach routine use.

## The Outlook

The almost overnight growth in the notoriety of radon in residences could be the needed stimulus. Presently, most of the large commercial dosimetry services are directly or indirectly participating in, or examining, the radon measurement business. The incentives are great; there are more homes to potentially monitor than radiation workers. The emergence of local statutes requiring a radon measurement as a part of the sale of a residence expands the market size.

The radon business has attracted the interest of small, entrepreneurial firms also. In early 1988, over 1,000 firms were seeking enrollment in the U. S. Environmental Protection Agency's Radon Measurement Proficiency Program. Many of these smaller firms use the analytical services of the larger dosimetry firms. With the overall business climate in the United States, the radon business presents the features of a competitive environment.

The seeds have been planted for a reemergence of privately supported research and development. A large potential market exists. Competition exists. Promising technologies exist. If the development expenditures are made, personnel monitoring systems could benefit.

Solid state nuclear track detection is one method for passive, long-term radon monitoring. CR-39 and cellulose nitrate are two track detection materials that can also be used for personnel neutron monitoring. Large scale use of these materials for radon assessments could stimulate material improvements, automation and economies of scale. The current use of CR-39 in the United States for neutron monitoring is insufficient to warrant significant research in these areas. Undoubtedly, successes for radon could be transferred easily to the neutron application.

Finally, the maturing radiation industry could create future shortages of radiation measurement technical professionals. Slow growth industries are handicapped for the process of attracting new talent. The first generation of professionals who were challenged by the radiation measurement demands of a fledging nuclear industry, are retiring. Graduate programs devoted to teaching research skills are not thriving as they were. A resurgence of corporate radiation measurement research could attract needed people.

Forecasters are predicting labor shortages for many businesses. By aggressively seeking new markets and becoming more competitive, commercial dosimetry services can establish the framework to attract new talent. Commercially, this talent must be able to translate the ideas and laboratory demonstrations from research facilities into usable, marketable products.

The perspective of this commercial dosimetry services supplier is that of being on the threshold of a new period of technical advancement. The door is cracked. Soon, it will become clear if it will open fully.

IMPLEMENTATION OF THE DEPARTMENT OF ENERGY  
LABORATORY ACCREDITATION PROGRAM (DOELAP)  
AND THE NEW EXPOSURE REPORTING REQUIREMENTS

PAUL NEESON  
U. S. DEPARTMENT OF ENERGY  
CHICAGO OPERATIONS OFFICE

The Department of Energy has initiated DOELAP in an effort to standardize on optimum state-of-the-art external dosimetry technology, and to identify anomalies in dosimetry performance in order to determine areas of needed research. The program is analogous to the National Voluntary Laboratory Accreditation Program (NVLAP), but with three essential differences: a) more stringent tolerance levels, b) a built-in provision for applied research, and c) application to a wider spectrum of source terms and dosimetry needs.

Accreditation of external dosimetry programs is now mandatory for DOE operations. Requirements are established in DOE Order 5480.15, which consists of a basic Order and two companion documents, the Handbook (DOE/EH-0026, for operational procedures) and the Standard (DOE/EH-0027, for performance criteria). To initiate the accreditation process, a formalized application is submitted, which describes the dosimetry and defines the irradiation categories in which the dosimeter(s) will be tested. The dosimeters are sent to the DOE-Radiological and Environmental Sciences Laboratory (RESL) at INEL for performance testing, and site assessment is performed at the organization's facilities, to evaluate its handling of dosimetry data and documentation. The DOELAP Oversight Board eventually reviews the results of these functions and makes appropriate recommendations to DOE-HQ. Accreditation is formally granted by HQ and is valid for two years.

Certain organizations may be exempted from DOELAP accreditation. Generally, these are smaller operations which utilize commercial dosimetry services and which have low radiation exposures. In such cases, exemption from DOELAP can be granted if the dosimetry system(s) is NVLAP accredited.

The organizations within DOE-Chicago Operations Office (CH) exhibit a wide spectrum of dosimetry systems and applications. There are "in-house" systems, and commercial services provide dosimetry for large and small operations. Table 1 shows the salient features of selected CH laboratories' external dosimetry programs, with data taken from CY 1987. (Full titles are listed in the Appendix.)

To achieve DOELAP accreditation, ANL-E, BNL, FNAL, and MIT-Bates will undergo both performance testing and site assessments. ANL-W and NBL need only site assessments, since their dosimeters' performance testing will be completed by their servicing organizations, i.e. RESL and ANL-E, respectively. PPPL will have a site assessment, but will not need to submit dosimeters for performance testing, since essentially the same dosimeter will be tested by FNAL. This type of option will be available to any other DOE laboratory. However, Ames and SERI, for example, in view of their low exposures, may opt to apply for DOELAP exemption utilizing the NVLAP accreditation which exists for their dosimeters.

Testing of commercial dosimeters will be spearheaded by BNL and FNAL. Figure 1 is a DOELAP application category listing, showing the categories in which BNL's and FNAL's dosimeters will be tested. At the present, these and all other commercial dosimeters used at CH laboratories are provided by the R.S. Landauer Co. (RSL). The current intention is for a) BNL to pursue accreditation for RSL NTA, Lexan, and CR-39 dosimeters exposed to a moderated ( $^{252}\text{Cf}$ ) spectrum; and b) FNAL to pursue accreditation for RSL film (beta-gamma), and NTA and Lexan exposed to an unmoderated spectrum. Once such an accreditation is established, it can be applied to any other DOE laboratory using this or similar RSL dosimetry. As an example of the latter, the RSL G dosimeter contains the same type film for beta-gamma as does the P, but the P also has NTA for neutron detection. It would appear that these two dosimeters would be equivalent for beta-gamma accreditation. Decisions on technical equivalence will be made by the Performance Evaluation Program Administrator (at RESL).

To summarize DOELAP activities, CH laboratories will either pursue DOELAP accreditation, or exemption based on low dose equivalent and existing NVLAP accreditation. Once DOELAP accreditation is established for a specific dosimeter, it can be utilized by any other DOE Laboratory using the same or equivalent dosimetry, to avoid duplication of effort.

DOE laboratories have been required to submit radiation exposure reports for several years. Starting with CY 1987 data, the reports for external exposures will conform to new requirements as promulgated by DOE Order 5484.1A. The new system is intended to develop more exact exposure data and to provide for better trend analyses.

The previous system required individual reports on terminated/visitor personnel during the year, and summary (non-personal) reports yearly. The new system involves reporting of individual personnel exposure data on an annual basis only. Figure 2 shows the specific elements required for each individual

reported, along with the field sizes and locations for automated systems. A separate report is required for each employee and resident non-employee, and for each visitor having a positive exposure. (Note: Specific internal and extremity exposure reporting elements are still under development.)

The REMS automated data entry program has been developed by the Systems Safety Development Center (SSDC) of EG&G, Idaho, Inc., for use in developing the new exposure reports. The program follows the exact format of Figure 2. It is available on floppy disk and can be used in any IBM PC compatible system. It is especially useful for smaller laboratories which do not have great numbers of personnel monitored. (Data may also be submitted on hard copy if desired.)

The larger laboratories are developing their own automated systems for preparation of the reports. For those served by RSL, there is an additional step - data from the tape supplied by RSL must be extracted and combined with specific laboratory information (e.g. individual occupational codes) to produce the final report. The first to complete this was PPPL. They were assisted by SSDC, who developed a utility program to read the RSL tape and combine PPPL data into the proper format. BNL may have to develop a separate utility program due to differences in their RSL service. However, any of the programs developed for production of exposure reports are available for use by any other DOE laboratory.

The completed reports are transmitted to CH. A duplicate copy is forwarded by CH to SSDC, who operates the DOE Central Repository and develops the Annual Reports of DOE Radiation Exposures. The reports retained at CH are entered into the Radiation Exposures (RADEX) program, which combines CH laboratories' data and produces several tabular and graphic displays. Figures 3 and 4 are examples of RADEX output. The RADEX program is currently being updated (by ANL-E personnel) to receive and process data in the new format. Information on the updated program can be useful and available to any DOE field office or laboratory.

This first year of working with the new reporting requirements involves a level of effort, especially in developing the new automated systems. Any new systems developed, e.g. data entry programs or RADEX programs, will be available to interested parties.

TABLE 1  
SELECTED CH LABORATORIES  
EXTERNAL DOSIMETRY PROGRAMS - 1987

<u>Laboratory</u>	<u>Service</u>	<u>Type</u>	<u>Dosimeters</u>	<u>CDE (man-rem)</u>
ANL-E	in-house	TLD, albedo	2500	34
ANL-W	RESL in-house	TLD, albedo	2700	45
BNL	commercial	RSL P,B,E	3000	175
FNAL	commercial	RSL P,H,E	2300	58
PPPL	commercial	RSL H	1300	7
MIT-Bates	in-house	TLD, albedo	1700	9
Ames	commercial	RSL K	64	<1
NBL	ANL-E in-house	TLD	66	<1
SERI	commercial	RSL G	17	<1
U. of Michigan	commercial	RSL G,H	24	2

RSL Dosimeters:

- B - Kodak Type 2 plus CR-39
- G - Kodak Type 2 only
- E - Lexan polycarbonate
- H - Kodak Type 2 plus NTA and cadmium shield
- K - TLD
- P - Kodak Type 2 plus NTA

FIGURE 1

DOELAP TESTING CATEGORIES  
FOR BNL AND FNAL DOSIMETERS

<u>CATEGORY</u>	<u>DOSIMETER DESIGNATION</u>				
	<u>BNL</u>		<u>FNAL</u>		
	<u>B</u>	<u>P+E</u>	<u>P</u>	<u>P+E</u>	
I.	Low-Energy Photon (High Dose)			X	
II.	High-Energy Photon (High Dose)			X	
IIIA.	Low-Energy Photon			X	
IIIB.	Low-Energy Photon (Plutonium)				
IV.	High-Energy Photon			X	
VA.	Beta				
VB.	Beta (Uranium)			X	
VC.	Beta (Special) $^{90}\text{Sr-Y} + ^{204}\text{Tl}$			X	
VI.	Neutron $^{252}\text{Cf}$ {	Moderated	X	X	
		Unmoderated			
VIII.	Mixtures:				
	III AND IV			X	
	IV AND V			X	
	III AND VI	X	X		X
	IV AND VI	X	X		X

FIGURE 2

ANNUAL RADIATION DOSE SUMMARY

<u>Item</u>	<u>Example Code or Data</u>	<u>Field Size (Characters)</u>	<u>Column Range</u>
1. Calendar year of reported data	1987	4	1-4
2. Social security number	123456789	9	5-13
3. Name of monitored individual			
a. First name or initial	JOHN	15	14-28
b. Middle name or initial	Q	12	29-40
c. Last name	DOE	15	41-55
4. Birth year	1942	4	56-59
5. Sex (F or M)	M	1	60-60
6. Beginning of monitoring date (MMDDYY)	010187	6	61-66
7. End of monitoring date, end of visit date, or termination date (MMDDYY)	123187	6	67-72
8. Employment status	A	1	73-73
A = Monitored worker	(see TABLE 1)		
T = Terminated employee			
V = Monitored Visitor			
N = Nonemployee radiation worker			
9. Organization code	0567002	7	74-80
10. Facility type code	(see TABLE 2)	2	81-92
11. Occupation code	(see TABLE 3)	3	83-85
12. Annual whole body dose			
External penetrating (dose equivalent) (including neutron)		7	93-99
- Neutron (dose equivalent)		7	100-106
13. Annual shallow dose (dose equivalent)		7	160-166

NOTE: Internal and extremity reporting elements are under development.

FIGURE 3

SAMPLE OF RADEX OUTPUT

Page No. 1  
05/10/88

ANL - EAST

RADIATION EXPOSURE SUMMARY INFORMATION

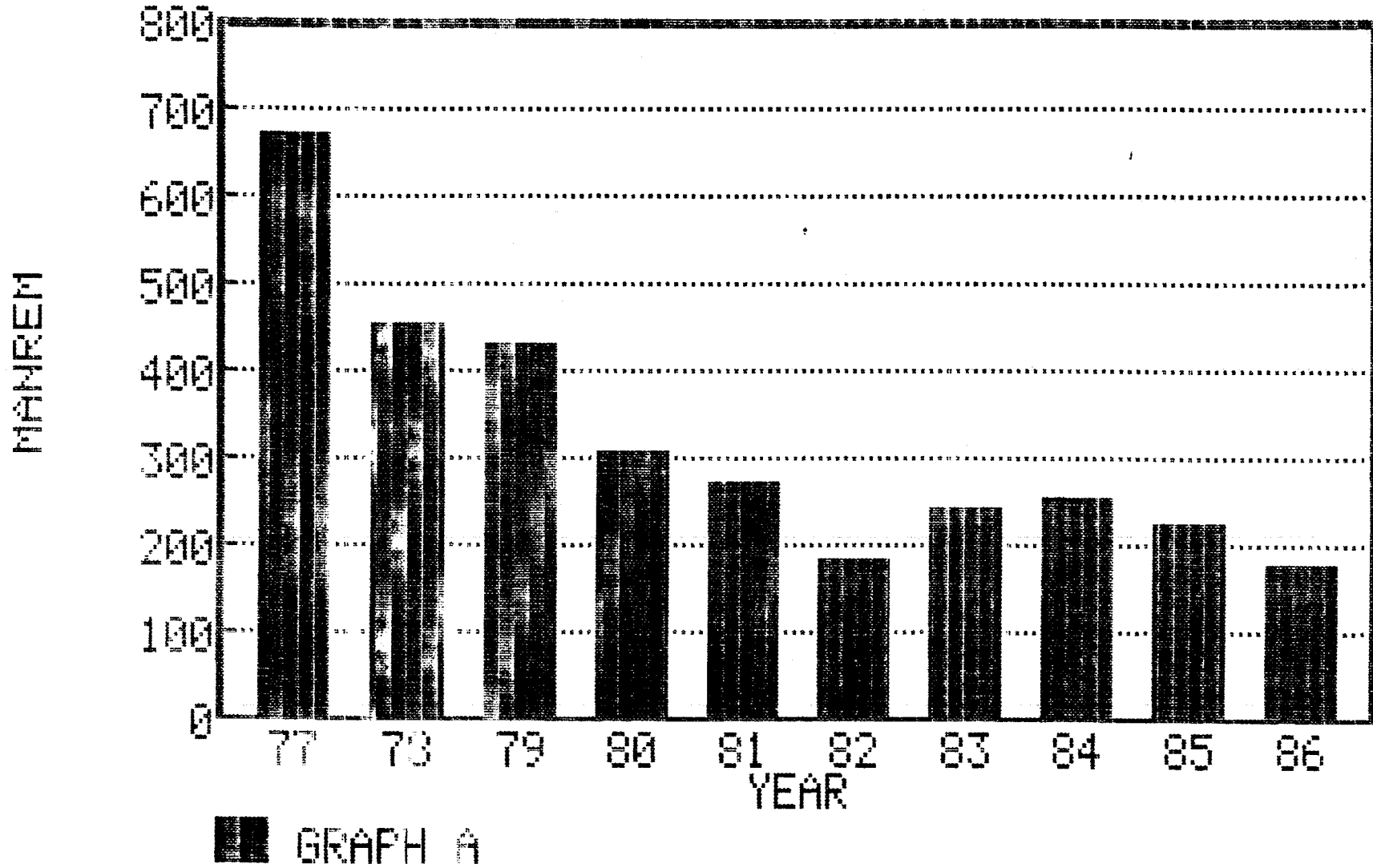
FRACTION OF MONITORED INDIVIDUALS WITH DOSE EQUIVALENT  
IN EACH RANGE

YEAR	TOTAL													TOTAL MAN REM	MAN-REM EMPL	PER FACILITY TOTAL
	NO. BADGED	< NONE	.100-	.250-	.500-	.750-	1.000	2.000	3.000	4.000	5.000	6-12				
1977	3159	0.733	0.159	0.043	0.026	0.014	0.010	0.012	0.002	0.001	0.000	0.000	0.000	196.844	0.062	4.0
1978	3194	0.806	0.132	0.026	0.015	0.008	0.006	0.007	0.001	0.000	0.000	0.000	0.000	113.609	0.036	4.0
1979	3242	0.841	0.110	0.024	0.011	0.006	0.003	0.005	0.001	0.000	0.000	0.000	0.000	80.723	0.025	4.0
1980	2675	0.813	0.124	0.030	0.017	0.007	0.004	0.004	0.001	0.000	0.000	0.000	0.000	82.416	0.031	4.0
1981	2535	0.817	0.127	0.021	0.017	0.010	0.004	0.003	0.001	0.000	0.000	0.000	0.000	73.318	0.029	4.0
1982	2299	0.854	0.094	0.020	0.017	0.008	0.004	0.004	0.000	0.000	0.000	0.000	0.000	58.020	0.025	4.0
1983	2156	0.859	0.093	0.022	0.013	0.004	0.004	0.004	0.002	0.000	0.000	0.000	0.000	56.551	0.026	4.0
1984	2119	0.867	0.081	0.023	0.011	0.006	0.005	0.007	0.000	0.000	0.000	0.000	0.000	58.817	0.028	4.0
1985	2280	0.883	0.077	0.016	0.012	0.005	0.002	0.003	0.000	0.000	0.000	0.000	0.000	41.104	0.018	4.0
1986	2079	0.000	0.000	0.000	0.000	0.000	0.000	0.000	0.000	0.000	0.000	0.000	0.000	31.305	0.015	4.0
AVE.	2574	0.832	0.109	0.025	0.015	0.007	0.005	0.005	0.001	0.000	0.000	0.000	0.000	79.271	0.031	4.0

FIGURE 4

SAMPLE OF RADEX OUTPUT

# COLLECTIVE DOSE - BROOKHAVEN



APPENDIX

Abbreviations/Full Titles

ANL-E	Argonne National Laboratory - East
ANL-W	Argonne National Laboratory - West
BNL	Brookhaven National Laboratory
CH	Chicago Operations Office
CDE	Collective Dose Equivalent
DOE	Department of Energy
DOELAP	Department of Energy Laboratory Accreditation Program
FNAL	Fermi National Accelerator Laboratory
INEL	Idaho National Engineering Laboratory
MIT	Massachusetts Institute of Technology
NBL	New Brunswick Laboratory
NVLAP	National Voluntary Laboratory Accreditation Program
PPPL	Princeton Plasma Physics Laboratory
RESL	Radiological and Environmental Sciences Laboratory
RSL	R. S. Landauer, Jr. and Co.
SERI	Solar Energy Research Institute

IMPROVED PERFORMANCE OF A TWO-ELEMENT TLD BADGE  
FOR DETERMINING GAMMA AND BETA DOSES USING  
MULTIPLE LINEAR REGRESSION

Sam J. Cipolla and Raymond J. Powell  
Physics Department  
Creighton University  
Omaha, NE 68178

R. K. Stultz, C. Norris, M. Hawes, and B. Hearty  
Nuclear-Technical Services Division  
Omaha Public Power District  
Omaha, NE 68102

Introduction

The gamma/beta TLD badge used by OPPD consists of two TLD-700 chips (Harshaw G7 card), one of which (chip#2) is shielded by a 0.102 cm-thick aluminum filter, and the other (chip#1) is unshielded, as shown in Fig. 1. Standard procedure had been to determine the beta dose to the badge by subtracting the response of chip#2 from that of chip#1 and then dividing by a calibrated beta-sensitivity factor; the gamma dose was taken to be the response of chip#2 divided by the chip's gamma-sensitivity factor followed by the subtraction of the background dose. A problem with this procedure is penetration of energetic beta particles through the aluminum filter on chip#2 which causes an over-response. Due to the technique used to obtain the beta dose, this also results in an under-estimate of the beta dose. This problem has been corrected through application of multiple linear regression analysis on a large data base of pure gamma ( $^{137}\text{Cs}$ ), pure beta ( $^{90}\text{Sr}$ ), and mixed exposures. The outcome of the analysis is an algorithm that automatically corrects for penetration effects. Performance tests using the ANSI N13.11 standard [1] are presented to show the improvement.

TLD Processing Method

TLD chips are read out for 10 sec. at 300°C using a Harshaw model 2271 reader system. Prior to exposure, the chips are repeatedly annealed in the reader until the internal background response is less than 5 nC. After exposure, TLDs are left to fade for 3 days to allow the unstable low-

temperature traps to effectively decay; for longer fade times, a calibrated fading correction factor is applied to the responses. TLD badges used in exposure tests are accompanied by control badges to monitor in-transit background.

### Rationale for Shallow and Deep Dose Algorithms

For mixed beta/gamma exposures, the over-response of the OPPD TLD badge to the gamma dose and the under-response to the beta dose can be quantitatively described as follows. The non-penetrating beta dose  $D\beta'$  is obtained from

$$D\beta' = (R1 - S1 R2 / S2) / Snp \quad (1)$$

where R1 and R2 are the background-corrected responses (nC) of the chips, and S1 and S2 are the gamma sensitivities (nC/mrem) of the chips. The total responses R1 and R2 each have beta- and gamma-induced components:

$$R1 = R1\beta + R1\gamma \quad (2)$$

$$R2 = R2\gamma + R2\beta \quad (3)$$

$Snp$  (1.039 +/- 0.135 nC/mrem) is the average non-penetrating beta sensitivity, defined as

$$Snp = (R1 - S1 R2 / S2) / (D\beta - R2\beta / S2) \quad (4)$$

From eqn.'s (1) and (4), we see that

$$D\beta' = D\beta - R2\beta / S2 \quad (5)$$

where  $D\beta$  = true beta dose. The calculated gamma dose  $D\gamma'$  is obtained from

$$D\gamma' = R2 / S2 \quad (6)$$

Using eqn. (3) we get

$$D\gamma' = R2\gamma / S2 + R2\beta / S2 \quad (7)$$

$$D\gamma' = D\gamma + R2\beta / S2 \quad (8)$$

where  $D\gamma$  = true gamma dose. Define the beta-penetration ratio as

$$f = (R2\beta / S2) / (R1\beta / S1) \quad (9)$$

Using  $f$ , eqn.'s (5) and (8) become

$$D_{\beta}' = D_{\beta} - f R_{1\beta} / S_1 \quad (10)$$

$$D_{\gamma}' = D_{\gamma} + f R_{1\beta} / S_1 \quad (11)$$

The shallow dose  $D_s$  is obtained by adding the non-penetrating beta dose and the gamma dose:

$$\begin{aligned} D_s &= D_{\gamma} + D_{\beta} \\ &= D_{\gamma}' - f R_{1\beta}/S_1 + D_{\beta}' + f R_{1\beta}/S_1 \\ &= D_{\gamma}' + D_{\beta}' \end{aligned} \quad (12)$$

Consequently, when the determined beta and gamma doses are added together to obtain the shallow dose, the deep dose over-response (eqn. 11) and beta dose under-response (eqn. 10) compensate each other, resulting in a reliable estimate of the shallow dose. Indeed, the non-penetrating beta sensitivity was defined in eqn. (4) in order to achieve this outcome.

If we define the beta sensitivity  $S_{\beta}$  as,

$$S_{\beta} = R_{1\beta} / D_{\beta} \quad (13)$$

then eqn. (10) becomes

$$D_{\beta}' = D_{\beta} + f (S_{\beta}/S_1) D_{\beta}$$

or,

$$D_{\beta} = D_{\beta}' / (1 - F) \quad (14)$$

where we set  $F = f S_{\beta}/S_1$ . The deep dose  $D_d$  is defined as the gamma dose,  $D_d = D_{\gamma}$ . Using eqn.'s (11), (13), and (14), we get the result,

$$\begin{aligned} D_d &= D_{\gamma}' - D_{\beta}' (S_{\beta}/S_1)(f/(1-(S_{\beta}/S_1)f)) \\ &= D_{\gamma}' - D_{\beta}' F / (1 - F) \end{aligned} \quad (15)$$

Eqn. (15) shows that the deep dose is expected to be underestimated due to subtraction from the chip#1 response of the beta-penetration component included in the total response of chip#2. Note that if there is no penetration effect ( $f = 0$ ), then  $D_d = D_{\gamma}'$ , and the measured gamma dose reliably determines the deep dose. Likewise, eqn. (14) shows that the beta dose is over-estimated due to over-subtraction of the deep dose, and  $D_{\beta} = D_{\beta}'$  if  $f = 0$ .

Equation (15) is of the form,

$$D_d = D_{\gamma'} + C D_{\beta'} \quad (16)$$

where  $C = -F / (1 - F)$ . Equation (14) is of the form

$$D_{\beta} = A D_{\beta'} \quad (17)$$

with  $A = 1/(1 - F)$ . Since the expected relationships between the measured and true doses are linear (eqn.'s 16 and 17), multiple linear regression analysis of a sufficient data base should yield reliable values of the penetration-correction coefficients A and C.

### Multiple Regression Analysis Results

For the purpose of determining the penetration-correction coefficients, we employed a data base consisting of 30 TLD badges exposed to a  $^{137}\text{Cs}$  gamma source at dose levels between 100 and 7500 mrem, 30 badges exposed to a  $^{90}\text{Sr}$  beta source at dose levels between 160 and 7400 mrem, and 28 badges exposed to mixed doses from these sources, at gamma dose levels between 90 and 2100 mrem and beta dose levels between 120 and 2100 mrem. The exposure conditions were identical to those employed in NVLAP proficiency testing [2].

Standard multiple linear regression techniques [3] were used on a microcomputer (Apple IIe) to fit the measured gamma and beta doses (see eqn.'s (6) and (1), resp.) to the delivered doses. The form of the regression equations were:

$$D_{\gamma} = G_0 + G_1 D_{\gamma'} + G_2 D_{\beta'} \quad (18)$$

$$D_{\beta} = B_0 + B_1 D_{\gamma'} + B_2 D_{\beta'} \quad (19)$$

The results of the regression fits are:

$$D_{\gamma} = (0.935 \pm 0.011)D_{\gamma'} - (0.249 \pm 0.017)D_{\beta'} \quad (20)$$

$$D_{\beta} = (1.22 \pm 0.03)D_{\beta'} \quad (21)$$

where the parameters  $G_0$ ,  $B_0$ , and  $B_1$  in eqn.'s (18) and (19) were found to be statistically insignificant.

### Discussion of Regression Results

The gamma and beta dose formulas (eqn.'s 20 and 21) obtained from regression fits have the forms expected from

the analysis leading to eqn.'s (16) and (17). The reason that the coefficient  $G_1 = 0.935 \pm 0.011$  is not equal to 1 is probably due to a calibration drift in the TLD reader.

It is useful to compare the regression coefficients with values that can be calculated from calibration data. From the pure beta exposures of the data base, we find  $\langle f \rangle = 0.221 \pm 0.044$  and  $\langle S\beta/S1 \rangle = 0.731 \pm 0.088$  nC/mrem. Then, from eqn. (16), we get  $C = -0.193 \pm 0.064$ , and from eqn. (17), we get  $A = 1.19 \pm 0.28$ . These values are reasonably close to the regression results of  $-0.249 \pm 0.017$  and  $1.22 \pm 0.03$ , and thus present an approximate alternative method of obtaining the penetration-correction coefficients in the absence of a suitable data base for a regression fit.

From the regression fit eqn.'s (20) and (21), the deep dose would be determined as,

$$D_d = D_\gamma = 0.935 D_{\gamma'} - 0.249 D_{\beta'} \quad (22)$$

and the shallow dose would be

$$D_s = D_\gamma + D_\beta = 0.935 D_{\gamma'} + 0.971 D_{\beta'} \quad (23)$$

As expected from eqn. (12), the shallow dose estimate using regression (eqn. 23) is little different from simply adding the measured gamma ( $D_{\gamma'}$ ) and beta ( $D_{\beta'}$ ) doses.

Figures 2 - 5 show the interpreted deep and shallow doses plotted against delivered doses using the regression algorithm (eqn.'s 22 and 23).

### Performance Tests

Performance testing in a different exposure category is conducted each month on a set of 15 TLD badges sent to an independent testing laboratory. The performance criterion for doses under consideration here, as prescribed in ANSI N13.11, is

$$P = |B| + S \leq 0.50$$

where B and S designate, respectively, the bias and standard deviation of the performance quotient. The performance quotient is defined, for the  $i$ th TLD of the test set, as

$$P_i = [H_i' - H_i] / H_i$$

where  $H_i$  is the delivered dose and  $H_i'$  is the

interpreted dose. The bias is

$$B = \Sigma P_i / n$$

where the sum is extended over all n badges. The standard deviation is

$$S = [ \Sigma (P_i - \langle P \rangle ) / n ]^{1/2}$$

Performance testing using the standard method and the new algorithm (eqn.'s 22 and 23) on monthly test data are compared in Table 1. These results show that the performance quotient P is significantly lower using the regression algorithm in determining both the deep and shallow portions of mixed doses, although the shallow dose due to a pure beta exposure is determined equally well by either method.

### Conclusion

By analyzing the cause of poor performance of a two-element TLD badge in cases when the badge is exposed to energetic beta radiation, an algorithm has been developed to account for beta-penetration effects. If a suitable data base can be obtained, multiple linear regression analysis can be used to determine the correction coefficients in the algorithm. Short of this, the correction coefficients can be calculated from derived beta and gamma dose formulas and using appropriate calibration data from pure beta exposures.

We have demonstrated that performance is significantly improved in mixed beta/gamma exposures. Mixed neutron/gamma results have also been studied in the same manner and we have found that the standard method of determining deep and shallow dose is sufficient in this case.

### References

1. "Criteria for Testing Personnel Dosimetry Performance." ANSI N 13.11 (New York: American National Standards Institute), 1983.
2. LAP Dosimetry Handbook (U.S. Dept. of Commerce, NBS), May, 1985.
3. B. Flynn, Access, July/August, 1983.

Table 1. Performance Test Results.

Test	Shallow			Deep			Algorithm
	B	S	P	B	S	P	
1. Beta	0.004	0.104	0.108				Regr. Std.
	0.015	0.096	0.111				
2. Mixed	0.086	0.088	0.174	0.181	0.071	0.252	Regr. Std.
	0.143	0.096	0.239	0.449	0.136	0.585	
3. Gamma	0.171	0.065	0.236	0.144	0.099	0.243	Regr. Std.
	0.250	0.081	0.331	0.226	0.104	0.330	
4. Beta	0.106	0.133	0.239				Regr. Std.
	0.123	0.126	0.249				
5. Mixed	0.035	0.063	0.098	0.027	0.050	0.077	Regr. Std.
	0.266	0.118	0.384	0.081	0.055	0.136	
6. Gamma	-0.003	0.056	0.059	0.001	0.055	0.056	Regr. Std.
	0.063	0.061	0.124	0.066	0.061	0.127	
7. Beta	0.108	0.108	0.216				Regr. Std.
	0.121	0.091	0.212				
8. Mixed	0.025	0.157	0.182	0.069	0.053	0.122	Regr. Std.
	0.287	0.192	0.479	0.124	0.062	0.186	

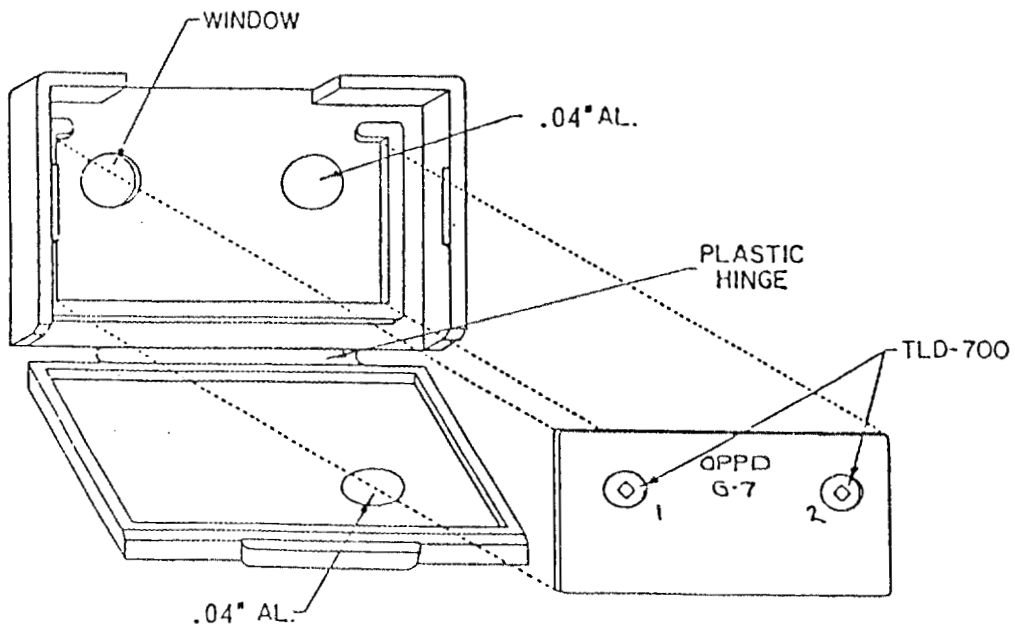


Fig. 1. Configuration of the Gamma/Beta TLD Badge.

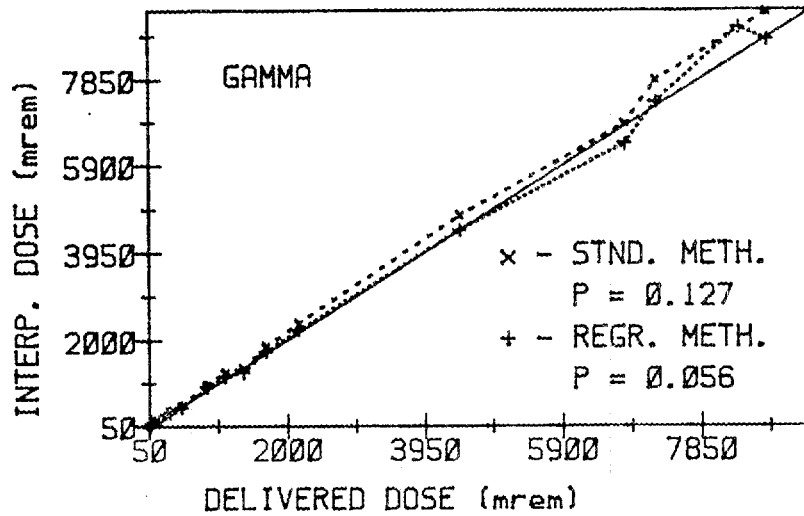


Fig. 2. Interpreted vs Delivered Deep Doses from  $^{137}\text{Cs}$  (Test 6). Lines connecting data points are used only to guide the eye. The solid line corresponds to perfect agreement between interpreted and delivered doses. P is the performance quotient.

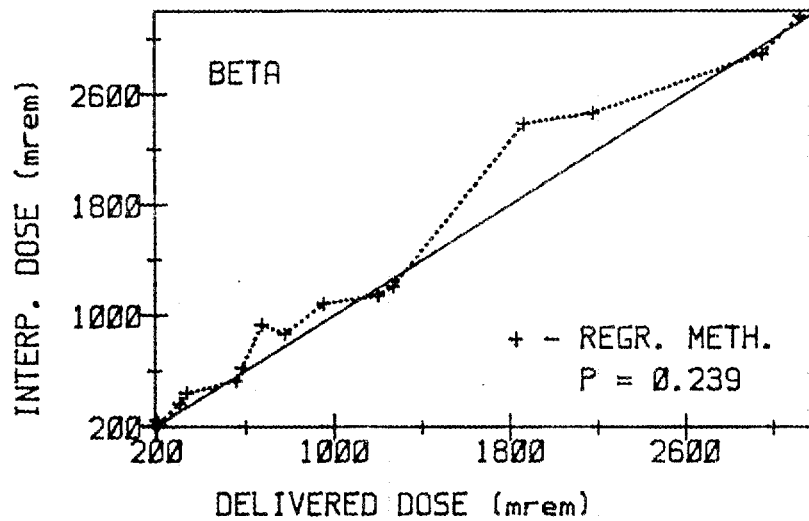


Fig. 3. Interpreted vs Delivered Shallow Doses from  $^{90}\text{Sr}$  (Test 4).

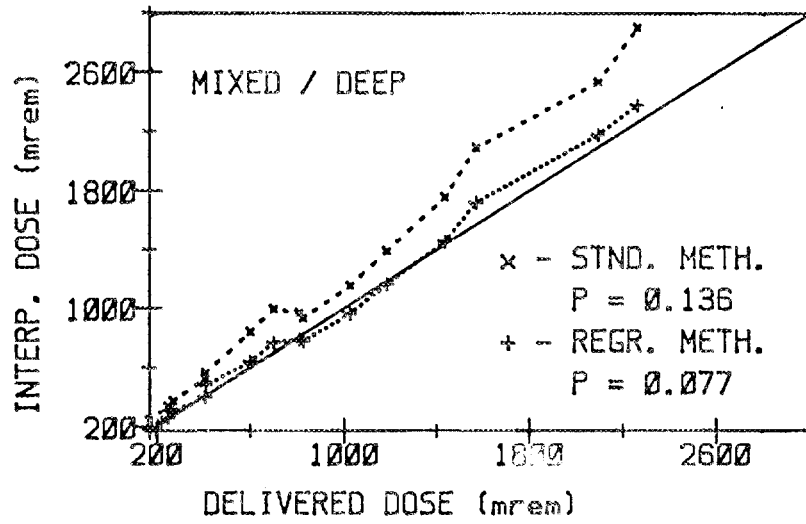


Fig. 4. Interpreted vs Delivered Deep-Dose Component from  $^{137}\text{Cs} + ^{90}\text{Sr}$  (Test 5).

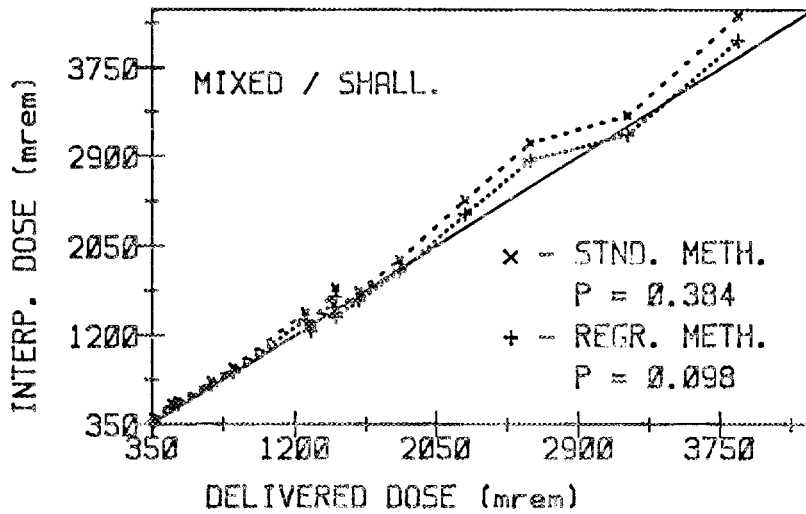


Fig. 5. Interpreted vs Delivered Shallow-Dose Component from  $^{137}\text{Cs} + ^{90}\text{Sr}$  (Test 5).

# THE ANGULAR ENERGY RESPONSE OF PERSONNEL THERMOLUMINESCENT DOSIMETERS

Pao-Shan Weng, Pin-Chieh Hsu\* and Teh-Chao Chen\*  
Institute of Nuclear Science  
Nuclear Science and Technology Development Center\*  
National Tsing Hua University  
Hsinchu 30043, Taiwan, R.O.C.

## ABSTRACT

The angular energy dependence of the response of two commercial thermoluminescent dosimeter systems was investigated. The first personnel dosimeter investigated was the Radi-Guard which is a multi-area LiF (TLD-700) locked in Teflon matrix and incorporated with a PB-2 holder developed by Teledyne Isotopes. The second one was the BG-7 which is comprised of two LiF (TLD-700) chips developed by Harshaw, but the TH-2 holder was fabricated at National Tsing Hua University. The angle of incidence was varied from perpendicular to parallel for  $^{90}\text{Sr}$ - $^{90}\text{Y}$   $\beta$  radiation,  $^{241}\text{Am}$  and  $^{60}\text{Co}$   $\gamma$  radiation. Experimental results are presented and discussed.

## INTRODUCTION

There are two commercial thermoluminescent dosimeter (TLD) systems available at National Tsing Hua University (NTHU) for personnel monitoring. They are the Radi-Guard dosimeter (RGD) from Teledyne Isotopes and the BG-7 from Harshaw. These two U.S. manufactured systems have long been used for both routine and research purposes.

The TLDs mentioned above are calibrated with perpendicular incidence of various types of radiation. Algorithms for computation of dose equivalent are developed based on the response of TLDs to perpendicular irradiation. The response of personnel TLDs, in fact, varies with angle of incidence, energy and irradiation type. In actual case the field conditions are much more complicated. The accuracy of the reported dose has therefore imposed some limitation.

The TLD irradiation under non-perpendicular radiation incidence is thus required.<sup>1</sup> The purpose of the study reported here is to characterize the angular response of two commercially available and widely used personnel TLDs in Taiwan for  $\beta$ ,  $\gamma$ , and  $\beta$ - $\gamma$  mixed fields.

## DOSIMETER SYSTEM

### 1. Radi-Guard Dosimeter

The multi-area TLD developed by Teledyne Isotopes has four main readout and four backup areas that can be read on the same company's TLD Model 8300 manual reader, which was used in this experiment. The RGD measures 31.8 mm x 44.4 mm x 0.40 mm. The standard phosphor for  $\beta$ - $\gamma$  personnel monitoring is  $^7\text{LiF}$  locked in Teflon matrix.<sup>2</sup>

The four main readout areas of the dosimeters are for normal use and four backup areas provide dose confirmation when required. If the readout of a main area has failed or an unexpected reading is found, the backup area may be read with the same resultant information supplemented by a glow curve output which may be examined for anomalies.

The badge (PB 2) for the RGD used in this experiment is made of plastic with the following filter array on both the front and back of the badge: (1) 2 mm plastic, equivalent to 2 kg/m<sup>2</sup>, (2) open window without any filter, and the black pouch which holds the RGD is equivalent to 0.0528 kg/m<sup>2</sup>, (3) 1 mm plastic plus 2 mm Al, equivalent to 7 kg/m<sup>2</sup>, and (4) 1 mm plastic, 1 mm Al, and 1 mm Cu, equivalent to 11 kg/m<sup>2</sup>.

The four backup areas have the same filters as the four main readout areas and are shown in Fig. 1. The filter array provides for a primary and backup readout of (1) penetrating exposure such as  $\gamma$  radiation in area 1, (2) skin exposure such as  $\beta$  radiation in area 2 (net readout difference between areas 1 and 2), and (3) energies of x,  $\gamma$ , and  $\beta$  radiation (ratio of areas 2, 3 and 4 to area 1).

The 8300 reader is engineered to read out eight independent areas from one RGD card. The card is heated in such a way that the total light output

from each area is integrated separately.

## 2. BG-7

The BG-7 card consists of two  ${}^7\text{LiF}$  (TLD-700) chips with nominal size of 3.2 mm x 3.2 mm x 0.38 mm (TLD 1) and 3.3 mm x 3.2 mm x 0.89 mm (TLD 2), respectively as shown in Fig. 2. The two TLD chips are bonded into Teflon film of 0.063 mm and mounted on an aluminum plate.

The TH-2 badge fabricated at NTHU is used together with the BG-7 card for personnel monitoring.<sup>3</sup> This badge has two parts. One is an open-window area which is used with the thin TLD 1 for penetrating dose evaluation. The other part consists of 0.4 mm PVC which is equivalent to 4.76 kg/m<sup>2</sup>. This PVC covered wall is used with the thick TLD 2 for penetrating dose evaluation. Filters can be added over TLD 2 to assure  $\beta$  stopping and to correct the over-exposure to low energy photons. The TH-2 badge is shown in Fig. 2.

The TL response was analyzed with a Harshaw Model 2000 B and Model 2271 automated TLD system. A linear heating rate of 20° C/s was used. The TL response was integrated up to 300° C. In order to minimize the fading effect, the TLD cards were read about 24 h after irradiation in this study. The detection limit was found about 0.1 mGy  $\pm$  30%.

## EXPERIMENTAL

The radiation sources used in this experiment can be categorized as  $\beta$  and  $\gamma$  radiations. They are listed in Table 1.

Table 1 Sources of radiation

Source	Type of radiation	Activity (MBq)	Max. and ave. $\beta$ energy (MeV)	Gamma energy (MeV)	Events per disintegration (%)
${}^{90}\text{Sr}-{}^{90}\text{Y}$	$\beta$	1850	0.546 ( ${}^{90}\text{Sr}$ )		100
			0.20 ( ${}^{90}\text{Sr}$ )		100
			2.28 ( ${}^{90}\text{Y}$ )		100
			0.93 ( ${}^{90}\text{Y}$ )		100
${}^{241}\text{Am}$	$\gamma$	3700		0.059	36
${}^{60}\text{Co}$	$\gamma$	3552		1.17	100
				1.33	100

The  ${}^{90}\text{Sr}-{}^{90}\text{Y}$  source was calibrated by the Physikalisch-Technische Bundesanstalt (PTB), Federal Republic of Germany. Its average energy can be taken as 0.8 MeV. The average  $\gamma$  energy of  ${}^{60}\text{Co}$  can be taken as 1.25 MeV.

## RESULTS AND DISCUSSION

The responses of bare TL elements (without the badge case) for  ${}^{90}\text{Sr}-{}^{90}\text{Y}$  vs. angle of incidence are shown in Fig. 4. The data reported are normalized to the response of the TL element where the  $\beta$  radiation is perpendicular. The response of the four elements decreases as angle of incidence increases as expected.

The normalized angular responses for the 59.5 keV  $\gamma$  radiation from  $^{241}\text{Am}$  for the above described TL elements excluding the TLD-700 chip without the badge case are shown in Fig. 5. The responses are fairly well behaved in this irradiation except near  $\pm 90^\circ$  where nearly all responses sharply decrease.

The effect of the badge case added will be discussed as below.

1. *TH-2 badge case.* The TL response of BG-7 card with TH-2 badge case, where chip 1 is with open window and chip 2 with PVC filter, for  $^{90}\text{Sr}$ - $^{90}\text{Y}$  vs. angle of incidence is shown in Fig. 6. The response of chip 2, as compared with chip 1, decreases as angle of incidence increases. This is attributed to the PVC filter and probably the thickness of chip 2. Similar irradiations were performed for the  $\gamma$  radiations from  $^{241}\text{Am}$  and  $^{60}\text{Co}$  respectively for the above described elements with TH-2 badge case; the responses are fairly well behaved in these irradiations except near  $\pm 90^\circ$  where all responses sharply decrease as shown in Figs. 7 and 8.

2. *PB-2 badge case.* The TL responses for four areas of RGD with PB-2 badge case for  $^{241}\text{Am}$   $\gamma$  radiation vs. angle of incidence are shown in Fig. 10. Unusual behavior was found for the area 4 with heavy filter. At  $\pm 90^\circ$  the large responses of area 4 were observed because the perpendicular filtration was not eclipsing the radiation source. Similar irradiations were performed for  $^{60}\text{Co}$   $\gamma$  radiation and the responses are fairly behaved as shown in Fig. 11.

The 0.4 m x 0.4 m x 0.12 m acrylic phantom used in the irradiation also created some effects on the TL response. It is recognized that the backscatter from a phantom provides a contribution to reported dose. As the phantom is turned to present its surface more nearly parallel to the incident radiation secondary electrons are scattered into the TL element increasing the electrons' contribution to reported dose. The TL responses with an acrylic phantom added are shown in Fig. 12. They are fairly well behaved because of the high-energy  $\gamma$  radiation from  $^{60}\text{Co}$  except BG-7 chip 2 due to its thickness and distance to the edge of the acrylic phantom.

Finally it comes to the mixed field radiation. Two mixed fields were provided:  $^{90}\text{Sr}$ - $^{90}\text{Y}$  and  $^{60}\text{Co}$  mixed field and  $^{90}\text{Sr}$ - $^{90}\text{Y}$  and  $^{241}\text{Am}$  mixed field. The former is a  $\beta$  field with high energy  $\gamma$  while the latter is with low energy  $\gamma$ . Both Figs. 13 and 14 show the TL responses. As expected the BG-7 chip 2 with PVC filter has lower TL response except at  $\pm 90^\circ$ . The thicker chip 2 has higher response for high energy  $\gamma$  than the thinner chip 1 at larger angle of incidence. The larger response for low energy  $\gamma$  observed at area 4 of RGD with heavy filter at large angles of incidence is due to the eclipse of the filter to the parallel radiation beam.

To eliminate the angular response, the response ratios of chip 1 to chip 2 of BG-7 with TH-2 badge case were investigated. For both high and low energy  $\gamma$  radiations, angular independence can be achieved using the response ratios described above as shown in curves a, b and c of Fig. 15. For mixed field radiation, high energy  $\gamma$  component causes the response ratios to decrease at larger incidence angles as shown in curve d of Fig. 15.

As the new operational quantities proposed by the International Commission on Radiation Units and Measurements such as the directional dose equivalent, penetrating and superficial individual dose equivalents are to

be applied in individual monitoring, the problem of angular response of personnel dosimeters needs further study.<sup>4,5</sup>

#### ACKNOWLEDGMENTS

Financial support from the Atomic Energy Council of the Executive Yuan is much appreciated.

#### REFERENCES

1. American National Standard Institute, *Criteria for Testing Personnel Dosimetry Performance*, ANSI N13.11, New York (1983)
2. P.C.Hsu and P.S.Weng, "Test of Teledyne Multi-area TLD for Mixed Beta-Gamma Personnel Monitoring," *Radiat. Protect. Dosim.* 14, 59 (1986)
3. T.K.Wang, P.C.Hsu and T.C.Chen, "A Personnel Dosimeter Using BG-7 and TH-2 Nadge for Beta and Gamma Dosimetry," *Radiat. Protec. Dosim.* 22, 49 (1988)
4. International Commission on Radiation Units and Measurements, *Determination of Dose Equivalents Resulting from External Radiation Sources*, ICRU Report 39, Bethesda, Maryland, U.S.A. (1985)
5. C.W.King, "The Angular Energy Response of a Personnel Dosimeter," 32nd Annual Meeting of Health Physics Society, Salt Lake City, Utah, U.S.A. July 5-9, 1987

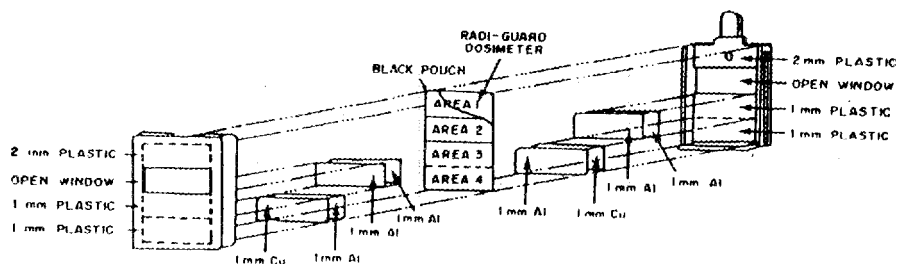


Fig.1 The multi-area TLD and the PB-2 holder.

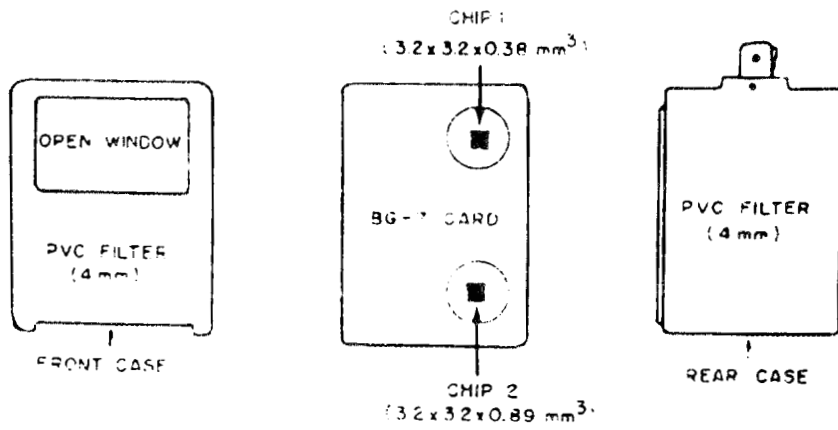


Fig.2 The BG-7 card and the TH-2 holder

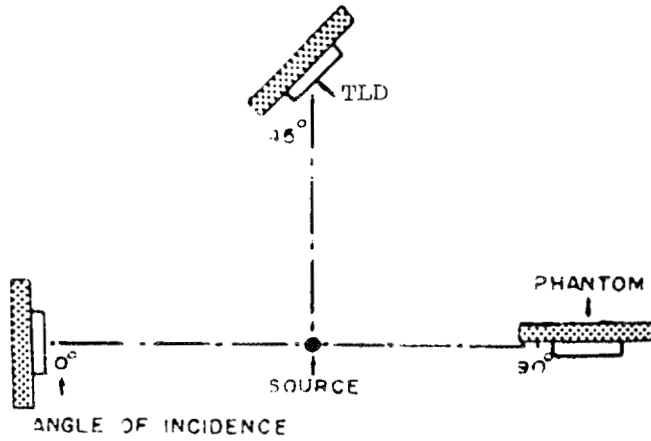


Fig.3 The irradiation array

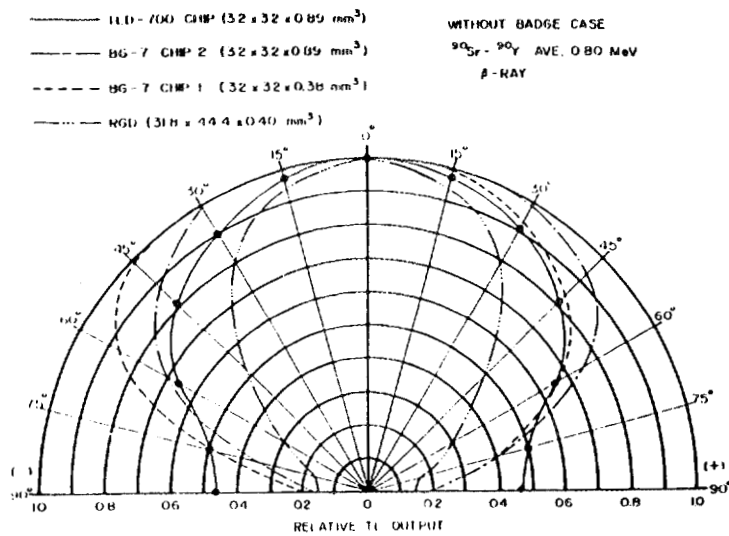


Fig.4 Angular dependence of TLD chips due to beta irradiation.

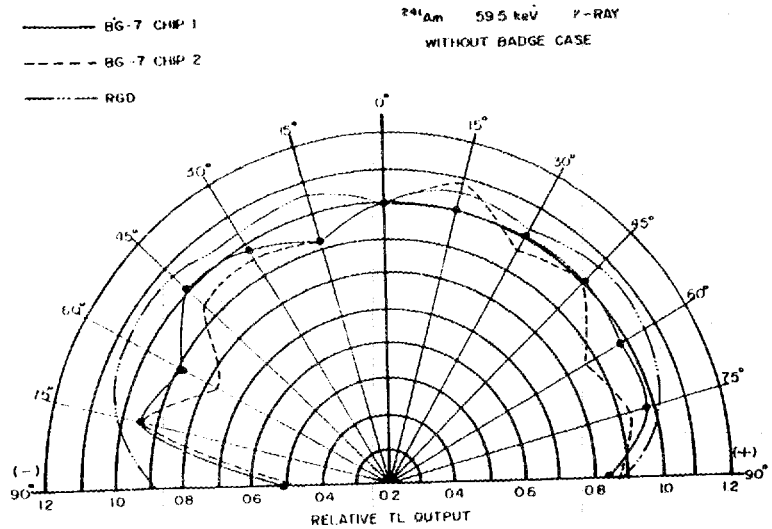


Fig. 5 Angular dependence of TL chips due to low energy gamma irradiation.

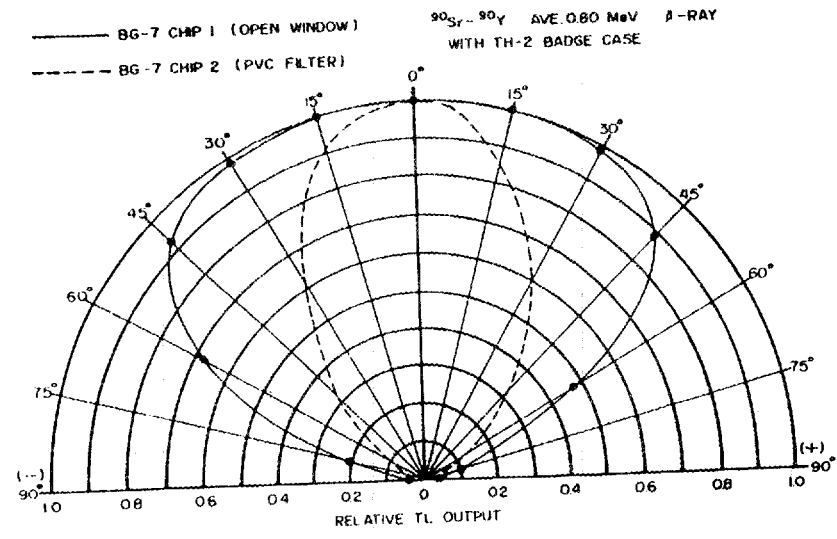


Fig. 6 Angular dependence of BG-7 with TH-2 holder due to beta irradiation.

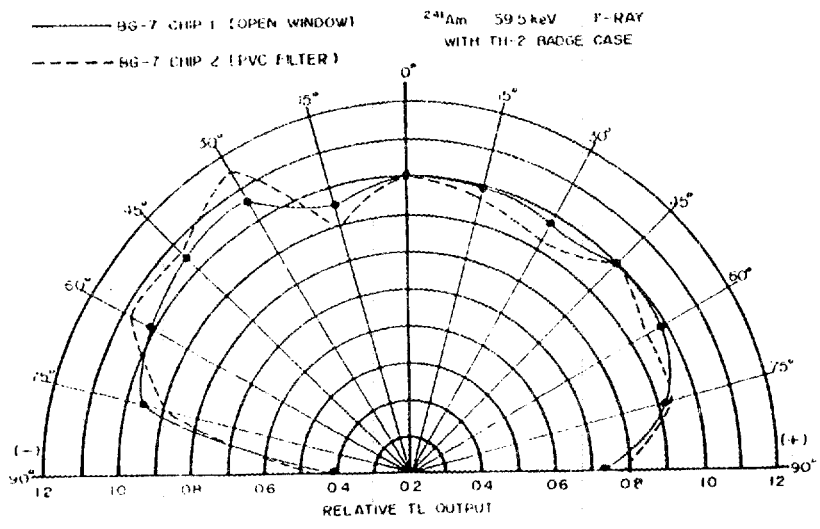


Fig. 7 Angular dependence of BG-7 with TH-2 holder due to low energy gamma irradiation.

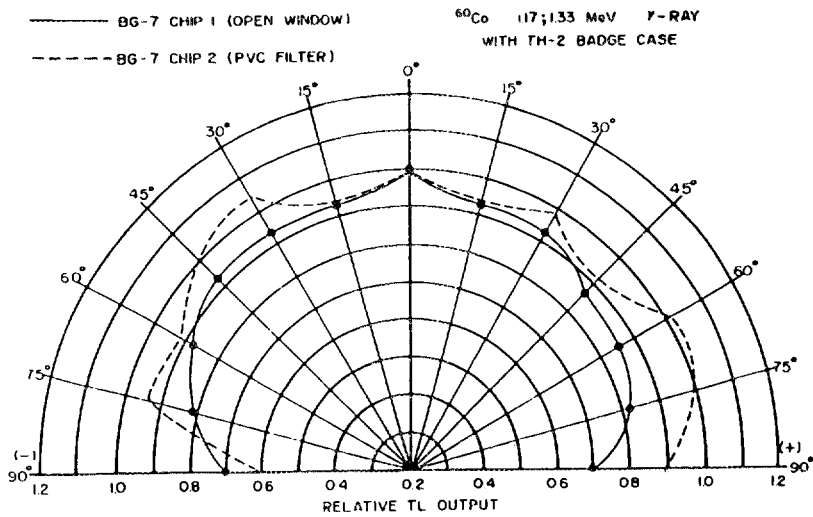


Fig. 8 Angular dependence of BG-7 with TH-2 holder due to high energy gamma irradiation.

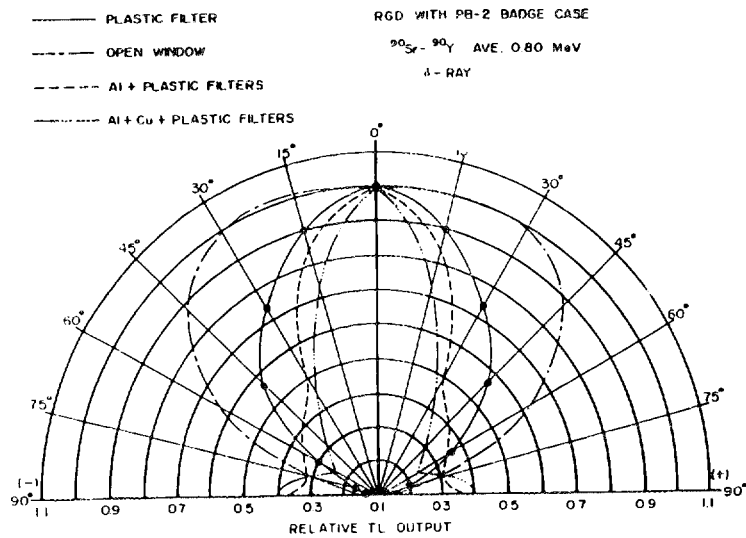


Fig. 9 Angular dependence of RGD with PB-2 holder due to beta irradiation.

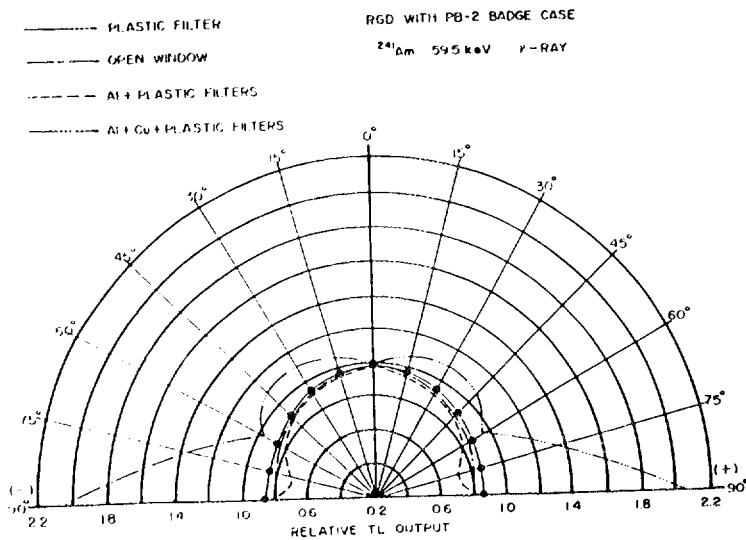


Fig. 10 Angular dependence of RGD with PB-2 holder due to low energy gamma irradiation.

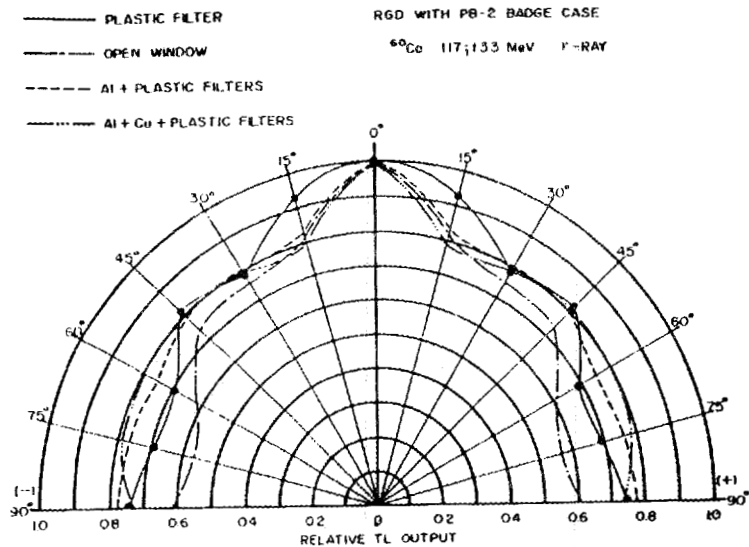


Fig.11 Angular dependence of RGD with PB-2 holder due to high energy gamma irradiation.

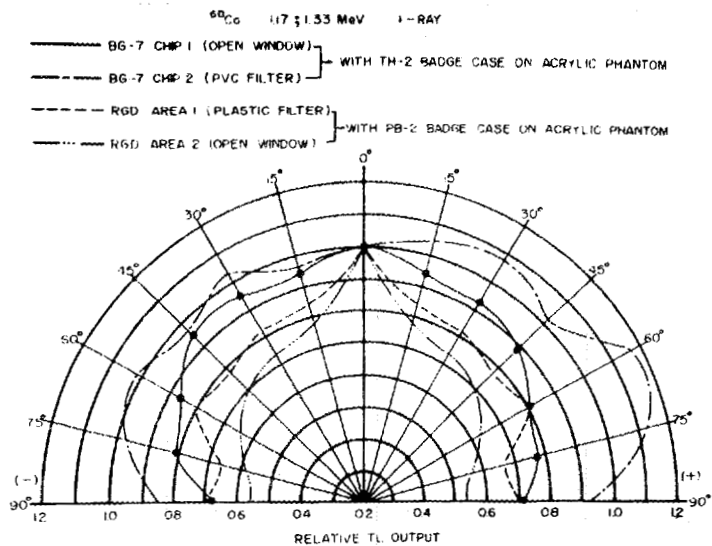


Fig.12 Angular dependence of two personal dosimeters with phantom due to  $^{60}\text{Co}$  gamma radiation.

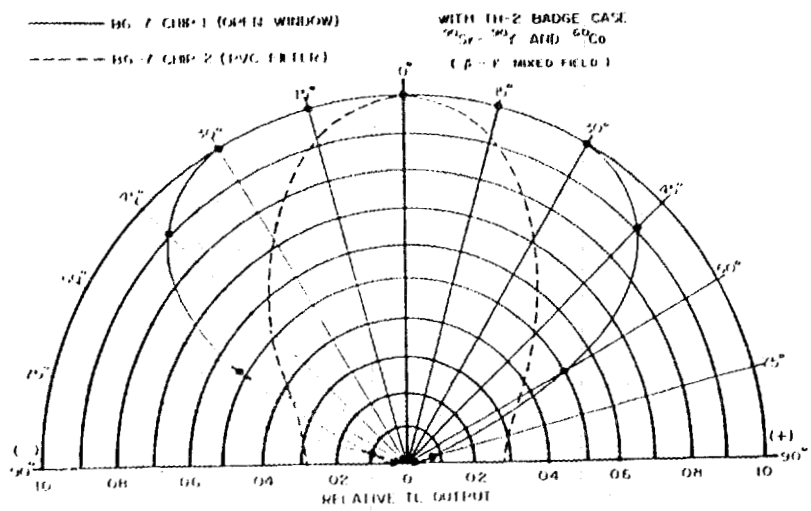


Fig.13 Angular dependence of BG-7 dosimeter due to beta-gamma mixed field irradiation with high energy gamma component.

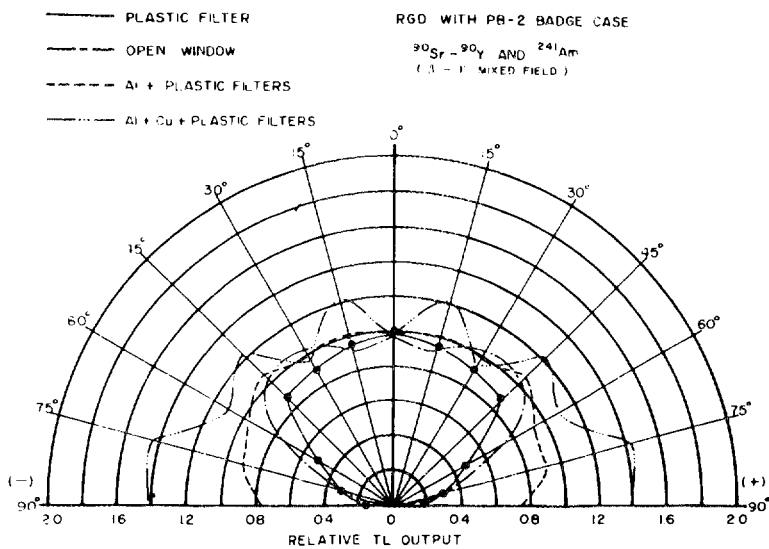


Fig.14 Angular dependence of multi-area dosimeter due to beta-gamma mixed field irradiation with low energy gamma component.

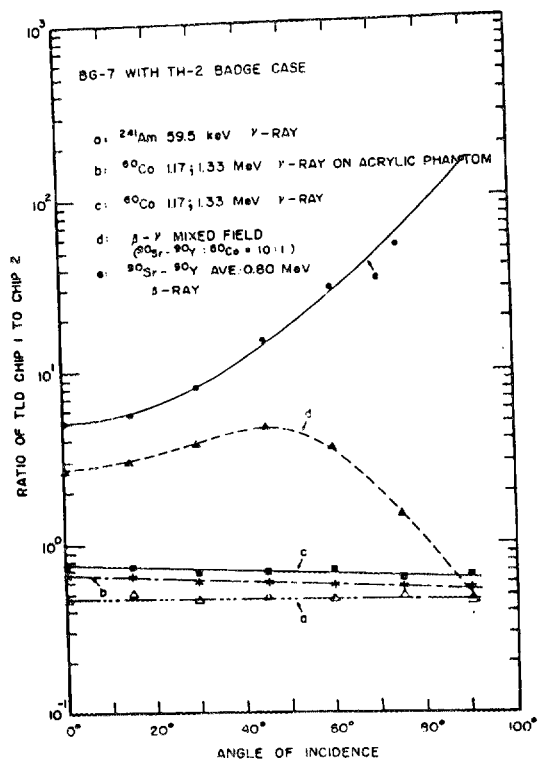


Fig.15 TL ratios versus angles of incidence of BG-7 dosimeter due to beta, gamma, and mixed field irradiation.

LINEARITY OF AND MINIMUM MEASURABLE DOSE FOR  $\text{Li}_2\text{B}_4\text{O}_7:\text{Cu}$  AND  $\text{CaSO}_4:\text{Tm}$   
TL-ELEMENTS USED IN A PERSONNEL/ENVIRONMENTAL DOSIMETER

Jeffrey Hoffman, Barak Ben Shachar\* and Gary L. Catchen  
(Department of Nuclear Engineering, The Pennsylvania State  
University, University Park, PA 16802).

\*Permanent address: Nuclear Research Center,  
Beer-Sheva, 84190, Israel.

Abstract

The TL-dose response was measured for  $\text{Li}_2\text{B}_4\text{O}_7:\text{Cu}$  and  $\text{CaSO}_4:\text{Tm}$  phosphors, in the useful range of personnel and environmental dosimetry (0.005-10 mGy). The relative standard deviations and the corresponding doses were fitted to a semiempirical expression, from which the minimum measurable doses were derived.

## I. INTRODUCTION

Panasonic UD-802 dosimeters, which are commonly used for personnel and environmental dosimetry, contain two  $\text{Li}_2\text{B}_4\text{O}_7:\text{Cu}$  and two  $\text{CaSO}_4:\text{Tm}$  phosphors. As Schulman et al.<sup>1</sup> initially demonstrated, the lithium borate elements are useful for personnel dosimetry because they have nearly tissue-equivalent responses, i.e.,  $Z_{\text{eff}}=7.3$ .<sup>1</sup> Although the phosphor,  $\text{CaSO}_4:\text{Mn}$ , is the most sensitive TL-material,<sup>2</sup> its TL-response is subject to rapid fading. But, Tm-doped calcium sulfate, which meets essentially all of Schulman's<sup>3</sup> requirements, shows little fading and is reasonably sensitive. Because Ca-based TL-materials are not tissue equivalent, they are not generally used for personnel dosimetry. Their sensitivity, however, makes them suitable for low-dose environmental measurements, and their inherently poor energy response can be improved by using metal absorbers. Since detailed information about the linearity of the dose-response over the useful range (0.005-10mGy) and the associated minimum measurable doses (MMD) were not available for the phosphors,  $\text{Li}_2\text{B}_4\text{O}_7:\text{Cu}$  and  $\text{CaSO}_4:\text{Tm}$ , we performed a series of measurements to determine the MMDs for each phosphor via the relative errors.

## II. RESULTS

Five UD-802 dosimeters were irradiated (using a  $^{137}\text{Cs}/^{137}\text{Ba}$  source), read, and annealed three times for each of 10 different doses. For each phosphor and dose, the mean and relative error (standard deviation divided by the mean) were calculated for a sample of 30 responses (2 phosphors x 5 dosimeters x 3 irradiations). Figure 1 shows the average TL-derived dose as a function of the primary-calibration-based dose. The derived doses were obtained by first converting the first and second readings (on the Panasonic Model 702 reader) to dose via individual element correction factors and global calibration factors and then subtracting the second reading from the first. For the lithium borate phosphor, the second readings tended to be much larger, which may be in part responsible for the larger relative errors reported below. Figure 2 shows the relative error, which is the standard deviation of 30 responses divided by the mean, as a function of the dose. To determine the MMD, we used the expression developed by Zarand and Polgar:<sup>4,5</sup>

$$\frac{\sigma}{D} = \left( \frac{A^2}{D^2} + \frac{1}{KD} + B^2 \right)^{1/2} \quad (1)$$

in which  $\sigma$  is the standard deviation and  $D$  is the dose. The parameters,  $A$ ,  $K$ , and  $B$ , were determined by direct linear regression. The MMD is defined as the dose at which the reproducibility,  $(\sigma/D) = 0.2$ . For the phosphor,  $\text{CaSO}_4:\text{Tm}$ , the MMD occurred at approximately 0.003 mGy (0.3 mrad). This result is in agreement with the results of Yamashita.<sup>6</sup> For the phosphor,  $\text{Li}_2\text{B}_4\text{O}_7:\text{Cu}$ , the MMD is in the range of 0.01-0.02 mGy (1-2 mrad). But, since the relative errors are

based on 30 measurements, the MMDs are rather small. For more typical sample sizes, we would expect the MMD to increase. To estimate the effect of sample size, we selected several subsets of sample size four from the sample of 30. A similar analysis showed that the MMDs increased by approximately a factor of 1.5. This result is interesting because the change in MMD with sample size is relatively small, that is, the change is not as large as what would be predicted by normal distribution theory.

### III. CONCLUSIONS

The response of the lithium borate phosphor is linear in the range from 0.01 to 10 mGy, and it can be used accurately for doses as low as 0.02 mGy. Similarly, the response of the calcium sulfate phosphor is linear in the range from 0.005 to 10 mGy, and it can be used accurately for doses as low as 0.003 mGy. This result is consistent with the application of this phosphor to low-dose environmental measurements.

### IV. ACKNOWLEDGEMENTS

We thank the Pennsylvania Power and Light Co., the Panasonic Industrial Co., and the Department of Nuclear Engineering for financial support for this project.

### V. REFERENCES

1. Schulman, J. H., Kirk, R. D., and West, E. J.: "Use of lithium borate for thermoluminescent dosimetry," CONF-650637, Proc. Int. Conf. on Luminescence Dosimetry, Stanford University, 1965.
2. Watanabe, K.: "Properties of  $\text{CaSO}_4:\text{Mn}$  Phosphor Under Vacuum Ultraviolet Excitation," Phys. Rev., 83, 785-797 (1951).
3. Schulman, J. H.: "Luminescence Dosimetry," (Edited by F. H. Attix), Part 1,3. USAEC, 1967.
4. Zarand, P. and Polgar, I., Nucl. Instrum. Meth., 205, 525-529 (1983).
5. Zarand, P. and Polgar, I., Nucl. Instrum. Meth., 222, 567-573 (1984).
6. Yamashita, T., Nada, N., Onishi, H., and Kitamura, S., Health Physics, 21, 295-300 (1971).

FIGURE 2 A : RELATIVE S.D. vs. DOSE for Li2B4O7:Cu

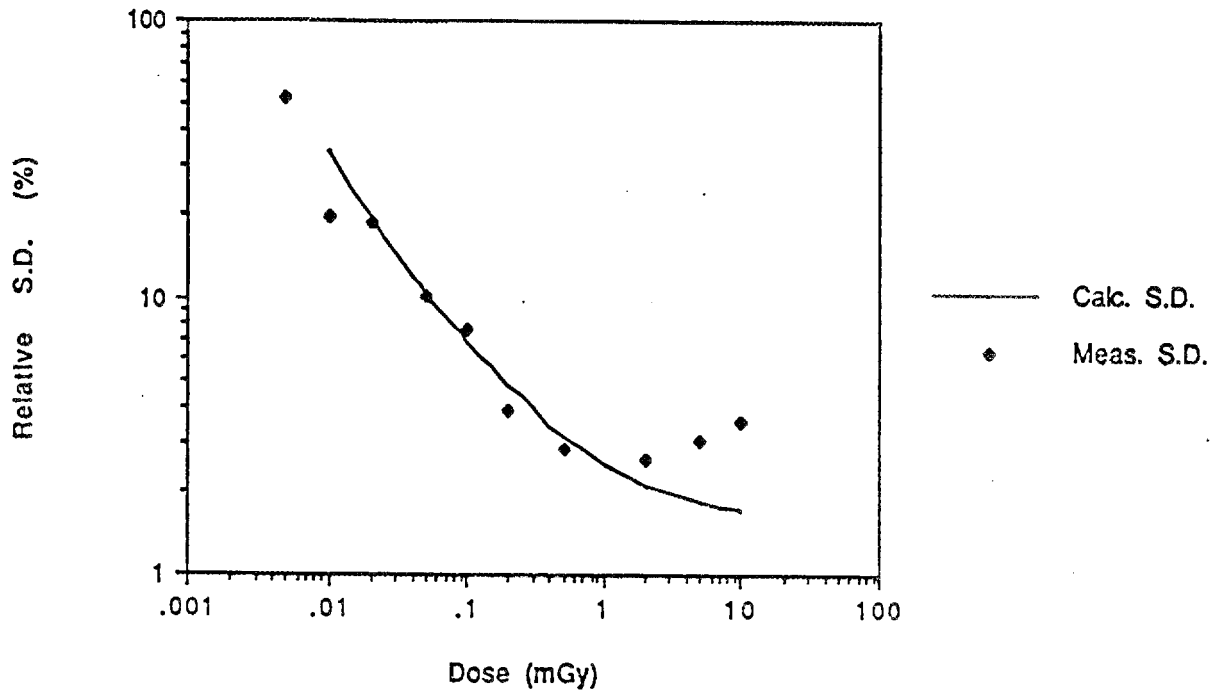


FIGURE 2 B : RELATIVE S.D. vs. DOSE for CaSO4:Tm

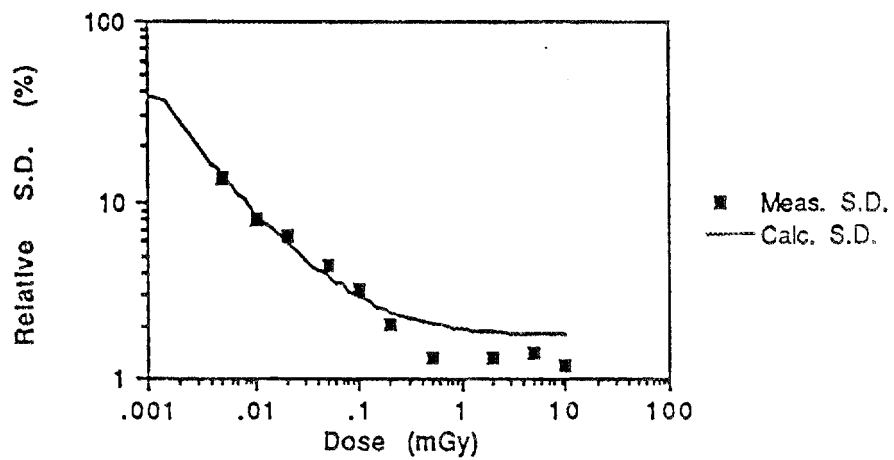


FIGURE 1 A : TL - DOSE RESPONSE of  $\text{Li}_2\text{B}_4\text{O}_7:\text{Cu}$ .

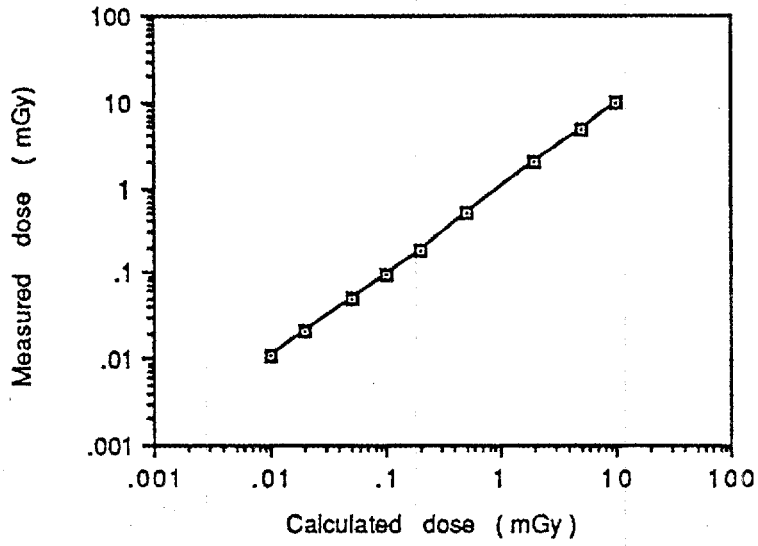
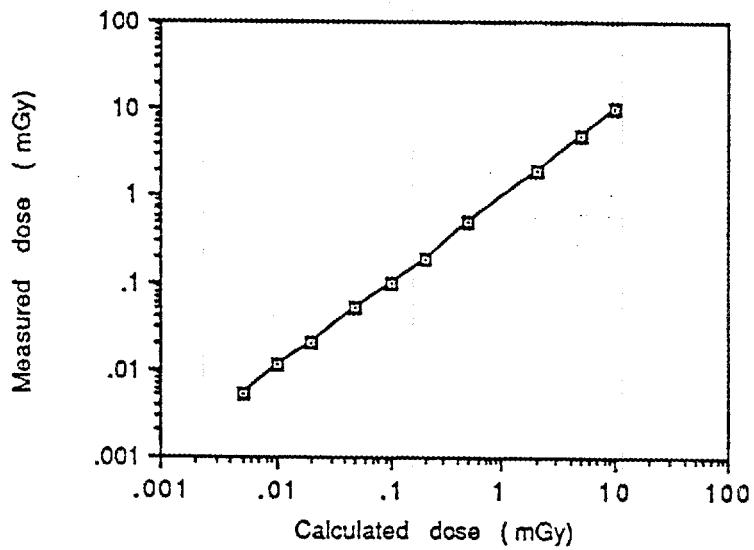


FIGURE 1 B : TL - DOSE RESPONSE of  $\text{CaSO}_4:\text{Tm}$ .



DOSE DETERMINATION ALGORITHMS FOR A NEARLY TISSUE EQUIVALENT  
MULTI-ELEMENT THERMOLUMINESCENT DOSIMETER

M. Moscovitch, J. Chamberlain and K. J. Velbeck  
Harshaw  
Crystal and Electronic Products  
6801 Cochran Rd.  
Solon, Ohio 44139

ABSTRACT

In a continuing effort to develop dosimetric systems that will enable reliable interpretation of dosimeter readings in terms of the absorbed dose or dose-equivalent, a new multi-element TL dosimeter assembly for Beta and Gamma dose monitoring has been designed. The radiation-sensitive volumes are four LiF-TLD elements, each covered by its own unique filter. For media-matching, care has been taken to employ nearly tissue equivalent filters of thicknesses of 1000 mg/cm<sup>2</sup> and 300 mg/cm<sup>2</sup> for deep dose and dose to the lens-of-the-eye measurements respectively. Only one metal filter (Cu) is employed to provide low energy photon discrimination. A Thin TL element (0.09 mm thick) is located behind an "open window" designed to improve the energy under-response to low energy beta rays and to provide closer estimate of the shallow dose equivalent.

The deep and shallow dose equivalents are derived from the correlation of the response of the various TL elements to the above quantities through computations based on previously defined relationships obtained from experimental results. The theoretical formalization for the dose calculation algorithms is described in detail, and provides a useful methodology which can be applied to different "tissue-equivalent" dosimeter assemblies. Experimental data has been obtained by performing irradiation according to the specifications established by DOELAP, using 27 types of pure and mixed radiation fields including Cs-137 gamma rays, low energy photons down to 20 keV, Sr/Y-90, Uranium, and Tl-204 beta particles.

Copyright, Harshaw/Filtrol, 1988

\* Patent applied for

## 1. INTRODUCTION

Although the need for improving the quality of personnel dosimetry systems is well recognized by the health physics community members and by the various authorities, there is no overall agreement about techniques and methodology which are required to achieve this goal. Some of the inconsistencies between the different dosimetry programs and systems have been recently demonstrated in a pilot performance test conducted by the Department of Energy Laboratory Accreditation Program (DOELAP) where as a group, the participants met the test criteria in only 38% of the tested categories<sup>(1)</sup>. All the participants experienced difficulties in any category that required low energy photons or mixtures of low energy photons with beta fields. The main reasons for the large variations in the test results and the poor performance in some of the test categories were identified as follows: 1) lack of evaluation and preparation of the system; 2) calibration problems; and, 3) dose calculation algorithms and dosimeters not designed to accommodate a wide range of radiation types and energies. This paper presents an improved multi-element TL dosimeter together with dose calculation algorithms which are designed to resolve those problems and to meet the ever growing demands of modern personnel dosimetry and obtain DOELAP<sup>(2)</sup> accreditation. In this paper we present the philosophy behind the dosimeter design, the dose calculation algorithm formalism, a comprehensive step-by-step methodology, and the results from a detailed experimental study that was conducted to calibrate and characterize this system.

## 2. DOSIMETER DESCRIPTION

The dosimeter is composed of two parts, a TLD card and a holder which carries the radiation modifying filters. The TLD card consists of four LiF:Mg,Ti TL elements of different thicknesses and compositions mounted between two PTFE sheets (0.0635 mm thick) on an aluminum substrate. Each TL element is covered by its own unique filter which provides different radiation absorption thicknesses to allow dose estimation for the various organs in risk. The element in position 3 is a thin (0.09 mm) solid TLD-700 chip protected from the environment by a thin, aluminized Mylar sheet (0.0625 mm thick). The shallow dose estimation is based on the response of this element; and, as a result of its reduced thickness (a factor of 10 thinner than the standard 3x3x0.9 mm TLD ribbons), the energy-dependent response to the low energy beta rays is improved. The elements in positions 1 and 2 are a thicker (0.4 mm) TLD-700, covered by a 1000 mg/cm<sup>2</sup> tissue equivalent filter and by a Copper filter respectively. The deep dose estimation is based on the response of element 1. The ability of the dosimeter to act as a crude energy spectrometer for low energy photons is based on the variation with energy of the photon attenuation characteristics of the Copper filter located in position 2. Position 4 is occupied by a neutron sensitive TL element, TLD-600, shielded by a tissue equivalent filter of 300 mg/cm<sup>2</sup> thickness, to enable dose estimation to the lens of the eye and to measure neutron dose in the absence of

thermal neutrons. Since the scope of this study was limited to deep and shallow dose estimation in the presence of mixed photon beta fields, the response of the dosimeter in neutron fields and the dose estimation to the lens of the eye are not discussed here. This configuration is a modification of the dosimeter described by Storm et al,<sup>(3)</sup> and which has been used since 1982 in the Los Alamos National Laboratory (LANL) Personnel Dosimetry Program. Care has been taken to use nearly tissue equivalent TL elements and tissue equivalent filters. A plastic filtration of 1000 mg/cm<sup>2</sup> for the deep dose estimation was preferred over lead filters, which are commonly used<sup>(4)</sup>. Lead filters introduce severe mismatch<sup>(5)</sup> between the sensitive dosimetric material (LiF) and the filter medium (Pb), which complicates the dose reading interpretation and reduces the TL signal per unit dose for low energy photons due to the strong attenuation of low energy photons in Lead. Those difficulties are further demonstrated in reference 6.

### 3. EXPERIMENTAL

The TL measurements were performed using the Model 8800 Automatic TLD Card Reader developed by Harshaw. The Model 8800 utilizes a non-contact heating technique based on pre-purified hot nitrogen gas. However, unlike any other hot gas TLD reader known to date, the Model 8800 employs a programmable, precisely controlled, linear time temperature profile. One of the most important requirements of a TLD reader is that the heating of the dosimeter elements should be reproducible. The reason is that the amount of radiation-induced Thermoluminescence is dependent on the thermal history of the material as well as on the heating rate during readout. A fully controlled heating cycle is therefore important, especially for low dose measurements. Usually a controlled heating cycle is accomplished by contact ohmic heating of the TL element. The contact heating method has some disadvantages, such as relatively short dosimeter life and large infrared signals associated with the heating element. The most important advantage of the contact heating method is its ability to continuously control the heating cycle using various feedback techniques. The "Time Temperature Controlled" non-contact heating technique applied in the Model 8800 shares this advantage of the contact heating approach without sharing its disadvantages.

For this series of tests, glow curves were recorded to a maximum temperature of 300°C at a heating rate of 25°C/sec. No high temperature annealing was applied and the preparation of the dosimeters prior to irradiation consisted of subjecting each dosimeter to one readout cycle through the reader. The residual TL signals using this reader anneal technique were found to be less than 0.5% at the Sr/Y-90 one rad level. All the irradiations to determine the Element Correction Coefficients and the Reader Calibration Factor were performed in the reader using an internal 0.5 mCi Sr/Y-90 irradiator with an automatic shutter. The reproducibility of the irradiator was found to be within 1% (one

standard deviation of 10 repeated irradiations) at the Sr/Y-90 500 mrad level. Also, no significant changes in the glow curve structure were observed due to repeated irradiation and readout. The TL signal is accumulated simultaneously from four TL elements via the charge integration technique using four thermoelectrically cooled Hamamatsu photomultipliers (Bialkali photocathode).

#### 4. THE ELEMENT CORRECTION COEFFICIENT METHOD

Since not all TL elements can be manufactured to have exactly the same TL efficiency, where TL efficiency (TLE) is defined as the emitted TL light intensity per unit of absorbed dose, individual Element Correction Coefficients (ECCs) have been applied. The method of ECC generation is based on relating the TL efficiency of each TL element of the entire dosimeter population (Field Dosimeters) to the mean TL efficiency of a small subset of this population which is used only for calibration purpose (Calibration Dosimeters). When the ECC is applied to the response of each individual TL element of any of the Field or the Calibration Dosimeters, its TL efficiency is virtually identical to the mean value of the Calibration Dosimeters group. The Element Correction Coefficient,  $ECC_{ij}$ , for element  $i$  in calibration card  $j$  is given by:

$$ECC_{ij} = \langle Q \rangle_i / Q_{ij} \quad (1)$$

when  $\langle Q \rangle_i$  is the average TL response for element  $i$  of the calibration card population and  $Q_{ij}$  is the response of TL element  $i$  in card  $j$ . Similar to (1), we define the Element Correction Coefficient  $ecc_{ij}$  for Field Cards as follows:

$$ecc_{ij} = \langle Q \rangle_i / q_{ij} \quad (2)$$

when  $q_{ij}$  is the TL response of element  $i$  in a field card  $j$ . For a detailed discussion of this concept see reference 7. Throughout this process, the inherent sensitivity of the Calibration Cards must remain constant. However, as we have shown in a previous publication<sup>(9)</sup>, the TLD cards used here can be subjected to hundreds of reuse cycles without any noticeable change in their TL efficiency.

#### 5. THE REFERENCE SOURCE AND THE CALIBRATION LABORATORY

To maintain a known relationship between the ability of the reader to convert stored TL information to measurable electric signals (charge or counts), it is convenient to express the ratio between the average TL response of the Calibration Cards and the delivered radiation quantity  $L$  in terms of one variable. Since the numerical value of this variable will be mainly dependent on the condition of the reader at a given date and time, it is appropriate

to name this variable "Reader Calibration Factor" (RCF), defined as follows:

$$RCF_i = \langle Q \rangle_i / L \quad (3)$$

when  $\langle Q \rangle_i$  is the TL response of a set of Calibration Cards exposed to a known quantity of radiation L.

The radiation quantity L can be expressed in any convenient units. We define the unit gU (generic unit) as the unit to express the quantity L. For example, 1 gU can be equal to the amount of irradiation delivered during a period of one second by a specific source with specific geometry to a dosimeter located at a set distance from the source. Since the definition of gU is somewhat arbitrary, once it is defined for a specific source and geometry, it will have any meaning only for this source, which is called the Local or Reference Source.

The last step of the system calibration consists of establishing the link to a set of various NBS calibrated sources located at a calibration laboratory. The calibration laboratory performs the irradiations and reports the delivered quantity in terms of Shallow dose and Deep dose for various radiation fields<sup>(10)</sup>. The method that was used to establish this link is described in the following sections.

## 6. SUPERPOSITION OF RADIATION FIELDS AND THE MIXTURE IDENTIFICATION FORMULAS

Since the dosimeter may respond differently (different gU/rem values) to different types of radiation fields or mixtures, its response has been experimentally characterized. The results of this characterization are used in the interpretation of the dosimeter readings for unknown dose and radiation field combinations. This requires knowing the type of radiation field or mixture that the dosimeter was subjected to, and to use this information to calculate the specific dose equivalent values. The only direct data from the dosimeter reading which is available for determining the radiation field type are the responses in units of gU from the different dosimeter positions,  $L_1$ ,  $L_2$ ,  $L_3$  and  $L_4$ . The TL element in position 4 is sensitive to neutrons<sup>3</sup> and is reserved for applications involving neutron fields. The remaining three elements form two independent ratios,  $L_3/L_1$  and  $L_3/L_2$ . Let us define a function  $f(x)$  to be the ratio  $L_3/L_1$  ( $f$ ) as a function of the ratio  $L_3/L_2$ , ( $x$ ).

The key issue in the dosimeter's ability to discriminate different radiation fields or to determine the relative contribution of components in mixed fields is the shape of this function and its rate of change for different energies and compositions. For a mixture of 2 model radiation fields "a" and "b" we assume that the

response of each TL element is the weighted sum or superposition of its individual response to fields "a" or "b" as if the other field did not exist. This assumption means that there is no interaction between the induced TL effects when the dosimeter is subjected to two or more different radiation fields. Although this assumption may seem to be straightforward, there are evidences in the literature that in some cases the TL response resulting from mixtures of radiation fields may not be additive. This effect is particularly noticeable with fast neutrons, where a decrease of 10% in the gamma TL signal was observed as a result of the tendency of fast neutrons to release the stored gamma induced signal from previous or simultaneous gamma irradiation<sup>(11)</sup>. However, if non-additivity effects exist for mixed beta gamma fields, they are expected to be small, and in fact our data shows that the assumption of superposition of radiation fields is valid to within few percent.

The superposition principle can be applied to determine f(x). Let N be the relative contribution of field "a" to the mixed field and assuming that only two fields exist, 1-N will be the relative contribution of field "b". If the delivered quantities are expressed in terms of Roentgen or rad in air, N and 1-N will be the weighting factor assigned to each field. The relative response,  $a_i$ ,  $b_i$  ( $i=1..4$ ) of each element to pure field "a" or "b" is defined as the response of the particular element in units of gU per unit of delivered dose in air when only one field is being used. Using the superposition principle, the relative response  $(ab)_i$  of element i to a mixture of fields "a" and "b" is as follows:

$$(ab)_i = Na_i + (1-N)b_i \quad (4)$$

Based on (4), the L3/L1 and L3/L2 ratios in a mixed field become:

$$L3/L1 = (ab)_3 / (ab)_1 = [Na_3 + (1-N)b_3] / [Na_1 + (1-N)b_1] \quad (5)$$

and similarly,

$$L3/L2 = (ab)_3 / (ab)_2 = [Na_3 + (1-N)b_3] / [Na_2 + (1-N)b_2] \quad (6)$$

Using x for L3/L2, we can then rewrite (6) in the form:

$$N = [b_3 - xb_2] / [x(a_2 - b_2) - (a_3 - b_3)] \quad (7)$$

Substituting N from (7) into (5) and using f(x) for L3/L1, we can then write (5) in the form:

$$f(x) = [b_3a_2 - a_3b_2]x / [(b_1a_2 - a_1b_2)x + (a_1b_3 - b_1a_3)] \quad (8)$$

Formula (8) is used to identify the mixture as follows: all the calibration constants  $a_i$  and  $b_i$  are determined once by performing calibration irradiations at an NBS traceable calibration laboratory for all the radiation fields of interest (all the possible a's and b's). The value of x (the ratio L3/L2) is then computed from the

response of the dosimeter, and  $f(x)$  computed for this particular  $x$  and for all the possible radiation field mixtures "a" and "b", which are used as model fields to simulate possible different model responses of the dosimeter to various radiation fields. Then the measured L3/L1 value is compared to all the calculated  $f(x)$  (all the possible computed L3/L1 ratios for the particular measured L3/L2 ratio) and the calculated value which is nearest to the measured L3/L2 ratio is selected to represent the required type of model radiation fields mixture, i.e. the identity of "a" and "b". Once "a" and "b" have been identified, (7) can be used to calculate the relative contribution of each component,  $N$  and  $1-N$  for fields "a" and "b" respectively. If none of the computed L3/L1 ratios is in close agreement with the measured one, the reading may have resulted from radiation fields different from those covered by the calibration, or the dose was too low to provide an accurate measure of the value of  $N$ . In this case, the dose is calculated based on the average value of the calibration constants shown in Table 2.

## 7. DEEP AND SHALLOW DOSE DETERMINATION

Once the value of  $N$  has been determined, the Deep and the Shallow dose are calculated from the TL response in units of  $gU$ ,  $R_1$  and  $R_3$  for elements 1 and 3 respectively. Let  $R_{a1}$  be the response of element 1 in units of  $gU$  when the dosimeter is exposed to  $d$  rem of deep dose and  $R_{a3}$  the response of element 3 in units of  $gU$  when the dosimeter is exposed to  $s$  rem of shallow dose using model field "a". Similarly, the variables  $R_{b1}$  and  $R_{b3}$  are defined for model field "b". The "model field calibration values"  $r_{a1}$ ,  $r_{a3}$  in terms of  $gU$  per "deep rem" and  $gU$  per "shallow rem" for field "a", are defined as follows:

$$r_{a1} = R_{a1}/d \quad [gU/rem] \quad (9)$$

and

$$r_{a3} = R_{a3}/s \quad [gU/rem] \quad (10)$$

similarly we define  $r_{b1}$  and  $r_{b3}$  for model field "b":

$$r_{b1} = R_{b1}/d \quad [gU/rem] \quad (11)$$

and

$$r_{b3} = R_{b3}/s \quad [gU/rem] \quad (12)$$

Using the superposition principle, we can now define the "mixed field calibration factors"  $r_{ab1}$  and  $r_{ab3}$  for deep and shallow dose respectively, to be:

$$r_{ab1} = Nr_{a1} + (1-N)r_{b1} \quad [gU/rem] \quad (13)$$

and,

$$r_{ab3} = Nr_{a3} + (1-N)r_{b3} \quad [gU/rem] \quad (14)$$

Finally, we can compute the deep and shallow dose from the TL response in units of gU,  $R_1$  and  $R_3$  for elements 1 and 3 respectively and using (13) and (14) as follows:

$$\text{DEEP DOSE} = R_1/r_{ab1} \quad [\text{rem}] \quad (15)$$

and,

$$\text{SHALLOW DOSE} = R_3/r_{ab3} \quad [\text{rem}] \quad (16)$$

## 8. RESULTS AND DISCUSSION

To implement and test the methodology described in the previous sections, a batch of 145 dosimeters was supplied to the calibration laboratory to be exposed to various types and amounts of beta and gamma radiation following the Department of Energy Standard for the Performance Testing of Personnel Dosimetry Systems<sup>(2)</sup> (DOE/EH-0027) irradiation procedures. Forty dosimeters, five in each field, were exposed to eight different "pure" radiation fields as specified in DOE/EH-0027 and summarized in Table 1. The responses of those dosimeters were used to generate the various calibration factors as described in the previous sections. Ten other dosimeters were exposed to the accident categories (I and II). However, the dosimetry at the high dose level and the fading corrections required are still under investigation. The remaining 95 dosimeters were irradiated using 19 different mixtures of photons and beta rays. The responses of both groups of dosimeters were used to test the dose calculation algorithm. The deep dose levels were in the range of 420 - 2000 mrem.

The calibration factors  $r_{ai}$  and  $a_i$  were calculated using the response of the dosimeters to the pure fields and the delivered deep dose, shallow dose and delivered exposure, or dose, supplied by the calibration laboratory. The results of this calculation for  $r_{ai}$  are shown in Table 2. Each calibration factor was computed averaging the response of five dosimeters which were exposed simultaneously to the same radiation field. The uncertainties shown in Table 2 represent one standard deviation from the average. and the percentage standard deviation is given in parentheses. When the L3/L1 ratio is plotted as a function of L3/L2, each mixture type is identified by its own unique pattern, i.e., Mixture Identification Curve (MIC). Typical results for various mixtures are shown in Figure 1, which illustrates a family of curves calculated using (8).

The ability to discriminate between photon and beta fields has been well demonstrated. However, there is no discrimination ability among M150, H150, and Cs-137 photon fields. From Table 2 we can see that the over-response of the dosimeter relative to Cs-137 is approximately 20-25% with M150 and about 10% with H150. Since there is no clear discrimination among these 3 sources, whenever one of them is identified in a mixture, the calibration factors ( $r_{abi}$ ) are set to the average of the individual  $r_{ai}$  values for those three photon fields. This procedure will overestimate the reported dose

from the M150 source by approximately 10-13% and underestimate the response to the Cs-137 and the H150 sources by approximately 10% and 3-5%, respectively. Although less pronounced, a similar situation may occur in some mixtures involving Tl-204 or Depleted Uranium. If we reexamine Table 2, we see that the shallow dose responses of these two beta sources are within 20%. Again, if the average of the individual calibration factors ( $r_{\alpha\beta}$ ) is used whenever Tl or DU are identified in a mixture, the maximum "built-in" overestimation or underestimation of the DU or Tl-204 dose respectively will be 10%.

The Mixture Identification Curve method was applied to all of the 135 dosimeters that were involved. Each dosimeter was treated as if it was exposed to a mixed field and the mixture components were identified and the relative contributions of each field, N and 1-N were calculated. The measured N values were compared to the N values as reported by the calibration laboratory ("delivered") for the mixed fields. The results of this comparison are shown in Table 3, and demonstrate good agreement between the measured and the actual contribution of the various radiation fields. No comparison was made for the two mixtures of Cs-137 with M150 or with H150 since no meaningful N values can be computed due to the overlap of their MICs. The reported Deep and Shallow doses were calculated from the dosimeter responses using formulas (9) to (16) and the calibration factors from Table 2. The results for each category were compiled using the guideline given in the DOELAP handbook for Personnel Dosimetry Systems<sup>(12)</sup>, when the "Bias", B is given by:

$$\bar{B} = 1/n \left[ \sum_{i=1}^n P_i \right] \quad (17)$$

where  $P_i$  is the fractional difference between the reported and delivered absorbed dose or dose equivalent for the  $i^{\text{th}}$  dosimeter, given by:

$$P_i = (\text{Reported}_i - \text{Delivered}_i) / \text{Delivered}_i \quad (18)$$

and the standard deviation:

$$S = \left[ \sum_{i=1}^n (P_i - \bar{B})^2 / (n-1) \right]^{1/2} \quad (19)$$

The  $|B|+S$  values for all of the 27 radiation fields involved are represented graphically in Figure 2 and compared to the current (solid line) and future (dotted line) DOELAP tolerance levels.

## 9. CONCLUSION

It has been shown that the dosimeter response can be used to identify the mixture type in a mixed beta-gamma field and to estimate the relative contribution of major components. Furthermore, it has been demonstrated that the accuracy of the system can be well within DOELAP tolerance limits.

## 10. REFERENCES

- ( 1) Carlson R. D., and Gesell, T. F., "The Department of Energy Laboratory Accreditation Program in Personnel Dosimetry: Results of the Pilot Performance Test", DOE/ID-12104 (1986).
- ( 2) DOE Standard for the Performance Testing of Personnel Dosimetry Systems, DOE/EH-0027 (1986).
- ( 3) Storm, E., Buslee, P. L., Blackstock, A. W., Littlejohn, G. J., Cortez J. R., Fultyn, R. V. and Lawrence, J. N. P., "The Los Alamos Thermoluminescence Dosimeter Badge", Radiat. Prot. Dosim., 1, 209-219(1982).
- ( 4) Plato, P., Leib, R., and Miklos., J., "Two Methods for Examining Angular Response of Personnel Dosimeters", Health Phys, 54, 597-606(1988).
- ( 5) Horowitz, Y. S., Moscovitch, M., Mack, J. M., Hsu, H. and Kearsley, E., "Incorporation of Monte Carlo Electron Interface Studies Into Photon General Cavity Theory", Radiat. Prot. Dos., Vol. 17, p. 437, (1986).
- ( 6) Soares C. G., Bright E. L., and Ehrlich., M., "Difficulties Encountered With Some Intermediate-Atomic Number Personnel Dosimeters Irradiated On-Phantom in Low-Energy Photon Beams", Health Phys., 54, 431-444(1988).
- ( 7) Plato, P., and Miklos., J., "Production of Element Correction Factors for Thermoluminescent Dosimeters", Health Phys., 49, 873-881, (1985).
- ( 8) Spanne, P. TL Readout Instrumentation, in "Thermoluminescence and Thermoluminescent Dosimetry", Vol. III (Y. S. Horowitz ed.), Chapter 1, CRC Press, Orlando, FL (1984).
- ( 9) Moscovitch, M., Bruml W., Velbeck, K. J. and Martis C., "The Reusability of a New TLD Card Type", Health Phys. Soc. Annual Meeting, Salt Lake City, (July 1987).
- (10) Hooker, C. D., Roberson, P. L., Gesell, T. F. and Carlson R. D., "Quality Assurance Manual for the Department of Energy Laboratory Accreditation Program for Personnel Dosimetry Systems", DOE/ID-12105 (1987).
- (11) Oltman, B. G., Kastner, J., Tedeschi, P., and Beggs, J. N., "The Effects of Fast Neutron Exposure on the LiF-7 TL Response to Gamma Rays", Health Phys., 13, 918 (1967).
- (12) "Handbook for the Department of Energy Laboratory Accreditation Program for Personnel Dosimetry Systems", DOE/EH-0026 (1986).

Table 1. Calibration Irradiations

Radiation Field		Energy
1	x-ray NBS filtered Technique - M30	20 keV
2	x-ray NBS filtered Technique - S60	36 keV
3	x-ray NBS filtered Technique - M150	70 keV
4	x-ray NBS filtered Technique - H150	120 keV
5	Gamma Cs-137	662 keV
6	Beta (Point geometry) Tl-204	760 keV (max)
7	Beta (Point geometry) Sr/Y-90	2300 keV (max)
8.	Beta (Slab geometry) Uranium	2300 keV (max)

Table 2: Pure Field Calibration Factors - gU/rem

Source	Deep Dose - $r_{a1}$	Shallow Dose - $r_{a3}$
1 M30	693.0 ± 11.1(1.6%)	837.6 ± 19.7(2.4%)
2 S60	942.9 ± 15.1(1.6%)	1008.1 ± 22.0(2.2%)
3 M150	805.4 ± 16.3(2.0%)	848.1 ± 10.9(1.3%)
4 H150	726.5 ± 39.6(5.5%)	737.2 ± 20.3(2.8%)
5 Cs-137	659.8 ± 14.5(2.2%)	667.7 ± 11.7(1.8%)
6 Tl-204	-----	498.0 ± 7.6(1.5%)
7 Sr/Y-90	-----	716.0 ± 10.9(1.5%)
8 Uranium	-----	408.6 ± 10.1(2.5%)

Table 3: Comparison Between Delivered and Measured N values

Mixture Components		Relative Contribution of Field "a" - N	
Field "a"	Field "b"	Delivered	Measured
M30	Cs-137	0.696	0.674 ± 0.012
S60	Cs-137	0.491	0.441 ± 0.096
M30	Tl-204	0.483	0.561 ± 0.028
S60	Tl-204	0.466	0.458 ± 0.021
M150	Tl-204	0.416	0.515 ± 0.088
H150	Tl-204	0.415	0.464 ± 0.071
M30	Sr/Y-90	0.474	0.471 ± 0.043
S60	Sr/Y-90	0.458	0.470 ± 0.052
M150	Sr/Y-90	0.407	0.457 ± 0.011
H150	Sr/Y-90	0.406	0.410 ± 0.023
M30	Uranium	0.483	0.385 ± 0.061
S60	Uranium	0.466	0.500 ± 0.041
M150	Uranium	0.416	0.421 ± 0.026
H150	Uranium	0.415	0.438 ± 0.034
Cs-137	Tl-204	0.493	0.441 ± 0.075
Cs-137	Sr/Y-90	0.484	0.402 ± 0.056
Cs-137	Uranium	0.493	0.406 ± 0.087

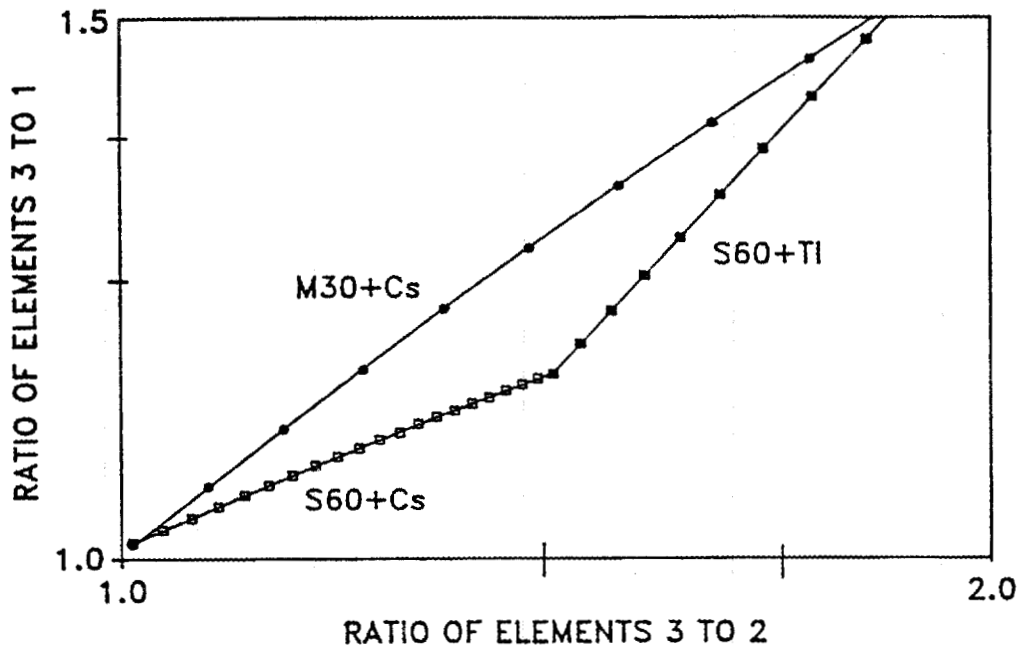


Figure 1

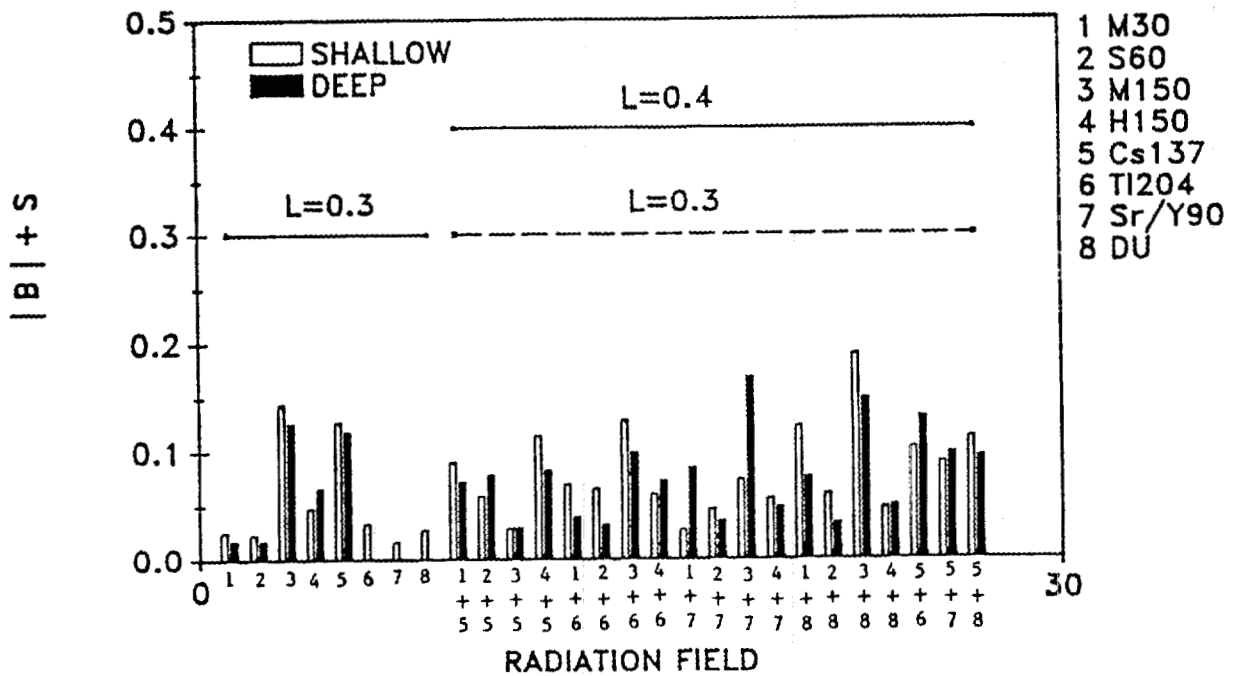


Figure 2

## ACCIDENT LEVEL DOSIMETRY WITH TLD

N. M. Moghari\*, Department of Radiation Science,  
Georgetown University  
R. T. Devine, Naval Dosimetry Center, Bethesda, MD

### ABSTRACT

Under the sponsorship of the Naval Dosimetry Center (NDC), a series of accident level irradiations were conducted at the Mount Weather Facility of the Federal Emergency Management Agency (FEMA). The irradiations consisted of two sets of exposures involving 50 8800-series TLD cards (DT-648/PD) with Cs-137 photons. The first set of irradiations ranged from 6 to 600 Rad. The purpose was to pre-irradiate the TLD cards, measure the superlinearity of the detector's responses, and then, clear the TLDs for the subsequent exposure. The second set of irradiations were conducted at the same dose levels and with the same TLD cards. The superlinearity of the detector responses were re-measured to establish the effect of accident level photon doses on the TLD responses.

### INTRODUCTION

The TLD response  $R(D)$ , defined here as the corrected measure dose is a linear function of the absorbed dose  $D$ :

$$R(D) = SD$$

where  $S$  is the slope of the line and is defined as the TLD response per unit absorbed dose. At high levels of absorbed dose,  $D > D_{su}$ , the TLD response becomes superlinear and saturates at dose  $D^*$  (Fig. 1). At doses

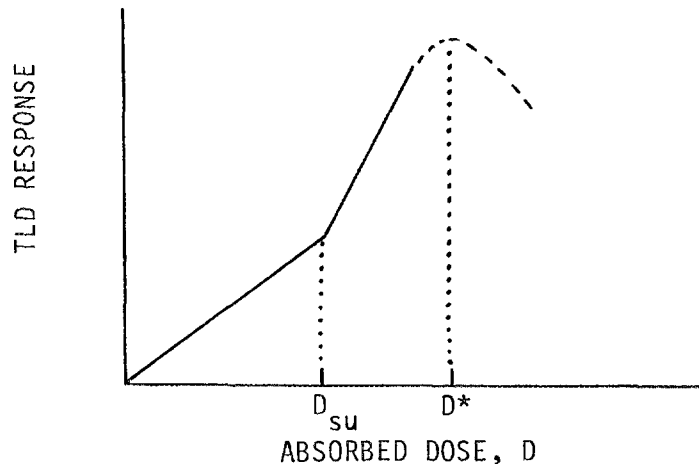


FIGURE 1. TLD RESPONSE VS. DOSE

\*Current affiliation: Control Data Corporation, UAI, 6003 Executive Blvd.,  
Rockville, MD 20852

above the saturation dose  $D^*$ , the TLD response diminishes rapidly at increasing levels of  $D > D^*$ . In the superlinear region, the TLD response is represented by Eq. 1:

$$R_{su}(D) = S_{su}(D) + C \quad \text{Eq. 1}$$

Theoretical models to explain the TLD superlinearity are proposed by several authors (Refs. 1-4) and their explanations are beyond the scope of the present work. For the purpose of this study, Eq. 1 is generally an appropriate representation of the TLD response behavior over the absorbed dose range of interest.

Following pre-irradiation of TLDs at dose levels beyond  $D_{su}$ , the thermoluminescence sensitivity of TLDs is generally enhanced. This sensitization process depends on the level of absorbed dose and the annealing procedures. Under special conditions, the sensitivity of TLDs can be increased by up to a factor of five (Ref. 5). Pre-irradiations to much higher dose levels will cause a permanent loss in the TLD sensitivity, generating desensitization of the TLDs.

To assess the effect of accident level photon doses on the 8800-series TLD responses, 50 8800-series LTD cards were pre-irradiated with Cs-137 photons. The absorbed dose range was 6-600 Rad. The superlinearity of the individual TLD chips were measured and expressed in terms of four superlinear slopes:  $S_{su}^i(D_1)$ , where index  $i=1,2,3,4$ , refers to individual TLD chips. After clearing the TLDs, a second set of irradiations at dose levels ranging from 6-600 Rad were conducted. Both photon irradiations and measurement of the responses were performed under near identical conditions. This superlinearity of the individual chips were re-measured and expressed in terms of a second set of superlinear slopes  $S_{su}^i(D_2)$ .

A comparison of  $S_{su}^i(D_2)$  vs.  $S_{su}^i(D_1)$  indicated that the pre-irradiation of the TLDs appears to reduce superlinearity of the responses. It was noted that compared to the TLD responses of the first irradiations, the pre-irradiated TLD responses showed a decreasing trend at increasing values of the absorbed dose.

## EXPERIMENT

The photon irradiations were conducted at FEMA's Jack C. Green Radiological Instrumentation Test Facility. The source consisted of a calibrated Shepherd Cs-137 source system. The first set of irradiations were conducted at a current source activity of 995 Ci and at a source-to-dosimeter distance of 178.7 Cm. At this distance, 50 8800-series TLD cards (DT-648/PD), divided into 10 batches of 5 TLD cards, were positioned on a platform, perpendicular to the horizontal direction of the photons source. Each batch was exposed to a specific dose, as shown in Table 1.

Table 1. Absorbed Dose per Batch

Batch Number	D (Rad)
1	6
2	96
3	168
4	240
5	288
6	360
7	400
8	450
9	500
10	600

The dosimeter readouts were performed 10 days following the irradiation at the Naval Dosimetry Center's TLD System 8800 Workstation. The time-temperature profile and the data processing of the measured data were based on standard NDC procedures and an NDC-developed computer code called: ALGORITHM 648DOSE (Ref. 6).

Prior to the second set of photon irradiations, the TLDs were cleared and re-grouped in the same batches of the first exposure. The slight source decay during the elapsed time between the first and the second exposure was calculated and compensated by reducing the source-to-dosimeter distance by 2mm. The second set of exposures, dosimeter readout, and data processing, were performed under identical conditions of the first set.

## RESULTS

The batch-average TLD chip responses were obtained by averaging the 5 corrected measured responses for each batch, and plotted vs. the absorbed doses. Figures 2-5 show the TLD chip responses for the first and the second set of exposures. The slopes of responses' superlinearity is reported in Table 2. The values of  $S_{su}^i(D_2)$  indicate that pre-irradiated

Table 2. Slopes of TLD Superlinearity

Chip i	$S_{su}^i(D_1)$	$S_{su}^i(D_2)$
1	1.235	1.009
2	1.266	1.069
3	1.197	0.964
4	1.225	0.844

chips 1 and 2 exhibit a reduction of superlinear trend at high absorbed doses whereas, chips 3 and 4 appear to display a loss of sensitivity,

particularly at high doses. The batch-average response for pre-irradiated chip 3 is 568 Rad for an absorbed dose of 600 Rad, the corresponding response for the unirradiated batch is 680 Rad. The corresponding values for pre-irradiated chip 4 are: 504 Rad for an absorbed dose of 600 Rad, and 680 Rads for the unirradiated response. These figures indicate that compared to the unirradiated condition, chips 3 and 4 exhibit a loss of 112 and 176 Rad, respectively.

These results indicate that the pre-irradiated TLDs at high levels of absorbed dose exhibit losses of sensitivity that are not restored by standard annealing process. Thus, these dosimeters become inadequate for a reliable re-utilization.

The obtained results indicate superlinear responses at absorbed doses lower than expected. This behavior may be partly attributed to the operational characteristics of the dosimeter chips and the TLD reader. Since in a hypothetical nuclear accident condition the readings are to be performed with some degree of urgency, the reader was not set up to conditions different than routine operational conditions. The decrease of sensitivity in the pre-irradiated dosimeters is, however, attributable to chip damage at high absorbed doses.

#### ACKNOWLEDGEMENT

We wish to thank Mr. Carl Siebentritt of FEMA for his permission to use the Cs-137 source system. We also wish to thank Mr. Bert Thompson of FEMA and Dr. Paul Blake of NDC for very useful discussions and the processing of the TLD cards.

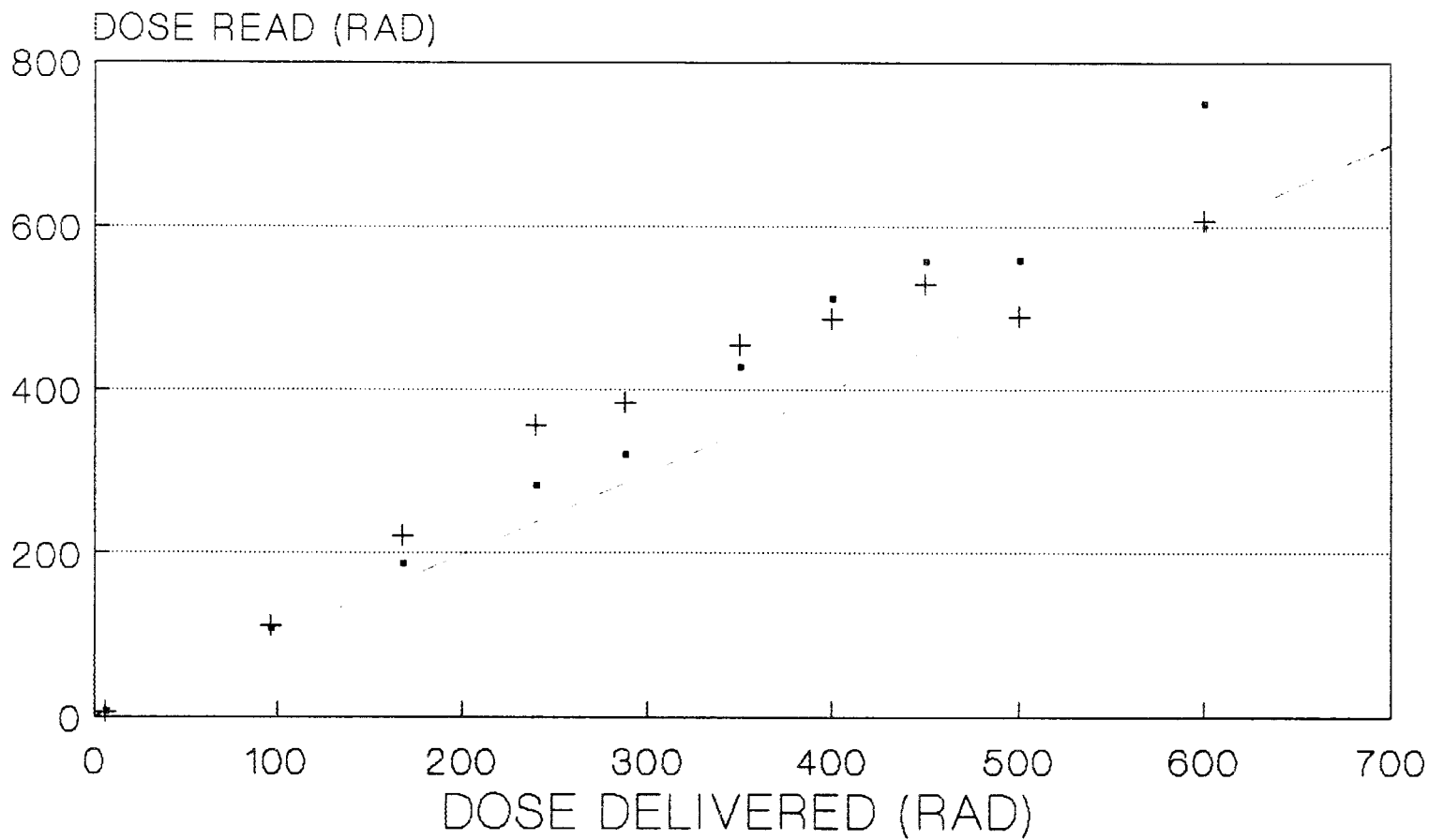
#### REFERENCES

1. Suntharalingam N and Cameron J R 1969 Phys. Med. Biol. 14 394
2. Stoebe T G and Wantanabe S 1975 Phys. Stat. Solid. (a) 29 11
3. Attix F H 1975 J. Appl. Phys. 46 81
4. Mayhugh M R 1970 J. Appl. Phys. 41 4776
5. Wilson C R, Dewerd L A and Cameron J R 1966 USAEC Rep. C00-1105-116
6. Devine R T, Moscovitch M and Blake P K 1988 US Naval Med. Comm. Ctr. Rep. (to be published under the report title: The US Naval Medical Command Dosimeter Algorithm)

FIGURE 2

# SUPRALINEARITY STUDY FOR DT-648

Comparison of two successive runs



• chip 1 (1)    + chip 1 (2)

(1) First Run, (2) Second Run

FIGURE 3

# SUPRALINEARITY STUDY FOR DT-648

Comparison of two successive runs

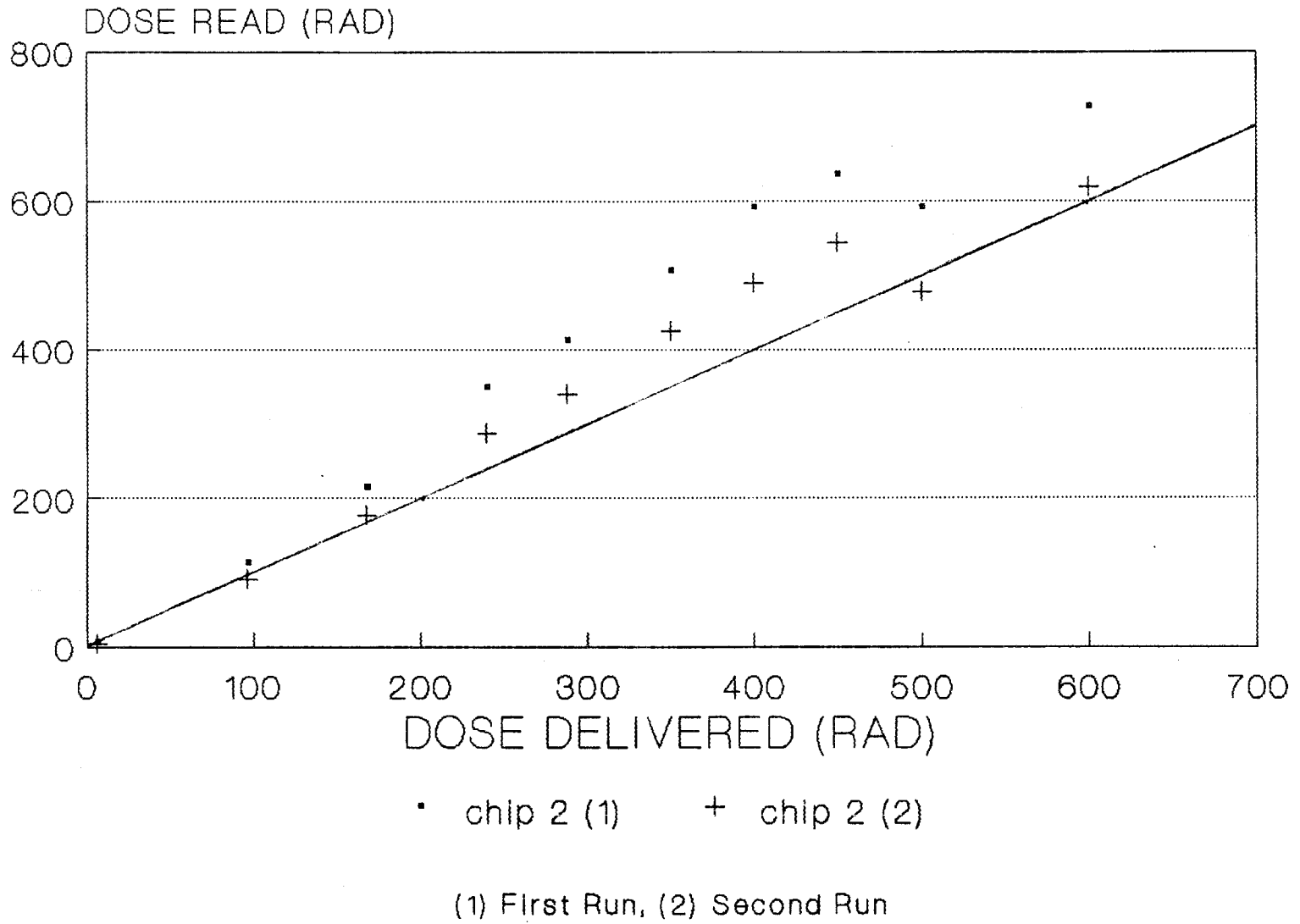
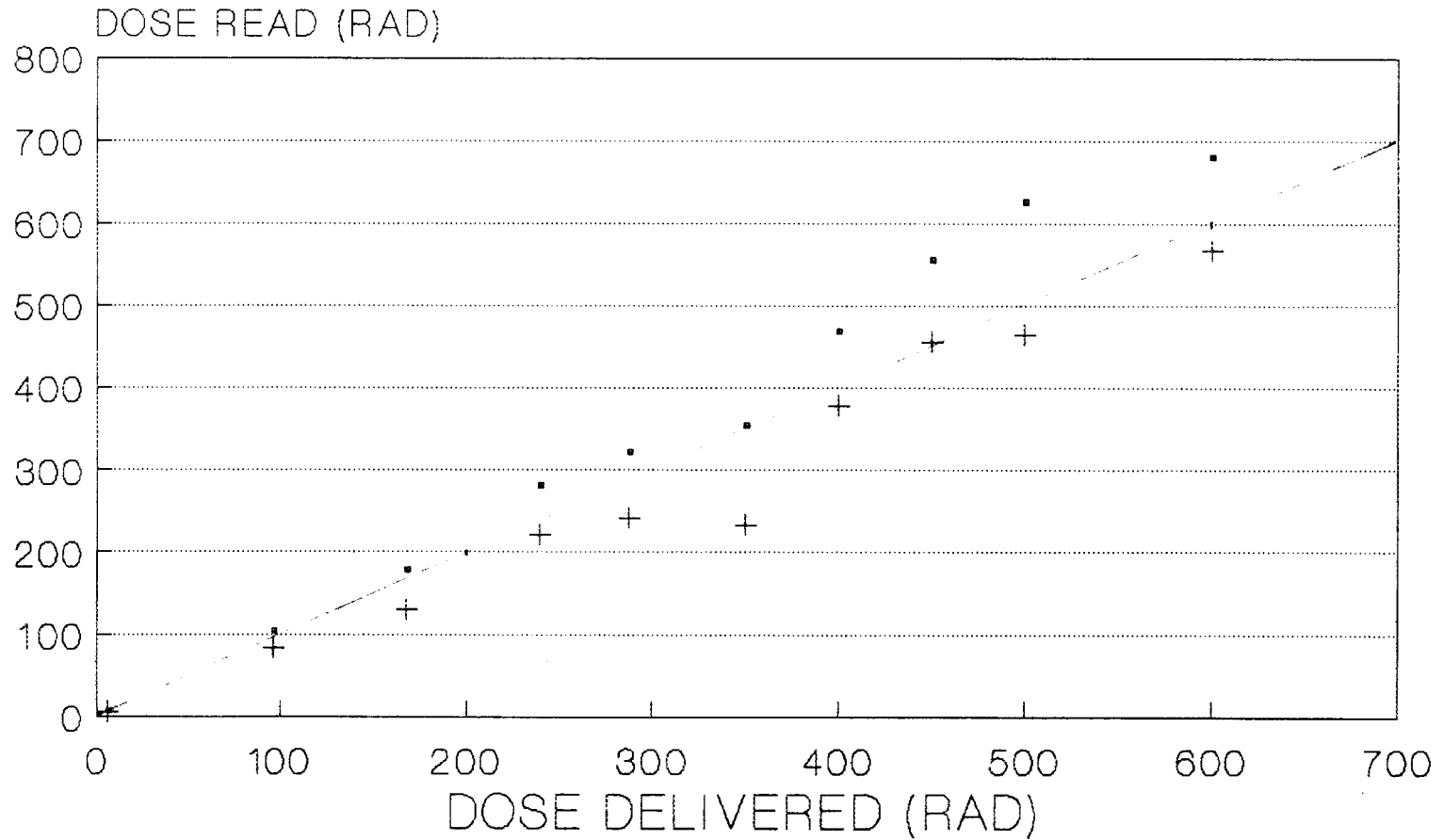


FIGURE 4

# SUPRALINEARITY STUDY FOR DT-648

Comparison of two successive runs



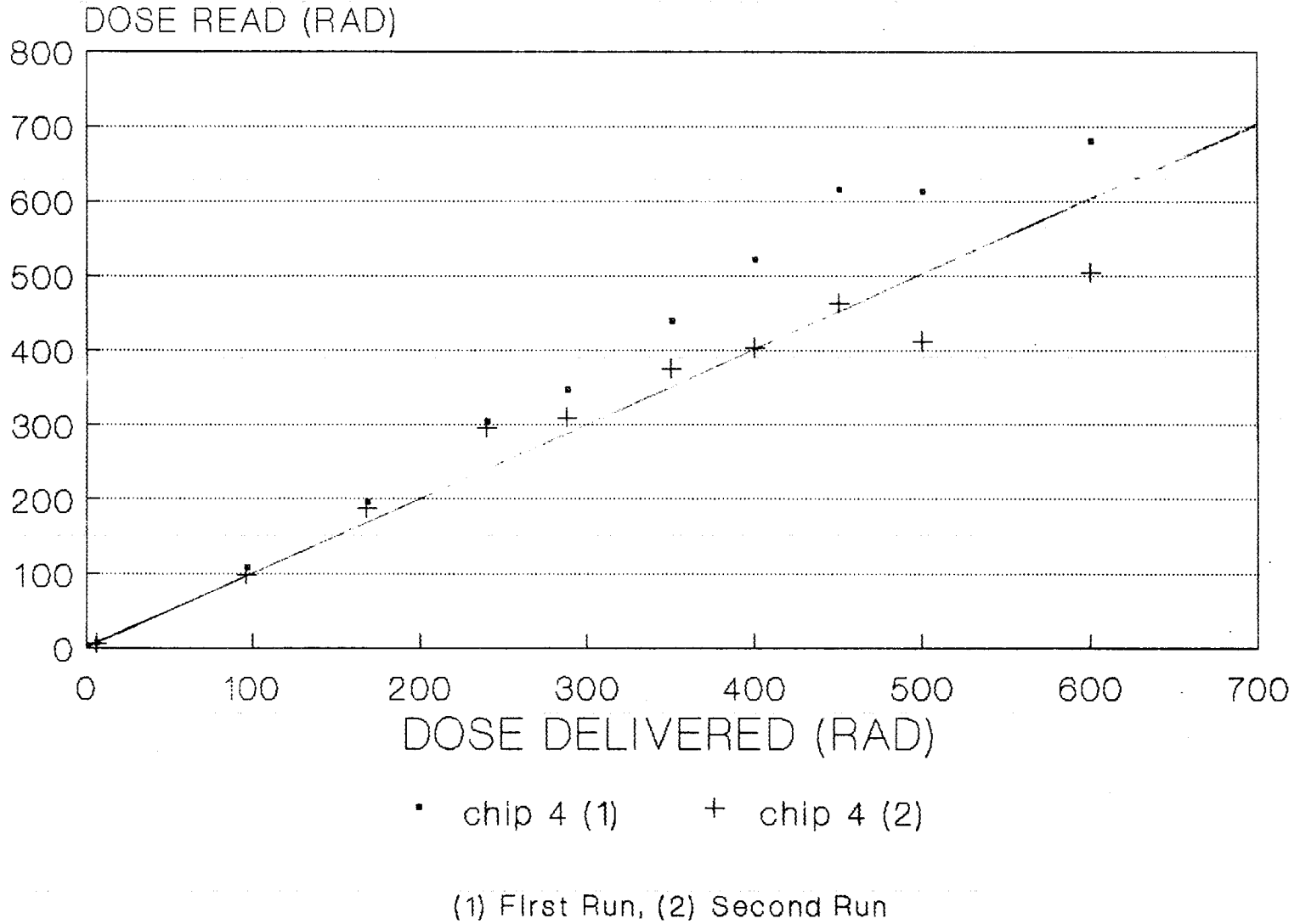
• chip 3 (1)    + chip 3 (2)

(1) First Run, (2) Second Run

FIGURE 5

# SUPRALINEARITY STUDY FOR DT-648

Comparison of two successive runs



DOE PERSONNEL NEUTRON DOSIMETRY EVALUATION  
AND UPGRADE PROGRAM

Leo G. Faust and Carl M. Stroud  
Pacific Northwest Laboratory  
Richland, Washington

Edward J. Vallario  
U.S. Department of Energy  
Washington, D.C.

ABSTRACT

The U.S. Department of Energy (DOE) sponsors an extensive research program to improve the methods, dosimeters, and instruments available to DOE facilities for measuring neutron dose and assessing its effects on the work force. The Total Dose Meter was recently developed for measuring in real time the absorbed dose of mixed neutron and gamma radiation and for calculating the dose equivalent. The Field Neutron Spectrometer was developed to provide a portable instrument for determining neutron spectra in the workplace for flux-to-dose equivalent conversion and quality factor calculation. The Combination Thermoluminescence/Track Etch Dosimeter (TLD/TED) was developed to extend the effective neutron energy range of the conventional TLDs to improve detection of fast-energy neutrons. An Optically Stimulated Luminescence Dosimeter is presently being developed for application to gamma, neutron, and beta radiation. An Effective Dose Equivalent System is being developed to provide guidance in implementing the January 1987 Presidential Directive to determine effective dose equivalent. Superheated Drop Detectors are being investigated for their potential as real time neutron dosimeters. This paper includes discussions of these improvements brought about by the DOE research program.

INTRODUCTION

The DOE Personnel Neutron Dosimetry Evaluation and Upgrade Program was initiated in October 1980. Its primary objectives are to assess current neutron dosimetry capabilities and develop improved personnel neutron dosimeters and instruments. The short-term goal of the program is to provide a portable field neutron spectrometer and an interim neutron dosimeter that are effective over the maximum practical energy range and dose. The long-term goal of the program is to improve our understanding of neutron exposure and to develop a total effective dose equivalent system.

Health risks associated with exposure to neutrons are still not well defined. However, it is known that neutrons are more damaging biologically than other types of radiations, such as gamma rays. Concern about the low-level effects of radiation dose is increasing, and the relative hazard for neutron radiation may be higher than has been assumed in the past. With the proposed increase in neutron quality factors, neutron dose and, therefore, neutron dosimetry will become more significant. Present dosimeters do not provide information about the quality of radiation to account for differences

in biological damage produced by neutrons and gamma rays. The minimum sensitivity of present neutron dosimeters is typically 50 mrem  $\pm$ 100%. When these dosimeters are exchanged on a monthly basis, there is a potential for missing up to 600 mrem per year. If neutron quality factors are increased by a factor of 2, the minimum sensitivity will be increased to 100 mrem and the potentially unaccounted-for dose will be increased to 1200 mrem per year.

It is necessary to know the neutron dose at various depths in the body as well as on the surface. In January 1987, President Reagan signed the "Radiation Protection Guidance to Federal Agencies for Occupational Exposure; Approval of Environmental Protection Agency Recommendations" (1) which adopts the methods of the International Commission on Radiological Protection (ICRP) Publication 26 (2). ICRP-26 recommends that the dose equivalent in non-uniform fields be determined by summing the dose equivalent to various specified tissues multiplied by a set of weighting factors.

National laboratories, private industry, and universities provide the technical support for this program. Research is accomplished by a combination of contracts and subcontracts that focus the best possible expertise on each task. The advice and recommendations of consulting committees are used to guide program development, and interactions with the National Bureau of Standards assure that measurements and results are consistent with national standards.

#### RECENT DEVELOPMENTS

A portable field neutron spectrometer, total dose meter, and combination thermoluminescence/track etch dosimeter (TLD/TED) have been developed and are being used to assess occupational radiation dose.

#### PORTABLE FIELD NEUTRON SPECTROMETER

Proper application of dose conversion and quality factors to calculate dose equivalents requires knowledge of the energy spectra of the neutron fields. If this information is not available, conservative factors are used in calculations, potentially inflating reported dose equivalents. Neutron source energy spectra are seldom well known in the workplace and may vary as operational conditions vary. A neutron spectrometer is needed to characterize these fields and a portable spectrometer is needed for monitoring these fields on a routine and as needed basis. Use of a field spectrometer increases accuracy by incorporating irradiation geometry in the field calibration of personnel dosimeters and instruments. With the exception of Bonner spheres, there are no portable field neutron spectrometers commercially available at this time.

Pacific Northwest Laboratory (PNL) has developed an innovative portable field neutron spectrometer that covers the ranges of neutron energies involved in the processing of plutonium. The unit is completely portable and can be carried into the workplace and set up quickly. It uses a modular design, so that it can be repaired in the field by exchanging modules. Two different types of detectors, each with built-in electronics, are used: a tissue equivalent proportional counter (TEPC) and a  $^3\text{He}$  proportional counter. The analysis module is mounted in a suitcase and based on a lap-top

computer that controls the data collection, analyzes the data, and displays the results to the operator. The differential neutron flux density as a function of neutron energy between 50 keV and 5 MeV is displayed graphically. The computer also calculates and displays average neutron energy, average neutron quality factor, and average dose equivalent. The analysis program uses the current values for quality factors and flux-to-dose equivalent conversion factor listed in NCRP Report 38 (3).

The  $^3\text{He}$  detector is sensitive to neutrons in the 50 keV to 5 MeV energy-range and can measure 0.1 to 100 mrem/hr depending on the size of the detector. The detector is self-calibrating using the 764 keV peak produced by slow neutrons. The unfolding algorithm used in the data analysis is programmed into the computer. Thus, measurements can be made by pushing a single button.

Quality factors are presently defined as a function of linear energy transfer (LET). The TEPC is used to determine LET distributions. Thus, quality factors and dose equivalents can be determined from first principles using TEPCs and appropriate algorithms. The TEPC covers the energy range from thermal to 20 MeV.

Agreement from the two different methodologies employed by the  $^3\text{He}$  detector and the TEPC lends credibility to the accuracy of the results. The spectrometer is effective in gamma/neutron fields up to 500:1.

A plan to convert the spectrometer to battery operation with an AC electrical charger will eliminate its sensitivity to electrical disruptions. As funds become available for this conversion, the power consumption and size of the spectrometer will be reduced to reduce its cost and increase its ease of use in the field. Also, Lawrence Livermore National Laboratory (LLNL) is developing plans to incorporate the NE-213 probe into the spectrometer which will expand its effective energy range to 20 MeV.

#### TOTAL DOSE METER

The total dose meter was developed jointly by PNL and EG&G/Santa Barbara Laboratory. It uses a single TEPC to measure the neutron and photon dose. The radiation reacts with the tissue equivalent plastic walls to form charged particle secondaries, which deposit energy through ionization in its cavity. At the low gas pressure in the cavity, most particles have a nearly constant LET in traversing the cavity. The ionization produced in the detector is proportional to the energy deposited in the gas cavity, and this value of energy deposition can be divided by the mass of the gas to determine the absorbed dose (energy per unit mass).

The TEPC used in the total dose meter simulates a tissue site diameter of one micron. A built-in empirical algorithm is used in the microprocessor to calculate the dose equivalent from mixed radiation and display the results on a liquid crystal. The microprocessor can be reprogrammed with a different algorithm to accurately determine dose equivalent if the neutron and/or photon quality factors are changed.

The total dose meter has an operating range of 1 mrem to 10 rem in the neutron energy range from thermal to 20 MeV with an alarm if the accumulated dose exceeds 100 mrem. It has a minimum sensitivity of 0.2 mrem for neutrons and displays results to the nearest mrem.

A reduction in power consumption and size of the total dose meter is planned to enhance its usefulness in the workplace.

#### COMBINATION THERMOLUMINESCENCE/TRACK ETCH DOSIMETERS

Most DOE facilities use thermoluminescence-albedo dosimeters (TLDs) which are relative inexpensive, easy to read out automatically, and reusable. TLDs effectively measure exposure to low-energy neutrons and indicate exposure to significant fast neutron radiation. However, their response drops quickly at neutron energies above 1 keV.

Proton recoil track etch dosimeters (TEDs) are insensitive to low-energy neutrons but are quite sensitive to neutrons above about 150 keV. Neutrons interact with hydrogen in specialized plastics or radiators producing recoil proton with high elastic scattering cross section. The polymer of allyl diglycol carbonate, CR-39, the monomer of which is produced by PPG Industries, Pittsburgh, Pennsylvania, is the plastic currently being used.

CR-39 is highly sensitive to chain scission from alphas, protons, neutrons, and heavy charged particles. It is not sensitive to beta or gamma radiation and does not rely on the albedo effect to detect fast neutrons. The damage tracks are enlarged to macroscopic size by electrochemical etching. Readout is normally accomplished using an optical microscope together with an image analyzer to determine the track density.

The combination TLD/TED has an effective neutron energy range from thermal to 18 MeV and enhanced accuracy at neutron energies above about 200 MeV.

Software is presently being developed by LLNL for DOE-wide application for the analysis of CR-39 data. Further research is planned to develop a badge that will reduce the angular dependence of the CR-39 and to expand the sensitivity of the CR-39 into the thermal energy range by loading boron into the radiator. U.S. Department of Energy Laboratory Accreditation Program (DOELAP) criteria for TEDs are in the early development stage.

#### ONGOING DEVELOPMENTS

Developmental work has begun on the following tasks and is expected to continue through fiscal year (FY) 1989.

#### OPTICALLY STIMULATED LUMINESCENCE (OSL)

Solid-state alkaline and alkaline earth crystals doped with metallic impurities have been used extensively for measuring ionizing radiations.  $\text{CaF}_2:\text{Mn}$ ,  $\text{CaF}_2:\text{Dy}$ , and  $\text{NaCl}:\text{Ag}$  gave radiation-dependent responses indicating that OSL properties exist in almost all impurity-doped salts. OSL research efforts through 1986 reported minimum detectable gamma exposures from one to 1,000 R.

PNL found that a lower limit of detection of 100 mR was possible at room temperature using CaF<sub>2</sub>:Mn and ultraviolet or Excimer laser stimulation and that this lower limit could be reduced to less than 1 mR by cooling the crystal to liquid nitrogen temperatures. This lower limit of detection can be further reduced by increasing the crystal size. OSL stimulation and readout is nondestructive. Approximately 10% decrease in signal occurs each time a crystal is read out. In addition, re-reading crystals after five months showed no loss of signal, indicating that fading will not be a concern.

OSL has potential applications in neutron, beta, internal, and environmental dosimetry, as well as in gamma dosimetry. The development of an OSL proton recoil dosimeter will be the focus of this research. CaF<sub>2</sub>:Mn will be ground into micron-size particles and cast into a plastic of high hydrogen content. The small size of the sensitive material should provide good neutron/gamma discrimination because the difference in energy deposition will favor proton recoil interactions. The variations in size and spacing of the particles will provide a means for obtaining neutron spectral information.

Developing optimal crystal material and OSL procedures will be challenging research for the future. Developing a phosphorescence-free plastic is essential to adapting OSL techniques to neutron dosimetry.

#### EFFECTIVE DOSE EQUIVALENT SYSTEM

The present system of dose limitation used by DOE is based on the maximum value of dose equivalent that results at any point in a cylindrical phantom of uniform composition subjected to a normally incident beam of radiation. This approach does not take into account the different radiosensitivities of various tissues in the body. The January 1987 Presidential Directive (1) mandates the determination of effective dose equivalent (EDE), but there is little guidance for this determination for external exposures. This task will thus develop a methodology to determine EDE and demonstrate a practical dosimetry system for its determination for external irradiations.

Preliminary calculations were started in FY 1987 using a Monte Carlo computer code, MCNP, and the Medical Internal Radiation Dose (MIRD) anthropomorphic phantom. Calculations demonstrated that EDE at various depths is less than dose equivalent based on measurements made at the surface of the body. The following seven tasks have been identified for this project:

- A comparison will be made of the state-of-the-art neutron transport codes to determine if significant differences result from the calculations themselves.
- When the Monte Carlo calculations are completed, a simple utility code containing the necessary conversion factors will be written to enable the calculation of EDE for specific work conditions (neutron spectra and irradiation geometry).
- The best phantom available for mathematical calculations is the MIRD-V phantom. This model will be modified to be more accurate

for external irradiations, and additional organs will be specified.

- The requirements of DOELAP and consistency with internal dosimetry methods for adding internal and external doses will be included.
- Provisions will be made for acquiring and incorporating field data on neutron energy spectra, kerma or absorbed dose, and irradiation geometry.
- Criteria will be established for dosimeter response, placement of dosimeter, and interpretation of multiple dosimeters in order to provide the information required concerning neutron energy spectra and irradiation geometry.
- Criteria and methodologies will be established for determining EDE for partial body irradiations and for coordinating with the methods used for internal dosimetry.

#### SUPERHEATED DROP DETECTOR

Apfel Enterprises is developing a Superheated Drop Detector (SDD) for the measuring of neutron dose. The SDD system being developed consists of superheated fluorocarbons suspended in a viscous gel. Charged particles or neutron recoils trigger nucleation in the superheated liquid drop, and the stored energy is released very quickly (the drops pop). The acoustic signals generated by the process are detected, amplified, filtered, passed through a discriminator, and displayed digitally.

Advantages of SDDs include their insensitivity to gamma rays, their flexibility to provide crude spectral data, and their flexibility for providing active or passive data.

Problems encountered with the first prototype SDD system included overflow of the detector vials and their temperature, dose rate, and energy dependence.

#### OPTICAL TRACK DETECTOR FOR NEUTRON DOSIMETRY

Oak Ridge National Laboratory (ORNL) is conducting a feasibility and practicality study for an optical track detector for neutron dosimetry.

When a charged particle enters or originates in a chamber, it leaves a trail of subexcitation electrons. In addition, the particle electronically excites the gas molecules, which quickly emit light. The optical radiation thus produced by the excited molecules is used to trigger a high voltage, damped RF pulse generator, which is applied across the electrodes of the chamber. The electrons in the particle track are rapidly accelerated back and forth under the influence of the oscillating field, gaining sufficient energy to excite and ionize the surrounding gas. The light emitted by the gas molecules from the electronic excitation is imaged simultaneously by two digital solid-state cameras scanning across two perpendicular planes. The camera images are stored and analyzed in a computer for three-dimensional reconstruction of the track. The data will

be related directly to dose and LET distributions. Algorithms for obtaining the neutron energy spectrum will also be developed.

#### LLNL PORTABLE NEUTRON SPECTROMETER

Lawrence Livermore National Laboratory (LLNL) has proven the feasibility of an improved portable neutron spectrometer that uses a compact liquid-scintillator detector with an optimum combination of sensitivity, resolution, and response function. A stable light pulser will be included for calibration. The gain in the detector system will be established using the signal produced in the photomultiplier, a light pulser. This circuit will also stabilize variations in photomultiplier gain that occur as a function of temperature. Gamma sources will not be required for calibration.

Computerized data accumulation techniques and data reduction programs will be developed to display the data in real time with minimum operator involvement. These programs will be optimized for use in the field.

#### CONCLUSIONS

The U.S. Department of Energy, through the Personnel Neutron Evaluation and Upgrade Program, has historically developed and evaluated new neutron measurement technologies. Because of these continuing efforts, state-of-the-art systems have been developed for DOE facilities, and the technologies have been transferred to the commercial sector.

All research proposals are evaluated by a peer review group and prioritized according to their likelihood of improving personnel neutron dosimetry and their applicability to field use at DOE facilities.

#### ACKNOWLEDGMENT

This work was performed for the U.S. Department of Energy under Contract DE-AC06-76RLO 1830.

#### REFERENCES

1. The President: Radiation Protection Guidance to Federal Agencies for Occupational Exposure; Approval of Environmental Protection Agency Recommendations, 52 Fed. Reg. 2822-34 (January 27, 1987).
2. International Commission on Radiological Protection (ICRP). 1977. Recommendations of the International Commission on Radiological Protection. ICRP Publication 26, Pergamon Press, New York, New York.
3. National Council on Radiation Protection and Measurements (NCRP). 1971. Protection Against Neutron Radiation. NCRP Report No. 38, Washington, D.C.

## COMPUTATIONAL INDIVIDUAL NEUTRON DOSIMETRY AT THE PTB

R Jahr, R Hollnagel, B R L Siebert  
Physikalisch-Technische Bundesanstalt, Braunschweig, FRG

### 1. INTRODUCTION

Individual dosimetry is complicated due to the fact that a multitude of different exposure situations must be envisaged. Here, irradiations from the frontal half-space are particularly important in practice. As an interesting example, the AP (anterior-posterior) exposures are considered by a neutron point source at variable distances from the trunk. The duration of the exposure for each distance is assumed to be adjusted such that the incident fluence at a point 10 mm below the 'representative location' of the trunk remains constant. It can then be shown<sup>(1)</sup> that the smaller the distance the more the individual dose equivalent,  $H(10)$ , at this location<sup>(2)</sup> exceeds the effective dose equivalent,  $H_{\text{eff}}$ . Great distances are obviously more critical, therefore fluence distributions of neutrons incident from sources at great distances, i.e. expanded fields<sup>(2)</sup>, are of chief consideration in our calculations.

The requirements which dosimeters must meet with respect to the direction ( $\Omega$ ) and energy ( $E$ ) dependence, depend on how much - besides the dose measurement - is additionally known of the radiation field, for instance from directional and spectrometric measurements. If the fluence distribution of incident neutrons with respect to  $\Omega$  and  $E$ , as it appears in a frame of reference fixed within the individual's trunk, is fully known and remains constant, then a simple dosimeter comprising only one single detector is usually sufficient. The dose equivalent (briefly termed 'dose' in the following) measured with such a single detector (Index 's') is

$$\tilde{H}_s = U_s \cdot M_1 \quad (1)$$

where  $M_1$  is the detector reading and  $U_s$  the calibration factor, i.e. a constant which is determined under calibration conditions. If the actual exposure conditions differ from these, then the measured dose  $\tilde{H}_s$  may deviate from the true dose  $H$ . For an ideal dosimeter, the relative response

$$r_s = \tilde{H}_s / H \quad (2)$$

should be equal to one, independent of the exposure conditions. This property is by no means satisfied for detectors such as albedo or track-etch detectors. These are not really dosimeters but only monitors, referred to as 'detectors' in the following. They fail if the actual exposure conditions deviate from the calibration conditions, and this must be reckoned with if

little or nothing is known about the  $\Omega$  and E fluence distributions of the incident neutrons. In the particular case of a radiation component incident on the individual's back, the trunk will shield such a single detector when worn at the front, thus giving rise to dangerous underestimates of the dose. In all these perhaps less frequent cases where single detectors fail, a trustworthy solution to the problem of the dose measurement is also needed. It is then usually not possible to avoid combining several 'badly' performing detectors to form a dosimeter system which is less dependent on the actual exposure conditions. It is fair to say that the investigation of such dosimeter systems is a general and important task in the individual dosimetry.

According to rather general superposition considerations<sup>(3,4)</sup> the measured dose  $\tilde{H}$  must be a linear superposition of the readings  $M_i$  (where  $i = 1, 2, \dots, I$ ) of the I detectors, making up the dosimeter system

$$\tilde{H} = \sum_i U_i M_i \quad (3)$$

$U_i$  are the calibration factors, i.e. a set of constants determined under calibration conditions. This raises two important questions. First, how can the  $U_i$  be optimized; secondly, how large is the deviation of the measured dose  $\tilde{H}$  from the true dose H under actual exposure conditions, i.e. what is the magnitude of the relative response of the dosimeter system, r? The latter is given by

$$r = \tilde{H} / H = \left( \sum_i U_i M_i \right) / H \quad (4)$$

and should be equal to one.

A general discussion of this problem can be found in<sup>(3,4)</sup>. Depending on the particular situation these questions can be dealt with either by expanding the fluence distribution of the incident neutrons in terms of 'standard fluence distributions', or by expanding the fluence-to-dose conversion factor in terms of the fluence response of the detectors. This is further explained in Sect. 2.

The first expansion will be applied to the example of an 'arbitrary' directional fluence distribution of incident neutrons, measured by a system of two identical albedo detectors worn on the chest and the back, respectively (Sect. 3).

The second expansion will be used in another example for a system of one albedo and one track-etch detector worn on the chest, if the exposure is restricted to the frontal half-space (Sect. 4).

## 2. CALIBRATION IN THE FRAMEWORK OF THE CONCEPT<sup>(3,4)</sup>

### 2.1 Basic Idea behind the Concept

Dealing with the first expansion, the actual fluence distribution of incident neutrons with respect to  $\Omega$  and E in a frame of reference fixed within the individual's trunk, is approximately expanded into a set of  $g = 1, 2, \dots, G$  different 'standard fluence distributions' encountered as more or less strong components in actual radiation fields<sup>(3,4)</sup>:

$$\phi_{\Omega, E} \cong \sum_g \phi_{\Omega, E}^g \quad (5a)$$

By integration over  $\Omega$  and  $E$

$$\phi \cong \sum_g \phi^g \quad (5b)$$

is obtained. The parameters  $\phi^g$  reflect the overall intensity with which the  $g$ -th normalized distribution, i.e.  $\phi_{\Omega,E}^g / \phi^g$ , contributes to the actual radiation field. Eq. (5a) can therefore represent a multitude of different radiation fields which differ in their 'fit parameters'  $\phi^g$  but have the same set of normalized standard fluence distributions.

The reading of the  $i$ -th detector, and the true dose, are composed of the fractions due to these field components:

$$M_i \cong \sum_g M_i^g \quad (6)$$

$$H \cong \sum_g H^g \quad (7)$$

Here,

$$M_i^g = \int_0^\infty \int_{4\pi} R_i(\Omega, E) \cdot \phi_{\Omega,E}^g \cdot d\Omega \cdot dE = \phi^g \cdot \langle R_i \rangle^g \quad (8)$$

$$H^g = \int \int P(\Omega, E) \cdot \phi_{\Omega,E}^g \cdot d\Omega \cdot dE = \phi^g \cdot \langle P \rangle^g \quad (9)$$

where  $R_i(\Omega, E)$  is the direction and energy dependent fluence response of the  $i$ -th anthropomorphic phantom and  $P(\Omega, E)$  the direction and energy-dependent fluence-to-dose conversion factor. The right-hand sides of these equations define the average values  $\langle R_i \rangle^g$ ,  $\langle P \rangle^g$  which in the following are considered to be well-known quantities:  $\langle R_i \rangle^g$  can be either measured by determining  $M_i$  and  $\phi^g$  (eq. 8) or calculated<sup>(5,9)</sup> from the experimental free-in-air responses, the backscattering from the phantom and the incident fluence distribution<sup>(6-8)</sup>  $\phi_{\Omega,E}^g$ .  $\langle P \rangle^g$  is usually calculated using the Monte Carlo method<sup>(3,4)</sup>.

The essential point of the concept<sup>(3,4)</sup> consists in deriving the calibration factors sought from the following set of equations:

$$\langle P \rangle^g \cong \sum_i U_i \cdot \langle R_i \rangle^g \quad (10)$$

where  $i=1,2,\dots,I$  and  $g=1,2,\dots,G$ . The number of detectors,  $I$ , is usually smaller than the number of radiation field components,  $G$ , and therefore the  $U_i$  are overdetermined. Eq. (10) can then be satisfied only approximately. According to eqs. (7,9,10,8,6,3), the true dose is

$$H \cong \sum_{i,g} U_i \phi^g \langle R_i \rangle^g = \sum_i U_i \sum_g M_i^g = \tilde{H} \quad (11)$$

The right-hand side is the dose measured by the dosimeter system. From this and eq. (4) the relative response of the dosimeter system in the actual exposure situation is obtained

$$r = \tilde{H} / H \cong 1$$

The fact that the right hand side is merely an approximation follows from eqs. (5a) and (10). It expresses the fact that the relative response of the dosimeter system will still depend on the actual exposure conditions, though to a lesser extent than in the case of a single detector.

The second expansion mentioned in Sect. 1 starts out from the fact that eqs. (8,9) are valid for an arbitrary distribution of incident neutrons and that it is therefore admissible to omit the upper index 'g'. the requirement that  $r \cong 1$  (see eq. 4) is then equivalent to

$$P(\Omega, E) \cong \sum_i U_i R_i(\Omega, E) \quad (12)$$

where the  $U_i$  are obtained as fit parameters. Using the analogue of eqs. (8,9) one arrives again at

$$\langle P \rangle \cong \sum_i U_i \langle R_i \rangle \quad (10')$$

The relative response for the arbitrary neutron distribution is then obtained from eq. (4) as

$$r = (\sum_i U_i M_i) / H = (\sum_i U_i \langle R_i \rangle) / \langle P \rangle \cong 1$$

## 2.2 Calibration Procedure

The calibration in the case of the first expansion is performed in three steps: In the first step, a physically significant expansion, eq. (5a), must be found. In the second step, the data of  $\langle R_i \rangle^g$  and  $\langle P \rangle^g$  must be determined as described in the previous section. In the final step, (3,4) (10) must be solved for the  $U_i$  using well-known mathematical algorithms. As a result, a set of calibration factors  $U_i$  is obtained which is to be kept constant for subsequent practical applications. In the case of the second expansion the  $U_i$  are obtained from eq. (12).

Calibration in a general, more complete sense requires an additional step, namely the determination of the relative response (eq. 4) for a variety of actual exposure conditions encountered in practice, i.e. a quality test of the dosimeter system, using the constant set of  $U_i$ .

## 2.3 Dose Quantities

Apart from some exceptional exposure situations, the effective dose equivalent  $H_{eff}$  is usually the most stringent primary limited dose quantity. Its fluence to dose conversion factors  $P_{eff}(\Omega, E)$  were approximately calculated<sup>(7)</sup> using the MIRD phantom. Thus, in principle  $H_{eff}$  can serve as the 'true dose',  $H$ , in the framework of our concept. In fact, this appears to be the only practicable procedure in our first example (Sect. 3).

On the other hand, the ICRU has proposed operational quantities in the ICRU sphere and, in the case of exposures from the frontal half-space, it would appear expedient to use such a quantity for individual dosimetry, too. We have argued<sup>(1)</sup> in favor of a quantity  $H^1(10)$  which can be very well approximated by the directional dose equivalent  $H'(10)$  defined by the ICRU<sup>(2)</sup>. The latter has therefore been chosen as the 'true dose' in the second example (Sect. 4).

### 3. FIRST EXAMPLE: TWO ALBEDO DETECTORS WORN ON CHEST AND BACK

The performance of albedo dosimeters in neutron fields with unknown directional distributions is investigated. The case in which one single albedo detector is worn on the chest only is compared with the case in which a second albedo detector is placed on the back of the individual.

The directional distribution of the incident neutron fluence is expanded in terms of three components incident from the AP (anterior-posterior), LAT (lateral) and PA (posterior-anterior) directions, corresponding to  $g = 1, 2, 3$  in eq. (5a):

$$\phi_{\Omega, E} \cong \phi_E \cdot \sum_{g=1}^3 \phi_{\Omega}^g \quad (13)$$

Here, the unknown directional fluence distribution is represented by the three arbitrary parameters  $\phi_{\Omega}^g$ . The common factor  $\phi_E$  corresponds to a normalized energy spectrum, for instance a  $D_2O$  moderated  $^{252}Cf$  or a monoenergetic neutron spectrum. In order to solve eq. (10) for the calibration constants  $U_i$ , the data of  $\langle R_i \rangle^g$  and  $\langle P_{eff} \rangle^g$  were needed. The former was taken from previous calculations of a simplified albedo dosimeter<sup>(5)</sup>, the latter from calculations of Wittman et al.<sup>(7)</sup>.

Before considering further the cases with one or two detectors, the well-known strong energy dependence of albedo detectors must be taken into consideration. This means that the relative responses in both cases,  $r$  (eq. 2) in the case of the single detector and  $r$  (eq. 4) in the case of the dosimeter system, will strongly depend on the energy. In other words, the addition of a second albedo detector cannot substantially improve the poor energy dependence. In order to formally eliminate the strong energy dependence, a 'relative directional response' can be defined by

$$\tilde{r} = r / r_s^1 = \frac{U_s^1}{r_s^1} \cdot \frac{\tilde{U}_1 \cdot M_1 + \tilde{U}_2 \cdot M_2}{H_{eff}} \quad (14)$$

where  $U_s^1$ ,  $r_s^1$  refer to the single dosimeter quantities introduced by eqs. (1,2) for the special  $g = 1$  or AP exposure condition. The definition of the 'relative calibration factors'  $\tilde{U}_i$  is obtained by comparing this equation with eq. (4):

$$\tilde{U}_i = U_i / U_s^1 \quad (15)$$

#### 3.1 A Single Albedo Detector on the Chest

Eq. (10) must be solved with  $I = 1$  (one detector) and  $G = 3$  (three field components), i.e.  $U_1$  is (over)determined by three linear independent equations. In view of the great importance of the AP exposure the first of these, i.e.  $g = 1$ , is usually chosen to determine  $U_1$ , thus neglecting the remaining two. Using eqs. (8,9,1,2) with  $r_s = 1$ , the calibration constant is obtained from the first eq. (10) as

$$U_1 = \frac{\langle P_{eff} \rangle^1}{\langle R_1 \rangle^1} = \frac{H_{eff}^1}{M_1^1} = U_s^1 \quad (16)$$

which according to eq. (15) is equivalent to the relative calibration factor

$$\tilde{U}_1 = 1 \quad (17)$$

The final step is the examination of the relative directional response  $\tilde{r}$  which is obtained from eqs. (14,17,6-9) using  $\tilde{U}_2 = 0$ :

$$\tilde{r} = \frac{U_s'}{r_s'} \cdot \frac{M'}{H_{eff}'} = \frac{U_s'}{r_s'} \frac{\sum_g \langle R_1 \rangle^g}{\sum_g \langle P_{eff} \rangle^g} \quad (18)$$

For a pure AP exposure, i.e.  $g = 1$ ,  $M_1/H_{eff}' = M_1^1/H_{eff}'^1 = \langle R_1 \rangle^1 / \langle P_{eff} \rangle^1$ .

Eqs. (2,1) then result in  $r_s^1 = U_s^1 M_1^1 / H_{eff}'^1$  and thus, as expected,

$$\tilde{r} = 1 \quad (19)$$

This result does not hold in the case of general directional distributions. For instance, for pure PA exposures, i.e.  $g = 3$ , the relative directional response  $\tilde{r}$  can be as small as 0.1 which is a dangerous underestimate of the true dose<sup>(10)</sup>. This reflects the simple fact that under these conditions the albedo detector is shielded by the trunk.

### 3.2 The System of Two Albedo Detectors

This case has been recently discussed<sup>(10)</sup>. The calibration factors  $U_1$  and  $U_2$  are determined by the three linear independent eqs. (10). The approximate solution was not obtained by the familiar least-squares method but by means of an algorithm similar to linear programming. Assuming a  $D_2O$ -moderated  $^{252}Cf$  spectrum, the following relative calibration factors were obtained

$$\tilde{U}_1 = 0.938 \quad \tilde{U}_2 = 0.515 \quad (20)$$

The relative directional response of the dosimeter system (eq. 14) in this neutron spectrum in which the AP, LAT, and PA components (i.e.  $g = 1,2,3$ ) are arbitrarily combined, was then shown<sup>(10)</sup> to be

$$0.90 \leq \tilde{r} \leq 1.04 \quad (21)$$

Fig. 1 shows the limits of  $\tilde{r}$  if the same calibration factors (eq. 20) are used in monoenergetic neutron fields with arbitrary AP, LAT and PA components.  $\tilde{r}$  never falls below 0.8, but for lateral exposures it can exceed 2.5 in the MeV range. The latter, however is a favorable increase in the poor albedo response at higher energies.

To summarize, the system of two albedo detectors is clearly superior to the single detector if the directional distribution of incident neutrons is unknown.

### 4. SECOND EXAMPLE: SYSTEM OF ALBEDO AND TRACK-ETCH DETECTORS

Track-etch detectors are known to be a good complement to albedo detectors if the energy dependence of the response is to be reduced. Here the second expansion mentioned in Sects. 1, 2 was considered to be adequate. The aim

of our recent study<sup>(11)</sup> was to investigate by means of calculational methods

- a) the energy dependence of the response on the phantom
- b) the influence of various directional distributions of the incident neutrons
- c) the influence of various distances between the dosimeter system and the phantom
- d) the reading ratio  $M_1/M_0$  of the inner and outer  $^6\text{LiF}$  detector of the albedo dosimeter<sup>1</sup> (see insert of Fig. 2)
- e) the contribution to the detector reading of neutrons backscattered from the phantom.

Regarding a) Fig. 2 shows the energy dependence of the relative response (with respect to  $H'(10)$ ) for various detector systems.  $A(\beta)$  refers to the response of the inner albedo detector,  $M_1$  (see insert of Fig. 2).  $G$  and  $G(\beta)$  refer to track-etch detectors whose free-in-air response was adopted from Griffith et al.<sup>(12)</sup>,  $G$  referring to a constant directional response,  $G(\beta)$  to a response proportional to  $\cos\beta$ . The terms  $B$  and  $B(\beta)$  are related to a track-etch detector coated with a hydrogenic radiator according to Benton et al.<sup>(13)</sup>, where a constant and a directional free-in-air response proportional to  $(1-\beta/90^\circ)$  respectively was assumed. The curves  $A(40^\circ) + G(\beta)$  and  $A(40^\circ) + B$  illustrate the improvement in the relative response if the two detectors are combined to a dosimeter system. The relative response of this system is further improved, if broad distributions of the incident neutrons are taken into account<sup>(14)</sup>.

The bandwidth of all curves shown in Fig. 2 is the envelope which results from the variation of exposure conditions mentioned as items b) and c): The directions of the incident neutrons were assumed to be limited by a cone with a half-aperture angle of  $10^\circ$ ,  $50^\circ$ ,  $90^\circ$ . The distances assumed were 0.1 and 5.0 cm.

Considering item d): The left hand side of Fig. 3 shows the envelopes of the reading ratios  $M_1/M_0$  for three albedo detectors with different collimation (see insert of Fig. 2). They increase monotonically with the energy and corroborate the known fact that the value of  $M_1/M_0$  is characteristic of a neutron spectrum. The left-hand side of the figure shows the fraction of albedo detector reading due to backscattering,  $M_1(\text{scatt})/M_1$ , too. This fraction is near 1.0 except for the energy range 1 eV to 10 keV, where the incident neutrons contribute up to 70 % to the reading.

The backscattering for track-etch detectors is shown on the right-hand side of Fig. 3. It is typically lower than for albedo dosimeters but still reaches values of up to 35 % in the case of the Griffith<sup>(12)</sup> detector (not shown in the figure).

## 5. SUMMARY AND CONCLUSIONS

As has been known for some time, the investigation of dosimeters composed of several detectors is important in individual dosimetry. The concept<sup>(3,4)</sup> offers a suitable formalism for this task. Computational methods are needed in particular in order to determine the calibration factors defined in eq. (3).

Calibration methods have been briefly discussed for these composed dose-meter systems and a plea made for calibrating the dosimeter on an anthropomorphic phantom and not on the ICRU sphere as recently proposed in the literature. In our opinion, the ICRU sphere is useful for defining dose quantities but not for affixing dosimeters<sup>(1)</sup>.

Computational methods are still needed not only to calculate the fluence-to-dose conversion factors but are also useful for calculating the detector responses as a function of influence parameters such as the distributions of energy and direction of incidence, the influence of the phantom and the distance between dosimeter and phantom. These methods allow the influences to be studied more systematically than in experiments.

The power of computational methods was illustrated in two examples. First, a system of two albedo detectors was shown to have good dosimetric properties even in radiation fields with unknown directional distributions of incident neutrons. In this case, the effective dose equivalent is an indispensable dose quantity.

Secondly, the effect of the influence parameters was studied for dosimeter systems of albedo and track-etch detectors worn on the chest. The directional dose equivalent appears to be an adequate dose quantity in this case.

#### ACKNOWLEDGEMENT

This work was supported by the Commission of the European Communities, Brussels, Belgium, under contract no. BI-6-012-D.

#### REFERENCES

- 1) R. Jahr, B.R.L. Siebert, W.G. Alberts. Seminar on implementation of dose-equivalent operational quantities into radiation protection practice, Braunschweig, 1988. (to be published in Rad. Prot. Dos.)
- 2) ICRU Report 39 (1985). International Commission on Radiation Units and Measurements.
- 3) B.R.L. Siebert, R. Hollnagel and R. Jahr. Phys. Med. Biol. 28 (1983)521.
- 4) B.R.L. Siebert, R. Hollnagel and R. Jahr. PTB-Report PTB-ND-21 (1983).
- 5) R. Hollnagel, R. Jahr, B.R.L. Siebert. Proc. 5th Sympos. Neutron Dos., EUR 9762, I, 123 (1983).
- 6) R. Jahr, R. Hollnagel, B.R.L. Siebert. Rad. Prot. Dos. 10 (1985)75.
- 7) A. Wittmann, A. Morhart, G. Burger. Rad. Prot. Dos. 12 (1985)101.
- 8) S.R. Wagner et al. Rad. Prot. Dos. 12 (1985)231.
- 9) R. Hollnagel, R. Jahr, B.R.L. Siebert. Rad. Prot. Dos. 20 (1987)25.
- 10) R. Jahr, R. Hollnagel, B.R.L. Siebert. 6th Sympos. Neutron Dos., München-Neuherberg, 1987 (to be published).
- 11) B.R.L. Siebert, R. Hollnagel, R. Jahr. IVth European Congress of IRPA, Salzburg, 1986 (to be published).
- 12) R.V. Griffith, et al. Rad. Prot. Dos. 1 (1981)61.
- 13) E.V. Benton, R.A. Oswald, A.L. Trank (1981). Health Phys. 40 (1981)801.
- 14) B.R.L. Siebert, R. Hollnagel, R. Jahr. Rad. Prot. Dos. 12 (1985)119.

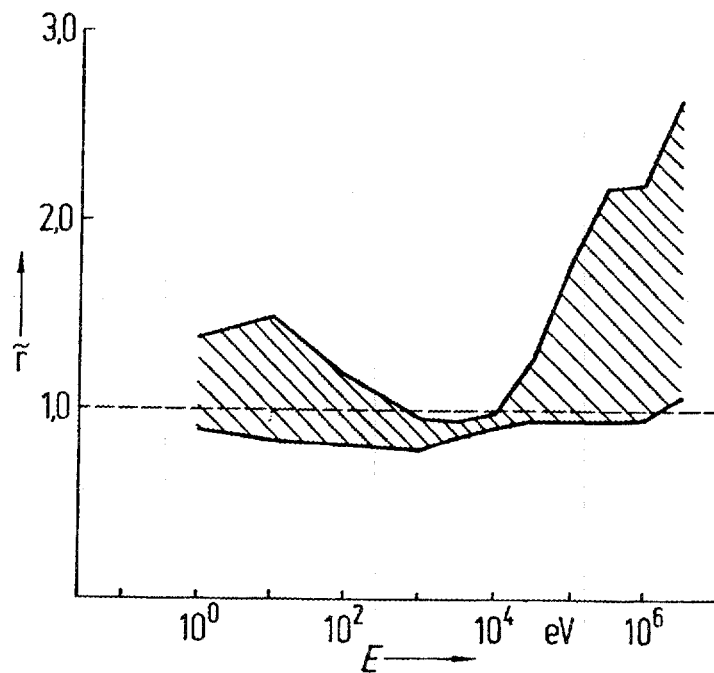


Fig. 1: Limits of the relative directional response for a system of two albedo detectors using the relative calibration factors eqs.(20)

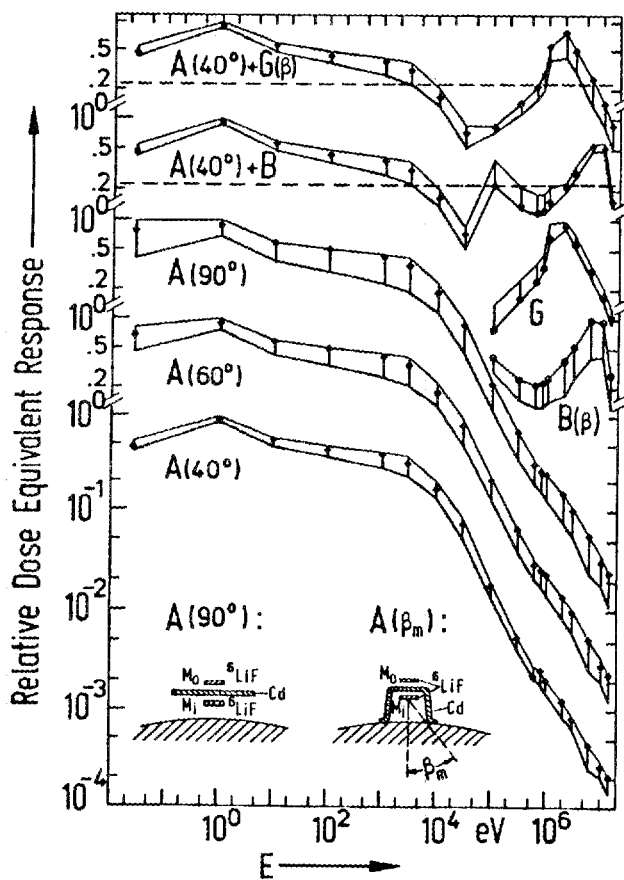


Fig. 2: Relative dose-equivalent response for various dosimeters vs. neutron energy. In the calculation for thermal energies, the screening of the phantom by the cadmium shield of the albedo dosimeter had not yet been taken into account. Thus the true response at this energy should be lower.

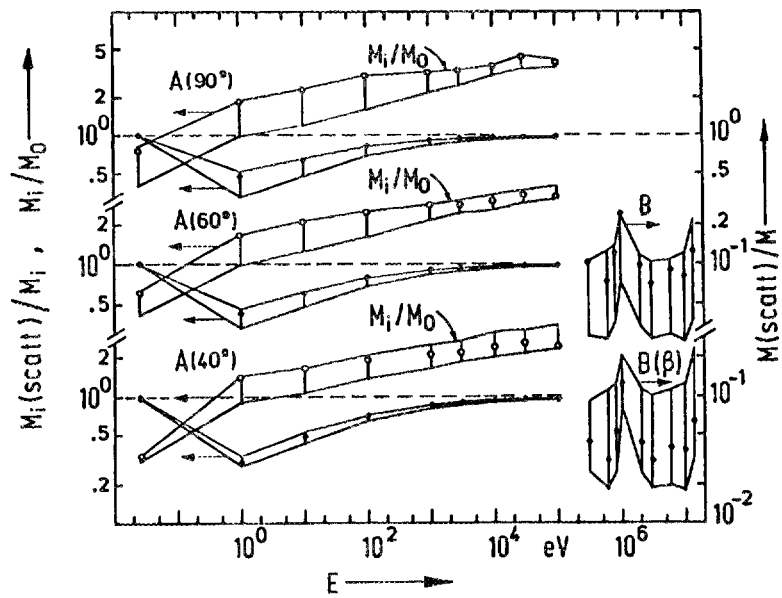


Fig. 3: Fraction of doseimeter reading due to neutron backscattering,  $M_i(\text{scatt})/M_i$ , and ratio of readings  $M_i/M_0$  for albedo doseimeters. The right-hand side shows  $M(\text{scatt})/M$  for track-etch detectors. For notation and comments see fig. 2 and text.

# PERSONNEL NEUTRON DOSIMETRY APPLICATIONS OF TRACK-SIZE DISTRIBUTIONS ON ELECTROCHEMICALLY ETCHED CR-39 FOILS\*

*Dale E. Hankins, Steven G. Homann, and Joane Westermark*

Hazards Control Department, Lawrence Livermore National Laboratory,  
Livermore, CA 94550

## ABSTRACT

The track-size distribution on electrochemically etched CR-39 foils can be used to obtain some limited information on the incident neutron spectra. Track-size distributions on CR-39 foils can also be used to determine if the tracks were caused by neutrons or if they are merely background tracks (which have a significantly different track-size distribution). Identifying and discarding the high-background foils reduces the number of foils that must be etched. This also lowers the detection limit of the dosimetry system. We have developed an image analyzer program that can more efficiently determine the track density and track-size distribution, as well as read the laser-cut identification numbers on each foil. This new image analyzer makes the routine application of track-size distributions on CR-39 foils feasible.

## INTRODUCTION

We have developed a personnel neutron dosimeter for use at the Lawrence Livermore National Laboratory (LLNL). The fast neutron detector consists of CR-39 plastic that is electrochemically etched at elevated temperatures. Electrochemical etching is preferred over chemical etching because it improves the neutron energy dependence and because the track sizes are larger, allowing them to be evaluated using automated readers. The dosimetry system<sup>1</sup> and the details of the electrochemical etching process<sup>2</sup> have been described in previous reports.

Although the electrochemical etching process alters the track size, we find that under the right etching conditions the distribution of the track sizes is related to the neutron energy even after the blow-up stage is completed. This relationship between track-size distribution and neutron energy can provide some general information on the incident neutron spectrum. At this time, the primary use of the track-size distribution information is to distinguish between foils having a neutron exposure and foils with a high background (caused by defects in the foil). Eliminating the results from high-background (defective) foils improves the accuracy of the dosimetry system and eliminates the need to etch additional foils from personnel badges.

## IMAGE ANALYSER DEVELOPMENT

An image-analyzer system has been developed at LLNL that enables us to determine the track density and track-size distribution on a CR-39 foil in the same time previously required to determine the track density with the formerly used Biotran colony reader. The image analyser consists of a Hewlett Packard Vectra computer (equivalent to an IBM AT personal computer) with 4 Mbytes of extended memory, a data translation frame grabber board, and a Dage model 650 camera connected to standard Nikon microscope. Approximately 1.5 minutes is now

---

\* Work performed under the auspices of the U.S. Department of Energy by Lawrence Livermore National Laboratory under Contract W-7405-Eng-48.

required to process each CR-39 foil; we hope to reduce this to less than one minute in the future.

The image analyzer displays the track-size distribution, the number of tracks, and percent of tracks in each of 20 bins. A printer records the track density (tracks/cm<sup>2</sup>) and the number of tracks and the percentage of tracks in each of the 20 bins.

The laser that cuts the CR-39 sheets into foils is also used to etch an identification number at one end of the foil. The image analyzer software is being modified to include pattern recognition of these numbers.

To fully automate the reading of the CR-39 foils, we are purchasing a computer-controlled stage for the microscope and a mechanism to automatically load and remove a foil from the microscope stage. When this is completed, the computer program will be rewritten to include the loading, identification, reading, unloading, and data storage to personnel dosimetry records.

### CHANGES IN ETCHING AND READING PROCEDURES

The best resolution of the track-size distributions occur when the foils are etched for three hours in place of the five hours we had been using for several years. Therefore, to make use of track-size distributions in our personnel neutron dosimetry program, the etching time was reduced to three hours, although this decreases the sensitivity of the foils. To partially compensate for this decreased sensitivity, we changed the orientation of the foils in the badge. The side of the foil to be etched is now positioned facing away from the wearer (toward the incident neutrons). The net result is a reduction in the sensitivity of the foils from 7 to about 5 tracks/cm<sup>2</sup>-mrem.

Previously six microscope fields of view (each about 0.09 mm<sup>2</sup>) were used to determine the track density on a CR-39 foil. This was changed to three larger fields of about 0.2 mm<sup>2</sup> by using a lower magnification on the microscope. This lower magnification eliminated the need to focus the microscope because of the increased depth of field (about 30 mils before changes in track density or track-size distributions become apparent). Our nominal CR-39 foil thickness is about 25 mils: Therefore, once we focus, no further focusing is required.

At the lower microscope magnification, the light intensity across the microscope's field of view is not uniform. This causes the reported size of a track to be dependent on where in the field of view the track is located. To solve this problem, the image analyser software was modified to include a light-intensity correction for each field of view.

### TRACK-SIZE DISTRIBUTIONS

The size of a CR-39 track depends on the incident neutron energy. When a CR-39 foil is exposed to neutrons, some of the neutrons react with hydrogen to produce recoil protons. These protons break chemical bonds along their paths in the CR-39. The etching rate along the path of a recoil proton is a function of the density of the chemical bonds that were broken. The highest density of broken bonds results from recoil protons (with the highest LET produced by neutrons having energies from about 500-700 keV. These protons produce the largest tracks. The recoil protons from neutrons with either lower- or higher-energy neutrons (up to 5.0 MeV) break fewer bonds and thus yield a reduced etching rate. At higher neutron energies, recoil carbon and oxygen atoms or alpha particles are created. These recoil atoms and alpha particles have higher LET than protons and create a high density of broken chemical bonds, and the etched tracks are larger than those produced by protons.

Track-size distributions obtained using a three-hour etch with a 30-minute blow-up cycle are shown in Fig. 1 for <sup>252</sup>Cf and monoenergetic neutron energies

between 152 keV to 16.2 MeV. We cannot precisely determine a specific neutron energy from these track-size distributions, but we can infer information on the approximate neutron energy, particularly in selected energy regions. The interesting feature of these distributions is that there are two distinct peaks, one occurring at neutron energies between 300-800 keV and the second starting at 800 keV up to 5.2 MeV. At 820 keV both of these peaks can be seen. Track-size distributions can be used to approximately determine the energy of monoenergetic neutrons that are between about 300 keV and 1.0 MeV. Above 1.0 MeV the track-size distributions are essentially the same out to 5.2 MeV.

For neutron energies from 13-16 MeV, the neutrons create recoil carbon and oxygen atoms that produce tracks larger than those produced by protons. Large tracks in the distribution can be used to identify exposures from high-energy neutrons; a correction for the underresponse of CR-39 at these neutron energies can be applied to the dosimetry results.

The effects on the track-size distributions caused by changing the etching time are shown in Fig. 2. Longer etching times increase the number of small tracks. This is particularly noticeable at 499 keV where a large increase in small tracks is very apparent. These small tracks can also be seen in the track-size distribution for the  $^{252}\text{Cf}$  neutron source. Since one of our primary interests in using track-size distributions is to determine if low-energy neutrons are present, three-hour etching cycles are preferred. At this time the preferred second stage (blow-up) time is 30 minutes, although we are investigating the effect and possible advantages of using 40 minutes. The number of large tracks in the track-size distribution at 14-16 MeV neutrons remain unchanged by changing the etching time.

Shown at the top of Fig. 3 are the track-size distributions obtained from foils exposed to  $^{252}\text{Cf}$  calibration sources and for foils with no neutron exposure. The tracks on the unexposed foil are caused by chemical defects, dirt, imperfections, abrasion, etc., on the foil. These background track-size distributions are significantly different from those caused by neutron exposures. This allows us to distinguish between tracks from neutron exposures and tracks from other causes. This improves the accuracy of our personnel neutron dosimeters by identifying and eliminating the readings from foils with high defect-caused backgrounds. It also enables us to determine if the second and third CR-39 foils in the personnel badge need to be etched and evaluated. Previously the second and third foils were evaluated if the first foil had a high track density. Now, if the track-size distribution on the first foil is from defect-caused background, we usually do not etch the second and third foils.

The average track-size distribution from foils worn by personnel exposed to spontaneous fission neutrons from Pu is shown in Fig. 3. The track-size distribution is flatter than that obtained with the  $^{252}\text{Cf}$  calibration source because the spectra of the neutrons in the field contain more low-energy neutrons from scattering, moderation, and shielding. Many of these neutrons are in the 300-800 keV region, which produces the largest track sizes (see Fig. 1). Adding tracks from these low-energy neutrons flattens the track-size distribution.

The results from a recent study at the Brookhaven National Laboratory (BNL) are shown in Fig. 3. Two spectral types were identified. One (field #2) contains high-energy neutrons and compares favorably with the track-size distributions from 14-16 MeV neutrons. The other (field #1) does not contain high-energy neutrons. A correction to the dose would be made for the badges exposed in "field #2" but no correction would be made for badges exposed in "field #1".

We are presently participating in a study at the University of California, Davis, campus involving high-energy monoenergetic neutrons. At this time only neutrons at 65 MeV have been used; the track-size distribution obtained is shown

in Fig 3. Other exposures with monoenergetic neutrons having energies between 5 and 65 MeV are planned.

Power-reactor leakage neutrons contain a large component of low-energy neutrons. The track-size distribution from one of these reactors is shown in Fig. 3. The low energy neutrons cause this track-size distribution to be flat. Foils exposed at other reactors have shown track-size distributions indicating even more low energy neutrons. At one reactor the track-size distribution was similar to that shown in Fig. 1 for 499-keV neutrons.

Occasionally some of the CR-39 foils have defects that appear as lines or groups of tracks. The tracks in these lines and groups are usually large and nearly all the same size. This apparently is caused by some surface defect that causes tracks to develop early in the etching process. The track-size distributions from these defects are unique, as shown at the bottom of Fig. 3.

Another unusual track-size distribution is shown in Fig. 3, labeled "bad foils". This is the track-size distribution that normally appears on the back or bad side of the foils. However, it has also been observed on the front of some defective CR-39 sheets.

It is not known why these distributions occur on some foils and not others, or why the back of the foils (side that was down during casting) always has a high background-track density. Frequently, a batch of sheets made at the same time will contain some sheets that are defective, while the others will be satisfactory.

#### ADDITIONAL STUDIES IN PROGRESS

We are investigating changing the evaluation procedure to improve the signal-to-noise ratio of our CR-39 foils. Figure 3 shows that about half of the defective and chemically caused background tracks occur in bins 1 and 2. For practical personnel dosimetry, we may be able to ignore the tracks in these bins. This would reduce the track density on the background foils by about 50%, but the track density on foils exposed to  $^{252}\text{Cf}$  (used for calibration) is reduced by only about 15-20%. The net effect is about a 40% reduction in the background track density. Our preliminary results show that this can be done without increasing the standard deviation of the background track density, which is typically  $\pm 30\%$ . If this procedure can be used, the effective dose equivalence can be reduced from the present 8-10 mrem to about 5-6 mrem. This means that the lower limit of detection (currently about 10 mrem) could be reduced to around 5 mrem. This lower limit of detection is very desirable if the Quality Factor (QF) is to be increased by a factor of 2, as has been proposed.

#### CONCLUSION

We have been able to improve the accuracy and efficiency of our personnel neutron dosimeters by using the track-size distributions on CR-39 foils. This has enabled us to identify and eliminate the readings from foils with high-defect or chemically caused backgrounds. This advance was made possible by the LLNL development of an image analyser designed for this application. We are working to fully automate the reading procedures for the CR-39 foils.

Some limited information on the energy of the incident neutron energy can be obtained by using track-size analysis. This information would be valuable in a dosimetry program if a person were exposed to either high-energy or reactor-leakage neutrons. In both cases a correction factor needs to be applied to the indicated dose to account for the underresponse of the CR-39 at these energies.

#### REFERENCES

## REFERENCES

- (1) Hankins, D.E., Homann, S., and Westermark, J., "The LLNL CR-39 Personnel Neutron Dosimeter," to be published in Radiat. Prot. Dosim. (in press).
- (2) Hankins, D.E., Homann, S.G., and Westermark, J., Personnel Neutron Dosimetry Using Electrochemically Etched CR-39 Foils, Lawrence Livermore National Laboratory, Livermore, CA, UCRL-95350 (1987).

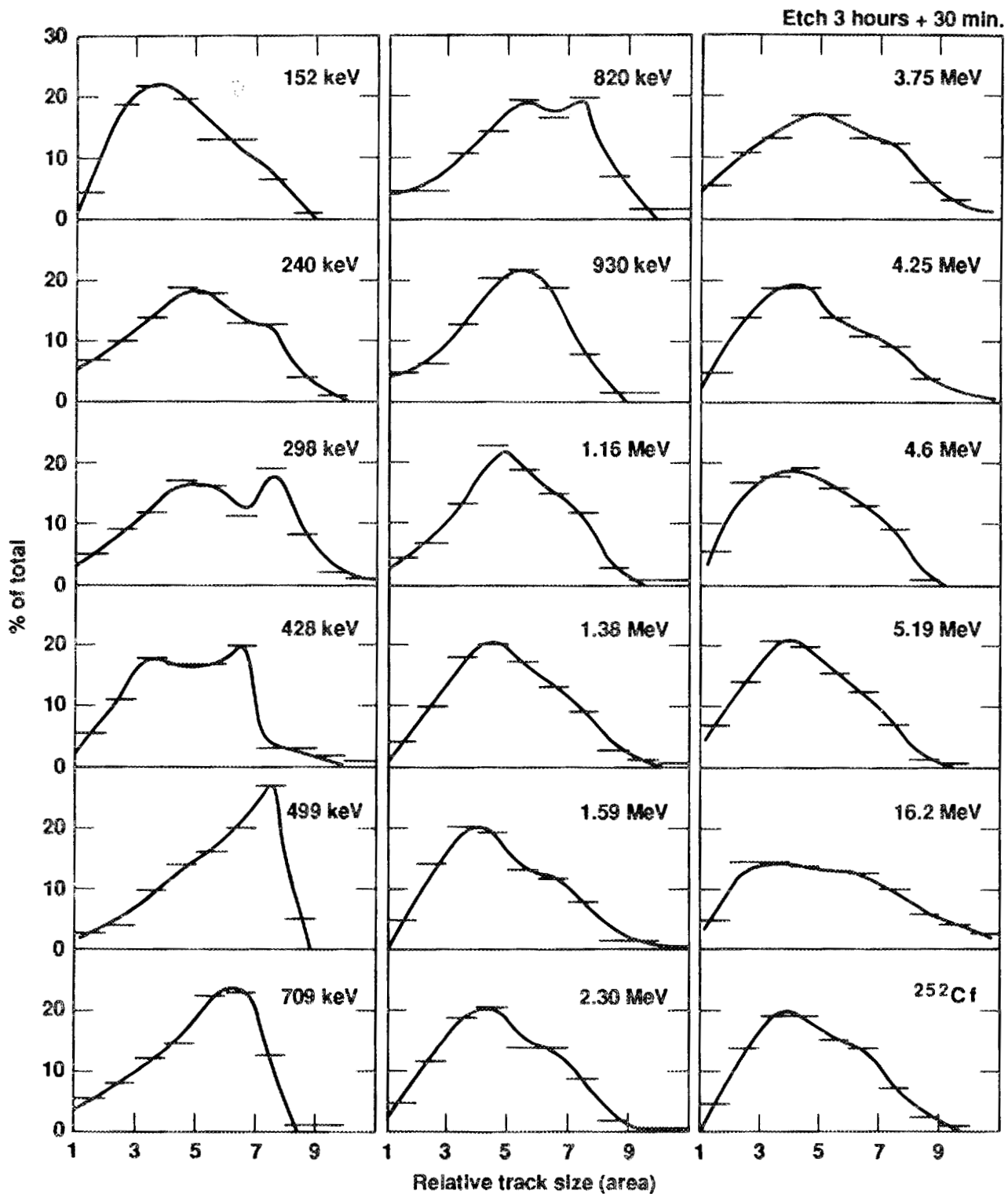


Figure 1. The track-size distribution on electrochemically etched CR-39 foils, obtained with monoenergetic neutrons. The etching conditions were 3 hours at 60 Hz with a 30 minute blow-up stage at 2000 Hz, 3000 V, 6.5 N KOH, and an oven temperature of 60°C.

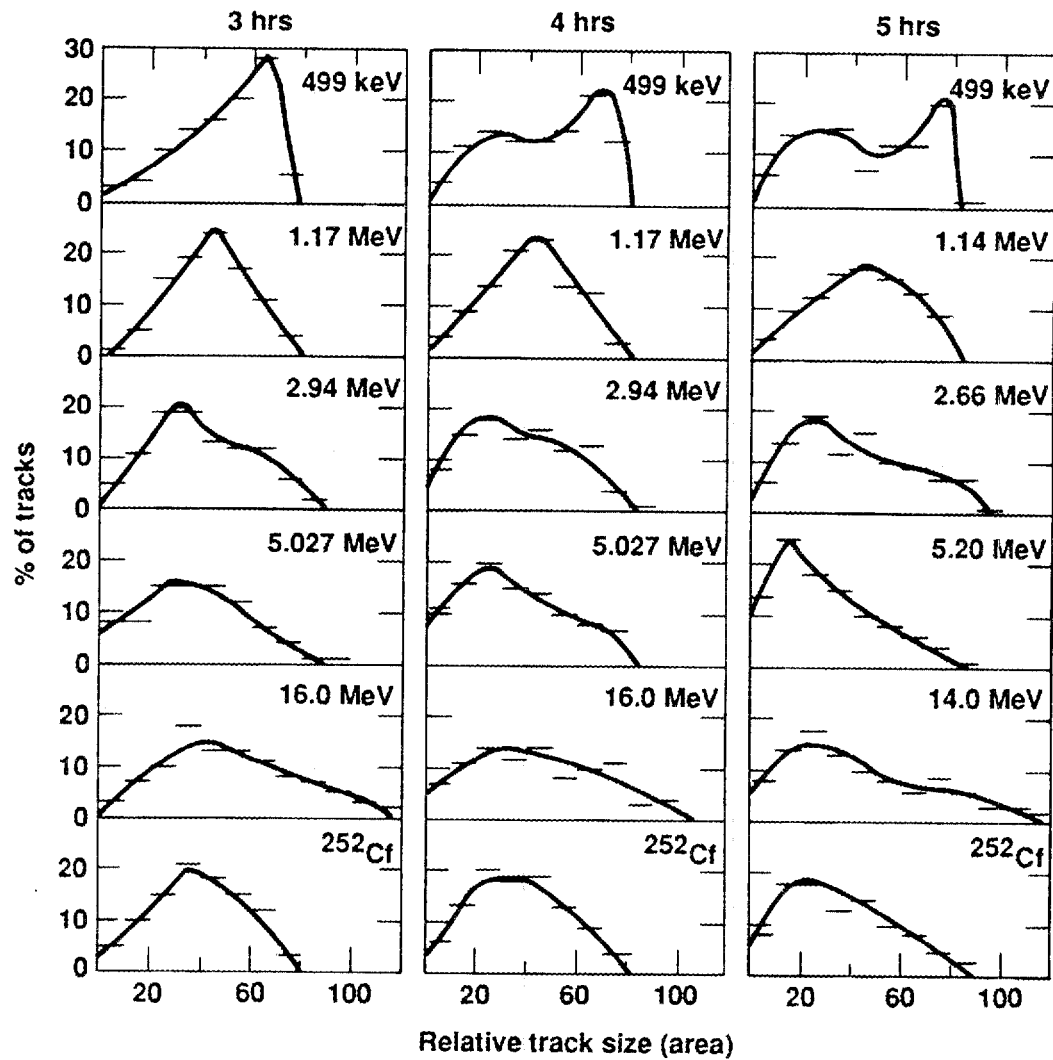


Figure 2. The track-size distributions at selected neutron energies etched using 3, 4, and 5 hours etching cycles. The track-size distributions are different depending on the etching time.

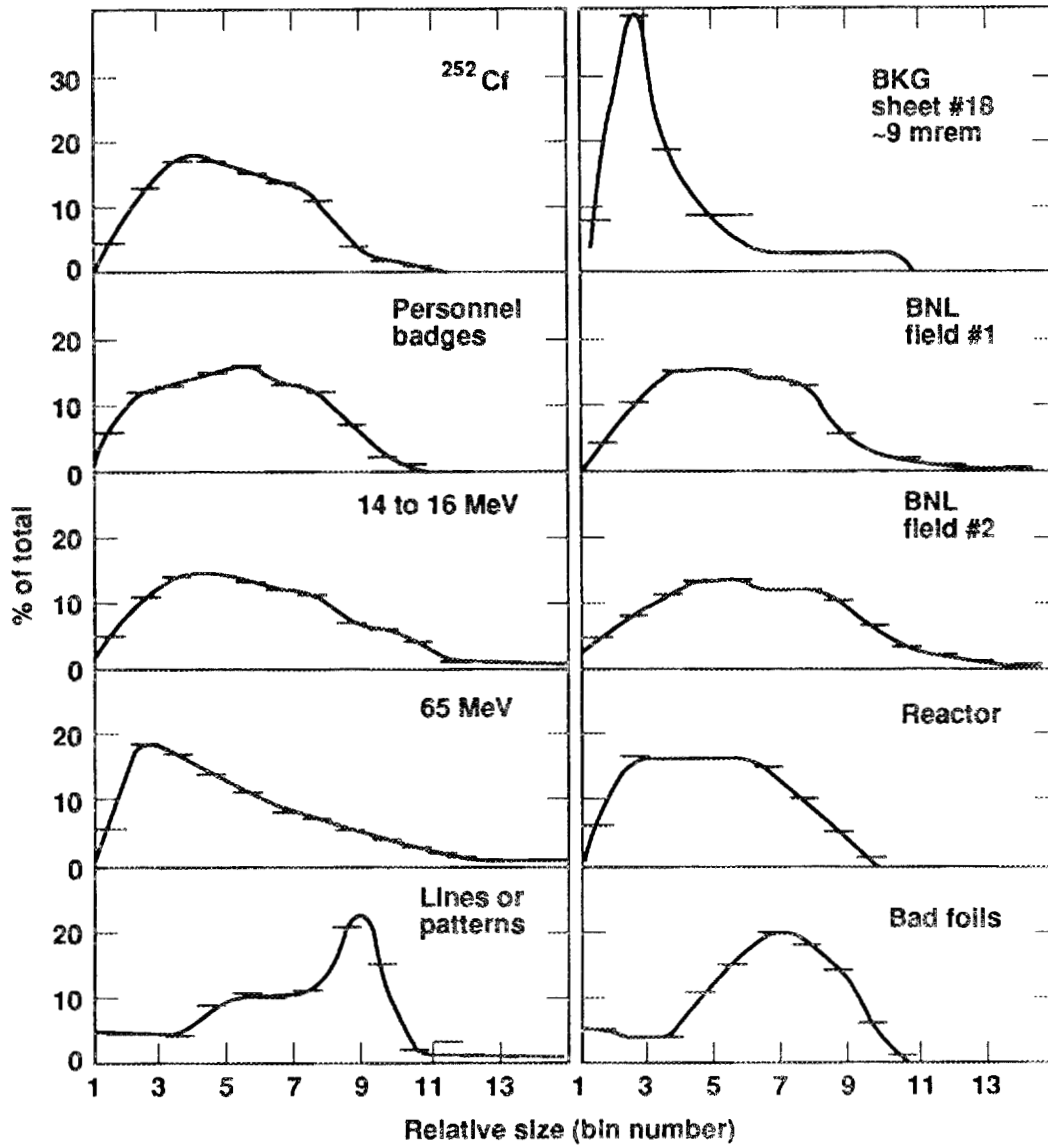


Figure 3. The track-size distributions on unexposed CR-39 foils, foils exposed to different neutron spectra and on defective foils. A three-hour etch cycle with a 30 minute blow-up stage was used.

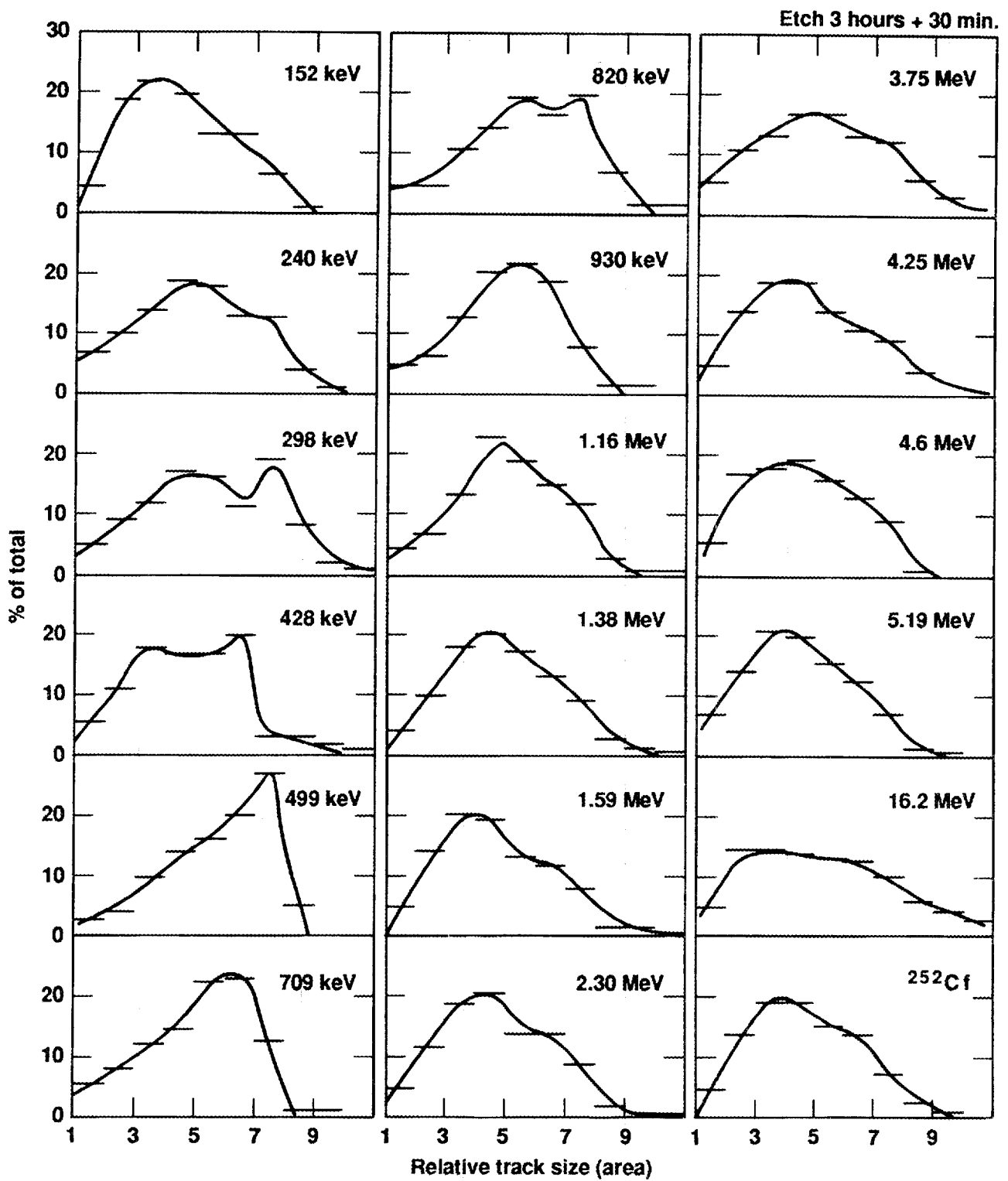


Figure 1. The track-size distribution on electrochemically etched CR-39 foils, obtained with monoenergetic neutrons. The etching conditions were 3 hours at 60 Hz with a 30 minute blow-up stage at 2000 Hz, 3000 V, 6.5 N KOH, and an oven temperature of 60°C.

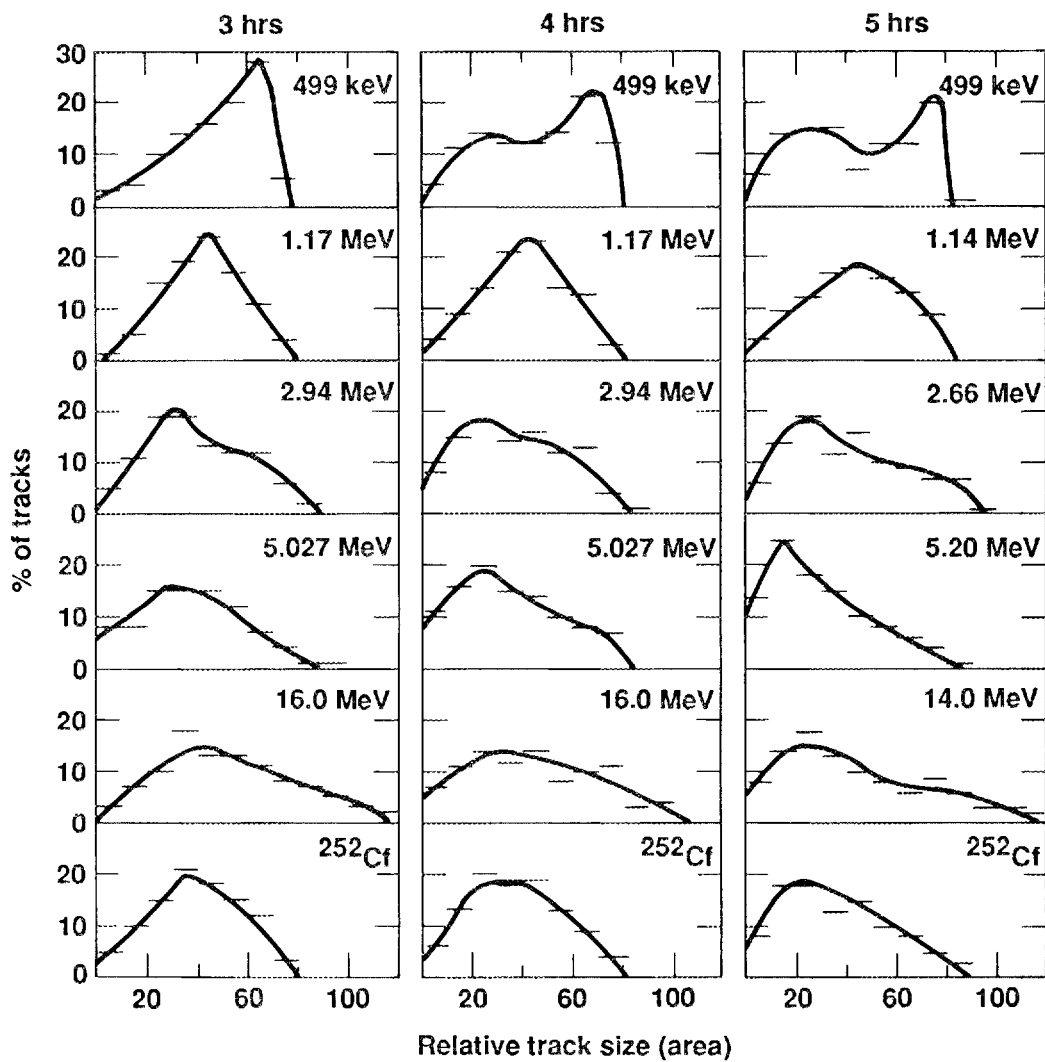


Figure 2. The track-size distributions at selected neutron energies etched using 3, 4, and 5 hours etching cycles. The track-size distributions are different depending on the etching time.

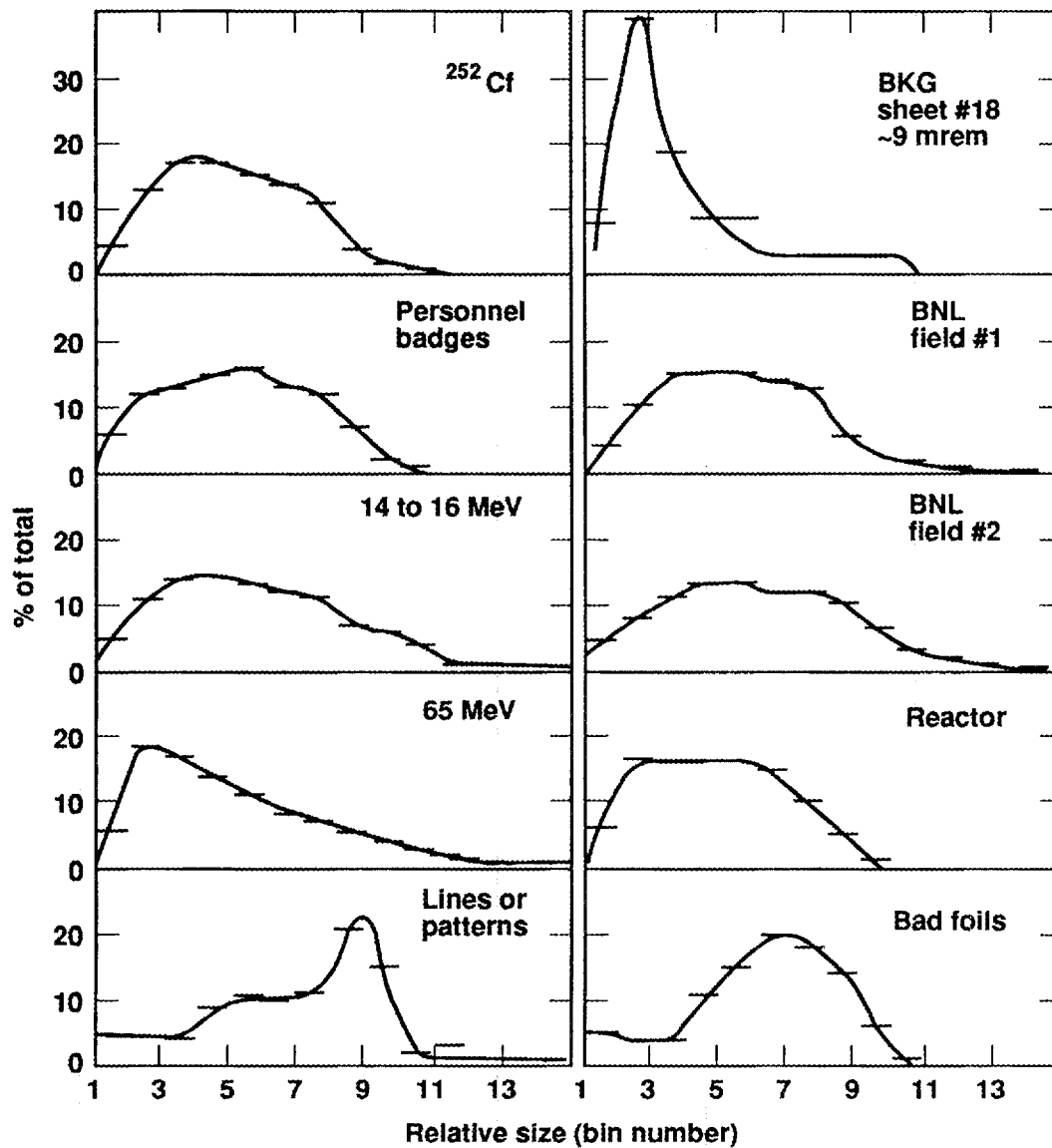


Figure 3. The track-size distributions on unexposed CR-39 foils, foils exposed to different neutron spectra and on defective foils. A three-hour etch cycle with a 30 minute blow-up stage was used.

## DEVELOPMENT AND IMPLEMENTATION OF A FAST NEUTRON MONITORING SYSTEM BASED ON PLASTIC TRACK DETECTORS

R.P. Bradley, F.N. Ryan  
Bureau of Radiation and Medical Devices

### INTRODUCTION

The Bureau of Radiation and Medical devices has provided neutron dosimetry services for Canadian industrial and research applications since the late 1960's. The programme used a nuclear emulsion film, Kodak NTA, as the personal dosimeter. Despite its two principle shortcomings, that of a relatively high energy threshold, approximately 700 keV, and highly labour intensive analysis technique, there was little else conveniently available for use. For quite a number of years we pursued, as did many laboratories, the possibilities of developing an albedo dosimeter based on paired thermoluminescent elements in some form of cadmium and plastic encapsulation. Some promise has been shown by this method and several major laboratories have designed and are currently using albedo dosimeters. At the first symposium on Personnel Radiation Dosimetry held in Knoxville in 1984, Dale Hankins of the Lawrence Livermore Laboratories, in his paper entitled, Improvements in the Etching of CR-39 For Large Scale Neutron Dosimetry, reported on his laboratories work with the polycarbonate, CR-39. Using this paper as a start and following up on similar work by W.G. Cross at the Chalk River Nuclear Laboratories, we have developed a replacement dosimeter. This paper will describe the principle features of the system introduced into routine use in Canada in October 1987.

### SYSTEM DESCRIPTION

#### 1) CR-39 Element Description

The CR-39 elements are cut from 50 cm x 65 cm sheets of the plastic which were purchased from American Acrylics and Plastics Inc. (1) When the sheets are received from the supplier, they are then sent out to be laser cut into 20 mm x 20 mm pieces. (2) One initial problem that needed to be addressed, was the labelling of the individual elements. It was proposed to use a bar code label attached to each element for identification purposes, but after trying numerous labels, adhesives, and surface protecting layers, this idea was discarded. None of the labels tried would stand up to the harsh processing conditions required for developing the damage tracks. It was then decided to develop a technique at the laser cutting stage to laser scribe

the elements on the back face so that they could be read from the front.

Once the elements have been numbered, they are then wrapped in heat shrink plastic tubing to provide a polyethylene layer which acts as a proton radiator for the energy spectrum which we are interested in covering. To make the scribed element I.D. number more visible, a piece of ordinary bond paper is placed in between the back of the CR-39 element and the heat shrink plastic.

## 2) Etch Chambers

We have designed our own etch chambers. They hold 36 CR-39 elements and are intended to allow etching of both faces of the CR-39 at the same time. The chambers are made of Lucite, with both halves serving as liquid electrodes. The chambers are very easy to assemble. Instead of "O" rings being used to form the seal, we have used rubber grommets which provide a larger surface area to maintain the integrity of both sides of a sealed cell. The opening in the grommet allows an area of 1.3 cm<sup>2</sup> to be etched. The power supply originally used for etching was one built by A.E.C.L. (Model AEP 5366). We were able to test different etching procedures at two fixed frequencies, 60 and 2000 Hz, and variable voltages. Once the protocol which we were to use had been established, it became necessary to investigate power supplies of greater capacitance. The A.E.C.L. power supply could only simultaneously drive two of our cells in the 2000 Hz mode. As it was necessary for us to use a minimum of 4 cells per day this would be unsatisfactory. We decided to use the programmable power supply made by Homann-Bell (Model CR1200B) which we calculated could supply the necessary amperage to 10 of our cells. As a result we realize substantial savings of costs and the time required to set up on a daily basis. It is very simple to operate and program the etching procedures, using the HP-41CX programmable calculator, which acts as the controller.

The only difficulties in using our cells is the pressure plate must be torqued down to an even pressure to ensure constant pressure over all the CR-39 elements. This is to prevent distortion, and a "blistering" effect on the surface of the CR-39 elements, which gives rise to an abnormally high background count.

## 3) Etching Procedure

The protocol used has three stages, the parameters of which are listed in Table 1. These settings were chosen to give a flat response curve over the energy range in which we were interested. The preliminary work was done in conjunction with a group at A.E.C.L. (3) as they had already established a working protocol which was appropriate for our objectives. Also, the chosen protocol closely resembles that which is reported by Dale Hankins, et al(4). As there had been quite a bit of development work done by these two laboratories using this technique, it was a simple matter to repeat the preliminary work to gain familiarity with it and thus, decrease our own development time.

It should be noted that in the original protocol, times for the first and second stages were respectively  $\frac{1}{2}$  hour and 15 minutes longer than those shown in Table 1. It was found through tests that decreasing the times by the above values made no difference to the background count nor to the sensitivity. Also in the development stage, an overnight humidity bath was used to eliminate any effect brought on by humidity differences during exposures. But again, as no discernible humidity effect was evident in the energy range of interest, this step was dropped. Through discussions with scientists at A.E.C.L., they concurred with our findings, and indicated that they had found similar results at lower energies. They were quick to point out that humidity does have an effect at energies higher than 5 MeV.

Table 1

	Pre-Etch	1st Stage	2nd Stage
KOH Normality	6.0	6.0	6.0
Voltage	0	1100	1100
Frequency	0	60 Hz	2000 Hz
Time	1 hour	4.5 hours	45 min.
Temperature	60°C	60°C	60°C

The chemical pre-etch stage is done to decrease the background count of the CR-39 elements by removing any surface flaws which might contribute to the count. The first Electro-Chemical Etching (ECE) stage forms the damage tracks in the plastic, while the second stage, the "Blow-Up" stage, increases the size of the holes thus allowing an automated counting method to be used.

The CR-39 elements are chemically pre-etched, and allowed to air dry before putting them into the cells and assembling the two halves. They are then placed into an oven and held at 60°C overnight (minimum 16 hours). The next morning, the cells are filled with KOH and electrodes inserted into each side. The power supply is attached and the control unit set to run for the 5  $\frac{1}{2}$  hour program. Once the cells have been disassembled, rinsed and dried, they are then reassembled with the dosimeters for the next day's etching and the sequence is repeated.

#### 4) Counting Apparatus

During the development stage of the project, we were using a commercial colony counter for counting the number of damage tracks. We have since purchased an Image Analysis software package from Gade-Data (5). This system allows us to snap an image from the microscope, store a binary image in the memory buffer of the image analysis board, and count the number of damage tracks per field of view. The complete list of hardware and software which we are currently using is listed in Table 2. An approximate value for the setup as listed is \$12,000 Canadian. This does not include the microscope, which we had previously purchased.

Table 2

Computer	Zenith Z-248 IBM AT compatible; 20 Megabyte Hard Drive; 360 K 5.25 Floppy Disk Drive; 1.2 Megabyte 5.25 Floppy Disk Drive; Zenith ZVM 1240 Monochrome Monitor; Intel 80287 Math Coprocessor
Additional Hardware	PCVISION-PLUS Framer Grabber (6) NEC Multisync RGB Monitor
Software	Gade-Data GIPS Image Analysis Program Ryan-McFarlan Fortran
Camera	COHU 4810 Solid-State CCD (7)
Microscope	Nikon Apophot Magnification used: 2.5 x before Camera Optics

The CR-39 elements are placed on the stage of the microscope and two areas of 3 mm x 4 mm are counted and the average taken to give the value for the element. Once the counts have been taken, the plaque ID and the counts are stored on diskette for processing and later reporting.

Figure 1 shows the characteristics of the counting system versus manual counting. It should be noted that there is an upper limit to the linearity of the counting system, a point after which the number of tracks detected by the system saturates. In typical exposure ranges (0-20 mSv) the response of the system is linear. The system's error in counting the same field of view is less than 0.1%. Reproducibility of the system is, therefore, extremely good.

The time required to count a single element depends on the number of damage tracks in the field of view, but a typical time is about 30 seconds to count 2 fields of view.

Since we etch both sides of the plastic, and use such low magnification in reading the elements, the system sometimes sees one damage track where there is actually two, one on the top surface, and another directly underneath on the bottom surface. We have assumed that the number of overlapping tracks is constant from element to element, and as such have included these tracks as part of the response curve. This is the only weakness of the present system.

#### BADGE CONFIGURATION

One of the objectives when this project first started out was to use one holder for both the regular service Beta/Gamma TLD dosimeters and the new CR-39 dosimeter. See Figure 2. After several tests, it was determined that we could put the CR-39 dosimeter behind our existing TLD dosimeter without any change in the response characteristics of the CR-39.

## BACKGROUND PROBLEMS

We found during the initial field testing of the CR-39 dosimeter that there was a difference in background from group to group. Most of these differences are due to the storage techniques used at each location ie, the dosimeters could be stored directly outside the exposure room, thus receiving a dose over long periods of time. These dosimeters would all have positive responses, while as it turns out, nobody had actually used neutron sources over the monitoring period.

Another variation in the background is due to the difference in the sheets of CR-39 received from the manufacturer. Each sheet is tested for a background count before being sent for cutting and numbering, and the sheets with similar backgrounds are used for dosimeters.

There has been one other contribution to the background count of the CR-39, and that is exposure to ambient light(8). Dosimeters left in a lighted room for extended periods of time have an increased background count.

To compensate for these problems, we have started issuing control dosimeters. The control is to be stored in the same location as the group's dosimeters, thus compensating for any erroneous exposures, any differences in handling, or difference in the original CR-39 sheet. All dose determinations are based on an individuals dosimeter compared to the control dosimeter.

## RESPONSE CHARACTERISTICS

### Angular Response

As others have shown (9,10), there is a certain angular dependance of the response of the CR-39. Figure 3 shows the angular response of our badge configuration. Note that at angles of incidence less than 45 degrees from the surface of the dosimeter, the response of the dosimeters drops suddenly.

We have taken 45 degrees as the angle above which there is no further response. Our sensitivity is determined then as the average of the response at the 90 and 45 degree exposures.

### Energy Response

The CR-39 dosimeter was exposed to protons of varying energies to determine the energy response of the dosimeter. Figure 4 shows the results of these tests.

The response curve of the dosimeter over the range we were interested in, 0.1 - 3.0 MeV, is fairly flat.

### Linearity

Figure 5 shows the linear response of the CR-39 dosimeter when exposed to a Pu/Be source. These exposures were done for us by A.E.C.L. The response of the dosimeter is linear up to about

4.0 mSv after which the sensitivity drops off. A large contributing factor is the nonlinearity of the counting system above this exposure. Manual counting extends the linearity of the system to much higher exposures. For evaluation of high exposures, we use the image produced by a microfiche reader and count a predetermined area using a touch sensitive pen connected to a counter.

The sensitivity of the CR-39 dosimeter is 6.75 Tracks/cm<sup>2</sup>/10 μSv.

#### CR-39 DOSIMETER VS. KODAK NTA FILM.

The following table outlines the differences between the CR-39 Dosimeter and the previously used Kodak NTA Film.

Table 3

	CR-39	NTA
Sensitivity	6.75 Tracks/cm <sup>2</sup> /10 μSv	1.61/mm <sup>2</sup> =10 μSv
Fading	None	20% reduction at 4 weeks
Energy Range	0.1 - 3.0 MeV	0.7 - 14 MeV
Gamma Sensitivity	None	Very Sensitive
Lower Limit	0.20 mSv @95% confidence limit	0.20 mSv @50% confidence limit
Upper Limit	4.0 mSv (auto) 10.0 mSv (manual)	5.0 mSv (manual)
Thermal Neutron Sensitivity	None	Sensitive under filtered conditions
Processing	Automatic	Manual
Reading	Automatic (30 sec/element)	Manual (1+ min/element)

#### FUTURE STUDIES

Of current concern is the background variation from sheet to sheet of CR-39, and the background induced from external variables. The next stage of the development is to modify the etching technique to etch only the "low" background side of the plastic. Wanting to continue to use the same etching apparatus, it should be a simple matter to fill one side of the etching cell with water rather than KOH. This is going to take some time as new calibration curves are required, and characterization of the system must be fully investigated.

Several other laboratories are investigating other sources of CR-39 plastic. One such supplier who has been supplying sheets of CR-39 with reported low backgrounds is Pershore Moldings, Pershore, England. The University of Bristol, also in the United Kingdom, is another. Both materials are to be investigated.

Another area of interest, is the expansion of the energy range of the dosimeter by modifying the etching parameters to extend sensitivity to energies higher than 3.0 MeV. This could prove helpful in special applications.

Lastly, the CR-39 has been investigated as a thermal neutron detector. By placing a substance containing Boron compounds on the back side of the detector, a highly sensitive thermal neutron detector is possible. This technique may serve, as well, for confirmation of doses received from fast neutrons.

#### DISCUSSION

Having completed one year of use of the new dosimeter we feel confident of its suitability as the chosen replacement for the nuclear emulsion neutron dosimeter. For the most part, comments from the users have been favourable. As stated above there is a need to continue work improving the inherent background of the material and system. Once these aspects are optimized we will have completed our initial assignment, having developed and implemented an efficient, reliable and easy to use personal neutron dosimeter.

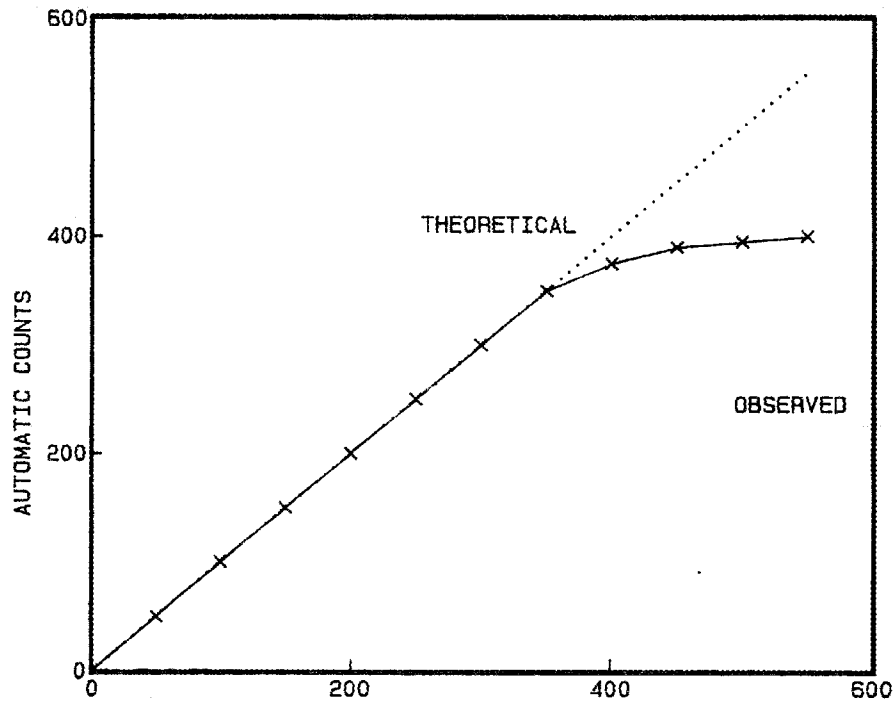
#### ACKNOWLEDGEMENTS

We would like to thank W.G. Cross and A. Arendja of the Chalk River Nuclear Laboratories, Atomic Energy of Canada Limited, for their continued help in the development of our system. Also thanks to D. Hankins of the Lawrence Livermore National Laboratory for his enlightening discussions.

#### REFERENCES

- 1) American Acrylics and Plastics Inc., 25 Charles St., Stratford Conn.
- 2) Laser Machining Centre, 64 Carnforth Rd., Toronto, Ontario.
- 3) Cross W.G., Arendja A., Atomic Energy of Canada Limited, Chalk River Nuclear Laboratories, Chalk River, Ontario.
- 4) Hankins D.E., Homann S., Westermarck J., "Personal Neutron Dosimetry Using Electrochemically Etched CR-39 Foils", URCL-95350, Lawrence Livermore National Laboratory.
- 5) Majborn B., "Automated Counting and Analysis of Etched Tracks in CR-39 Plastic", Radiation Protection Dosimetry, Vol. 17 (153-156), 1986.
- 6) Imaging Technology Inc., 600 West Cummings Park, Woburn, MA.
- 7) Cohu Electronics, 5755 Kearny Villa Road, San Diego, CA.
- 8) Hankins D.E., Lawrence Livermore National Laboratory, Personal Communication.
- 9) Harvey J.R., Weeks A.R., "A Neutron Dosimetry System Based on the Chemical Etch of CR-39", Central Electricity Generating Board, Berkeley Nuclear Laboratories, Berkeley, Gloucester, England.
- 10) Cross W.G., Arendja A., Ing H., "The Energy Dependence of Electrochemically Etched CR-39 Dosimeters to Neutrons", Atomic Energy of Canada Limited, Chalk River Nuclear Laboratories, Chalk River, Ontario. Presented at the Annual Health Physics Society Meeting, May 1985.

FIGURE 1  
MANUAL COUNTING VERSUS AUTOMATIC COUNTING



ERROR BARS ARE TOO SMALL FOR THE SCALE USED

FIGURE 2

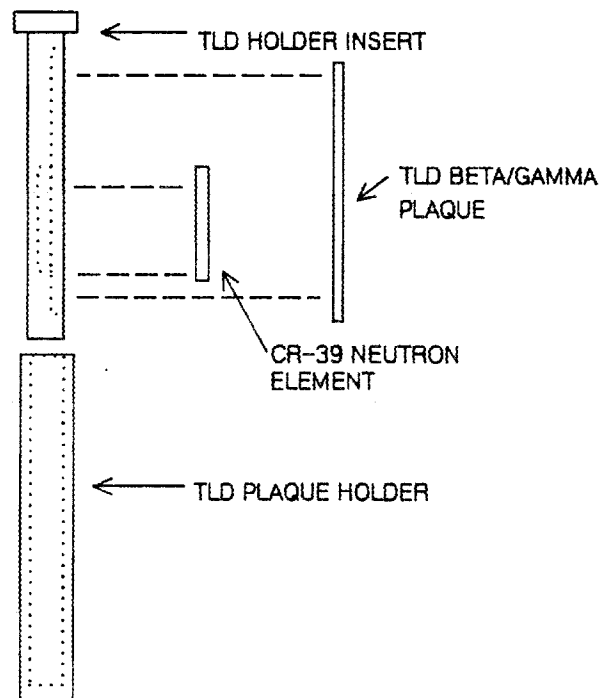
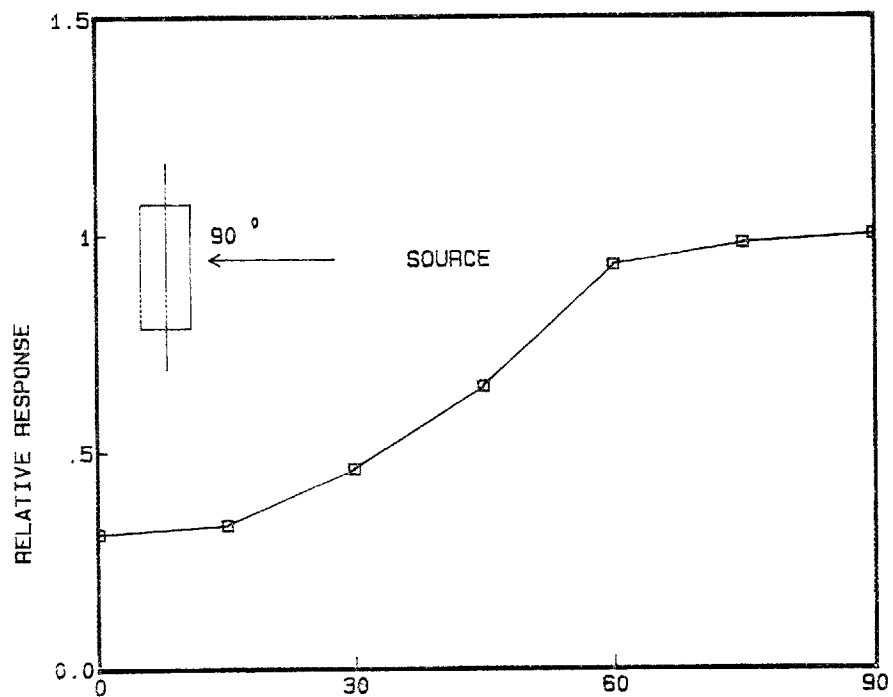
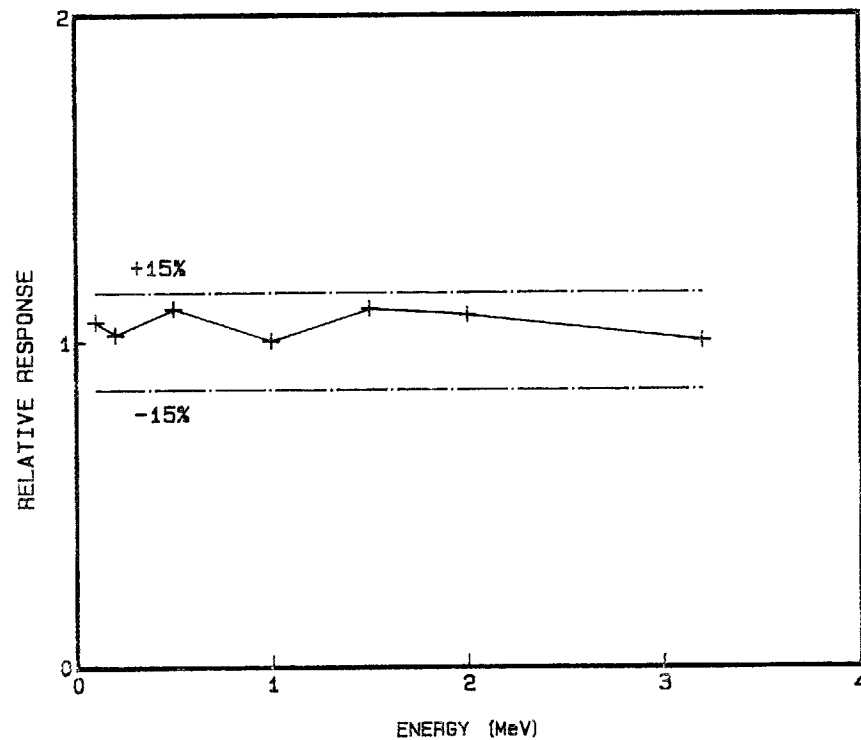


FIGURE 3  
ANGULAR RESPONSE OF CR-39 DOSIMETER



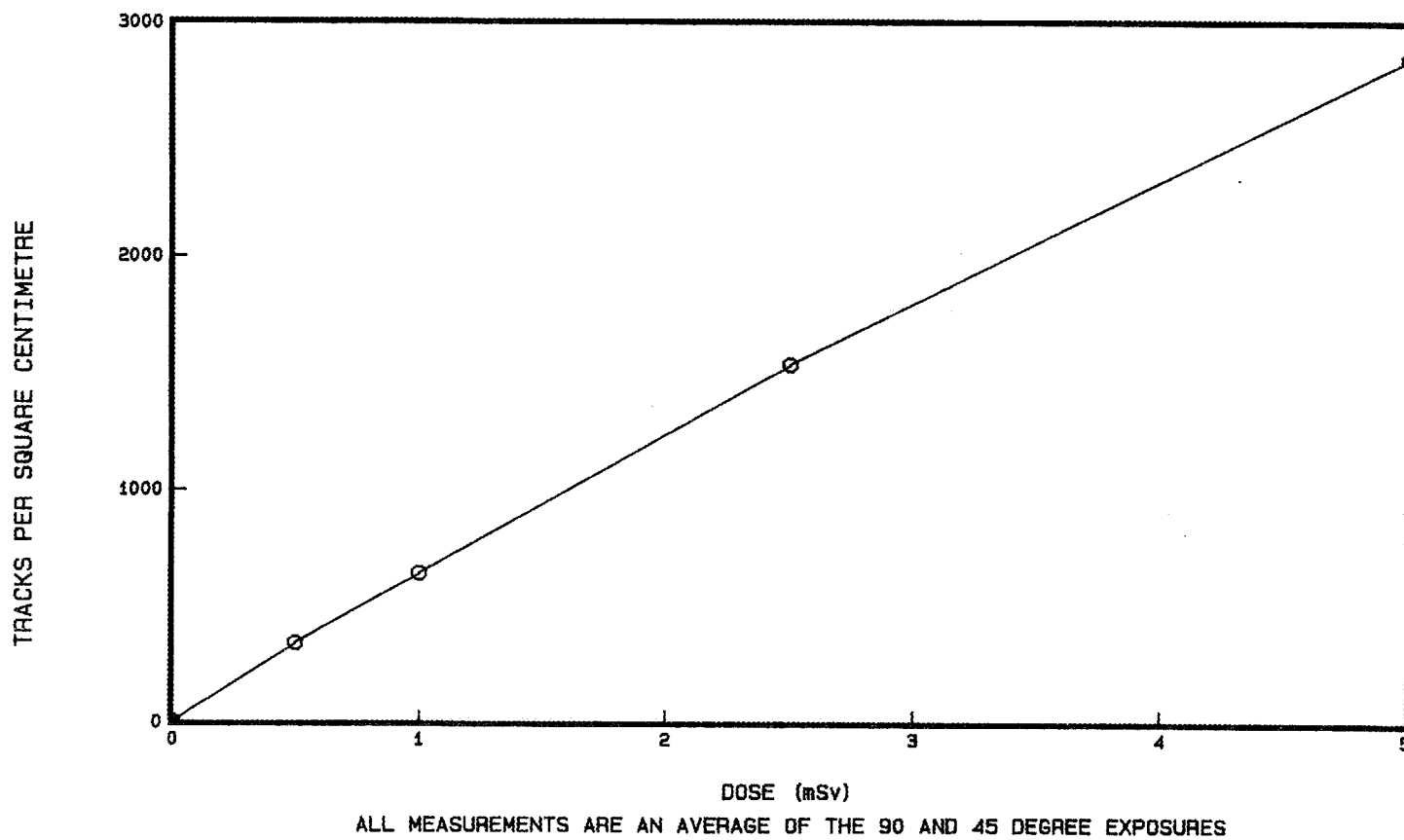
ANGLE OF INCIDENCE  
ERROR BARS ARE TOO SMALL FOR THE SCALE USED

FIGURE 4  
ENERGY RESPONSE CURVE OF CR-39 DOSIMETER



RELATIVE RESPONSE  
ENERGY (MeV)  
ALL EXPOSURES ARE AT 90 DEGREES INCIDENT TO THE DOSIMETER

FIGURE 5  
DOSE RESPONSE CURVE OF CR-39 DOSIMETER  
(AUTOMATIC COUNTING USED)



A REVIEW OF EXPERIENCE WITH PLUTONIUM EXPOSURE  
ASSESSMENT METHODOLOGIES AT THE NUCLEAR FUEL  
REPROCESSING SITE OF BRITISH NUCLEAR FUELS PLC

Dr R Strong  
Safety and Medical Services Department  
British Nuclear Fuels plc  
Sellafield  
Cumbria  
United Kingdom

## Introduction

British Nuclear Fuels plc and its predecessors have provided a complete range of nuclear fuel services to utilities in the UK and elsewhere for more than 30 years. Over 30,000 tonnes of Magnox and Oxide fuel have been reprocessed at Sellafield. During this time substantial experience has accumulated of methodologies for the assessment of exposure to actinides, mainly isotopes of plutonium. The purpose of the paper is to present some conclusions of contemporary work in this area.

For most of the period monitoring of personnel included assessment of systemic uptake deduced from plutonium-in-urine results. By the early 1980's it was apparent that the Langham function (1) predicted excretion rates which became progressively lower than observation as time increased (2)(3). The degree of underestimation had been shown (4) to approach an order of magnitude at 10,000 days post uptake.

## Development of A Urinary Excretion Function

Against this background Jones (5) developed a four-term exponential excretion function which represented the most probable level of excretion from subjects following known uptake of plutonium. Data for subjects whose urinary excretion was judged (6)(4) to be representative of persons in normal health, intravenously injected with Pu (IV) were used as the basis for deducing the excretion function:

$$\begin{aligned} f(t) = & 0.00475 \exp(-0.558t) \\ & + 0.000239 \exp(-0.0442t) \\ & + 0.0000855 \exp(-0.00380t) \\ & + 0.0000142 \exp(-0.0000284t) \end{aligned}$$

From the results of monitoring occupationally exposed persons at Sellafield this function was tested in two ways:-

Firstly, a comparison was made between the observed time development of excretion and the behaviour predicted by the excretion function, for two cases having intakes occurring in a limited and well defined time period, considerable excretion data above the limit of detection and no confounding effects associated with further exposure or translation from a non-systemic pool.

The second test was to compare uptake estimates with data obtained at autopsy on over 20 ex-plutonium workers at Sellafield. Assessments were performed by personnel having no knowledge of the autopsy data and it was possible to show that the value deduced for total uptake was insensitive to the choice of uptake regime within reasonable constraints determined by the work history of the individual. These estimates invariably exceed those from autopsy but were clearly more consistent with autopsy data than estimates based on the Langham function.

## Legislation In the UK

With full effect from 1 January 1986, new legislation - the Ionising Radiations Regulations 1985 - was brought into force in the United Kingdom.

The law gives effect to the recommendations of ICRP Publication 26 (7) in so far as dose limitation and dose limits are concerned.

Determination of committed dose equivalents or committed effective dose equivalents relies on determination of the increase of activity present in the relevant organs in the year. For long-lived long-retained radionuclides the dose equivalent actually received in the year of intake may be as little as one fiftieth of the committed dose. In these situations routine biological sampling may not be sufficiently sensitive to detect such small increments in exposure and therefore assessment of intake using personal or work-place air sampling is used. The UK system permits use of a quantity known as Compliance Index defined as:

$$\text{Compliance Index} = \frac{\text{External dose}}{\text{Annual Dose Limit}} + \frac{\text{Intake}}{\text{Annual Limit on Intake}}$$

If the Compliance Indices (stochastic and non-stochastic) are less than or equal to unity at the end of a year then compliance with statutory limits is demonstrated.

In order to demonstrate compliance with the law widespread use of personal air samplers (PAS) was introduced in 1986. The arrangements provided 500,000 PAS units annually to 3500 regular users. Special biological sampling was initiated on each occasion that a PAS result implied an intake greater than ten percent of the Annual Limit Of Intake as determined from ICRP Publication 30 (8) during a single work period of 8 hours. A protocol became necessary for the combination of biological and PAS results.

### Protocol For Interpretation of Biological Monitoring Results And Personal Air Sampler Results

The interpretation of biological monitoring results and personal air sampler (PAS) results relies on the use of standard ICRP models, for example as described in ICRP Publication 23 (9) and Publication 30 (8) unless data shows systematic departure from model prediction. In principle, and indeed in practice, urine sample results, faecal sample results and personal air sampler results can each imply different values for the intake being investigated and a protocol for the treatment of data is therefore required. Figure 1 shows the protocol used.

## Discussion of Results

The conclusions from assessments of suspected single acute exposure > 0.1 x Annual Limit on Intake are summarised below:

	1986	1987
Number of assessments	228	159
Assessment result implies intake greater than PAS result	14 (6%)	4 (2%)
Insufficient information to confirm or refute PAS result	114 (50%)	39 (25%)
Assessment result implies intake less than PAS result	100 (44%)	116 (73%)

In Figure 2 is plotted data pairs corresponding to the values of the assessment result and the PAS result for each suspect acute exposure which was investigated.

Figure 3 shows the results of faecal sampling in relation to urine sampling. Figure 4 shows the results of faecal sampling in relation to the PAS result.

The following comments can be drawn from these data:

- i there is no obvious correlation between PAS data, urine sample data and faecal sample data
- ii biological sample results generally imply intakes smaller than indicated by personal air sampler
- iii urine sample results generally imply intakes larger than indicated by faecal samples.

The latter observation should be interpreted with caution since the chemical limits of detection for plutonium (alpha) analysis ( $4 \times 10^{-4}$  Bq/litre for urine and  $7 \times 10^{-3}$  Bq/sample for faeces) tend to produce this effect. In addition, for some cases there is the confusing influence of low level chronic excretion.

Interpretation of biological sample data in terms of intake or uptake (as appropriate) has an uncertainty of typically  $\pm 60\%$  (95% confidence) based on a fit of the excretion data to the excretion function.

An intake of 1 x Annual Limit on Intake for lung Class W material can be as little as 120 Bq of alpha activity, which would be expected to give rise to systemic uptake of 15 Bq of plutonium (alpha). Such an increment in uptake is difficult if not impossible to discern in people occupationally exposed for tens of years. In cases like these the PAS result, by default, becomes used to assess compliance index and could indicate failure to demonstrate compliance with statutory limits. This situation is most unsatisfactory.

The basic difficulty arises because

- a the personal air sampler behaves as a statistical sampling device when operated in an environment having only a few to a few tens of particles per  $m^3$ ,
- b trivial levels of surface contamination, once transposed to the air sampler, can appear to indicate significant inhalation,
- c the absolute magnitude of statutorily significant uptake is small and implies increments in urinary excretion close to the limits of the existing assessment techniques,
- d when in doubt, model parameters are chosen to overestimate intake/committed doses for the purpose of demonstrating statutory compliance.

Little doubt exists that the protracted use of personal air samplers does provide a useful indicator of general environmental airborne contamination levels. Their use does not lead to an understanding which is different from that derived from installed air sampling equipment providing due account is taken of siting characteristics of this equipment. In addition, personal air sampling does provide a convenient means of identifying particular tasks or particular working methods which apparently give rise to localised enhanced levels of airborne contamination. In these respects timely information is produced for decision making by management. However, as is evident from the data presented, there is no clear relationship between significant PAS results and the evidence from biological sampling. Indeed this is a source of confusion. The dilemma arises through the importance which the assessment of intake necessarily assumes as a consequence of the ICRP Publication 26 (7) scheme of dose assessment (use of committed dose concept) and dose accounting (ascribing committed doses to year of intake) when applied to long-lived long-retained radionuclides.

Protection procedures intended to demonstrate proper control and limitation of individual radiation exposure depend for their effectiveness on the extent to which occupationally exposed people understand the underlying philosophy. Apart from a few specialists, most such people are not at ease with the concept of committed dose and show no signs of becoming so.

The dose accounting convention seems strange since it requires the summation of received dose (external dose equivalent) and dose to be received over the next 50 years if the individual lives long enough (arising from committed dose equivalents due to internally deposited radionuclides). Finally, the rather uncertain theoretical connection between intake and systemic uptake serves to confirm the sceptics' opinion that the underlying philosophy is hard to penetrate.

It must follow that there can be no adequate resolution within the formalism of ICRP Publication 26 (7) and therefore the Ionising Radiation Regulations 1985 in the UK. What is required is to divorce assessment of intake from assessment of dose equivalent, on the practical grounds that assessment of intake via personal air sampling is a useful tool for producing information about radiological conditions generally but is a poor guide to the magnitude of systemic uptake. Of course, over a period of some years employment there may be the prospect of urinary excretion of plutonium achieving a detectable level which could then be used to assess systemic uptake and dose equivalents to organs.

#### Acknowledgements

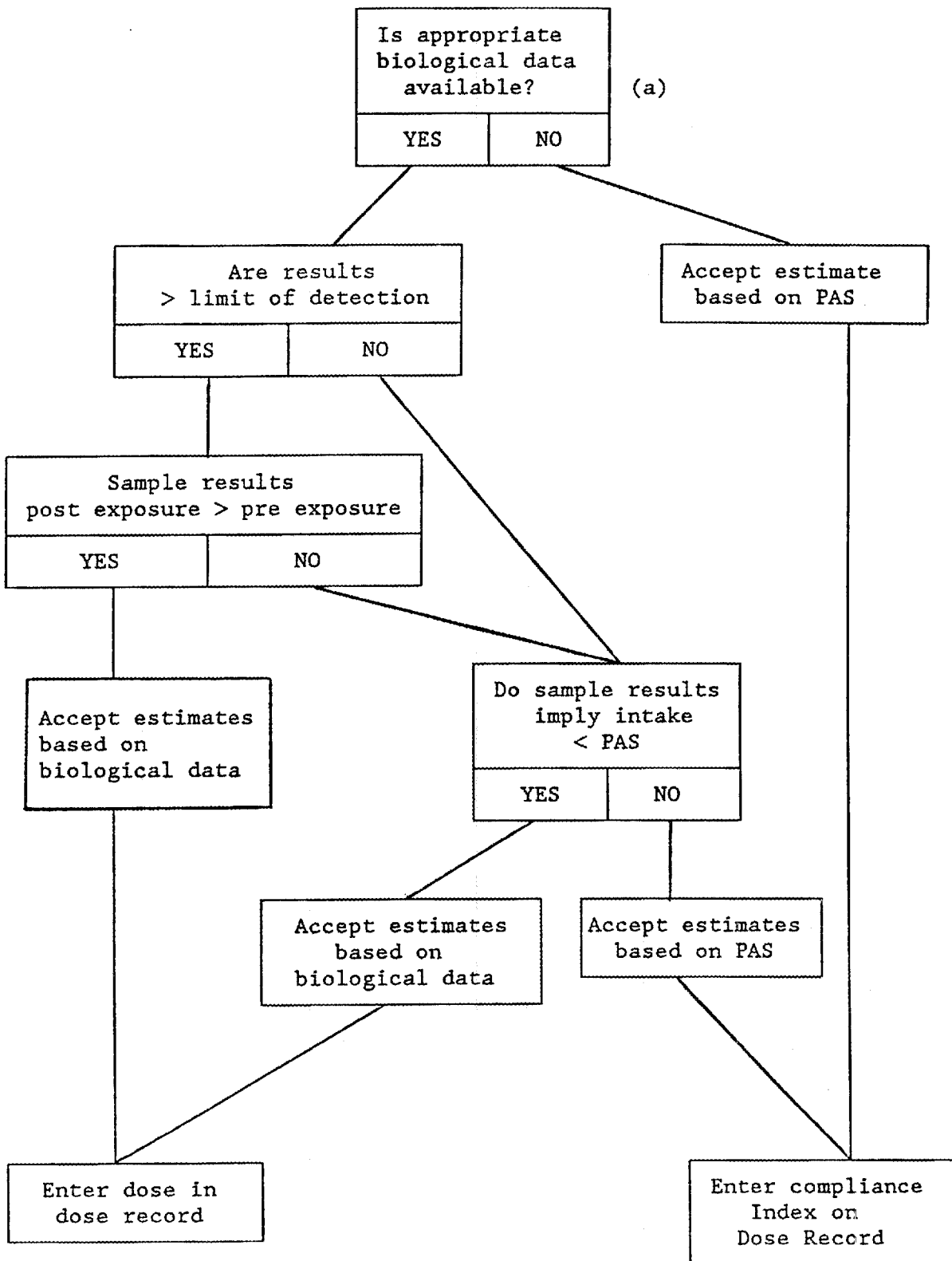
The author wishes to thank his many colleagues who have contributed to the work described here and to acknowledge the support of British Nuclear Fuels plc in the presentation of this paper.

Views expressed here are not necessarily those of British Nuclear Fuels plc.

## References

- 1 LANGHAM W H, BASSET S H, PAYNE S H and CARTER R E.  
"Distribution and Excretion of Plutonium Administered Intravenously to Man". Health Physics 38, 1031 - 1060 (1980) (Reprint of original work).
- 2 RUNDO J  
"Late Excretion of Pu Following Acquisition of Known Amounts" in "Actinides in Man and Animals" (Salt Lake City - RD Press)  
pp 253 - 260 (1981).
- 3 PARKINSON W W and HENLEY L C  
"A Proposed Long-Term Excretion Function for Plutonium". Health Physics 40 327 - 331 (1981).
- 4 RUNDO J, STARZY K, P M, SEDLET J, LARSEN R P, OLDHAM R D and ROBINSON J J.  
"The Excretion Rate and Retention of Plutonium 10000 Days After Acquisition" in "Diagnosis and Treatment of Incorporated Radionuclides". (Vienna : IAEA). STI/PUB/411, pp 15 - 23 (1976).
- 5 JONES S R.  
"Derivation and Validation of a Urinary Excretion Function for Plutonium Applicable over Tens of Years Post Uptake". Rad Prot Dos 11 19 - 27 (1985).
- 6 DURBIN P W.  
"Plutonium in Man : A New Look at the Old Data" in "Radiobiology of Plutonium". (Salt Lake City : JW Press). pp 469 - 530 (1972).
- 7 ICRP PUBLICATION 26  
"Recommendations of the International Commission On Radiological Protection". Pergamon Press (1977).
- 8 ICRP PUBLICATION 30  
"Limits For Intakes of Radionuclides By Workers". Pergamon Press (1979).
- 9 ICRP PUBLICATION 23  
"Report Of The Task Group On Reference Man". Pergamon Press (reprinted 1981).

Figure 1 : Protocol For Dealing With Biological Monitoring Data And PAS Results



Note a urine data is preferred for the assessment of systemic uptake  
 faecal data is preferred for the assessment of intake

FIGURE 2

# ASSESSMENT RESULT vs PAS RESULT

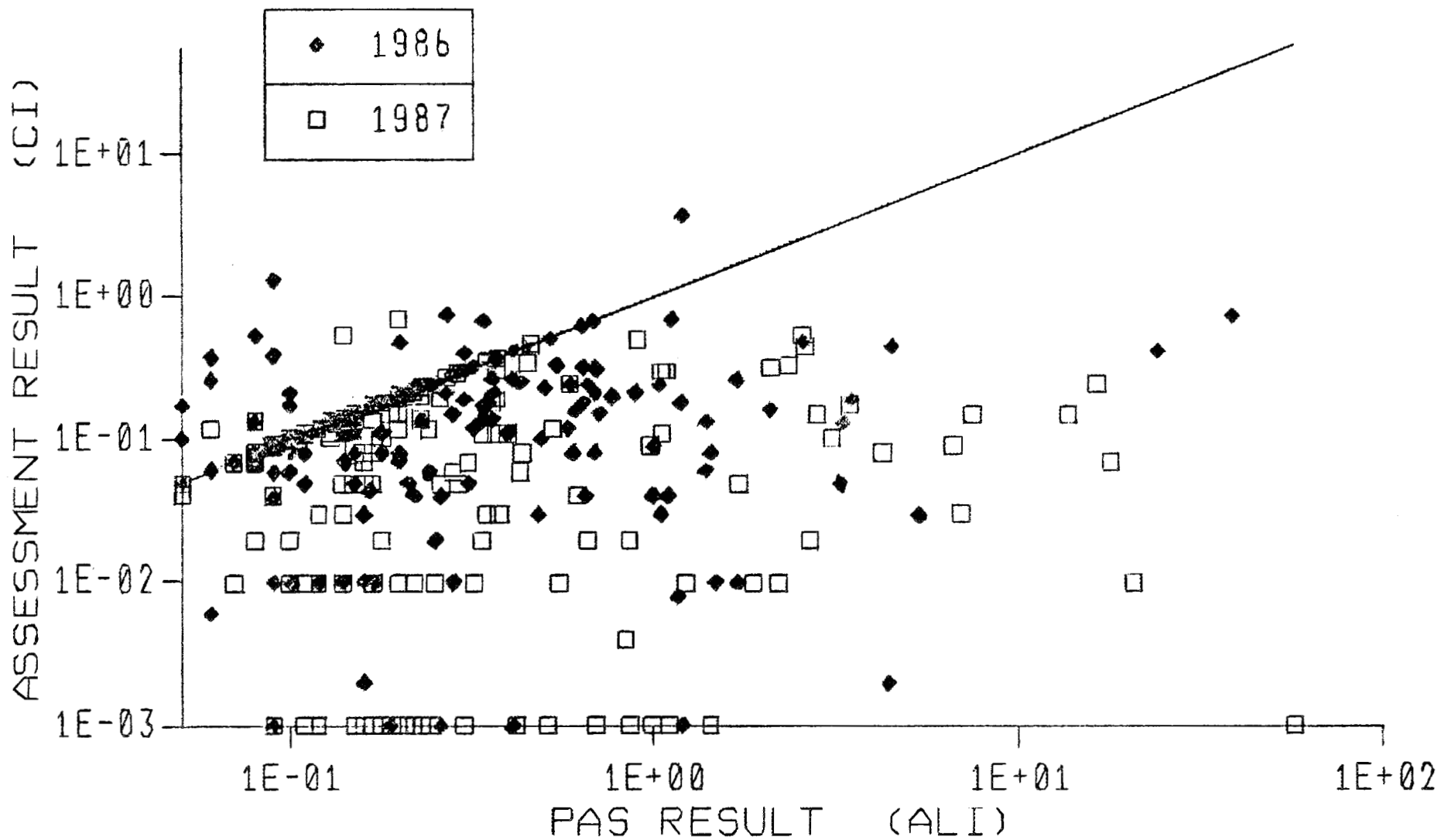
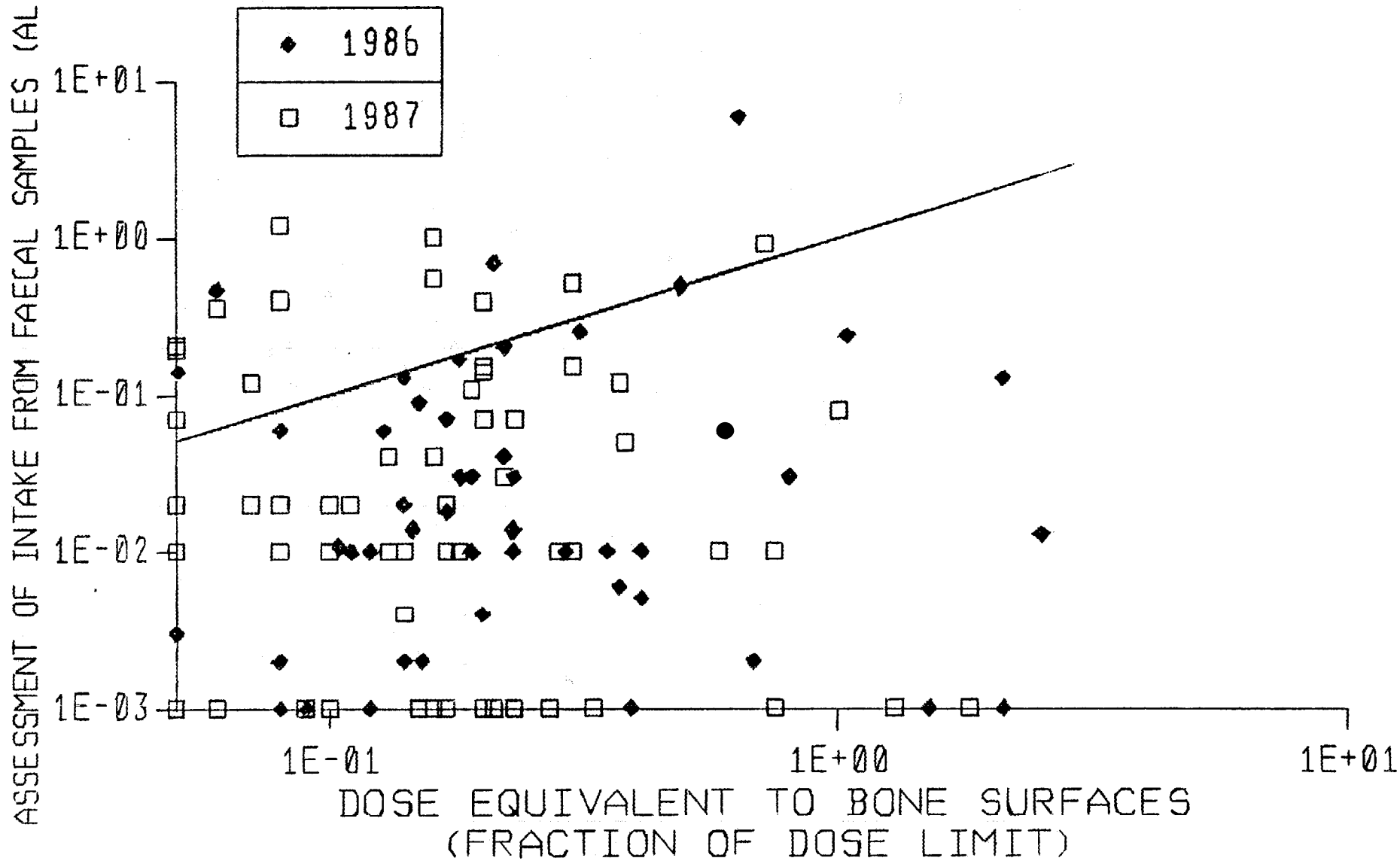


FIGURE 3

# FAECAL ASSESSMENT vs URINE ASSESSMENT





## ANALYSIS OF PARTICULATE CONTAMINATION FROM A PWR

Larry M. Hodgson  
Arkansas Tech University  
Russellville, AR 72801

Orville W. Cypret  
Arkansas Power & Light Co.  
Russellville, AR 72801

Roy R. Culp  
Arkansas Tech University  
Russellville, AR 72801

### INTRODUCTION

Within the last few years several nuclear power plants have reported what the Nuclear Regulatory Commission has referred to as *excessive skin exposures* as a result of contamination from small, discrete particles of radioactive material. The sources of contamination have been traced to fuel cladding failures, primary system leaks, and activated foreign matter. Once these particles, often called "fleas" or "hot particles", have been disseminated throughout a power plant, they are difficult to detect and control.

In this study, several samples of particulate contamination found at two pressurized water reactors on personnel or in controlled access areas were closely examined. If the sample contained a single particle, it was isolated, micro-photographed, and analyzed for gamma and x-ray emission. Some of the particles were further examined using a scanning electron microscope and assayed with x-ray fluorescence. The computer code QUINCE was used to estimate possible skin doses from such particles.

### PROCEDURE

The hot particle samples generally were received in the laboratory wrapped in the gray duck tape that was used for decontamination. Some came still embedded in pieces of clothing, when the contamination could not be removed with tape. The first step in the analysis was to determine the approximate location of the activity by surveying the sample through a small hole in a sheet of lead. The radioactive material was then removed from the cloth or tape by cutting away the sample until only a small amount of non-radioactive material remained with the active particle. This work was performed with the aid of a Bausch & Lomb stereo zoom microscope with a magnification of 10 to 70X. The hot particle was generally mixed with other bits of dirt and grit. The tip of a scalpel was used to remove each suspect particle from the remaining

material to check for radioactivity. Once the hot particle was located, it was placed on a piece of clear tape and covered with a plastic "bubble" obtained from a pharmaceutical packaging material known as a "blister pack".

Particle isolation, especially for the smallest ones, required patience and determination. However, once the particle had been identified and isolated, much was learned from its study. An Olympus stereo microscope with four fixed stages from 6.3 to 40X was used to photograph the particles. This microscope was equipped with an Olympus camera and an additional 2X camera mount, giving an over all photographic magnification of 86X. (The photographs shown here have been reduced slightly. The photograph in Figure 9 has a magnification of 43X.)

Once the particles had been isolated, a repeatable and precise geometry was available for gamma spectroscopy. If activity was high enough, the particle was counted at a position 10 cm from the detector face. Those of very low radioactivity were counted at the detector face. Counts at both positions were used to determine the geometry factors for detector efficiency correction.

The gamma analysis was performed using an ORTEC GMX-13180 detector and an ORTEC Model 918 ADCAM (multi-channel buffer) connected to an IBM PC-XT. The net peak areas and peak backgrounds were calculated with the analysis software supplied by ORTEC. The detector was calibrated using an 11 nuclide source with traceability to National Bureau of Standards. Detector efficiency was determined by fitting the peaks of the calibration standard to a function of the form

$$\epsilon(E) = ( X_1 \ln(E) + X_2 \ln(E^2) + X_3 \ln(E^3) + X_4 \ln(E^5) + X_5 \ln(E^7) ) / E .$$

where  $\epsilon(E)$  is the efficiency as a function of energy E, and  $X_n$  are the fitting parameters.

Some of the sample particles were analyzed with x-ray fluorescence (XRF) and a scanning electron microscope (SEM). The smaller particles had to be cleaned in an organic solvent to remove the adhesive, since the electrons could not penetrate it. Some were too small to be seen using this technique. It is suspected that they sank into the adhesive of the mounting tape. X-ray fluorescence was used to characterize the metal content of the activated particles and the medium for the fission products.

The small size of hot particles allows them to come into close contact with the skin, delivering extremely high doses to very small areas. Potential skin doses that could have been delivered by particles selected from this study were determined with the computer code QUINCE, which uses the same algorithm to calculate skin dose as VARSKIN. The calculations assumed that the particle was resting directly on the skin, and that skin density was 7 mg/cm<sup>2</sup>.

## RESULTS

Table 1 summarizes the properties of the particulate contamination samples examined during this study. Most of the samples consisted of a single particle. The exceptions were samples 9 and 17, which contained cesium, and sample 21, a swipe containing evenly distributed  $^{58}\text{Co}$ . Photographs of several of the particles are presented in Figures 1-10. The major gamma emitting radioisotopes identified for each sample and their estimated activities are given in Table 2. It is interesting to note the rather small number of isotopes involved.

The isolated particles ranged in size from about 2  $\mu\text{m}$  to 500  $\mu\text{m}$ . The larger particles were clearly visible to the naked eye, whereas the smaller ones were barely distinguishable, even at a magnification of 70X. Particle 2 (Figure 1), a 3  $\mu\text{m}$  fuel flea, was one of the smallest particles studied. Such particles may become airborne, thus presenting a respiratory protection problem. This particle is seen in the photo as a speck located at the corner of the clear tape to which it is attached.

Particle 15, which was the most active source of the mixed fission products and was deemed typical of this class of particles, was examined under the electron microscope. The image was not of great interest, but analysis of the x-ray fluorescence indicated that the particle was primarily composed of uranium and possibly contained a significant quantity of plutonium. This observation verified the fact that fuel pellet fragments had been introduced into the plant environment.

Particle 7, which was a pure source of  $^{106}\text{Rh}$  gammas, was determined to contain about 95% ruthenium, which is a fission product and the parent of the  $^{106}\text{Rh}$ .  $^{106}\text{Ru}$  emits a beta particle whose average energy is 1.4 MeV. This large concentration of ruthenium indicates a purification process for this element. Particle 1 was similar to particle 7, except that it had much less activity.

The size of the smaller particles is on the same order of magnitude as the fibers from which cotton thread is woven. The particles are tiny enough to move through the weave of typical anti-contamination clothing, blue jeans, t-shirts, etc., and come to rest on the skin. They also may become lodged in the fibers from which the thread is spun and are difficult to remove by laundering. Photographs of this type clothing, taken at the same scale as the particles, are presented in Figures 11 and 12.

The larger particles were activation products. One exception, particle 18, was what appeared to be a resin bead (Figure 9). This was the largest hot particle found. The large particles varied considerably in size and shape, but all typically contained sources of  $^{60}\text{Co}$ . Some appeared to be corrosion products (Figures 2 and 10), while others appeared to be uncorroded bits of metal (Figures 3, 5, and 8). Some of the larger particles were studied with the SEM and XRF. Generally these particles contained mostly chromium, nickel, and iron, with small amounts of titanium. Particle 12 (Figure 6), a small but relatively active source of  $^{60}\text{Co}$ , was the only one found to contain large quantities of elemental cobalt. Because of the large neutron cross-section and low ac-

Table 1. Description of 21 particulate contamination samples found at two PWRs on personnel or in controlled access areas. If the sample contained a single particle, it was isolated, micro-photographed, and analyzed for gamma and x-ray emission. Some of the particles were observed with a scanning electron microscope and assayed with x-ray fluorescence.

Particle	Description
1	Pure source of $^{106}\text{Rh}$ gammas. Appears as a speck 3 $\mu\text{m}$ in diameter.
2	Contained fission product isotopes. Appears as a speck 3 $\mu\text{m}$ in diameter.
3	Black, irregular shaped, 350 $\mu\text{m}$ in diameter, scaly, contained mainly $^{60}\text{Co}$ .
4	Contained fission product isotopes, appears as a speck 5 $\mu\text{m}$ in diameter.
5	Metallic oblong disk, 225 $\mu\text{m}$ across the long axis, 150 $\mu\text{m}$ across the short axis, and 10 $\mu\text{m}$ thick. Contained $^{60}\text{Co}$ , $^{58}\text{Co}$ , and $^{57}\text{Co}$ . It was similar to particle 10.
6	Cigar shaped particle, black with gold reflections, 250 $\mu\text{m}$ long and 60 $\mu\text{m}$ in diameter. Only $^{60}\text{Co}$ was detected. XRF indicated a Metallic make up of 23% Cr, 18% Fe, and 58% Ni.
7	Pure source of $^{106}\text{Rh}$ gammas. Appears as a speck 10 $\mu\text{m}$ in diameter. XRF analysis showed the surface of the particle to contain 95% ruthenium.
8	Contained fission product isotopes, appears as a sphere 15 $\mu\text{m}$ in diameter.
9	The sample looked like soil. During the initial stages of isolation $^{137}\text{Cs}$ , $^{134}\text{Cs}$ , $^{60}\text{Co}$ , and $^{58}\text{Co}$ were found to be evenly distributed throughout the sample. No further isolation was attempted.
10	Particle was a Silvery Metallic disk with a dark area in the center. It was 230 $\mu\text{m}$ in diameter and 10-15 $\mu\text{m}$ thick. Activity was primarily $^{60}\text{Co}$ with some $^{58}\text{Co}$ and $^{54}\text{Mn}$ .
11	Contained fission product isotopes, appears as a speck 3-5 $\mu\text{m}$ in diameter.
12	Spherical, dark, glassy looking, 15 $\mu\text{m}$ in diameter. Activity due only to $^{60}\text{Co}$ . XRF analysis showed Metallic make up to be primarily Co and Cr.
13	Spherical, dark, glassy looking, 15 $\mu\text{m}$ in diameter. Contained fission product isotopes.
14	Gold colored, irregular shaped, brittle looking, 150 $\mu\text{m}$ across. Mainly $^{60}\text{Co}$ . XRF showed a metal make up of 20% Cr, 26% Fe, 52% Ni, and 1% Ti. 15
15	Contained fission product isotopes, appears as a speck 5-6 $\mu\text{m}$ in diameter. XRF showed this particle to contain a large amount of uranium and probably plutonium.
16	Contained fission product isotopes, appears as a speck 5 $\mu\text{m}$ in diameter.
17	During the early stages of isolation, $^{137}\text{Cs}$ was found to be evenly distributed over the sample. No further isolation was attempted.
18	This particle was identified as a 500 $\mu\text{m}$ resin bead.
19	Particle was black, thin and brittle, 400 $\mu\text{m}$ across. Activity was due mainly to $^{60}\text{Co}$ .
20	Contained fission product isotopes, appears as a speck 2 $\mu\text{m}$ in diameter.
21	This sample consisted of evenly distributed $^{58}\text{Co}$ particulate. Particles were too small to be identified individually.

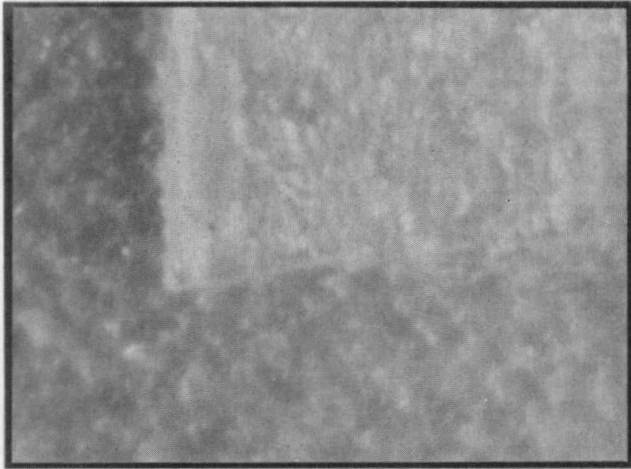


Figure 1. Hot Particle #2

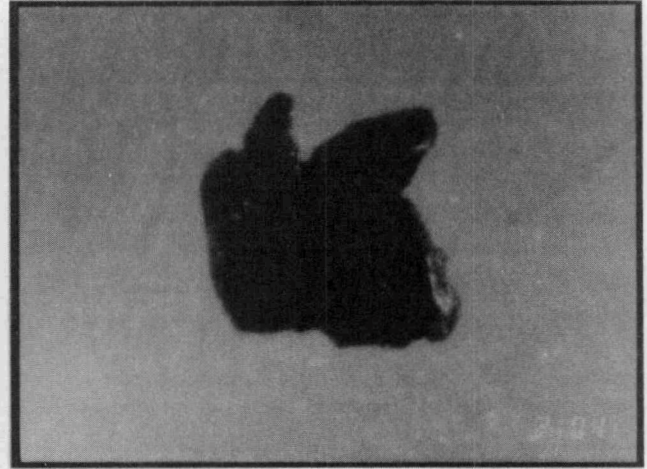


Figure 2. Hot Particle #3



Figure 3. Hot Particle #5



Figure 4. Hot Particle #8



Figure 5. Hot Particle #10

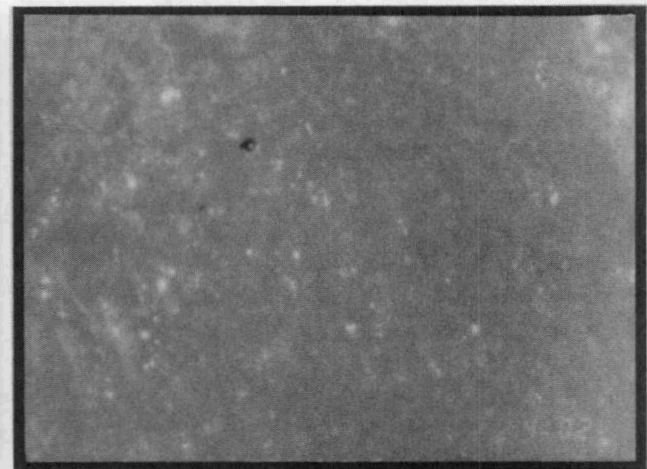


Figure 6. Hot Particle #12

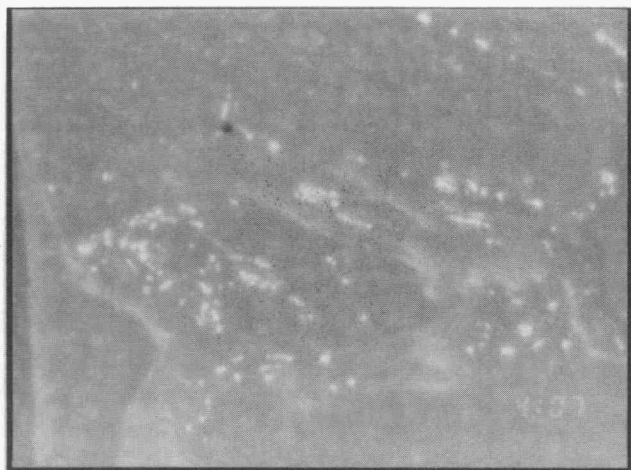


Figure 7. Hot Particle #13

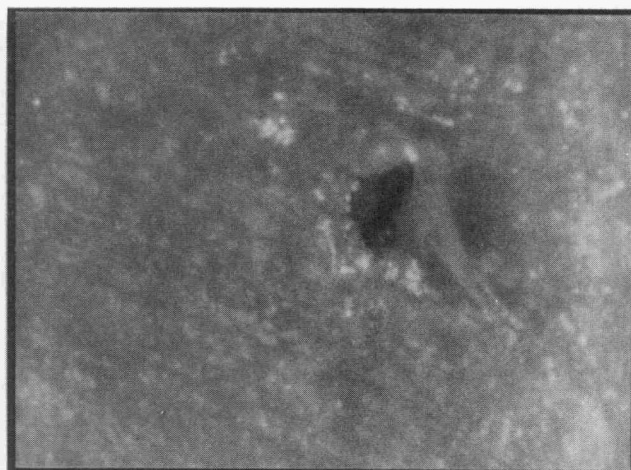


Figure 8. Hot Particle #14

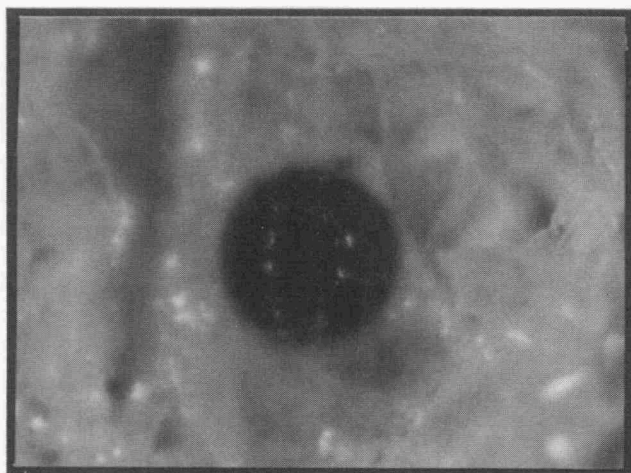


Figure 9. Hot Particle #18

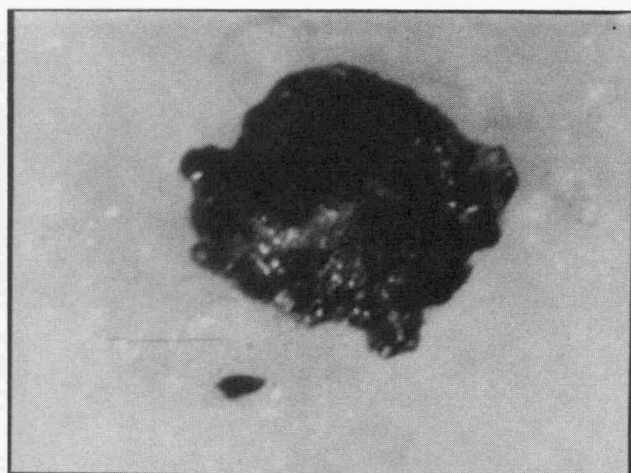


Figure 10. Hot Particle #19



Figure 11. Cloth from Anti C's



Figure 12. Cloth from blue jeans

Table 2. Summary of the gamma emitting isotopes found in the samples of particulate contamination and their activities in disintegrations per second. These isotopes consisted of fission products and activation products. The fission product bearing particles, referred to as fuel fleas, were found to be tiny bits of uranium. The activated metals were from various sources, probably mixtures of corrosion and wear products.

Fuel Fleas								
Particle	$^{144}\text{Ce}$	$^{106}\text{Ru}$	$^{154}\text{Eu}$	$^{155}\text{Eu}$	$^{95}\text{Nb}$	$^{95}\text{Zr}$	$^{103}\text{Ru}$	$^{141}\text{Ce}$
#2	60	14	0.6	0	8	4	1.1	0.9
#4	52	113	36	19	0	0	0	0
#8	110	47	0	0	48	24	7	3
#13	140	17	0.9	0	2.4	1.2	0	0
#15	380	30	6	4	1.2	0.9	0	0
#16	120	90	2.8	1.5	0.6	0.6	0	0
#20	25	130	4.1	2.8	4	2	0	0
Purified Fission Products								
Particle	$^{106}\text{Ru}$	$^{137}\text{Cs}$	$^{134}\text{Cs}$					
#1	160	0	0					
#7	4,500	0	0					
#9	0	609	240					
#17	0	3,000	0					
Activated Metals								
Particle	$^{60}\text{Co}$	$^{58}\text{Co}$	$^{57}\text{Co}$	$^{54}\text{Mn}$	$^{110\text{m}}\text{Ag}$	$^{137}\text{Cs}$	$^{134}\text{Cs}$	
#3	121,000	0	0	2,912	0	0	0	
#5	745	246	14	34	0	0	0	
#6	4,700	0	0	0	0	0	0	
#10	6,450	105	0	670	0	0	0	
#11	0	0	0	0	470	0	0	
#12	11,400	0	0	0	0	0	0	
#14	1,745	0	0	27	0	0	0	
#18	120	48	3.1	30	0	39	13	
#19	92,800	0	35	7,676	0	0	0	
#21	5.8	46	0	0.7	3.8	0	0	

tivation threshold for  $^{59}\text{Co}$ , very small quantities of cobalt normally found in steel will produce high activities of  $^{60}\text{Co}$ .

The typical particles that were selected for skin dose estimation included two fuel particles (#4 and #15), the pure ruthenium particle (#7), and two activation particles (#3 and #12). The two fission product particles showed dose rates of 0.5 to 1.0 rem/hr for a  $1\text{ cm}^2$  area of skin. These were the most active of the fuel particles studied. The pure ruthenium particle, which had more than ten times the activity of the fuel particles, but was also much larger, had an estimated skin dose value of about 0.5 rem/hr to a  $1\text{ cm}^2$  area. The large, relatively active  $^{60}\text{Co}$  source particle would deliver a dose at an estimated rate of 325 rem/hr to an area of  $1.0\text{ cm}^2$ . The smaller, but much less active  $^{60}\text{Co}$  source would deliver about 30 rem/hr to  $1.0\text{ cm}^2$ .

## OBSERVATIONS

Fission products in irradiated fuels have been classified into four groups<sup>1</sup>. The first group contains the fission product gases, which include Kr, Xe, Br, and I. Fission products which form metallic precipitates compose the second group. These are Mo, Tc, Ru, Rh, Pd, Ag, Cd, In, Sb, and Te. The third group includes Rb, Cs, Ba, Zr, Nb, Mo, and Te. These are the fission products which form oxide precipitates. The last group consists of those fission products which dissolve as oxides in the fuel matrix. These elements include Sr, Zr, Nb, Y, La, Ce, Pr, Sm, Nd, and Eu.

The isotopes in the fuel fragments found in this study were the longer lived gamma emitters from the last three groups, namely Ce, Ru, Eu, Sb, Cs, Nb, Zr, and Ag. The ones found in concentrated states, i.e. Ag, Ru, and Cs, have interesting mobilities and purification processes. The source of radioactive zirconium may be from the activation of zircalloy rather than fission, or a combination of the two. The presence of  $^{110\text{m}}\text{Ag}$  may also be due to activation, as silver is a common impurity in copper.

A similar study of hot particles was performed for Southern California Edison by Battelle Pacific Northwest Laboratories in June 1987. According to a draft copy of a report<sup>2</sup> on this work, ten of more than 1000 suspected fuel particles were analyzed. The source of the ten particles was a fuel rod that was broken in the fuel handling pool during rod replacement. These particles were very large in comparison to the ones studied here, ranging from 1500 to 5000  $\mu\text{m}$  in size, with dose rates at 30 cm ranging from 15 to 200 mR/hr. The radionuclides that predominated in the Battelle study were basically the same ones found in the particles from this study. However the  $^{95}\text{Zr}$  and  $^{95}\text{Nb}$  contents were much higher in the Battelle study. The source of these isotopes was attributed to fission products.

The skin dose estimation for the Battelle study was done for only one particle and used the computer code VARSKIN, which uses the same algorithm for calculation as used in QUINCE. The dose rate for the particle, which was primarily  $^{144}\text{Ce}/^{144}\text{Pr}$  and  $^{106}\text{Ru}/^{106}\text{Rh}$ , was estimated at over 400 rem/hr for a  $2\text{ cm}^2$  area. (This value would have been considerably higher if it had been reported for a  $1\text{ cm}^2$  area.) It was noted in this report, however, that injury due to

such doses to relatively small areas of skin tissue are insignificant, citing the work of Reece, et al<sup>3</sup>.

## CONCLUSIONS

This preliminary study has indicated that most of the samples which were examined were indeed particulate in nature. For the most part, the bulk of the radioactivity could be isolated to one particle. About half of these particles were "fuel fleas", i.e. they represented fuel cladding failure, and about half were from the activation of metal fragments.

The particles that bore fission product isotopes were small, on the order of 2  $\mu\text{m}$  to 15  $\mu\text{m}$ . Particles this size will fit through the spaces in cloth weaving. It is evident that they can become trapped within the cotton fibers and not be dislodged in the laundry. The particles that bore activation product isotopes were generally larger, on the order of 150-350  $\mu\text{m}$  in diameter.

A small number of radioisotopes accounted for most of the gamma activity. The particles found in this study included (1) activated metals containing Co, Fe, Cr, and Mn radioisotopes, (2) activated silver, (3) uranium bearing the fission products Ce/Ru/Nb/Zr/Eu, (4) purified Ruthenium where  $^{106}\text{Ru}$  was the only identifiable gamma emitter, (5) a resin bead, (6) evenly distributed cesium bearing compounds, and (7) finely divided  $^{58}\text{Co}$ . The mode of isotopic purification which produces particles bearing pure  $^{106}\text{Ru}$ ,  $^{137}\text{Cs}$ , and  $^{110\text{m}}\text{Ag}$  needs further investigation.

Though potential beta skin doses are often large, actual tissue damage from external contamination is slight. The detection of radiation from small hot particles is difficult, therefore survey monitors could possibly fail to detect the less active particles under routine use.

## REFERENCES

1. Heiko Keleykamp. The chemical state of fission products in oxide fuels at different stages of the nuclear fuel cycle. Nuclear Technology, Vol. 80, March 1988.
2. Moeller, M.P., G.A. Stoetzel, and S.E. Merwin. Fuel Particle Analysis Including Instrument Response. Battelle Pacific Northwest Laboratories. June 1987.
3. Reece, W. D., Harty, L. W. Brakenbush and P.L. Roberson, 1985. "Extremity Monitoring: Considerations for Use, Dosimeter Placement, and Evaluation." NUREG/CR-4297, U.S. Nuclear Regulatory Commission, Washington, D.C.

A TIME TEMPERATURE CONTROLLED NON-CONTACT  
AUTOMATIC TLD SYSTEM  
METHODOLOGY FOR PERFORMANCE EVALUATION

K. J. Velbeck and M. Moscovitch  
Harshaw  
Crystal and Electronic Products  
6801 Cochran Rd.  
Solon, Ohio 44139

ABSTRACT

This paper documents the test procedures and results pertaining to a new four chip TLD dosimeter, TLD card type 8801, when evaluated in the System 8800 TLD Card Reader developed by Harshaw. The reader is automatic and uses hot nitrogen gas for non-contact heat transfer. The heating method is unique in the sense that it employs a closely controlled, linearly ramped time temperature profile. Since the overall performance of the equipment used in radiation protection dosimetry has a major role in the final determination of the dose equivalent, we have developed and implemented a methodology for the performance evaluation of the Model 8800 Reader and its associated TL dosimeters. Nine test procedures were performed, including Dose Response and Repeatability, Batch Uniformity, Card Reusability and Endurance, Fading, Thermal Neutron Sensitivity, Residual Signal, and Element Thickness. The results of each test are reported and discussed.

Copyright, Harshaw/Filtrol, 1988

## 1. INTRODUCTION

Reliable methods of detecting and measuring radiation are of general interest in various radiation dosimetry applications and are particularly important in the fields of personal radiation protection and environmental radiation monitoring. In both of these applications, a large number of dosimeters are routinely processed so that dosimeter reusability and the preservation of initial dosimetric properties have both an operational and an economic impact. This paper presents the results from a series of experiments designed to test that the overall TLD System 8800 Card Reader and its associated dosimeter cards is repeatable and maintains a consistent dose response.

## 2. EXPERIMENTAL

The TLD System 8800 Card Reader used in this experiment utilizes a non-contact heating technique based on a stream of hot nitrogen gas flowing over a tightly encapsulated LiF-TLD element. The gas temperature is constrained to following a specified Time Temperature Profile (TTP) by a sensor within 1 mm. of the TL element. A TTP consists of three independently controlled areas; preheat, data acquisition, and anneal as shown in Figure 1. It is important for a TLD reader that the heating of the dosimeter elements be controlled and reproducible. This requirement is due to the fact that the amount of radiation-induced thermoluminescence is dependent on the thermal history of the material as well as on the heating cycle during readout. A fully controlled heating cycle is, therefore, extremely important especially for low dose measurements. Usually the heating cycle is applied and controlled by contact ohmic heating of the TL element. The contact heating is advantageous in its continuous control of the heating cycle using various feed-back techniques. However, this is not accomplished without two drawbacks; a relatively short dosimeter lifetime and large infrared signals associated with the heating element. The present "Time Temperature Controlled" Non-Contact heating method is unique in comparison to other existing heating techniques<sup>(1)</sup> by sharing the advantage of precise temperature control without creating the problems of decreased dosimeter life and extraneous signals.

The type 8801 TLD card incorporates four LiF TL dosimeter elements encapsulated between two thin sheets of PTFE. This card type has been designed and produced with minimal air entrapment to provide optimal heat transfer efficiency from the hot nitrogen stream to the encapsulated TL element. The 8801 type dosimeter card consists of four 3mm x 3mm TLD elements, of the following types and thicknesses:

<u>Position</u>	<u>Type</u>	<u>Thickness</u>
1	TLD-700	0.4 mm
2	TLD-700	0.4 mm
3	TLD-700	0.09 mm
4	TLD-600	0.4 mm

The TL signal is accumulated via the charge integration technique from four TL elements simultaneously using four thermoelectrically cooled photomultiplier tubes with bialkali photocathodes.

For each test, a set of 20 cards was randomly selected from a typical batch of 900 production cards. All cards were prepared before irradiation. A Sr/Y-90 beta source (previously referenced to Cs-137 gamma) and a water moderated Am-Be neutron source were used to perform the various irradiations. Glow curves were recorded to a maximum temperature of 300°C at a heating rate of 25°C/sec. No high temperature annealing was applied and the preparation of the dosimeters prior to irradiation consisted of subjecting each dosimeter to one readout cycle. In each case, the test results were evaluated at the 95% confidence level for the mean of a normal distribution. Therefore, the test results shown in the following tables, with the exception of Table 8, represent the upper limit of the confidence interval, which is the mean value plus two standard deviations of the mean.

### 3. TEST RESULTS

#### DOSE RESPONSE

Twenty cards were prepared, irradiated to twenty different randomly selected dose levels in the range from 10 mrad to 100 rad. The results are shown in Table 1 for two dose ranges in terms of average deviation from linearity based on a straight line fit. In the range of 10 to 100 mrad, an uncertainty in the delivered dose of approximately 8% is believed to contribute to most of the reported deviation from linearity; however, this is subject to further investigation.

Table 1 Dose Response - Linearity

Irradiation range	Percent Deviation from linearity			
	TLD 1	TLD 2	TLD 3	TLD 4
10mrad - 100mrad	11%	8%	13%	9%
100mrad - 100rad	3%	3%	3%	3%

For each TL element position, dose response curves in the dose ranges 10 mrad to 100 mrad are presented in Figure 3. The graphs clearly demonstrate that within the deviations shown in Table 1, the system is linear down to 10 mrad. Special attention should be given to TLD 3 which shows linearity down to 10 mrad even for a thin (.09mm) LiF element which is used for beta and low energy photon dosimetry. Further tests were made continuing the low dose measurements down to 1 mrad. In the range of 1 - 10 mrad, a special background subtraction technique was implemented after the measurements were taken. The technique consisted of individual element background subtraction based on extrapolating the background curve under the glow peaks on both sides of the curve outside the region

of the peaks, as shown in Figure 4. For low temperature background subtraction, the average of the first few data points is simply subtracted from each channel and is assumed to be constant during the time of acquisition that is usually in the order of seconds. Then, point b is automatically identified to indicate the location of the high temperature infrared (IR) background signal. The IR is then fitted by a simple exponential based on Plank's black-body radiation formula. Figure 5 shows the dose response down to 1 mrad.

We now turn to a consideration of the dose response at higher dose levels. As expected, above 100 rads LiF:Mg,Ti exhibits supralinearity. Figure 4 shows the relative TL dose response curve,  $f(D)$ . In the linear region,  $f(D) = 1$ ; while in the supralinear region  $f(D) > 1$ , requiring proper correction at the high dose levels.

#### REUSABILITY

To test the reusability of the dosimeters two sets of 20 cards were prepared, irradiated to 500 mrad and read. One set was stored while the other was recycled through 500 reading cycles. The two sets of cards were then irradiated and read. Using two sets of cards accounts for any change in the reader response during the recycling period. The following results are presented in terms of the average reduced response of the reused dosimeters following 500 readout cycles, as compared to the cards which were stored (i.e., not reused).

Table 2 Card Reusability

	TLD 1	TLD 2	TLD 3	TLD 4
Average Response Reduction following 500 readout cycles	7%	7%	9%	8%

Graphic results are also presented in Figures 7 and 8 showing the normalized response and relative batch standard deviation vs. number of reuses. Also shown are representative glow curves for 1 and 2000 reuse cycles. Similar results were obtained by extending the number of recycles up to 2000 through the reader. The preservation of peak position and width versus number of reuses are shown in Figure 9.

.....

$$* \quad f(D) = \frac{TL(D)/D}{TL(D_0)/D_0}$$

Where: TL(D) is the TL signal corresponding to dose D and TL(D<sub>0</sub>) is the TL signal corresponding to dose D<sub>0</sub>, when D<sub>0</sub> is selected to be in the linear region of the dose response curve.

The remainder of this section will briefly describe the results of other tests performed on the dosimetry system.

#### BATCH UNIFORMITY

Twenty cards were prepared, irradiated to 100 mrad and read. The following results are presented in terms of the percentage relative standard deviation of the mean of the response of that element type for all 20 cards.

Table 3 Batch Uniformity

	TLD 1	TLD 2	TLD 3	TLD 4
Percentage Standard Deviation	8%	9%	11%	8%

#### REPEATABILITY OF RESPONSE

Ten successive measurements of each of 20 cards are taken after preparation and irradiation to 100 mrad. For each TL element the percent standard deviation of the mean response of 10 successive measurements has been computed. This value has been averaged over the 20 cards and the results are shown in Table 4.

Table 4 Repeatability of Response

	TLD 1	TLD 2	TLD 3	TLD 4
Average Percentage	1.04%	1.37%	1.44%	0.90%
Standard Deviation				

#### ENDURANCE

The 20 cards that were recycled 500 times in the Reusability test were tested in 4 different categories including bar code readability, card physical condition, glow curve completeness (Teflon seal quality), and visual inspection. The results showed that a single element on one of the twenty cards produced an incomplete glow curve. Otherwise, all tests were passed.

#### FADING

Twenty cards were prepared, irradiated to 100 mrad and stored in the dark for a period of 77 days. They were then read, exposed again and then read again. The unfaded and faded response values were used in determining the results which are the reduced response due to fading.

Table 5 Fading

	TLD 1	TLD 2	TLD 3	TLD 4
Response Reduction	14%	12%	16%	12%

The fast fading Peaks 1 and 2, with half lives of 5 minutes and 12 hours respectively, are not included in these measurements; however, Peak 3 with a half life of approximately 5 months is included. By subtracting out Peak 3 using the method of Computerized Glow Curve Deconvolution<sup>(3)</sup>, the fading effect can be minimized.

#### THERMAL NEUTRON SENSITIVITY

Twenty cards were prepared and irradiated to 300 mrad neutron dose from a water moderated Am-Be source. The cards were read and the results are presented as the percentage response of the non-neutron sensitive elements TLD 1,2,3 (TLD-700 type) relative to the neutron sensitive element TLD 4 (TLD-600 type).

Table 6 Neutron Sensitivity

	TLD 1	TLD 2	TLD 3
Neutron Response	3%	3%	2%

Since no environmental gamma contributions were subtracted, the values shown in Table 6 represent an upper limit of the thermal neutron sensitivity of the TLD-700 elements relative to the TLD-600 element.

#### RESIDUAL TL SIGNAL

Twenty cards were prepared and irradiated to 500mrad. They were read and then reread. The results are in terms of the ratio of reread response to the initial read response. Note that the response reported includes a constant background signal.

Table 7 Residual Signal

	TLD 1	TLD 2	TLD 3	TLD 4
Response ratio	0.5%	0.2%	0.3%	0.3%

## ELEMENT THICKNESS

One hundred TLD elements (before encapsulation in cards) were randomly selected and measured to determine their thickness. The results are presented in terms of nominal thickness and the percentage standard deviation of the mean.

Table 8 Element Thickness

	<u>.4mm element</u>	<u>.09mm element</u>
Average	.4mm	.09mm
Std. Dev.	1.62%	4.01%

## 4.0 CONCLUSION

The Model 8800 Reader and type 8801 dosimeter card constitute a dosimetry system capable of providing sufficiently accurate and consistent measurements to enable reliable dose calculations.

## 5.0 REFERENCES

- (1) Julius, H. W., "Instrumentation in Thermoluminescence Dosimetry", Radiat. Prot. Dosim., 17, 267-273(1968).
- (2) Moscovitch, M. and Horowitz, Y. S., "Microdosimetric Track Interaction Model Applied to Alpha Particle Induced Supralinearity and Linearity in LiF:Mg,Ti", Radiat. Prot. Dosim., 17, 487-491(1986)
- (3) Moscovitch, M., "Automatic Method for Evaluating Elapsed Time Between Irradiation and Readout in LiF-TLD", Radiat. Prot. Dosim., 17, 165-169(1986)

6.0 FIGURES

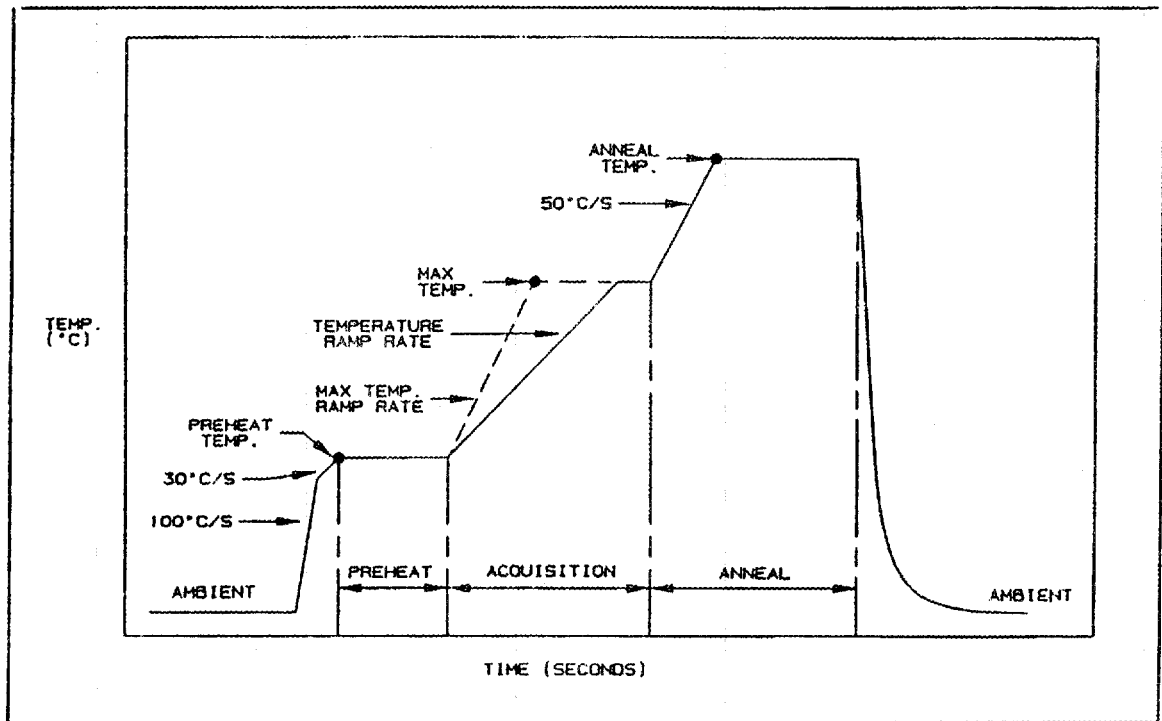


Figure 1  
Typical Time Temperature Profile

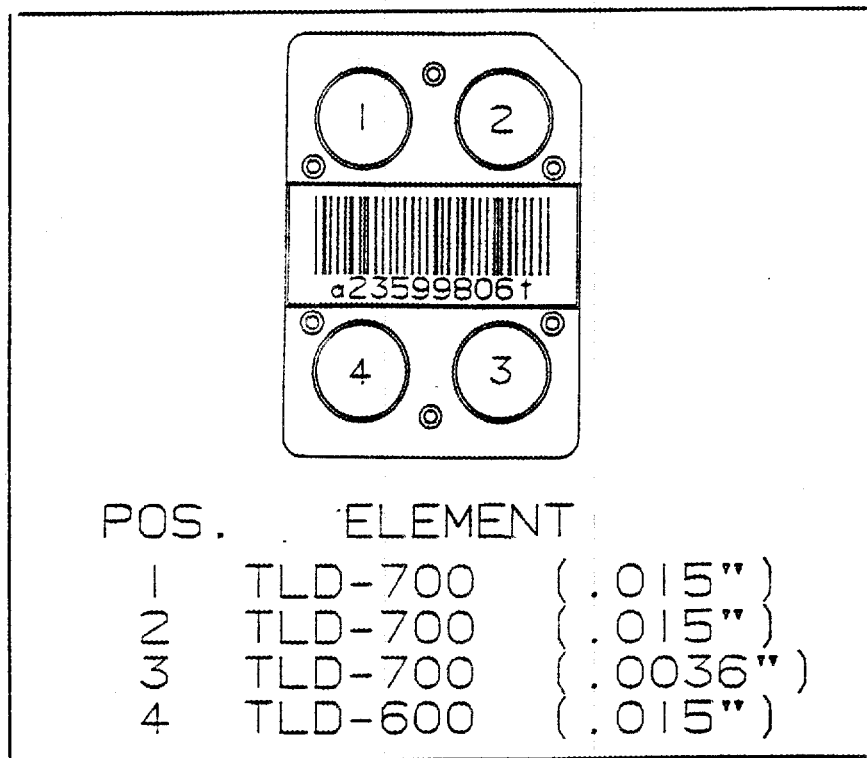


Figure 2  
8801 TLD Card

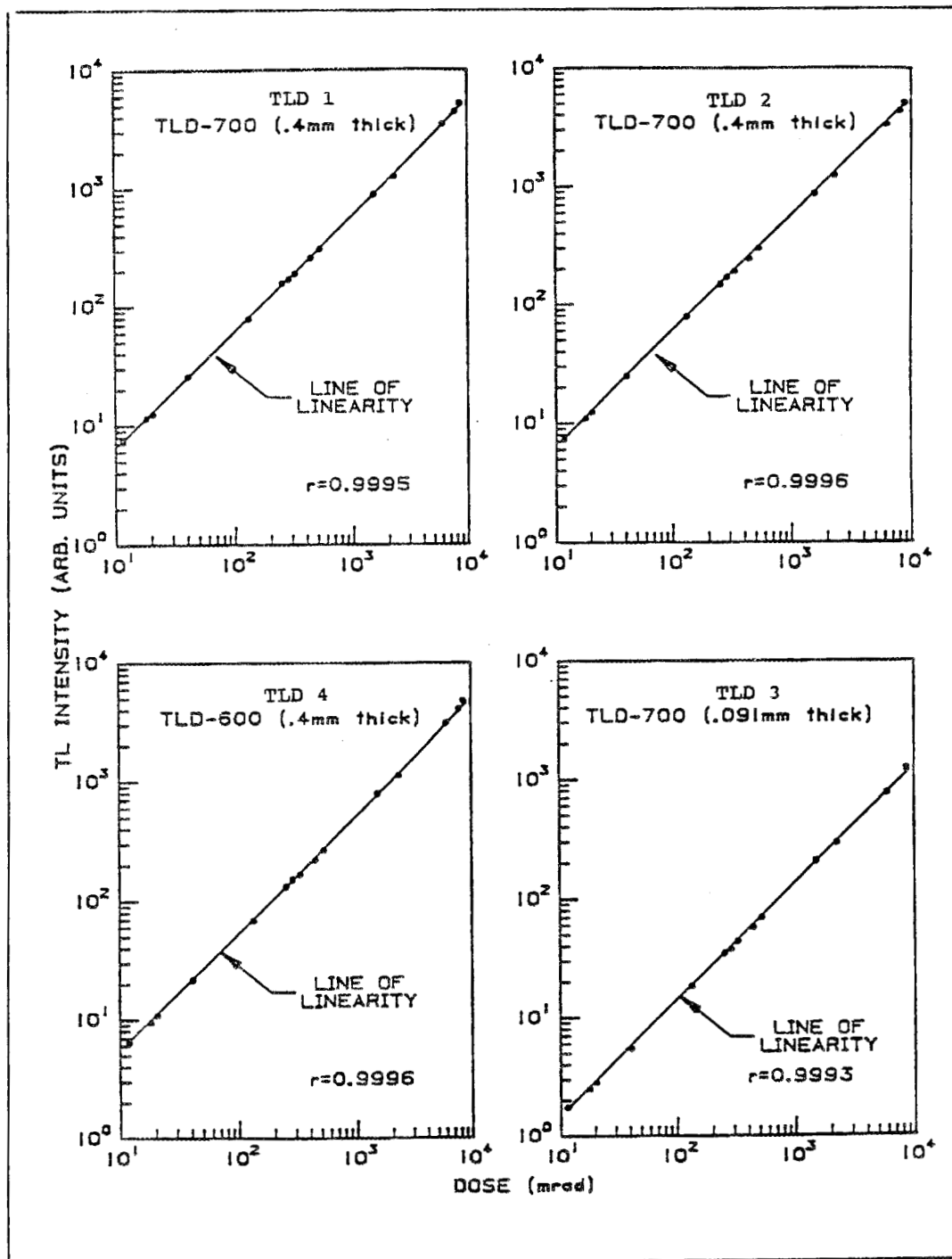


Figure 3 Response Linearity

TL as a function of dose in the linear dose response region of LiF:Mg,Ti

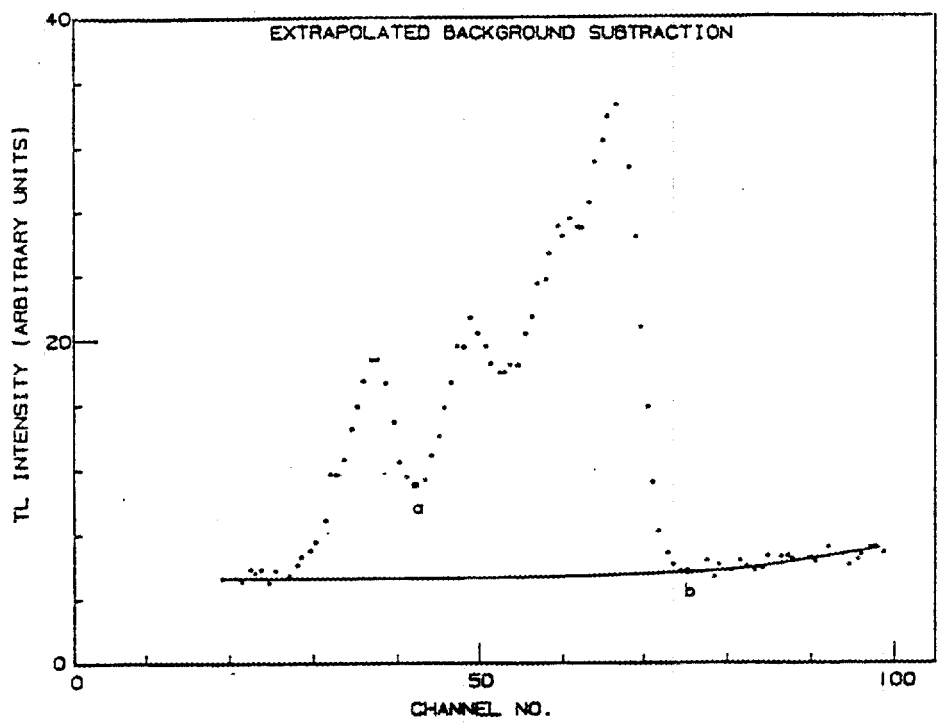


Figure 4  
Background Subtraction

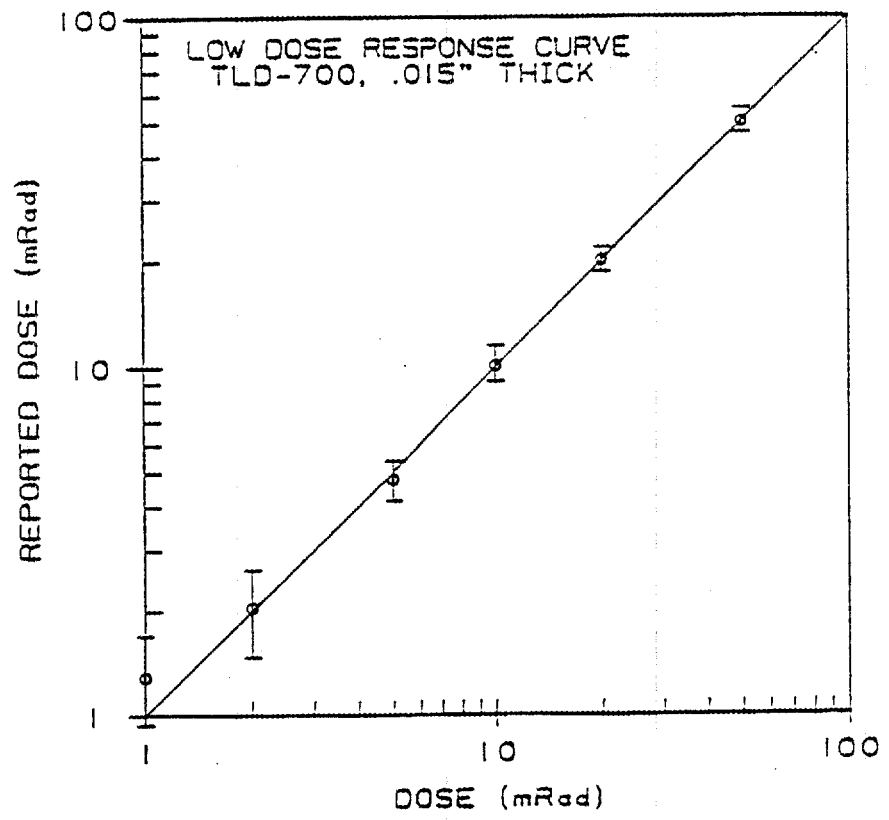


Figure 5  
Low Dose Linearity

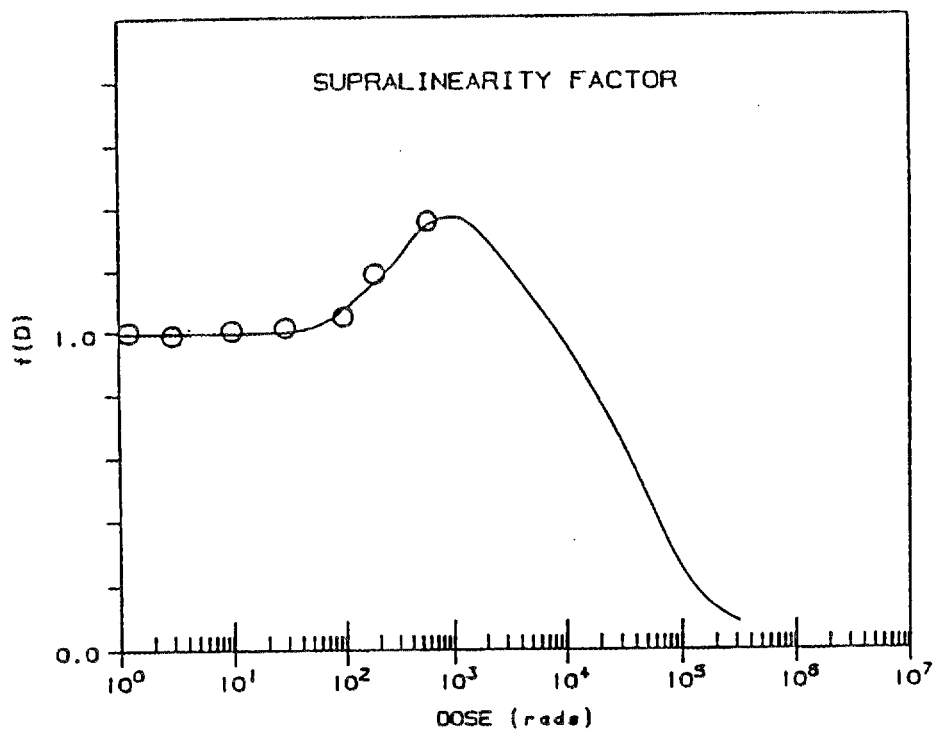


Figure 6  
TL Dose response curve for LiF:Mg,Ti

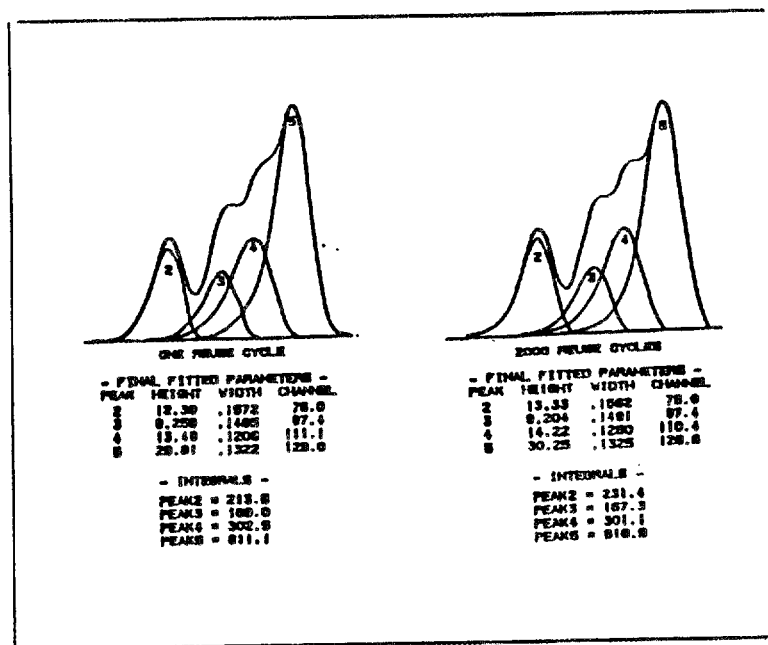


Figure 7  
Example of glow curves before and after 2000 reuse cycles.

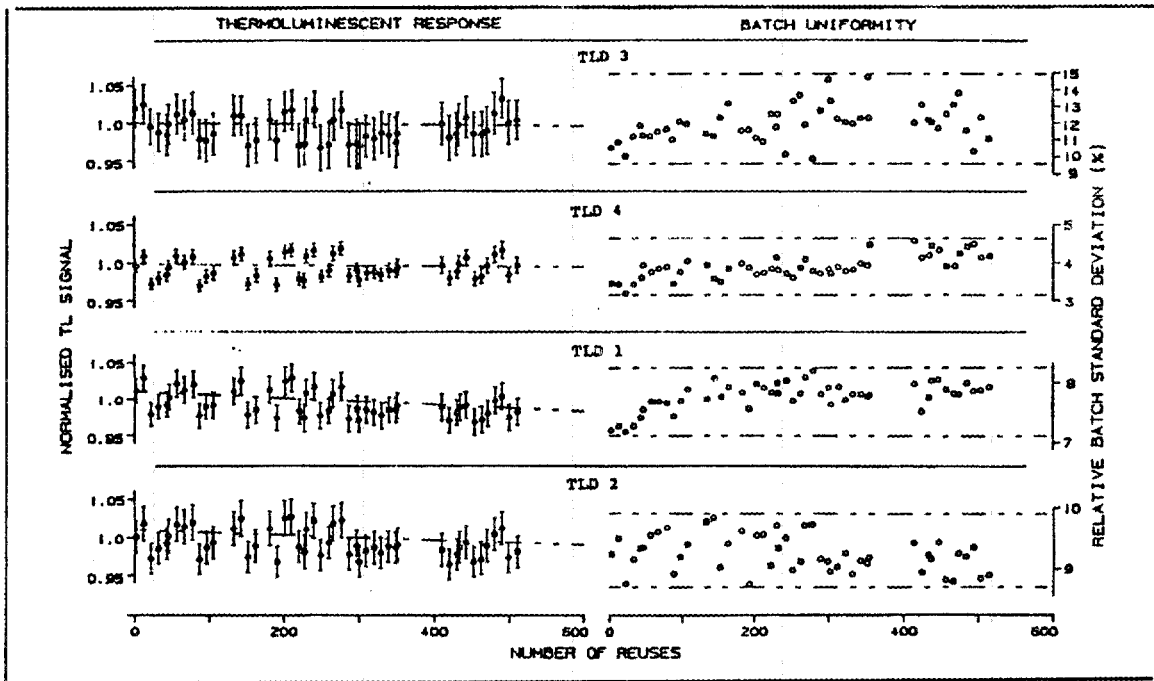


Figure 8  
TL response and batch uniformity as a function of the number of reuse cycles.

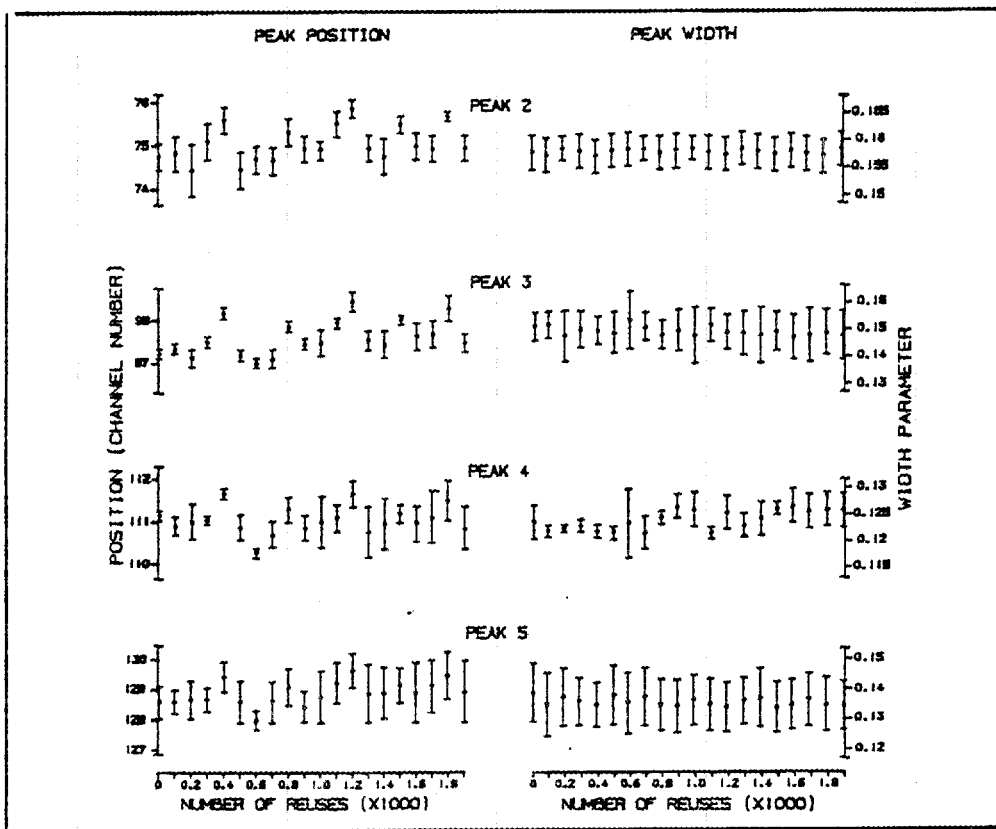


Figure 9  
Glow curve characteristics as a function of the number of reuse cycles.

QUALITY ASSURANCE PACKAGE FOR ROUTINE THERMOLUMINESCENCE  
DOSIMETRY PROGRAM

R. A. Tawil, G. Bencke, and M. Moscovitch  
HARSHAW  
Crystal & Electronic Products  
6801 Cochran Rd.  
Solon, Ohio 44139

ABSTRACT

The Quality Assurance Package presented here specifies a set of reader-related hardware diagnostics and calibration procedures and automatically maintains audit trails of generated and derived thermoluminescence data. It specifies acceptable performance criteria for the reader and dosimeter assemblies; tracks and controls Readout Cycle Temperature Profiles; and ensures that the acquired data is verified.

The quality of the generated glow curves is tracked by the real-time application of Computerized Glow Curve Deconvolution to reference dosimeters that may be mixed with field dosimeters during readout sessions.

This package is supported by a menu-driven software system using vertical auto-selection menus, lotus-style horizontal menus, data entry menus with automatic error checking, and pop-up windows. The menu system is supported by an extensive HELP file; data EDITING is password-protected, and a journal is maintained for each editing session as part of the audit trail. Files for the Raw Data and Derived Dose results are maintained and managed in seven databases.

The paper provides an in-depth analysis of each of the procedures, specifies data validation criteria, and presents samples of the reports generated.

Copyright, Harshaw, 1988

## I. GENERAL DESCRIPTION

The objective of this paper is to describe the Quality Assurance Package of the Radiation Evaluation and Management System (TLD REMS) software system originally developed by Harshaw for personal dosimetry applications.

The TLD-REMS software system was developed to control the reader operations, including the acquisition, storage, processing (including dose computation), retrieval, reporting, and disposition of TLD data. The REMS is an integral part of a thermoluminescent dosimetry (TLD) workstation which includes a personal computer and one or more TLD Card Readers in a configuration such as that shown in Figure 1. It accommodates the characteristics of several different readers and provides a common interface to a central computer system. The REMS is designed to operate under DOS or under a UNIX multi-user environment. Password security is required for certain functions of the REMS and a Utility is provided to enable the user to add, delete, and change password hierarchies. A user without a password may generally access data for viewing. With password security, the user may also edit various data, change the data acquisition set-up parameters, and change the Time-Temperature Profiles (TTP) applied to the TL element by the reader during the data acquisition cycle. Data can be archived to a diskette, restored from diskette, and deleted from the system. However, no data can be deleted from the data base unless it has first been archived. The system is menu driven using vertical and panel style menus, pop-up menu windows, and data entry panels with automatic error checking, and is supported by an extensive help message system. Four color pallets are utilized to enhance the utility and interpretation of menu items.

REMS stores the instrument calibration data and the corresponding Readout TTP, reader performance and quality control related data as produced by the instrument during its operations, dosimeter element correction data, glow curves, and computed exposures. Exposure data is stored in the TLD data base in sets of records known as Group Files. Data may be selected from the data base for review and disposition by Group and by certain characteristics of the data itself. The standard data bases are as follows: Group Files, Group Summary File, Quality Control Dosimeters, Element Correction Coefficients, Reference Light, PMT Noise, Electronics Quality Control, and Log Files. This last database is a collection of the comments made by the operator at the initiation and termination of activities that utilize the REMS acquisition functions.

The Quality Assurance Package described here was developed to offer users sufficient capabilities to ensure the validity, reproducibility, and traceability of the data bases maintained. It consists of procedures for Reader Quality Assurance, and procedures to monitor and control the performance of the Reader during the Acquisition of TL Data.

## II. READER QUALITY ASSURANCE

The instrument Performance Quality Assurance consists of the Electronics QC, Reader and Dosimeter Calibration procedures, and procedures to exercise and test the different subsystems of the TL Data Acquisition System. The last set of procedures enables the operator to specify operating tolerances during the routine operations of the Reader. A summary of these procedures is presented in Figure 2.

The Electronics QC function polls the electronics subsystem parameters that affect the conversion of the TL-generated light to charge pulses represented by the Glow Curve. The parameters are identified in Figure 3, and serve to determine that the instrument is properly adjusted. By means of the Execute Photronics Calibration option, the operator maintains the reader's electronic adjustments, monitors the data from the acquisition system, and interactively calibrates the current-to-frequency Digitizer/Interpolator electronics. Furthermore, these activities enable the operator to define and establish reader performance criteria for those parameters which are automatically monitored during the data acquisition cycle of the Reader while in normal production dosimetry operation. A complimentary function is the Daily QC. The operator invokes this function at Power Up or according to a pre-established schedule in order to perform diagnostics on the reader hardware including the RAM, PROM, and REFERENCES, and to generate the report shown in Figure 3.

The Reader Calibration option is used to establish the Reader Calibration Factor (RCF), or the average response of the reader to a subset of Calibration Cards created from the Generate Calibration Cards. The purpose of this procedure is to establish Element Correction Coefficients of a set of cards relative to the mean of their response and without reference to a specific Reader calibration. To generate a set of Calibration Cards, the selected cards are cleared and exposed to a known radiation,  $D_0$ , and read out in the normal manner. For each element position  $j$  of card  $i$ , the average response,  $Q(j)$ , is computed and used to generate element correction coefficient  $ECC(i,j)$ , according to:

$$ECC(i,j) = \frac{Q(j)}{Q(i,j)},$$

$Q(i,j)$  is the reported charge for element  $j$  of card  $i$ .

To establish the RCF, a statistically representative number of Calibration Cards is cleared, exposed to a known amount of radiation, and read out. An average response for each position on the card is computed according to the following relationships:

$$RCF(j) = \frac{\langle(Q_0)_j\rangle}{D_0}$$

$$\langle(Q_0)_j\rangle = \frac{\sum_{i=1}^k (Q(i,j)*ECC(i,j))}{k}$$

Where:

- RCF(j) - Reader Calibration Factor for card element position j
- D<sub>0</sub> - Nominal Irradiation Value
- ECC(i,j) - the Element Correction Coefficient for dosimeter element j of card i
- k - total number of cards included in the sample

Note that the RCF thus generated is specific to the Time-Temperature Profile (TTP) applied during the Readout Cycle. For the rest of this paragraph, reference is made to Figure 4, which identifies the set of parameters defining the TTP. It is obvious that the  $\langle(Q_0)_j\rangle$  value is dependent on the selections made for the Calibration Region values, the preheat temperature and its duration, the maximum temperature attained, the acquisition period and the temperature ramp rate.

Traceability to an NBS Standard may be established according to the following procedure. A statistically representative number of Calibration Cards is cleared and exposed to an absolute dose D<sub>0</sub>' at a facility with an NBS standard. The cards are read out in an uncalibrated reader after the application of the Electronics QC Procedures; the average response  $\langle Q(j)'\rangle$  for each element position (j) is computed as previously specified. The same set of cards is then exposed to a nominal value D<sub>0</sub> by the local irradiation facility and the corresponding  $\langle Q(j)\rangle_0$  is computed. The ratio of  $\langle Q(j)\rangle/\langle Q(j)'\rangle$  when folded in by multiplying with the RCF provides the traceability. This procedure must be repeated any time the local irradiator configuration is altered or changed.

Another menu item is the Card Calibration. Its purpose is to create an Element Correction Coefficient (ECC) for each dosimeter element on every card in the system in order to normalize their responses. To generate ECCs, all cards are cleared and exposed to a

known radiation. The cards are then read using a calibrated reader. The  $ECC(i,j)$ , position  $j$  in card  $i$ , is the ratio of the 'nominal irradiation value' to the measured response. The computation process is initiated and proceeds automatically, rejecting any cards with a sensitivity outside the limits set by the operator as acceptable.

### III READER MONITORING DURING READOUT CYCLE

The parameters that are monitored and the procedures that are applied during the Readout Cycle are summarized in the Acquisition Setup Menu, Figure 5. Access to this menu for the purposes of data editing is password protected since the values here are utilized to check the reader for acceptable performance. Among the conditions which are set here are the PMT Noise Check Interval and the corresponding acceptable performance range for each element position on the card. The same logic is also applied in monitoring the Reference Light. These two checks are applied to determine the performance of the PMT and the electronic gain stability of the system. This data is maintained by REMS in independent data bases.

Data quality and integrity during acquisition are further assured by means of a hierarchical system of messages exchanged between the reader and REMS. Perhaps the most significant tracking by the system is the instantaneous temperature of the hot gas during the read cycle, which is applied to control the heater logic and is displayed on the system screens in real time. Additionally, the instantaneous temperature and corresponding digitized light output pairs are stored in the database. The glow curve record includes 200 pairs of temperature and intensity values, generating the display seen in Figure 6. During acquisition of these values, several reliability tests are being performed. These include checking the various sensors; checking for an electronic circuit failure; and deviation of more than  $10^{\circ}$  C in heater temperature from the control input signal. If the system fails any of these reliability tests, orderly shutdown is initiated with the appropriate error messages displayed.

The last procedure of the Quality Assurance Package that will be discussed here is the application of COMPUTERIZED GLOW CURVE DECONVOLUTION TO QC CARDS (CGCD). QC cards are a set of cards that are selected from the Calibration Cards, exposed to a known dose, and inserted in line with other cards while prepared for Readout. The QC cards are identified by the system, and deconvolution is applied immediately after the Glow Curve generation is completed. CGCD enables tracking and determining the stability of the Glow Curve Peak Positions, reflecting the repeatability of readout cycle temperatures; the Peak Width, reflecting the efficiency of heat transfer from the heater to the TL element across the protective cover; and the Peak Heights, reflecting the stability of the gain of the reader. These are checked against the tolerances specified in

Figure 5, with the appropriate actions taken. This figure also shows the five dose thresholds used to control the disposition of the TLD data records received while processing cards. These thresholds apply to Field Cards only. If any of the TL elements on the card exceed the specified level, the action described will be triggered.

### Summary

The Quality Assurance Package described herein features three sets of functions that are invoked in preparation of the reader or during Field Card or dosimeter readout sessions. One set of functions is aimed at calibrating the reader subsystems; the other set addresses the various calibration procedures aimed at establishing traceability of the data generated; and the third is aimed at monitoring and tracking the TL Readout Cycle stability and efficiency during routine operations.

This Package is incorporated in a system, REMS, that is menu-driven using vertical, auto-selection menus, lotus-style horizontal (panel) menus, data entry panels with automatic error checking, and pop-up windows. The menu system is supported by an extensive help file.

### Acknowledgments

The authors acknowledge with thanks the helpful discussions with W. Wilder, and express appreciation to C. Martis and D. Herrick for their part in the development of this package.

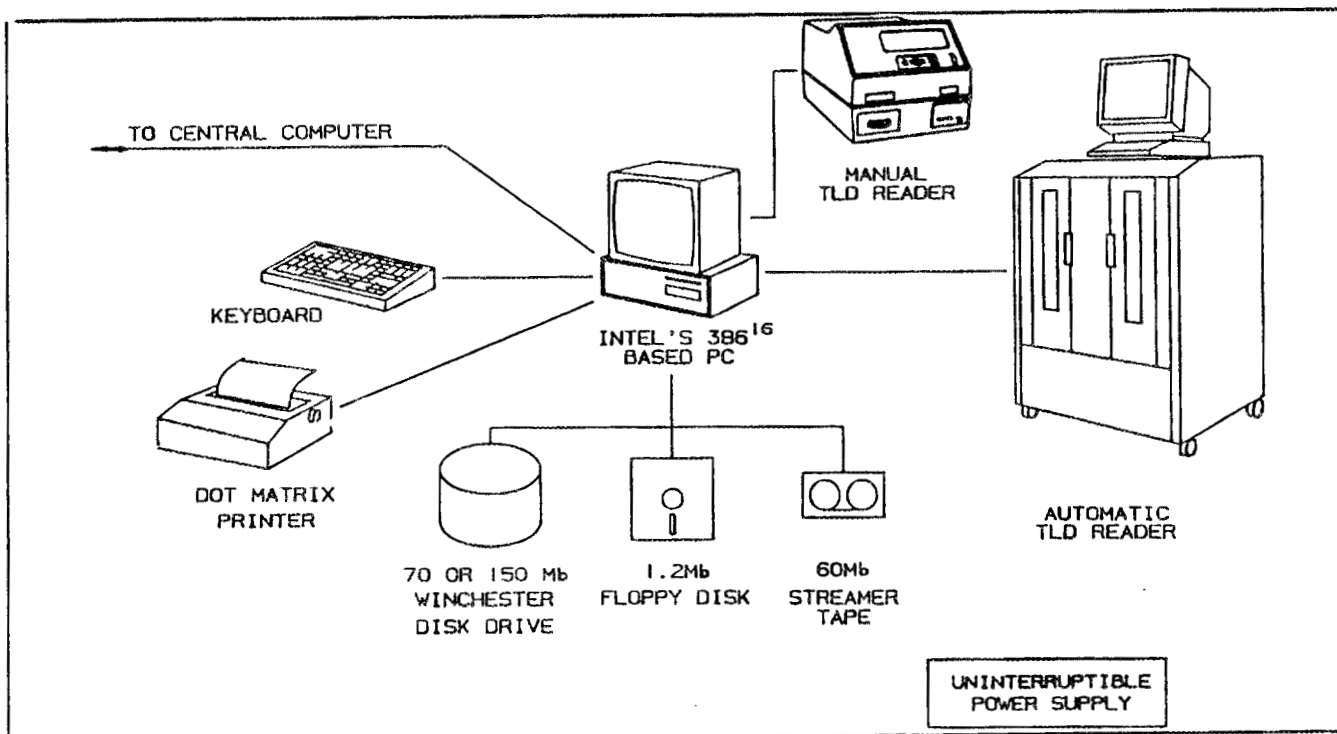


Figure 1  
Typical TLD Workstation

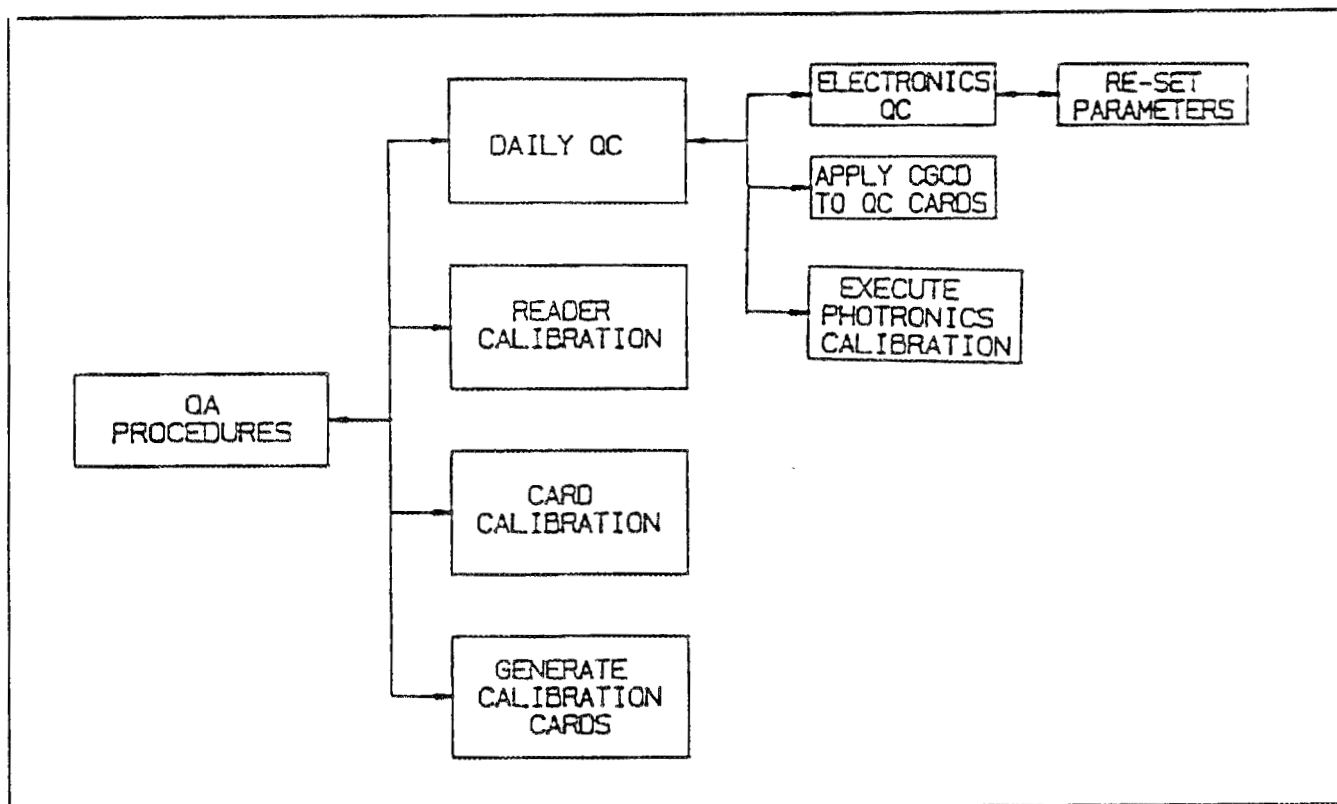


Figure 2  
TLD REMS Q A Procedures

Daily Q C Electronics Q C	Customer Name Harshaw TLD-REMS		14-Sep-1988 10:27 pm	
Date 14-Sep-1988	Time 22:17:45		Reader Number 16	
	(i)	(ii)	(iii)	(iv)
Photronics Version	15	15	15	15
RAM Read/Write test	pass	pass	pass	pass
PROM Checksum test	pass	pass	pass	pass
Plus 15 volt supply	pass	pass	pass	pass
Minus 15 volt supply	pass	pass	pass	pass
D/A Reference test	pass	pass	pass	pass
	Mean	SDev	Mean	SDev
Temperature	28.3	0.36 %	31.00	0.00 %
High Voltage	853	0.03 %	918	0.00 %
Plus 15 Volts	14.87	0.02 %	14.93	0.02 %
Minus 15 Volts	14.99	0.00 %	14.90	-0.0 %
D/A Reference	0.190	0.03 %	0.183	0.00 %
Ground	-0.03*	0.00	-0.00*	0.00
Reference Light	159.9	0.61 %	240.1	0.64 %
PMT noise	0.144	8.46 %	0.195	9.89 %
	Mean	SDev	Mean	SDev
	29.29	0.00 %	30.02	0.00 %
	899	0.00 %	827	0.00 %
	14.95	0.02 %	14.95	0.00 %
	14.88	0.00 %	14.89	0.00 %
	0.100	0.00 %	0.103	0.00 %
	0.004	0.00	0.004	0.00
	170.2	0.99 %	185.6	1.02 %
	0.258	3.11 %	0.113	8.32 %
Start Electronics Q C	PrtScrn	Re-set Parameters	Return to Daily Q C	

Figure 3  
Electronics QC Report Screen

Data Acquisition Time Temp Profile	Customer Name Harshaw TLD-REMS		14-Sep-1988 11:00 pm	
Date Edited 12-Sep-1988	Edited by WILDER			
Calibrated 12-Sep-1988				
Profile 10	Title plain cards			
	( i )	( ii )	( iii )	( iv )
roi1	[ 1 , 50 ]	[ 1 , 50 ]	[ 1 , 50 ]	[ 1 , 50 ]
roi2	[ 51 , 100 ]	[ 51 , 100 ]	[ 51 , 100 ]	[ 51 , 100 ]
roi3	[ 101 , 150 ]	[ 101 , 150 ]	[ 101 , 150 ]	[ 101 , 150 ]
roi4	[ 151 , 200 ]	[ 151 , 200 ]	[ 151 , 200 ]	[ 151 , 200 ]
Calibration Region	[ 1 , 200 ]	[ 1 , 200 ]	[ 1 , 200 ]	[ 1 , 200 ]
Preheat temperature	30	30	30	30
time	0	0	0	0
Temperature rate	30	30	30	30
Maximum	300	300	300	300
Acquire time	10	10	10	10
Anneal temperature	0	0	0	0
time	0	0	0	0
Calibration factor	1.058	0.961	0.359	0.891 nC/gU
Average PMT noise	0.1943	0.2081	0.3023	0.1624 nC
Average Reference light	159.66	237.01	167.34	190.36 nC
Next	Previous	Undo	Restore	Report
				Return

Figure 4  
Time Temperature Profile Screen

Note: Data on these two Figures are included for illustrative purposes only, these values may not be realistic for most cases.

Data Acquisition Acquisition Set-Up	Customer Name Harshaw TLD-REMS	14-Sep-1988 11:18 pm
Date Edited 14-Sep-1988	Edited by WILDER	
PMT Noise Interval 18	Reader Record Glow Curves	
Ref Light Interval 8	Display Format Glow Curves	
Apply Calibration none	Print Format Computed Exposure	
	Transmit Format noTransmission	

	( i )	( ii )	( iii )	( iv )	
PMT Noise Range [	0 , 200 ]	0 , 200 ]	0 , 200 ]	0 , 200 ]	pC
Ref Light Range [	100 , 150 ]	100 , 150 ]	100 , 150 ]	100 , 150 ]	nC
QC Card Range [	250 , 350 ]	250 , 350 ]	250 , 350 ]	250 , 350 ]	

If reading exceeds:

- 9000000 , halt machine and sound alarm
- 8000000 , re-read same dosimeter
- 1000 , mark record with warning flag
- 0 , for [ Cal. Region ] save curves and exposure
- 0 , for [ Cal. Region ] save exposure only

Return to Acquisition

Figure 5  
Acquisition Set-up Screen

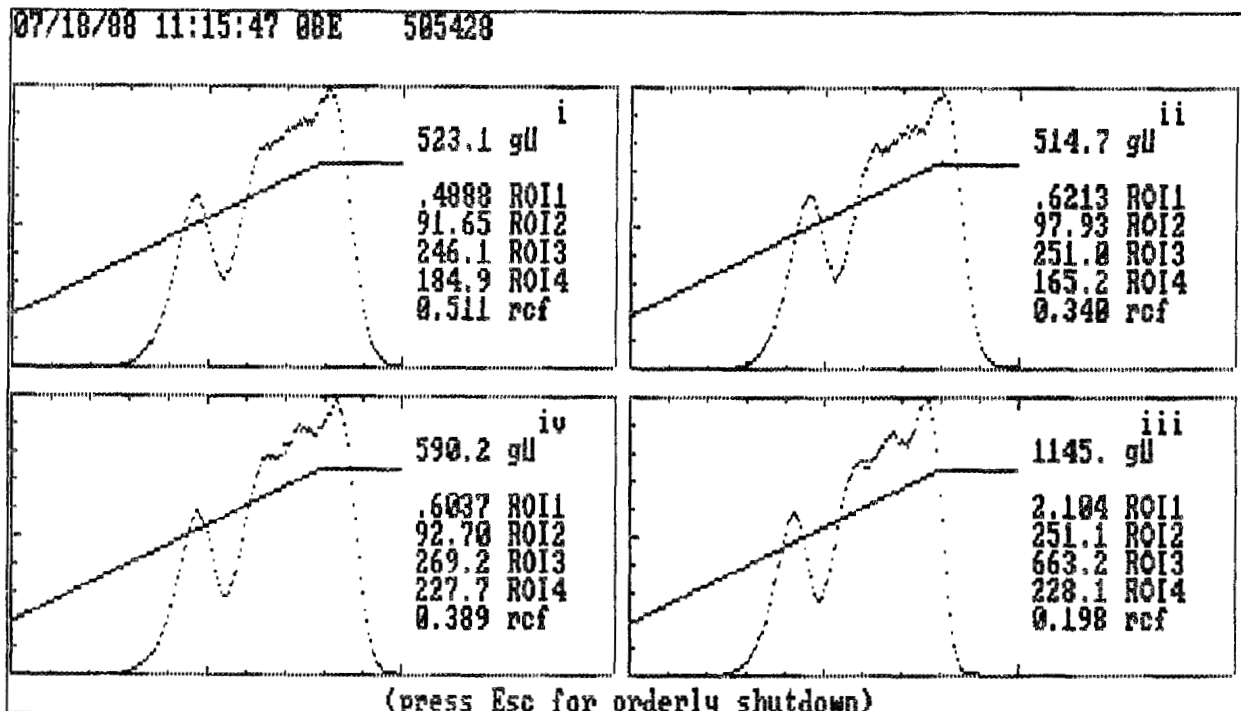


Figure 6  
Glow Curve and Temperature Display Screen

Note: Data on these two Figures are included for illustrative purposes only, these values may not be realistic for most cases.

**FACTORS AND STRATEGIES IN THE OCCUPATIONAL MONITORING  
OF PERSONNEL IN MEDICAL ANGIOGRAPHY**

**Stanley H. Benedict, Jeffrey H. Kleck, and James E. McLaughlin  
Radiation Safety Office, Department of Community Safety  
University of California at Los Angeles, Los Angeles, California**

## **FACTORS AND STRATEGIES IN THE OCCUPATIONAL MONITORING OF PERSONNEL IN MEDICAL ANGIOGRAPHY**

**Stanley H. Benedict, Jeffrey H. Kleck, and James E. McLaughlin  
Radiation Safety Office, Department of Community Safety  
University of California at Los Angeles, Los Angeles, California**

Angiographic procedures which include extensive fluoroscopy are among those which can produce the highest radiation exposure of hospital workers. The introduction of hemiaxial projections, and vascular fluoroscopic boost imaging methods has increased diagnostic accuracy, but it has also increased the physician's exposure to scattered radiation. Medical facilities in angiography and catheterization vary in regards to type of equipment and training of personnel. The health physicist for a facility is compelled to initiate a program to measure the potential exposure from a facility as well as assist in the training of personnel to minimize the exposure. Training of the medical personnel also includes techniques of exposure monitoring which for some individuals is more practically attained by utilization of a double badge program. This is especially important in the University setting where new residents and fellows are being introduced to the facility.

### **MEASURING STAFF EXPOSURE IN ANGIOGRAPHY LABS**

Modern angiography equipment must be capable of performing peripheral, visceral, and interventional procedures. Biplane, magnification, multiangulation, and spot filming capabilities are also desirable. Fortunately power requirements have decreased in recent years as a result of the introduction of rare earth screen-film systems and the incorporation of carbon fibers into tabletops and film changer faceplates. As a result, generators with relatively lower power outputs, and x-ray tubes with smaller focal spots are used. Multiangulation rotational mounting units, some of which contain "fluoro boost" potential, have been developed in recent years by the equipment manufacturers. These units have major advantages for clinical diagnosis, but their designs have major drawbacks in regards to personnel exposure (Levin, 1982).

X-ray tube and generator technology power requirements for serial film angiographic procedures have diminished considerably during the past decade. In the early 1970s, it was believed that 150-200 kW generators were required for serial film angiography. However, high-powered generators coupled with large focal spot x-ray tubes are no longer necessary or desirable for visceral or peripheral angiography. This results from advances in rare

earth screen-film systems and the incorporation of carbon fiber into angiographic tabletops and the faceplates of serial film changers. Equipment that incorporates these developments may utilize power outputs of 40-60 kW for most angiographic procedures, even in large patients. Unfortunately, to outfit a facility with all of the latest developments is very costly, and many angiographic-catheterization facilities undergo partial renovation to include replacement of selected components which may decrease or increase the subsequent exposure to the operators. Moreover, manufacturers use unique configurations for mounting and shielding x-ray tubes, as well as varying efficiencies for image intensifiers, tube outputs, etc. These factors lead to significant variations in radiation protection against leakage and scattered radiation. Since radiation exposure to the operator is not usually provided in the specifications of equipment, it should be measured upon completion of the renovation.

Using a RANDO phantom, a technique has been developed to compare radiation scatter to personnel from various units. In particular, this paper will focus on the comparison of a new facility (with a high efficiency prototype image intensifier) and a considerably older facility. The method utilizes an MDH survey meter to generate a series of exposure grids at designated distances from the source of scatter (ie. the RANDO phantom).

A common set-up in both facilities, anterior-posterior technique, onto the chest of the phantom was utilized to compare the scatter and leakage radiation to the operator. The new facility was a 2 million dollar system specifically manufactured for the UCLA Medical Center by Phillips Medical System, Inc. The older facility used in the comparison was 16 years old and contained a variety of new and old components. The phantom was placed in standard orientation on the tables in both rooms with the image intensifier located roughly 2-inches anterior to the phantom. The x-ray beam was incident on the phantom from beneath the table at a fixed distance. In both cases the 9-inch image intensifier was utilized.

A cardiologist, (either resident or attending) normally stands adjacent to the couch and roughly 1 to 2 feet from the edge of the image intensifier. This is the position of minimum distance to the patient/scatterer and hence the highest exposure to personnel. A matrix at one foot intervals and various feet above the floor was set-up to determine the estimation of exposure to personnel at the position of the cardiologist. This scatter-exposure grid was utilized for comparison of the two facilities. Floor tiles of 1-foot square were used to measure exposure from 1 to 4 feet from the edge of the image intensifier. A mobile intravenous holder was taped in intervals of 1 to 6 feet and was utilized to measure distances above the floor. The series of 6x6 foot grids formed adjacent to the phantom/image intensifier totalled to 4 matrices with the first set at 1-foot and the last set at 5-feet from the phantom.

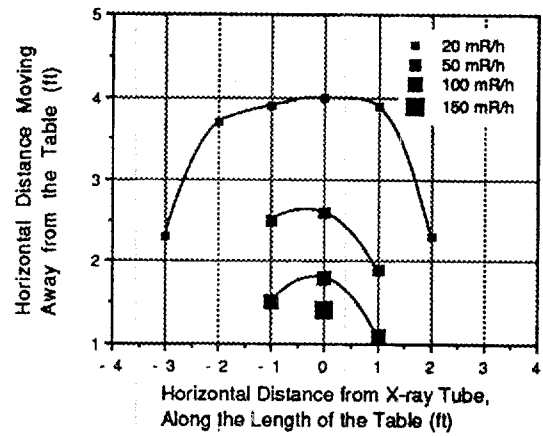
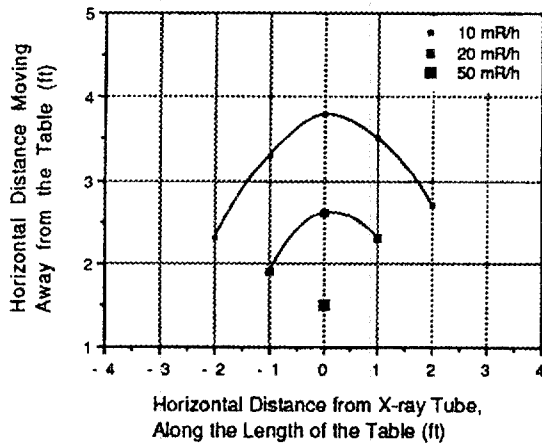
The fluoro unit was utilized for the comparisons since this has been determined to be the greatest exposure to the personnel (Kosnik, 1986; Balter, 1978; Gertz, 1982). The fluoro unit in the new facility was automatically set at 67 kVp and 1.5 mA. The fluoro technique for the older unit was manually set upon acquisition of an appropriate image from the overhead monitor and was 75 kVp and 1.6 mA.

The survey data is presented in figures 1 and 2. The data for the two facilities have been input into a spread-sheet program which enables equivalent distances and exposure rates for the two facilities to be compared and analyzed. In an effort to minimize the possible comparisons a representative height of 3-feet above the floor was chosen to present the variations in exposure rate from the two facilities. One can see that the exposure rate from the older unit is much greater than the new one. In fact, at distances of 1 foot from the image intensifier the exposures between the two facilities vary by a factor of 3 to 5. The relative ratios of exposures decrease rapidly to roughly a factor of 2 as the distance increases to 5-feet from the phantom. These exposure curves serve not only to compare the quantity of leakage and scatter from a given facility, but also aid in subsequent radiation safety instruction and education of operators.

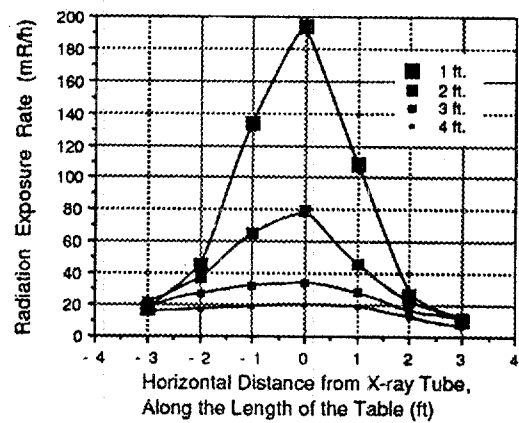
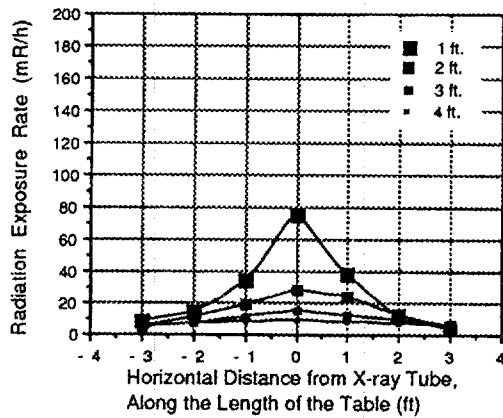
A final remark on the exposure comparisons to personnel in angiographic facilities regards the facility and not just the characteristics of a given x-ray tube assembly alone as a contributor to increased exposure. An older facility may have reliability problems which can not only be an annoyance, but serve to increase staff radiation exposure. Such reliability problems would include: cassettes jamming in the bucky, shutter and iris problems affecting beam field size, table mobility problems, size of the room, and film processor problems. These variables which are difficult to quantify in terms of increased exposure to personnel (especially in terms of retakes required), should most definitely be considered when justifying renovation or replacement of a facility.

#### **STAFF EXPOSURE MONITORING (DUAL BADGE PROGRAM)**

Personnel involved in medical angiography often exceed the established quarterly conservative limits for radiation exposure set at 1250 mrem. The radiologists work in high radiation fields and use protective apparel that include lead aprons, eye protection and thyroid bibs. Interpretations of applicable state regulations (California Administrative Code, Title 17, Radiation Regulation Controls) and NCRP guidelines concerning proper wearing of personnel monitoring devices for radiologists disagree (NCRP 57; Wiatrowski, 1980). A program of dual badge monitoring has been developed to distinguish exposure from effective whole body dose.



**Figs. 1A and 1B:** Radiation iso-exposure curves at varying distances from the image intensifier measured with an MDH survey meter at 3-feet above the floor. Fig. 1A (left) is the exposure from a new fluoroscopic facility and Fig. 1B (right) is the exposure from an old facility.



**Figs. 2A and 2B:** Radiation exposure at varying distances from the image intensifier measured with an MDH survey meter at 3-feet above the floor. Fig. 2A (left) is the exposure from a new fluoroscopic facility and Fig. 2B (right) is the exposure from an old facility.

All personnel involved in angiographic procedures wear a protective apron while in the facility. Section 30307 (17 CAC) states that protective aprons of at least 0.25 mm lead equivalent shall be worn in fluorographic installations. However, section 30309 also requires gonadal shielding of not less than 0.5 mm lead equivalent shall be used for patients who have not passed the reproductive age. In an effort to minimize the probability of providing the patient with "inadequate" gonadal protection during a given procedure all lead aprons at the UCLA Medical Center are 0.5 mm lead equivalent. Hence the personnel are provided with lead shielding of twice the lead equivalent required.

In addition to the 0.5 mm lead equivalent aprons the radiologists are supplied with thyroid bibs (0.5 mm lead equivalent) and lead glasses (0.75 mm lead equivalent). With this additional protective attire, the commonly accepted critical organs outside of a lead apron (lens of the eye and thyroid) are shielded.

NCRP Report No. 57 entitled, "Instrumentation and Monitoring Methods for Radiation Protection" states that *"When the trunk of the body is largely shielded by protective clothing it would be improper to wear a single dosimeter on the outside of such clothing since doses to the wholebody, the gonads, and most of the red bone marrow would then be greatly overestimated. Measurements have shown that, when a lead-rubber apron is worn by radiological personnel conducting fluoroscopic procedures, the exposure of the face and neck will exceed the exposure recorded under the apron by factors between 6 and 25. Under these circumstances the thyroid gland and the lens of the eye will become the critical organs, and their exposure should be monitored . . . If only one dosimeter is worn and one of its purposes is the estimation of "wholebody" dose, it is recommended that it be worn on the trunk under the apron."*

Obviously, the determination of actual effective dose is complicated if one is to consider weighting factors of the red bone marrow to the exposed areas of the body (ie. head and arms). However, for general practical reasons the effective whole body dose is most closely aligned to the under the apron dosimeter reading. Considering the protective apparel worn by radiologist includes glasses and bibs which protect the critical organ outside of the apron, it is only very recently that the California Department of Health Services has concurred with the notion of badge placement and interpretation of effective whole body dose previously outlined. In general, this has meant that when a radiologist exceeded the quarterly limits on his outside badge (usually a resident or fellow) a formal report of presumptive overexposure had to be filed with the state. This is a time consuming and inefficient use of the health physicist's time, especially at a large and busy University facility where such reports might have to be filed every quarter!

Figure 3 presents typical monthly exposures for a cardiology fellow and an attending staff cardiologist. It is evident from the figure that the fellow is exposed to more radiation during his/her first years than the attending staff cardiologist. This is attributable to the fact that the fellow is slower for a given procedure (learning curve) and that frequently the staff oversees many of the procedures and as such is able to step back and minimize his/her exposure. Finally, it is important (and not surprising) to note from the figures that the under the apron badges frequently only receive between 2 and 8% of the exposure of the outside badge.

Recent amendments (August 15, 1988) from the State of California, Supervising Health Physicist, Machine Radiation Control Section regarding personnel monitoring for radiologists have incorporated the intent of the dual badge program. The policy now states that:

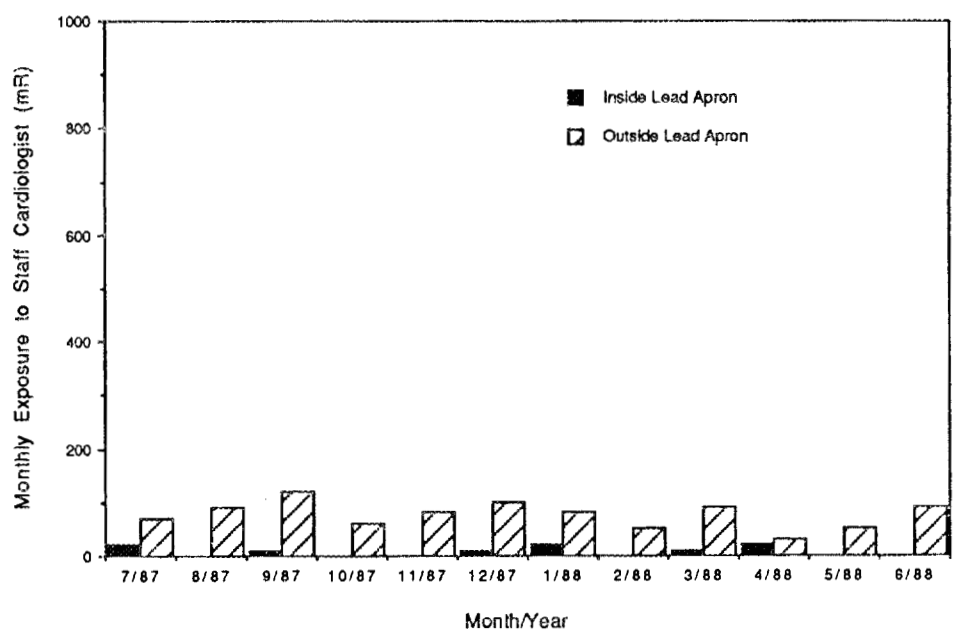
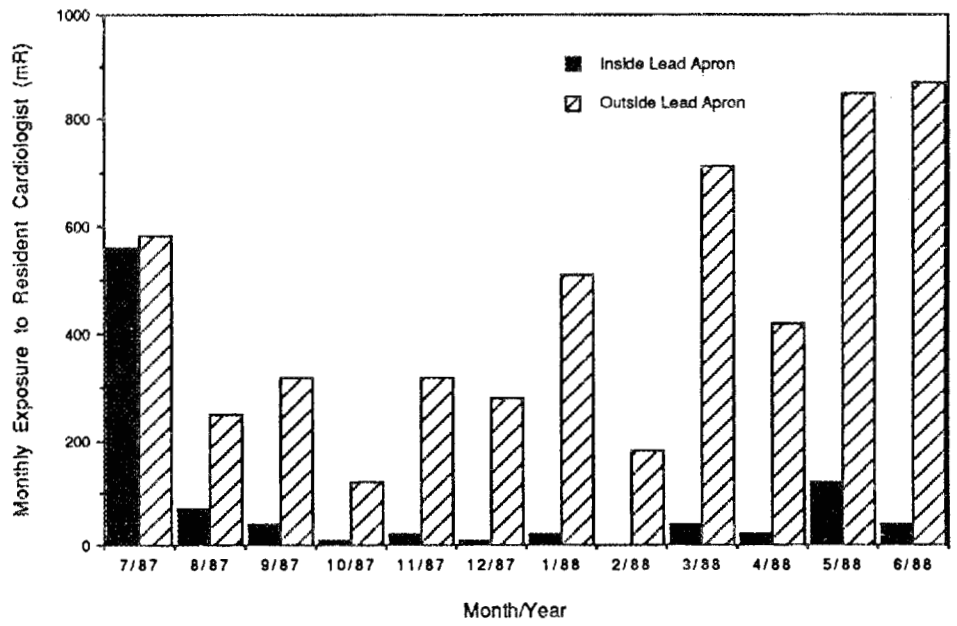
1. *When a single monitoring device is used by a radiation worker, it must be worn where it will monitor the most exposed organ of the body. Thus, placement of the device on the chest, finger or at the waist should be adequate to detect exposure to the whole body, extremities or gonads, respectively.*

2. *If a leaded protective apron is worn, it greatly reduces exposure to the body and to the film badge of workers in diagnostic radiology. Under this condition the head will generally become the most exposed organ, and the monitoring device shall be worn at the top or collar and outside the apron. For practical consideration we (the California State Dept. of Health Services) may assume that this location will receive about the same exposure as the head.*

3. *Should another dosimeter be worn under the apron, and if the worker affirms that adequate eye and thyroid protection is always worn when radiation is being used, we (the California State Dept. of Health Services) shall accept the reading of the under-apron dosimeter as the whole body exposure.*

With this third and final condition for badge monitoring laid out by the California State Dept. of Health Services, the University shall now be able to monitor exposure of a given individual by means of the outside badge, but not be required to complete a presumptive overexposure report unless the inside badge exceeds the state limits (ie. 1250 mrem per calendar quarter).

The implications for this program are two-fold. In order for the program to be effective the health physicist must be assured that the second dosimeter is used and that all of the protective apparel is worn by the radiologist in the program. Finally, in reporting exposures to other institutions (out of state and otherwise) the outside badge should be considered as an exposure, and the inside badge the effective whole body dose.



**Figs. 3A and 3B:** Typical monthly exposures for cardiologists wearing dual dosimeters (inside and outside lead apron). Fig. 3A (top) is for a second year resident cardiologist and Fig. 3B (bottom) is for a staff-attending cardiologist.

## CONCLUSION

Equipment in angiographic/catheterization facilities vary in their exposure potential to medical personnel. Due to the exceptional cost of the equipment refurbishing a facility may be performed on a piece by piece basis whereby the subsequent exposure to personnel is difficult to discern. A considerable change may occur in a given facility with the installation of new equipment, more than likely the exposure to personnel from new equipment should be decreased, but some devices (ie. "fluoro boost" units) may greatly exceed previous exposures. It is recommended that when a facility has been altered or replaced that a scatter survey be performed. A method has been described to measure the scatter from various angiographic facilities utilizing a RANDO phantom and an MDH survey meter. The method is simple to perform and is a good indicator of personnel exposure comparison of one facility to another. This exposure data, in addition to the clinical capabilities of a system can also be utilized to justify replacement or renovation of a facility.

Radiologists serving a fellowship in angiographic facilities commonly exceed the limits for radiation exposure when the reading for a dosimeter worn on the outside of a lead apron is considered. If the radiologist wears protective apparel which shields the commonly considered critical organs outside of the lead apron then the exposure outside of the protective clothing greatly overestimates the effective whole body dose. A program has been installed which utilizes dual badges for the radiologists. In this manner the health physicist can determine the radiation to which an individual has been exposed as well as the effective whole body dose. This dual badge program has recently been accepted by the California Department of Health Services and as such minimizes unnecessary reporting of presumptive overexposure of radiologists.

## REFERENCES

- G. M. Ardran and P. S. Fursdon, "Radiation Exposure to Personnel During Cardiac Catheterization", *Radiology* Vol. 106:517-518 (March 1973)
- S. Balter, F. M. Sones, and R. Brancato, "Radiation Exposure to the Operator Performing Cardiac Angiography with U-arm Systems", *Circulation* Vol. 58, No. 5, pp. 925-932 (1978)
- K. Faulkner and B. M. Moores, "An Assessment of the Radiation Dose Received by Staff Using Fluoroscopic Equipment", *British Journal of Radiology*, Vol. 55: 272-276 (1982)

A. Feldman, "Factors and Strategies in Selection of Instruments for Radiation Surveys Around Medical X-ray Installations", *Health Physics* Vol. 38, pp. 679-681 (April 1980)

E. W. Gertz, et al, "Improved Radiation Protection for Physicians Performing Cardiac Catheterization", *American Journal of Cardiology*, Vol. 50:1283-1286 December 1982

M. Gustafsson and A. Lunderquist, "Personnel Exposure to Radiation at some Angiographic Procedures", *Radiology* Vol. 140:807-811 (Sept. 1981)

W. R. Hendee and E. L. Chaney, "Diagnostic X-ray Survey Procedures for Fluoroscopic Installations - Part I: Undertable Units", *Health Physics* Vol. 29 (August 1975), pp. 331-337

M. P. Judkins, "Guidelines for Radiation Protection in the Cardiac Catheterization Laboratory", *Catheterization and Cardiovascular Diagnosis* Vol. 10: 87-92 (1984)

L. T. Kosnik, "Personnel Exposure in the Cardiac Catheterization Laboratory", *Health Physics* Vol. 50, No. 1, pp. 144-147, (January 1986)

D. C. Levin and L. Dunham, "New Equipment Considerations for Angiographic Laboratories", *American Journal of Radiology*, Vol. 139:775-780 (Oct. 1982)

E. L. McGuire, M. L. Baker, and J. F. Vandergrift, "Evaluation of Radiation Exposures to Personnel in Fluoroscopic X-ray Facilities", *Health Physics* Vol. 45, No. 5 (Nov. 1983) pp. 975-980

NCRP Report No. 57, "Instrumentation and Monitoring Methods for Radiation Protection", May 1978, National Council of Radiation Protection  
F. G. Rueter, "Physician and Patient Exposure During Cardiac Catheterization", *Circulation*, Vol. 58, No. 1, pp. 134-139 (July 1978)

W.A. Wiatrowski, "The Recommended location for Medical Radiation Workers to Wear Personnel Monitoring Devices", (Letter to the Editor) *Health Physics*, Vol. 38, pp. 434-435 (March 1980)

## ACKNOWLEDGEMENTS

We gratefully acknowledge the UCLA Department of Radiological Sciences and the Med-Cardio Division for their support and cooperation with the Radiation Safety Office.

VINTEN EXPOSURE MEASUREMENTS OF THE SALEM UNIT 1  
LOWER CORE BARREL

Patrick T. Glennon

Public Service Electric & Gas Company

Introduction

On November 6, 1987, the lower core barrel of Salem Unit I was removed from the reactor vessel and placed in the refueling pool as part of the unit's ten year inspection program. This paper deals with the supporting actions of the dosimetry group of PSE&G.

Prior to the move of the lower core barrel, Westinghouse predicted dose rates at one foot in water as a function of axial distance along the core barrel (Attachment 1). This prediction was used in planning the health physics requirements associated with the move. It was agreed that a measurement of the axial dose rates would either lend confidence to the predictions or identify weaknesses in them.

Vinten dosimeters were chosen for making the measurements for the following reasons:

1. They are watertight. Since they would be immersed in water for two hours, this was an important consideration.
2. They are thin. Despite their being watertight, they were encased in laminae to eliminate contamination from contact with the water in the pool. Their thin flat geometry enabled laminae to be used rather than plastic bags. This eliminated the problem of buoyancy which would have occurred had fifty plastic bags been affixed to the pole.
3. They are capable of measuring a large range of doses. The dose rates were expected to range from background to hundreds of rads per hour.

Vinten Dosimetry System

The Vinten system is an English system using LiF phosphor ( $6 \text{ mg/cm}^2$ ) attached to a thin polyamide strip ( $6 \text{ mg/cm}^2$ ) and covered by a thin ( $3 \text{ mg/cm}^2$ ) aluminized foil. The dosimeter resembles a Band Aid (TM) adhesive bandage with the pad (phosphor) being nearer one end rather than at the center. (See Attachment 2).

After irradiation, the dosimeters are manually mounted on stainless steel mounting plates. The mounting plates are then loaded into a magazine and placed on the automatic sample changer. (See Attachment 3) The appropriate button or buttons (for single or automatic feed) are pressed as desired and the dosimeter is moved over the bar code reader and deposited in the Vinten Toledo Reader drawer. If the auto mode was selected and the code is not successfully read in three attempts, the dosimeter is ejected without being processed. If the "single step with code read" mode was selected and the code is not successfully read in three attempts, the dosimeter is read but a space to manually enter the code number is left in the printout.

The automatic sample changer inserts the drawer into the reader and the hot finger is raised to the bottom of the mounting plate. The dosimeter is preheated in an optional pre-heat cycle according to the parameters chosen (temperature, time, and ramp rate). For dosimeters the pre-heat cycle is normally used. The dosimeter is then heated as dictated by similar parameters for the read cycle. During this part of the process the output from the PMT is measured and displayed. Either of two optional anneal cycles may or may not follow the read cycle. When processing dosimeters, an anneal cycle is normally not chosen since the dosimeters are disposable.

After the dosimeter has cooled to less than approximately 130 °C, the reading is printed and the automatic sample changer withdraws the drawer and deposits the dosimeter into either of two containers located inside and outside the automatic sample changer. The inside container is used for those dosimeters whose barcodes were successfully read and the outside container for those whose barcodes were not successfully read. While the drawer is withdrawn, the Toledo Reader automatically integrates the counts from an internal light source and modifies internal parameters to ensure stability. After these self checks, the process is repeated if the auto mode was selected.

### Core Barrel Irradiation

Laminated Vinten dosimeters were fastened onto a pole at intervals of 2, 6, or 12 inches depending on the expected dose rate gradients. The pole was then placed approximately one foot from the lower core barrel and parallel to it. The pole was removed after two hours. The dosimeters were removed from the pole and wiped of standing water. Due to time constraints, the dosimeters were not removed from the laminae until the following day. To accurately reflect any dose that might be delivered from possible contamination, the background dosimeter was kept in the same bag as the test dosimeters. The next day (November 7, 1987) the

dosimeters were removed from the laminae and tested for contamination. After confirming that there was none, they were forwarded to Dosimetry.

### Calculations

On January 18, 1988, the dosimeters were read using the Vinten Toledo reader. In addition to the test dosimeters, dosimeters irradiated to known doses ranging from 500 mR to 1,000 R were read to act as reference points.

Upon analyzing the results of the reference point dosimeters, it was apparent that the dosimeters did not respond linearly over the dose range since the light output per delivered mrem increased at the higher doses.

To apply the correct conversion factors to the entire range of doses, it was necessary to generate a curve of dose conversion factor versus net counts. Dosimeters were irradiated over a range from 50 mrem to 1750 Rem. Doses were chosen to result in 21 approximately log-equal intervals to ensure the capability of drawing a smooth curve. On February 8, 1988, the dosimeters were processed and the graph drawn. Error bars were drawn based on 1.96 standard deviations (95% confidence) for each data point.

Using the dose conversion curve (Attachment 4), the data from the lower core barrel read was converted to gross dose. The transit dose was subtracted to yield net dose. The net dose was then divided by the two hour irradiation time to arrive at dose rate.

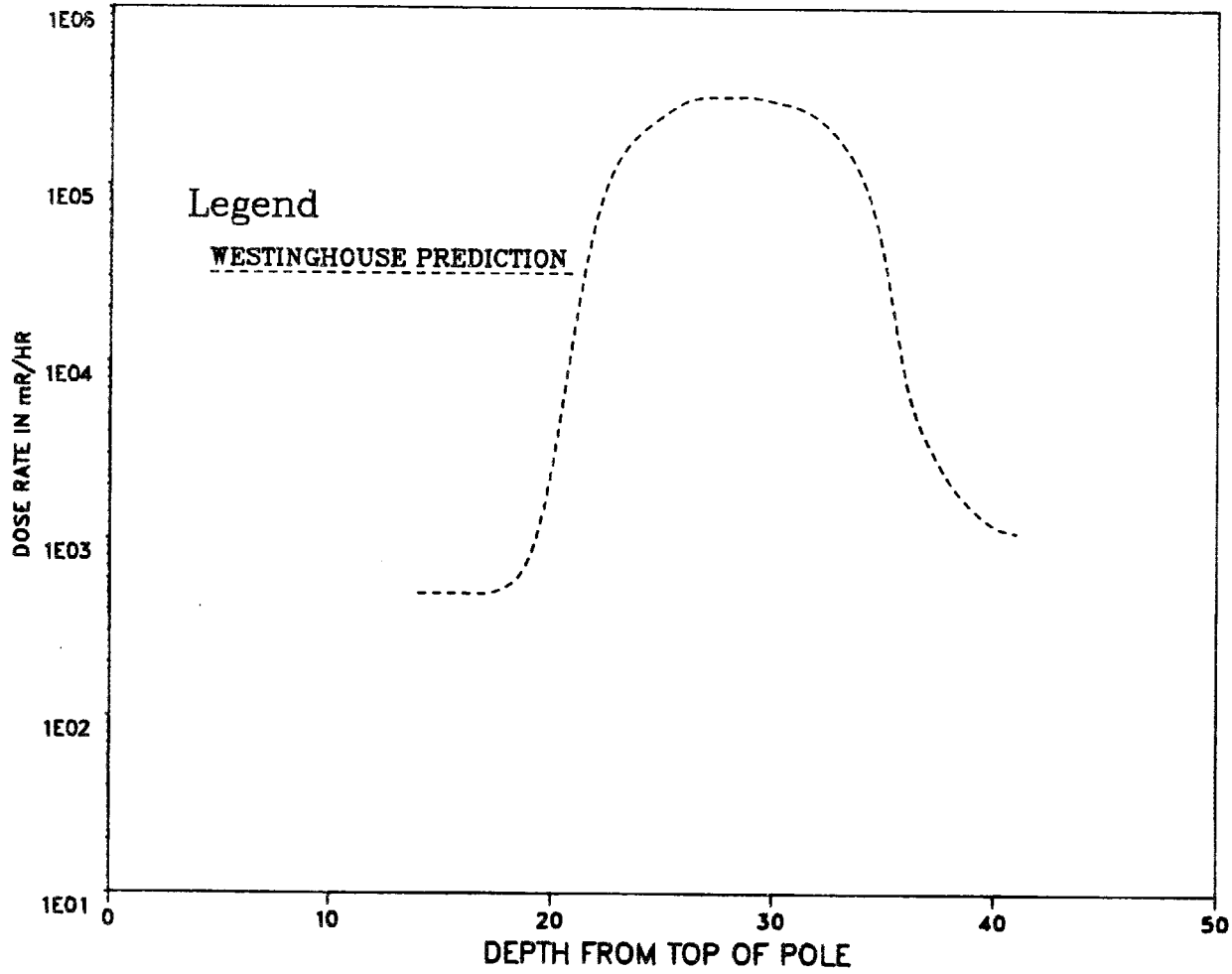
As a check of the dose conversion curve, the curve was used to determine the dose to the spiked dosimeters which were read with the core barrel dosimeters. The results were all within ten percent of the expected doses and most were within six percent (Attachment 5). This is judged to be a confirmation of the dose conversion curve.

The dose rates were then plotted as a function of axial distance along the pole (Attachment 6).

### Conclusion

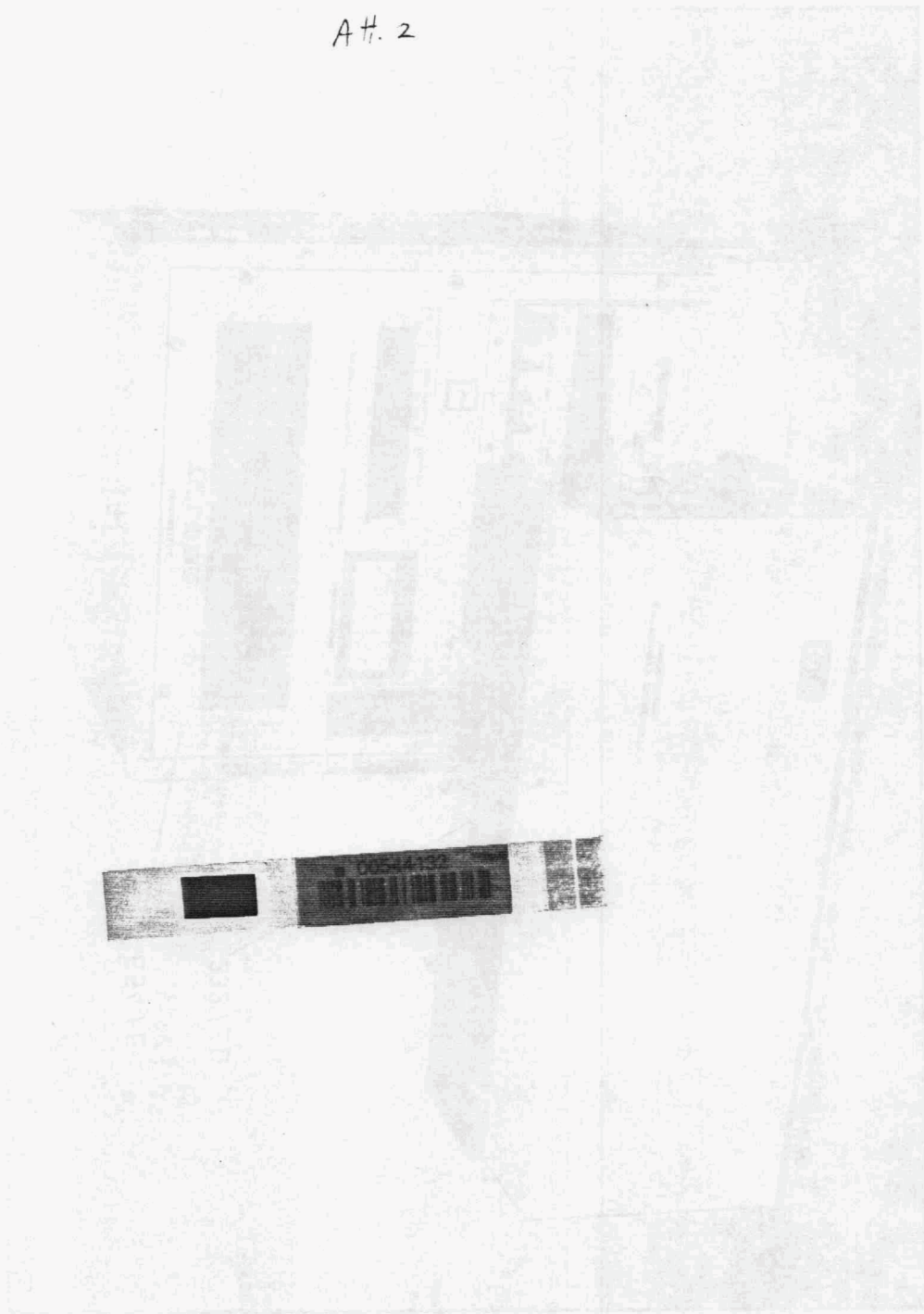
Attachment 7 presents the first page of conclusions from the initial Westinghouse report (underlining added). Attachment 8 shows the results of the Vinten measurements and the predictions from Westinghouse plotted on the same graph. As can be seen from Attachment 8, the results are consistent with the Westinghouse prediction and thus the conclusion is that the Westinghouse prediction is verified by the Vinten measurements.

### SALEM LOWER CORE BARREL DOSE RATES (mR/HR)

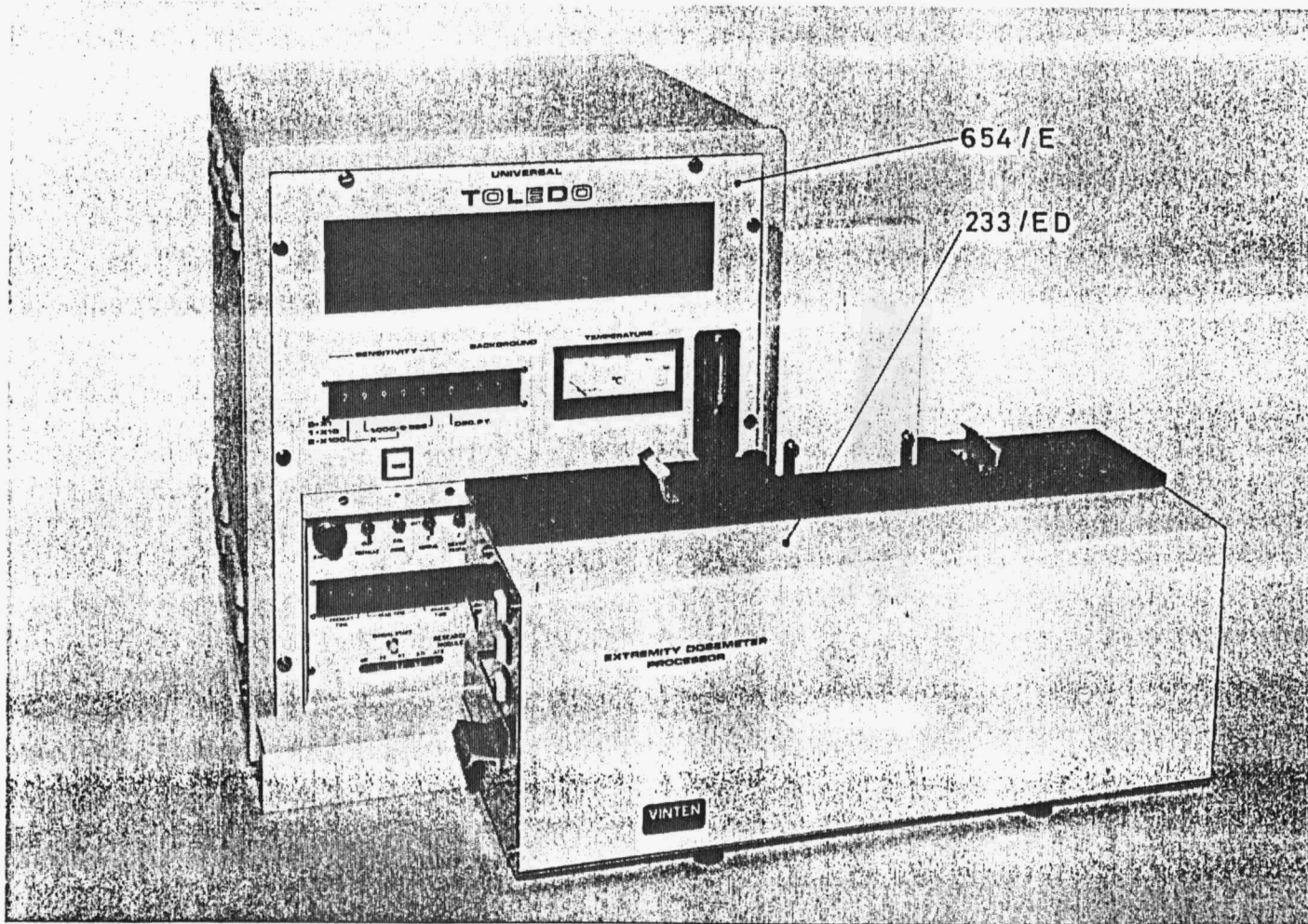


Att. 2

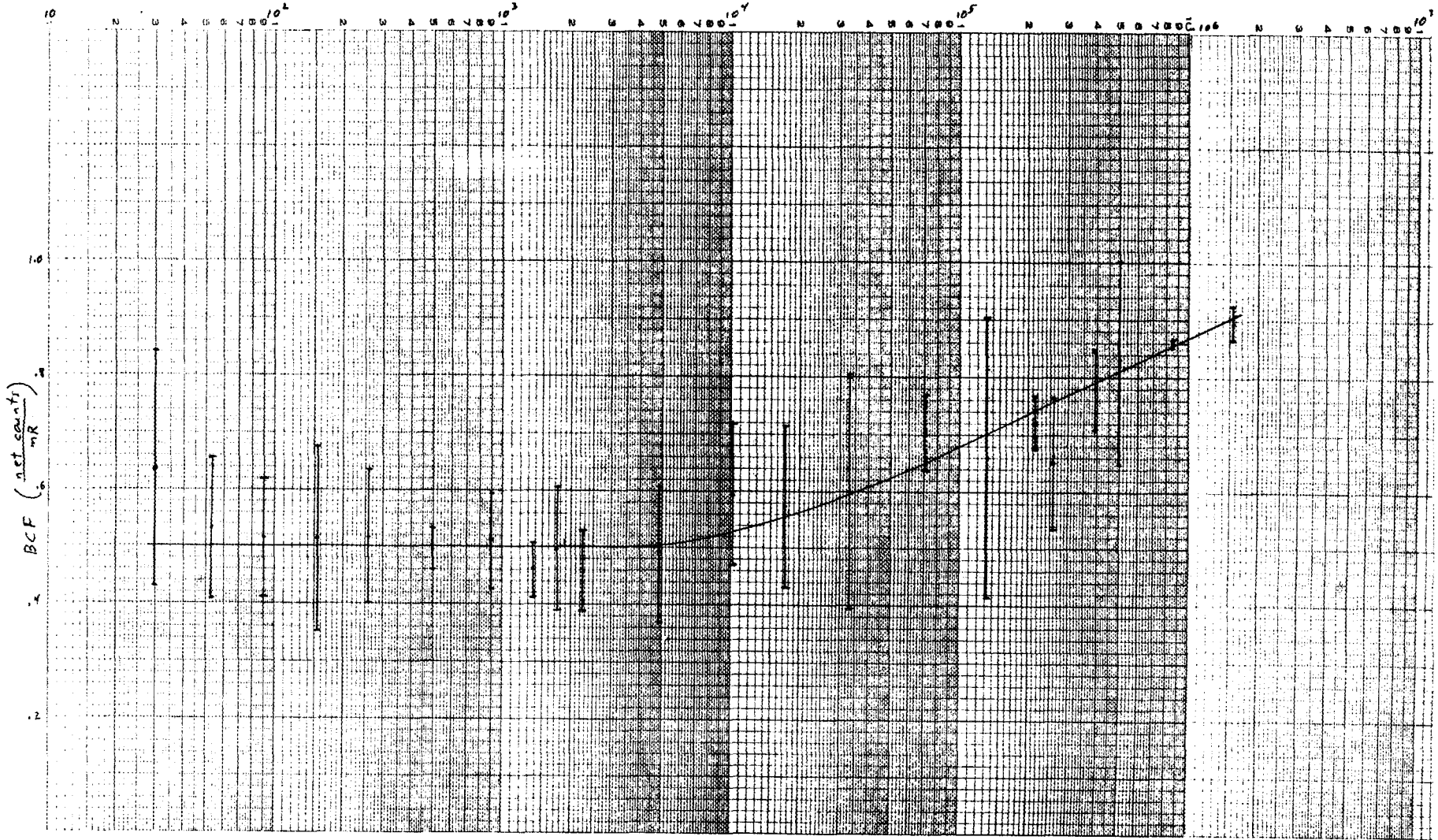
THE CITY SYSTEM



THE 654 X SYSTEM



AH. 3

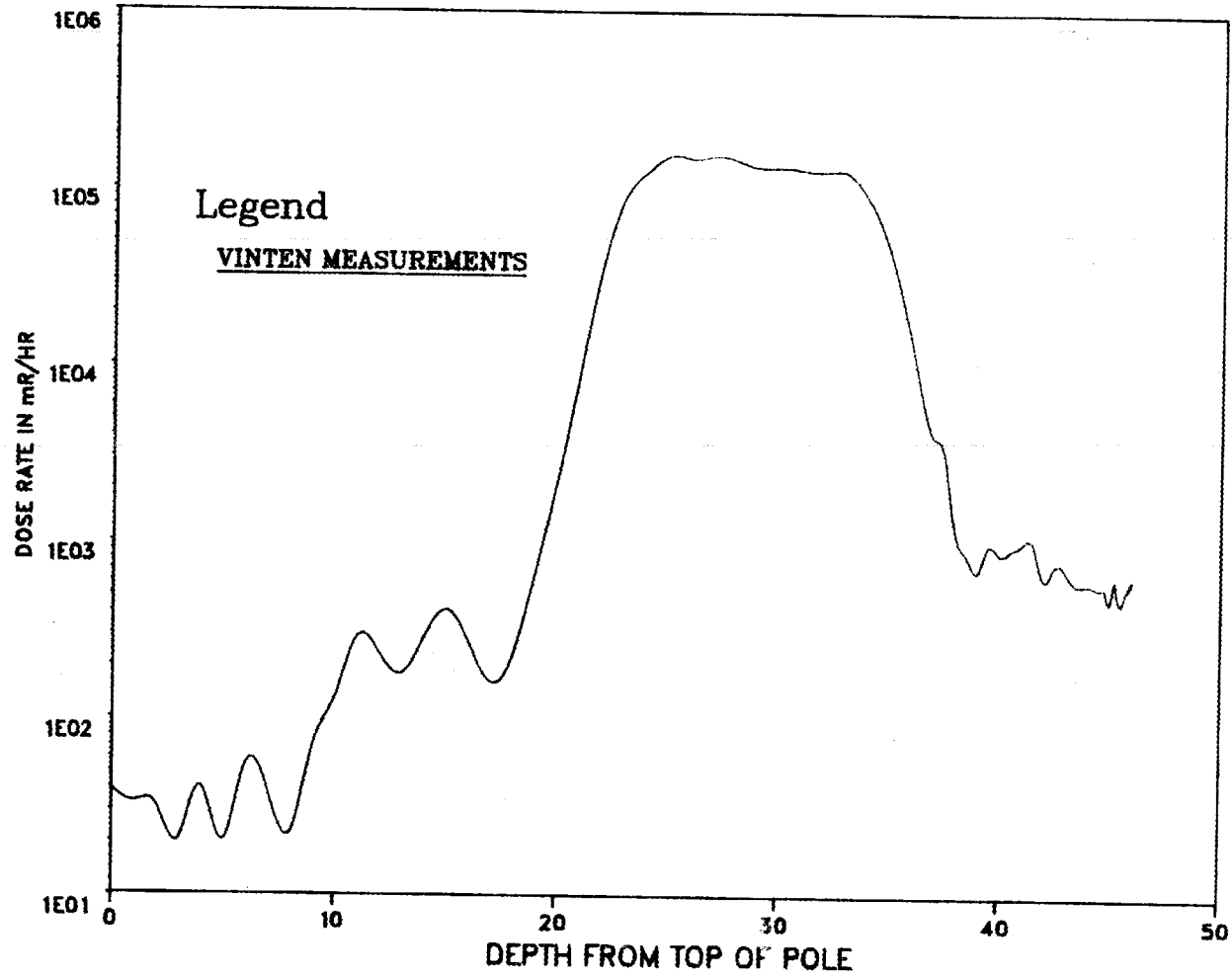


**ATTACHMENT 5**  
**SPIKED DOSIMETERS**

<u>Expected</u>	<u>Reported Average</u>	<u>% Diff</u>
500 mR	488	-2
100 R	109.5	10
200 R	208	4
300 R	327.5	9
400 R	407.5	2
500 R	529	6
600 R	587	-2
1000 R	1074.5	7

These are the values obtained using the calibration curve which was generated using different dosimeters on a different date.

# SALEM LOWER CORE BARREL DOSE RATES (mR/HR)



A #. 6

Att. 7

WESTINGHOUSE CLASS 3

WCAP-11635

EVALUATION OF EXPOSURE RATES FROM THE  
SALEM UNIT 1 REACTOR LOWER INTERNALS ASSEMBLY

J. Sejvar

WORK PERFORMED FOR PUBLIC SERVICE ELECTRIC AND GAS COMPANY

August 1987

Approved: *F. L. Lau*  
F. L. Lau, Manager  
Radiation and Systems Analysis

Although the information contained in this report is nonproprietary, no distribution shall be made outside Westinghouse or its Licensees without the customer's approval.

Westinghouse Electric Corporation  
Nuclear Technology Systems Division  
P.O. Box 355  
Pittsburgh, Pennsylvania 15230

6776e:1d/101587

Att. 7 (cont'd)

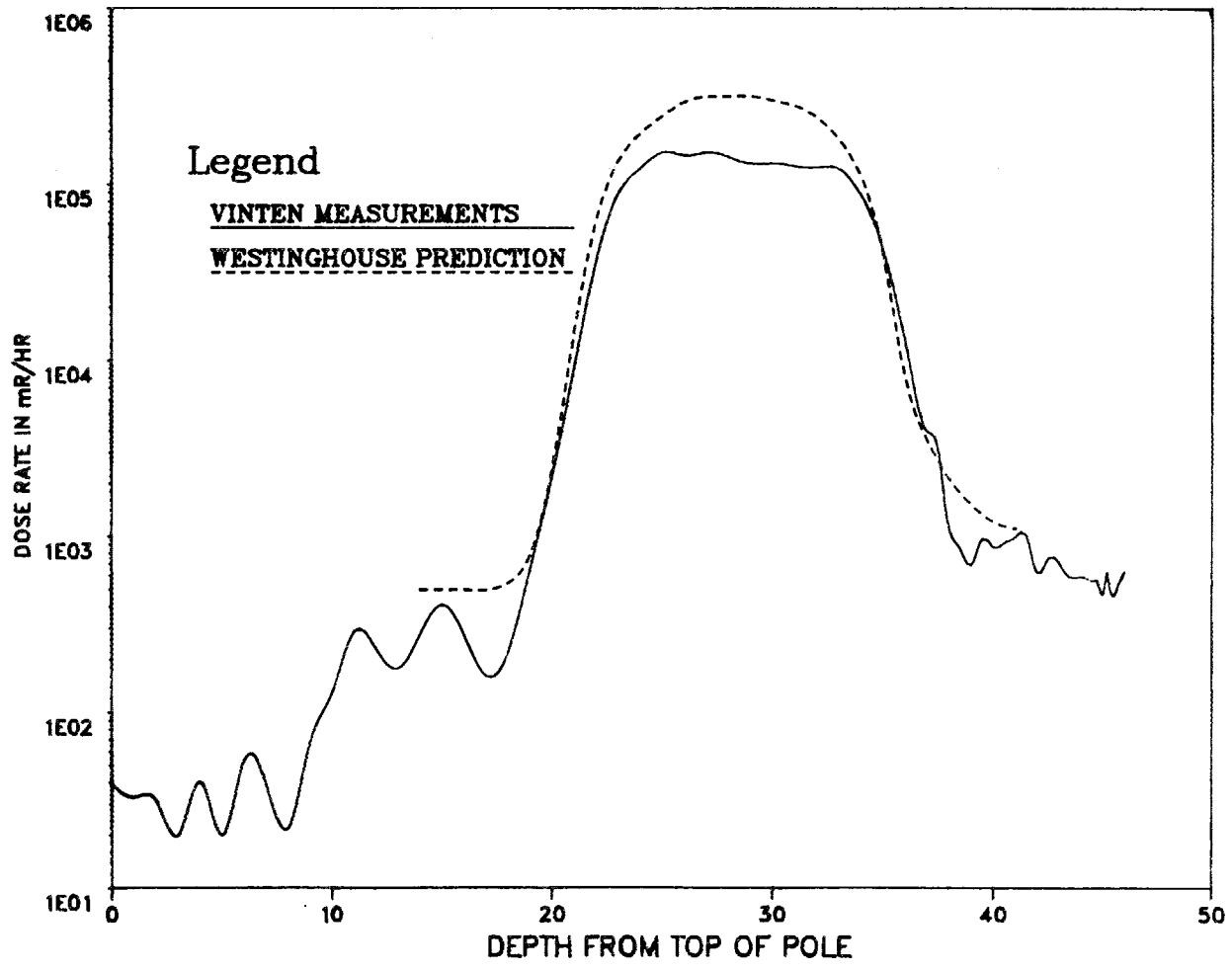
SECTION 4  
CONCLUSIONS

Reliable prediction of dose rates from the lower internals is a difficult task, owing to relatively large geometric variations in the magnitude and distribution of the activation source strengths associated with a number of source regions and the ill-behaved nature of crud deposits. However, the potential for unacceptably high radiation fields, during the transfer of the lower internals, require that the anticipated dose rates be considered in the pre-planning of this activity.

The analyses summarized in this report provide best estimate dose rate information at various locations and with various water cover and supplemental shielding configurations for use in preparing for the Salem Unit 1 lower internals handling activities. Uncertainties in the dose rate contribution of the various sources are minimized by the use of state-of-the-art neutron transport and shield analysis computer codes as well as actual plant materials data (i.e., cobalt impurity measurements). These measures lead to a relatively high confidence level in the determination of the sources and dose rates resulting from the activated lower internal components. However, the dominant source throughout most of the Salem Unit 1 internals handling operations is expected to be the deposited crud for which significant variations from plant to plant have been observed. Prior plant experience and measured radiation fields have thus been reviewed to aid in establishing the deposited corrosion product (crud) source and to verify the "reasonableness" of the results. Considering the various uncertainties associated with the development of the dose rate data in the Salem Unit 1 lower internals evaluation, it is estimated that the calculated radiation fields will be within a factor of 2 of the actual values. Further, it is anticipated that the measured dose rates from deposited corrosion product sources will tend to be lower, rather than higher, than projected.

A.H. 8

### SALEM LOWER CORE BARREL DOSE RATES (mR/HR)



## DOSIMETRY OF AN IN-CORE DETECTOR EXPOSURE ACCIDENT

Morse Olin  
Virginia Power  
Innsbrook Technical Center  
5000 Dominion Boulevard  
Glen Allen, Virginia 23060

William T. Bartlett  
Environmental Evaluation Group  
P.O. Box 3149  
Carlsbad, New Mexico 88220

### Abstract

Three technicians at the Surry Nuclear Power Station were exposed to high radiation levels from an activated cable while manually extracting a stuck in-core detector. The actual positioning of the detector was unknown and cable activation was not anticipated. As the activated cable entered the work platform area, exposure rates exceeded 1000 R/hr. The primary cable activity was found to be Mn-56 in a shielded line source geometry. The positioning of the individuals, shielding, short exposure times and unusual instrument responses created difficulties in dose assessment. The calculational methodologies and resulting dose assignments are discussed.

### INTRODUCTION

On February 8, 1988, the "A" in-core neutron flux detector at Surry Unit 2 became stuck in the reactor core during the monthly flux map and could not be withdrawn with the drive unit. Twenty-four days later, on March 3, 1988, two instrument technicians and a health physics technician entered the Unit 2 containment while the reactor was at full power. The lead control room technician was in direct communication with the work crew. The work crew was unable to free the stuck detector. After discussions with the control room technician it was decided to manually pull the cable to a point where the detector could be inserted into a permanent storage shield. As the detector neared the crane shield wall, and the point of insertion to the storage shield, the health physics technician noted rapidly increasing exposure rates. The job was immediately terminated and all three technicians moved to a low dose area. The health physics technician immediately checked exposures by reading their self-reading dosimeters (SRDs) and then returned to the work area to verify the exposure rates. This survey indicated exposure rates from 100 R/hr to greater than 1000 R/hr. The three technicians then exited the containment and returned their dosimetry to Health Physics. Results of processing the thermoluminescent dosimeters (TLDs) indicated whole body exposures from 275 mrem to 524 mrem as shown in Table 1.

**TABLE 1: Results of SRD and TLD Measurements**

	SRD (mR)	TLD (mrem)	
		Gamma	Beta
Health Physics Technician	240	275	38
Instrument Technician No.1	538	347	0
Instrument Technician No.2	555	524	35

Upon evaluation of the incident, it became apparent that the three technicians were exposed to a non-uniform radiation field and that the dosimetry provided may not have reflected the proper dose assessment. After an extensive review of the incident a calculational model was developed to determine better dose estimates for the three technicians.

#### **ASSUMPTIONS**

Basic parameters for development of the dose assessment model were determined through an exhaustive investigation of the incident. A mock-up of the in-core drive system was constructed and used in a reenactment of the event. Other information was obtained from computer activation analysis and subsequent radiation surveys of the in-core detector and drive cable.

The activity of the detector and drive cable were determined by calculating the neutron activation during the irradiation time by using the computer code, ORIGEN. The results of the activation analysis revealed the detector cable, not the detector, was the primary source of exposure. The drive cable had a total activity of approximately 224 Ci, while the in-core detector contained about 13.7 Ci of activation products. The relative isotopic distribution is shown in TABLE 2. Manganese-56 is approximately 92% of the activity and accounts for 99% of the gamma exposure rate. The decay data for Mn-56 is shown in Figure 1. The detector cable is also shielded by a stainless steel tube casing about 0.11 inch thick.

Figure 1

## **Mn-56 Decay Data**

$$T_{1/2} = 2.576 \text{ hours}$$

$$E_{\beta\text{max}} = 2.85 \text{ MeV}$$

$$\gamma_1 = 0.847 \text{ MeV (99\%)}$$

$$\gamma_2 = 1.811 \text{ MeV (29\%)}$$

$$\gamma_3 = 2.110 \text{ MeV (15\%)}$$

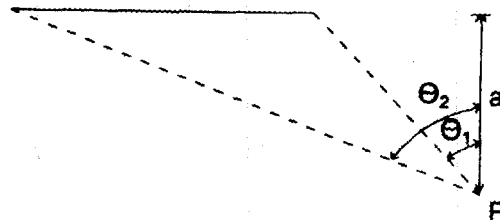
Through a reenactment of the event it was determined that the cable was being withdrawn at a rate of about 2 inches per second. When the high radiation was encountered the I & C technician pushed about six inches of the detector cable back into the casing at a rate of about 1 inch per second. A summary of the time-in-motion information is shown in Table 3.

The relative positions of the three technicians are shown in Figure 2. The highest exposed portions of the HP technician and Instrument technician No. 2 were the shin (extremity) and knee (whole body). Instrument technician No. 1's elbow position was used for whole body and extremity calculations because it appeared to be the nearest body part.

#### CALCULATIONAL MODEL

A computer spreadsheet model was devised to calculate the dose from a line-at-a-point to a point with interposed shielding. The model considers the furthest extraction of the activated portions of detector cable and calculates exposure from each 2 inch reference point over the time of exposure.

The basic line source equation, shown below, was used for determining the photon flux:



$$\phi = \frac{S}{4\pi a} (\theta_2 - \theta_1)$$

where:

- $\phi$  - photon flux (photons/cm<sup>2</sup>)
- S - source strength (dis/sec-cm)
- a - distance (cm)
- $\theta_1$  - angle (radians)
- $\theta_2$  - angle (radians)

The exposure rate was determined from the following equation:

$$ER = 1.827 \times 10E-8 \phi E hv \text{ uem/@ } f$$

- where: ER - exposure rate in air (R/sec)
- hv - photon energy (MeV)
- uen/p - energy absorption coefficient (cm<sup>2</sup>/gm)
- f - photon abundance/disintegration
- $\phi$  - photon flux (photons/cm<sup>2</sup>)

**TABLE 2: Isotopic Distribution in Activated Detector Cable**

Isotope	Half-Life (hrs)	Activity (Ci T=0)	Activity (%)
Na-24	14.97	0.07	0.03
Mg-27	0.16	0.34	0.15
Al-28	0.04	8.05	3.59
P-32	342.72	0.43	0.19
Cr-51	664.80	1.86	0.83
Mn-54	7492.80	0.55	0.25
Mn-56	2.58	206.80	92.41
Fe-55	23476.00	1.94	0.87
Fe-59	1068.00	0.98	0.44
Co-58	1701.00	0.18	0.08
Co-60	46165.00	0.01	0.00
Co-60m	0.17	0.54	0.24
Mo-99	65.94	1.37	0.61
Mo-101	0.24	0.34	0.15
Tc-101	0.24	0.34	0.15
Total >		223.79	100.00

**TABLE 3: Time-In-Motion Information**

Time (Seconds)	Reference
0*	High Scale Measurement, HP Tech. moves to back of "A" Drive Unit
5 - 7	HP Tech. at back of "A" Drive Unit
11 - 15	Inst. Tech. No. 1 and No. 2 stand up.
15 - 20	Inst. Tech. No. 2 at back of "B" Drive Unit, then leaving the area.
20 - 24	Inst. Tech. No. 1 at back of "B" Drive Unit, then HP Tech and Inst. Tech No. 1 leaving area.
27 - 29	All beyond "B" Drive Unit

\* Activated cable begins to enter area 12 to 15 seconds prior to T=0, and all individuals positioned as in Figure 2.

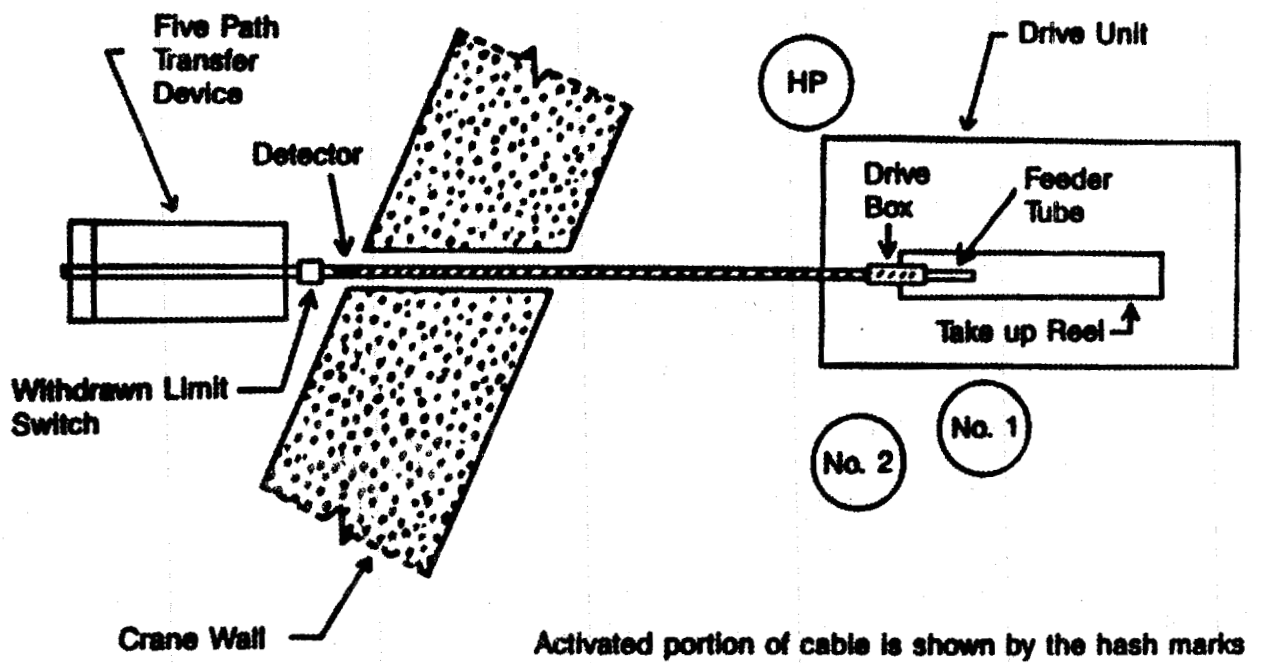


FIGURE 2 - Positions of Individuals During Exposure Event

For each of the geometries shown in Figures 3, 4 and 5 a separate spreadsheet was prepared. The technicians exposure to the activated cable occurred several seconds before rapidly increasing exposure rates were noted by the HP technician. Each spreadsheet calculates the exposure to a specified geometry for a time determined during reenactment. The position of the activated cable at its furthest extraction was broken up into 28 two inch reference points. For each second of exposure, the activity in mCi/cm for each reference point is recorded. The activity for each reference point is then summed to give the total activity over the exposure time. Using the line source and exposure rate equations described above the total exposure for each energy and reference point is calculated. The exposures for each reference point and energy are then summed to obtain the total exposure. Calculated exposures are shown in Table 4.

**TABLE 4. Calculate Incident Exposures (mrem)**

	TLD (chest)	Whole Body	Extremity
HP Technician	129	532	843
Instrument Technician No.1	836	1495	1495
Instrument Technician No.2	799	1598	1965

The assigned dose was determined by taking the ratio of the measured TLD response to the calculated TLD exposure and multiplying this ratio by the calculated whole body or extremity dose. For example, the portion of the whole body receiving the highest exposure during the incident for the health physics technician was his knee. To estimate the dose to the knee the measured TLD result of 170 mrem was divided by the calculated exposure to the TLD of 129 mrem. This result is then multiplied by the calculated exposure to the knee of 532 mrem to obtain health physics technician's assigned whole body dose of 701 mrem or  $170/129 \times 532 = 701$ . The measured response of the TLD worn by instrument technician No.1 is much lower than the self reading dosimeter and calculated exposure. It appears that the TLD was shielded so the dose assessment for instrument technician No. 1 was calculated using the TLD response of instrument technician No. 2. Table 5 lists the dose assessment for the incident. Table 6 list the exposure for the first quarter of 1988.

**TABLE 5: Dose Assessment for Incident (all units in mrem)**

	Whole Body	Extremities
HP Technician	707	1263
Instrument Technician No.1	958	1004
Instrument Technician No.2	1018	1310

**TABLE 6: Dose Exposure Summary for First Quarter 1988**

	Whole Body	Extremities
HP Technician	1124	1724
Instrument Technician No.1	1005	1046
Instrument Technician No.2	1042	1329

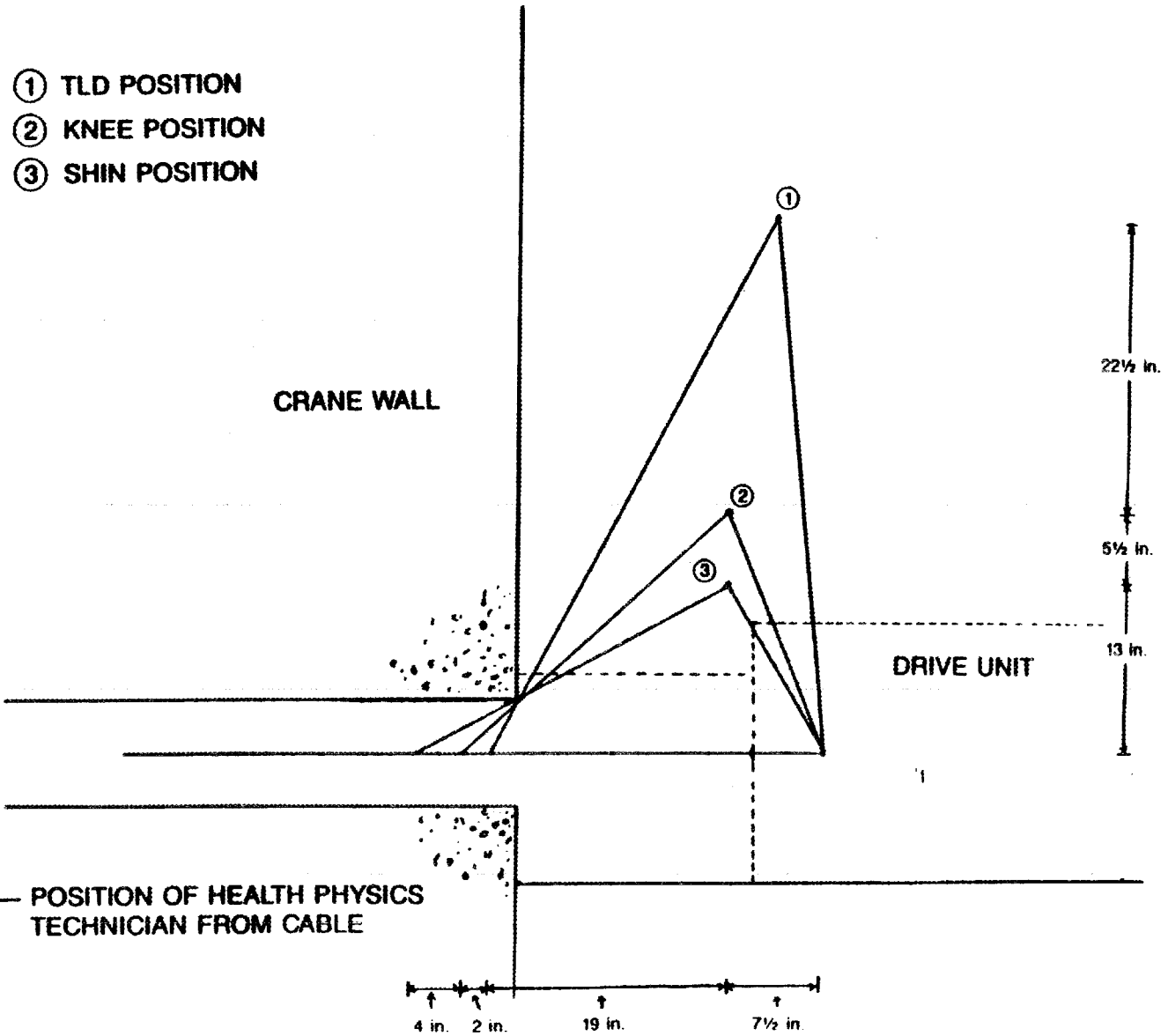


FIGURE 3 — POSITION OF HEALTH PHYSICS TECHNICIAN FROM CABLE

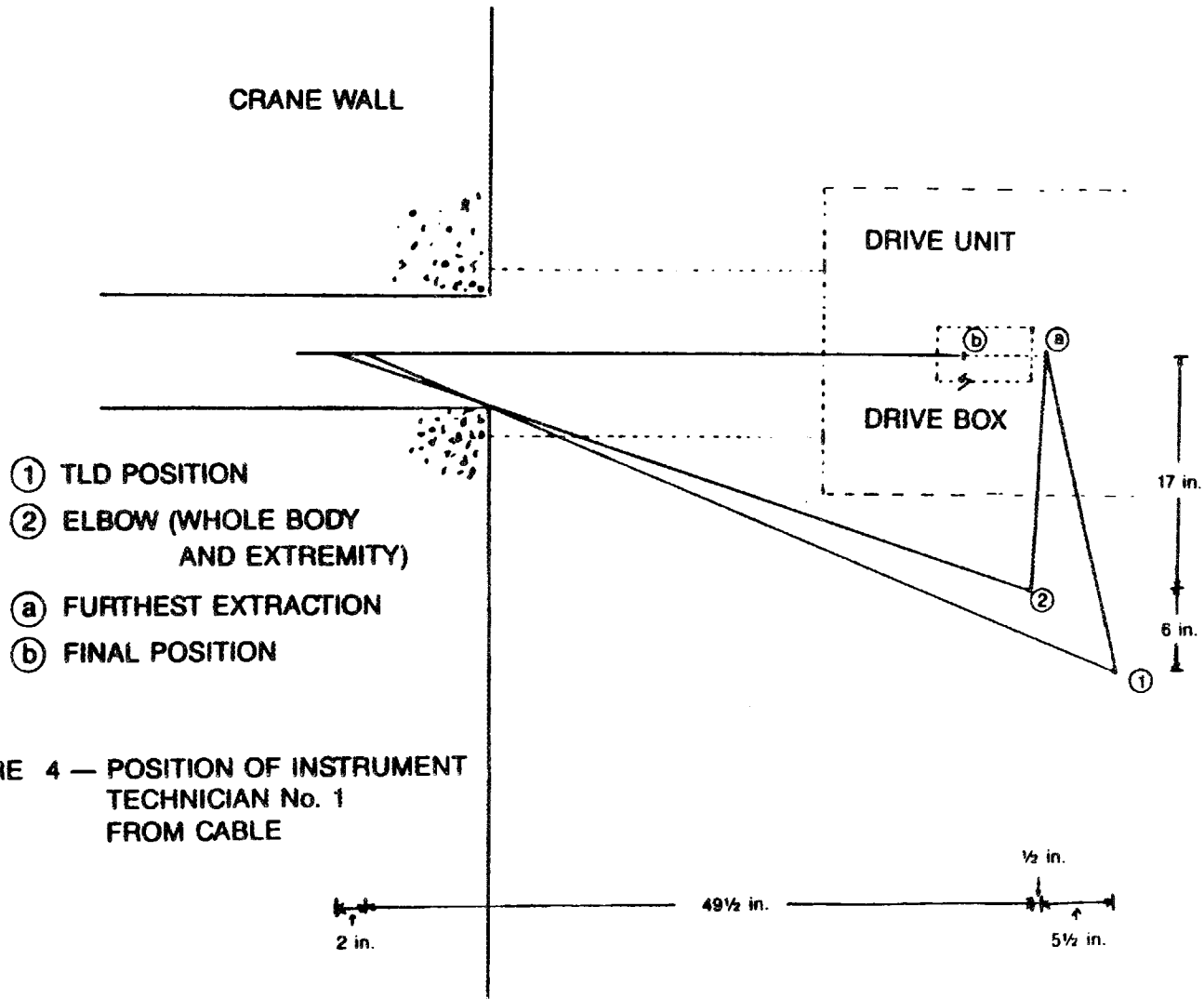


FIGURE 4 — POSITION OF INSTRUMENT TECHNICIAN No. 1 FROM CABLE

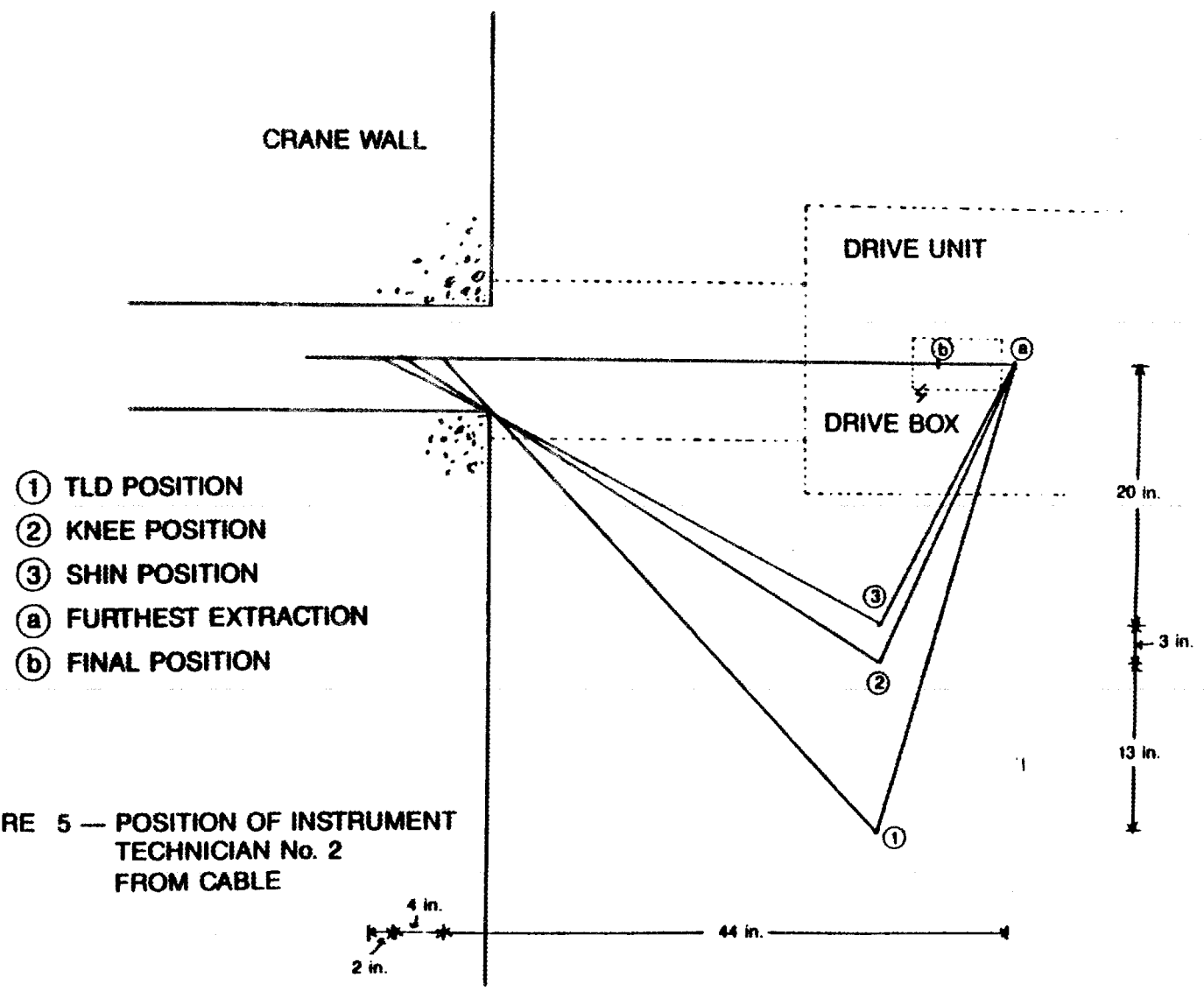


FIGURE 5 — POSITION OF INSTRUMENT TECHNICIAN No. 2 FROM CABLE

## CONCLUSIONS

Dose Assessments were performed for three technicians exposed to radiation fields in excess of 1000 R/hr. Because non-uniform, high exposure rates were not anticipated, additional dosimetry was not worn by the technicians. Extremity and whole body dose assessments were performed using doses measured by TLDs worn at the chest level and a computer spreadsheet model. The final dose assessments revealed that dose received was much greater than that indicated by the TLD, but the dose was not great enough to be classified as an overexposure.

## REFERENCES

1. Morgan, K. Z., Turner J. E., Principles of Radiation Protection, John Wiley and Sons, Inc., New York, 1967.
2. Virginia Power Nuclear Engineering, Technical Report 377-VEPCO ORIGIN Code, May 1984.

ESTIMATING RADIATION DOSES FROM REACTOR ACCIDENTS

Aileen Jeffries  
Aby Mohseni

Emergency Response Section  
Office of Radiation Protection  
Department of Social and Health Services  
Washington State

## ABSTRACT

In order to plan for emergency response to reactor accidents involving large radiation releases, it is necessary to determine the medical resources, such as diagnostic laboratory tests, hospital facilities and convalescent care, needed to care for a large population exposed to radiation. A determination of the needed medical resources is difficult because of the widely varying sensitivity humans exhibit to radiation exposure and because of the large number of assumptions involved in predicting radiation dispersion.

This paper demonstrates a simple method for approximating medical needs in response to a severe reactor accident. The method requires a model for radiation dispersion from the accident and data for population distribution surrounding the reactor. With this information, tables developed in this paper may be used to project medical needs. The needs identified by this methodology may be compared against the actual medical resources of nearby communities to determine the size of the area impacted.

## Introduction

This paper was developed by the Emergency Response Section of the Office of Radiation Protection, Department of Social and Health Services, for the State of Washington. It is part of a much larger report, Nuclear Accident Response Study, which assessed the state's ability to provide medical response during a severe nuclear accident. The Washington State Legislature commissioned this study in light of the Chernobyll incident, which called into question the adequacy of our medical resources to cope with a nuclear accident in our state.

## Background on Radiation Effects on Humans

The effects of receiving significant doses of radiation in humans are divided into three general categories.

- o Early and continuing effects, such as radiation sickness
- o Late effects following a period of years, such as cancer
- o Genetic effects in children of those exposed, such as birth defects

Early and continuing effects manifest themselves within a year of exposure. They are due to acute radiation exposure and usually limited to persons exposed in areas very close to the reactor. Late effects show up in 2 to 40 years and genetic effects show up in succeeding generations. The doses that result in the last two categories of effects are generally characterized as low level doses affecting the people physically removed from the plant by a large distance.

Those individuals in the first category would require immediate and long-term medical treatment. Those individuals in the second and third categories will generally not seek medical attention until the effects manifest themselves. However, we expect that those individuals who are more sensitive to radiation: infants, children and pregnant women, will seek immediate medical attention because they will be alerted to do so by authorities.

## Determination of Radiation Exposure

There are many different ways of estimating radiation exposure.

- o From a personal dose measuring device, dosimeter, such as a film badge worn by the individual at the time of exposure
- o From calculations of exposure based on models of the accident and the individuals location during the accident

- o From medical assessment of physical symptoms and blood tests

All of these methods have inherent inaccuracies and at best a dose determination is only an estimate. Dosimeters may have low or high readings depending on which side of the body is exposed relative to the dosimeter and how much the badge is shielded by clothing. Calculations have many uncertainties and are generally conservative resulting in an overestimation of dose. The calculations are complicated by certain conditions such as precipitation which creates an irregular deposition and could result in an underestimation of dose. Also, these first two methods do not take into consideration the individuals sensitivity to radiation.

Physicians prefer to base their diagnosis on the third method, an individual's physical symptoms and blood tests. This method has the advantage of incorporating the individuals sensitivity to radiation into the physician's determination, but people who have non-average symptoms might be missed. From this determination we may "infer" a received dose, but in so doing we assume the greater or lesser sensitivity of a large number of individuals averages to the typical individual physical response for a given amount of radiation.

### Observation of Symptoms

In order to make the transition from physical symptoms to inferred dose, we relied heavily on two papers which described clinical symptoms and signs and related them to ranges of radiation exposure. Dr Fred Mettler and Dr Robert Ricks' paper, Medical Management of Radiation Accidents [5] estimates radiation exposure that would cause nausea, diarrhea and lowered lymphocyte count. A second paper, The Medical Technologist and the Radiation-Accident Victim [6], relates absolute lymphocyte count to significance of injury. In addition to these two papers, we used data from the space program research. NASA has researched the effects of acute radiation on bioastronauts and published tables relating possible fatality to exposure.[7]

### Relationship of Symptoms and Exposure

This paper combined NASA data with the medical data to create an extended table, Table 3, that identifies symptoms and indicates the diagnostic procedure that would be used for those symptoms. This table then gives the range of lymphocyte count/cc that would be expected for an "average individual" with the symptoms indicated. From this it infers a radiation dose and indicates a short term prognosis from the inferred dose.

In order to put this broad range of information together it is necessary to make critical assumptions. The most important being that the response of many individuals may be grouped as average responses over ranges of symptoms and exposures. Obviously, this table is a first approximation to the actual situation, but it is necessary to attempt to quantify the number and types of radiation injuries from radiation exposure.

Table 3: Diagnostic work to Determine Radiation Doses

RADIATION SYMPTOMS AND PROGNOSIS

Symptom of Radiation	Diagnostic Procedure	Lymphocyte Count/cc after 48 h	Inferred Dose Rem	Short Term Prognosis
Sickness				
No symptoms, but possible exposure to radiation	None for general population. (Sensitive popul. discussed later)	NA	< 50	No short term effects
No symptoms or mild symptoms, but known exposure	History, complete blood count (CBC), lymphocyte count at 12 and 48 hours	> 2000	10-100	Good. No serious disability
Nausea, vomiting, anorexia within 6 hours	History, CBC, lymphocyte count every 6 hours for 48 hours, possible hospitalization	1200-2000	100-200	Guarded. No deaths anticipated
Nausea, vomiting, anorexia within 4 hours, diarrhea, minor hemorrhage	History, CBC, lymphocyte count every 6 hours for 48 hours, blood type, diff. and platelet daily for up to 6 weeks, hospitalize	500-1200	200-350	Guarded. 20% deaths within 60 days
Nausea, vomiting, anorexia within 2 hours, diarrhea hemorrhage, fever, emaciation, other severe symptoms	Above treatment plus intensive care	< 500	> 350	Poor. Lethal injury for 50% or more within 30 days.

To clarify the information presented in Table 3 in terms of whether or not an individual will survive a particular dosage, we can estimate as follows. A person in the area who was exposed to a dose under 50 rem will not have obvious symptoms. Individuals exposed to between 100 and 200 rem will be ill, but will not usually die. Those individuals exposed to over 200 rem will require hospitalization and may die. Fifty percent of those exposed to over 350 rem die and those exposed to over 550 rem usually die [7]. These ranges cannot be exact because an individual's sensitivity to radiation varies with age, sex and health.

Using Table 3, the next step is to infer needed hospital and convalescent care from the symptoms and relate this to inferred dose. This was done by discussions with health care professionals and is shown in Table 4.

Table 4: Hospital and Convalescent Care

Inferred Dose (In Rem)	Hospital Care		Convalescent	
	Low	Intensive Terminal	3 months	6 months
10 to 100	5%			
100 to 200	25%	25%		
200 to 350		80%	20%	80%
Over 350		50%	50%	50%

Both diagnostic work and hospital care have evolved rapidly in the last ten years. The proposed tables will doubtless be modified as better input is obtained, but they served the useful purpose of allowing us to take the next step and project medical demands from a radiation emergency given a real population at risk.

Projected Medical Response for Two Scenarios

In order to estimate the population in each of the above dose categories, this paper uses the calculated dose received at various distances from the accident and the actual number of people living or working at those distances. A plant in southwest Washington, Trojan, was used for the population distribution. We did not consider the Trojan plant staff in this study, but they are sure to be severely impacted by an accident. We estimated the number of pregnant women to be 1.6% of the general population (NUREG/CR-4214)[8] and the number of infants and children to be 24% of the population (1985 U. S. Census estimate for Cowlitz County.) These two groups are especially sensitive to radiation and represent an additional impact on medical resources because we assume the authorities will instruct members of these groups to present themselves for blood chemistry workups even if they manifest no symptoms.

This study presents two accident scenarios. The first, PWR-3, represents the third worst accident listed in Reactor Safety Study presented in the Accident Spectrum section.[1,2] PWR-3 accident predicts the dispersal of radioactivity close to the

plant. The conservative assumptions of no rain, a moderate wind and neutral atmospheric conditions give a middle range exposure from this accident.[3] We assume 90% of the population is evacuated after four hours and the remaining 10% are evacuated after 24 hours. (Obviously, 100% evacuation before radioactivity is released would result in no exposure and is the preferred action.)

Table 5 shows the number of people in each exposure category, separated into two groups, those who were evacuated after four hours and those who were evacuated 24 hours after the accident. The population is divided into sensitive and general populations. The sensitive population is tabulated for exposures greater than 10 rem (>10) but less than 100 rem. The number of people is then totaled by exposure.

Table 5: Estimated Dosages for Scenario 1

RADIAL DISTANCE MILES	NUMBER PEOPLE	WHOLE-BODY AVG DOSE IN SECTOR REM	NUMBER OF PEOPLE IN EACH CATEGORY									
			SENSITIVE POPULATION		GENERAL POPULATION							
			FORTUS	CHILDREN	>10	>100	>200	>350	>550			
			>10 REM	>10 REM	REM	REM	REM	REM	REM			
90%	1	122	650	0	0	0	0	0	0	0	122	
	2	60	488	0	0	0	0	0	60	0	0	
	4 HOURS	3	228	280	0	0	0	0	228	0	0	0
		4	212	182	0	0	0	212	0	0	0	0
		5	137	111	0	0	0	137	0	0	0	0
10	44468	59	711	10672	33084	0	0	0	0	0		
10%	1	14	3250	0	0	0	0	0	0	0	14	
	2	7	2340	0	0	0	0	0	0	0	7	
	24 HOURS	3	25	1170	0	0	0	0	0	0	0	25
		4	24	748	0	0	0	0	0	0	0	24
		5	15	520	0	0	0	0	0	15	0	0
10	4941	279	0	0	0	0	4941	0	0	0		
TOTAL	50251			711	10672	33084	348	5169	76	191	50251	

Table 6 was constructed using Tables 3 and 4 and shows the number of people in each exposure group who would require diagnostic procedures and hospital admittance.

Table 6: Scenario 1 Diagnostic Procedures and Hospital Admittance

DIAGNOSTIC PROCEDURE AND HOSPITAL ADMITTANCE				HOSPITAL CARE			CONVALSCENT TIME	
POPULATION SEGMENT	DOSE REM	DIAGNOSTIC PROCEDURE	NUMBER OF PEOPLE	STANDARD	INTENSIVE	TERM	3 MONTH	6 MONTH
GENERAL	10 - 100	HISTORY, CBC, LYMPHOCYTE 12,48	33084	1654				
GENERAL	100 - 200	HISTORY, CBC, LYMPHOCYTE 6 FOR 48	348	87	87			
GENERAL	200 - 350	HOSPITAL CARE	5169		4135	1034	4135	
GENERAL	OVBR 350	HOSPITAL CARE, INTENSIVE	266		133	133		133
PREGNANT WOMEN	OVBR 10	HISTORY, CBC, CHROMOSOME	711					
CHILDREN	OVBR 10	HISTORY, CBC, CHROMOSOME	10672					
TOTALS				1741	4355	1167	4135	133

In general, the medical community recommends that individuals receiving doses in the range of 10 to 100 rem have a medical history and a complete blood count (CBC) taken. In addition, they recommend a lymphocyte count 12 hours and 48 hours after exposure. If the CBC indicates the individual has received a higher dose, this person would be placed in a different classification.

The second accident scenario, PWR-5, represents a less serious accident. We chose to picture the weather as the same as in Scenario 1--no rain, moderate wind and neutral atmospheric conditions. A PWR-5 accident releases less radioactivity than a PWR-3 accident, so the health impact of delayed evacuation is not as serious. Table 7 shows the estimate of affected individuals for Scenario 2.

Table 7: Estimated Radiation Doses for Scenario 2

RADIAL DISTANCE MILES	NUMBER PEOPLE	WHOLE-BODY AVG DOSE IN SECTOR REM	NUMBER OF PEOPLE IN EACH CATEGORY								
			SENSITIVE POPULATION		GENERAL POPULATION						
			PORTUS	CHILDREN	>10	>100	>200	>350	>550		
			>10 REM	>10 REM	REM	REM	REM	REM	REM		
90%	1	122	26	2	29	90	0	0	0	0	
	2	60	20	1	14	45	0	0	0	0	
	4 HOURS	3	228	10	0	0	0	0	0	0	
		4	212	5	0	0	0	0	0	0	
		5	137	3	0	0	0	0	0	0	
10	4468	2	0	0	0	0	0	0	0		
10%	1	14	91	0	3	10	0	0	0	0	
	2	7	65	0	2	5	0	0	0	0	
	24 HOURS	3	25	33	0	6	19	0	0	0	0
		4	24	20	0	6	17	0	0	0	0
		5	15	11	0	4	11	0	0	0	0
10	4941	6	0	0	0	0	0	0	0		
TOTAL	50251			4	64	198	0	0	0	0	266

Notice that even for the people evacuated 24 hours after the accident the dose level is estimated to be below 10 rems. Table 8 shows the number of people who would require medical assistance in this scenario.

Table 8: Scenario 2 Diagnostic Procedures and Hospital Admittance

POPULATION SEGMENT	DOSE REM	DIAGNOSTIC PROCEDURE	NUMBER OF PEOPLE	HOSPITAL CARE		CONVALESCENT TIME			
				STANDARD	INTENSIVE	TERM	3 MNTH	6 MNTH	
GENERAL	10 - 100	HISTORY, CBC, LYMPHOCYTE	12,48	198	10				
GENERAL	100 - 200	HISTORY, CBC, LYMPHOCYTE	6 FOR 48	0	0	0			
GENERAL	200 - 350	HOSPITAL CARE		0	0	0	0		
GENERAL	OVER 350	HOSPITAL CARE, INTENSIVE		0	0	0		0	
PREGNANT WOMEN	OVER 10	HISTORY, CBC, CHROMOSOME		4					
CHILDREN	OVER 10	HISTORY, CBC, CHROMOSOME		64					
TOTALS					10	0	0	0	0

## Summary and Conclusion

The two accidents considered in this paper were both quite severe and have low likelihood of occurring. They were selected to demonstrate the range of results that can be obtained by the technique developed in this paper. Notice that in each scenario the bulk of the work of medical assistance is in taking case histories and in providing laboratory blood analysis.

Other issues need additional work. For example, those individuals who are sensitive to radiation should be examined even if their exposure was less than 10 rem. For example, a fetus may be damaged at doses as low as 10 rem. Pregnant women will need chromosome analysis to determine doses in this range. Abortion and counseling may be needed. Children are more sensitive to radiation than adults and chromosome tests may also be needed for them.

The whole issue of future liability is another important consideration. We believe liability considerations will provide an incentive to the owners of the reactor to accurately determine dose rates to the general population down to 10 rem. This again calls for chromosome tests. Since one out of three people in an exposed population would develop cancer even if they had not been exposed to radiation from the accident, there is a high likelihood that one-third of those individuals exposed could initiate lawsuits. Chromosome analysis done at the time to determine the accident exposure would be important to the outcome of these suits. These analyses must be done between two and three weeks after exposure to accurately determine dose rates as low as 10 rem. This analyses requires the culture of lymphocytes; it takes one week to process; and it costs approximately \$1000.00 (Mettler, private communication).

This paper has demonstrated a simple method for approximating medical needs in response to a severe reactor accident. The method requires a model for radiation dispersion from the accident and data for population distribution surrounding the reactor. With this information, Tables 3 and 4 may be used to project medical needs. At the present, the medical needs identified include medical history, laboratory work, hospital beds and convalescent care. The medical needs identified by this methodology may be compared against the actual medical resources of nearby communities to determine the size of the area impacted.

## REFERENCES

- [1] U. S. Nuclear Regulatory Commission. Overview of the Reactor Safety Study Consequence Model, (NUREG-0340), 1977.
- [2] U. S. Nuclear Regulatory Commission. Reactor Safety Study: An Assessment of Accident Risks in United States Commercial Nuclear Power Plants, WASH 1400 (NUREG-75/014), 1975. Available from NTIS, Springfield VA.
- [3] U. S. Nuclear Regulatory Commission. Dose Calculations for Severe LWR Accident Scenarios, (NUREG 1062), 1984.
- [4] U. S. Nuclear Regulatory Commission. Implications of the Accident at Chernobyl for Safety Regulation of Commercial Nuclear Power Plants in the United States (NUREG-1251), draft for comment.
- [5] Mettler, F. A.; Ricks R. C. Medical Management of Radiation Accidents. Contemporary Diagnostic Radiology. 5:1-6; 1982.
- [6] Berger, M. E.; Thompson, D. W.; Ricks, R. C.; Kaufmann, D. The Medical Technologist and the Radiation-Accident Victim. American Society for Medical Technology. 47: 829-834; 1981.
- [7] Webb P. Bioastronauts Data Book. National Aeronautics and Space Administration; 1975. Washington D.C. NASA SP-3006.
- [8] U. S. Nuclear Regulatory Commission. Health Effects Model for Nuclear Power Plant Accident Consequence Analysis, (NUREG/CR-4214), 1985.

# THE CALIBRATION OF NEUTRON SENSITIVE SPHERICAL DEVICES WITH A D<sub>2</sub>O-MODERATED <sup>252</sup>Cf SOURCE AT CLOSE DISTANCES

H Kluge, K Weise, J B Hunt\*  
Physikalisch-Technische Bundesanstalt, Braunschweig,  
Fed. Rep. of Germany,  
\* National Physical Laboratory, Teddington, United Kingdom

Neutron personal or area monitoring devices used in radiation protection have to be calibrated before any reliance can be placed upon the readings obtained in practice. If a device is to be used in environments rich in low energy neutrons, then the D<sub>2</sub>O-moderated <sup>252</sup>Cf source (diameter 30 cm) is preferred to more conventional radionuclide neutron sources.

The fractional contribution to the device readings due to neutrons scattered by the walls, the floor, the ceiling and the air may be reduced, and the dose equivalent rate increased, if the calibration is carried out in close proximity to the moderated source assembly. In this situation, the device readings must be corrected for non-uniform illumination of the device. The necessary geometric correction factor applicable to the calibration of spherical devices with the physically large spherical source has been developed and compared with measurements made with devices of different diameters and different responses as a function of neutron energy. The influence of the scattering effects was investigated by performing the measurements in two different sized rooms.

## 1 Introduction

In general, all neutron personal or area monitoring devices used in radiation protection work have to be calibrated before any reliance can be placed upon the readings obtained in stray neutron fields. Such calibrations are usually carried out by irradiating the device with a physically small neutron source of known emission rate. The neutron fluence response of the instrument is then obtained from its reading and from the calculated or measured neutron fluence at the position of the device but in its absence, i.e., the 'receptor-free' situation. This fluence response may be transformed to the dose equivalent response by use of the appropriate neutron fluence to dose equivalent conversion factor.

The choice of the most appropriate source for the calibration of the device depends upon both the spectrum of the field in which the device is to be used, and upon the variation of its response with incident neutron energy. It is highly desirable to choose a calibration source that has a significant fraction of its neutron spectrum over the same range of neutron energies that will be encountered in practice. If the device is to be used in environments rich in low energy neutrons, then the heavy-water moderated californium spontaneous fission source (D<sub>2</sub>O-moderated <sup>252</sup>Cf) /1/ is preferred to more conventional radionuclide neutron sources.

Earlier work carried out at the National Physical Laboratory (NPL) and the Physikalisch-Technische Bundesanstalt (PTB), demon-

strated that the D<sub>2</sub>O-moderated <sup>252</sup>Cf source assemblies constructed at NPL and PTB produced the same fluence rates, normalised to the known source emission rates of the bare <sup>252</sup>Cf source placed at the centre of the assemblies /2/. It was also demonstrated that the leakage spectra were very similar in both the intermediate and fast neutron energy ranges. The analysis of data obtained with spherical devices, taking into account all the scattering effects, is now well understood at source centre to detector centre distances D<sub>0</sub> ≥ 80 cm in both large and small calibration rooms.

The aim of the present work was to investigate the dependence of the response of spherical devices at much smaller centre-to-centre separation distances D<sub>0</sub>, and to try to explain any departures from the inverse-square law. The response of spherical devices due to a physically small radionuclide source as a function of the separation distance, at both small and large distances, is well understood /3/. Departures from the inverse square-law at close distances can be explained in terms of a geometric correction /4/ that takes into account the finite size of the detector and the divergence of the incident neutron fluence. If the response of a spherical device could be understood at such close distances, for a physically large source such as the D<sub>2</sub>O-moderated <sup>252</sup>Cf source, then calibrations could be carried out over the full operational range of typical devices using neutron sources with relatively low emission rates. This would reduce the initial cost of the source to the calibration laboratory and ease the problems associated with its handling.

## 2 Method

The calibration factor, N, is defined as the quotient of the conventionally correct value of the measurand at the place of measurement (dose equivalent to be specified, H, in the absence of the measuring instrument) and the reading, M, of the measuring instrument:  $N = H/M$ .

For standard conditions of irradiation, where the neutrons are incident from one direction only in a broad, parallel beam, for instance the ambient dose equivalent, H\*(10), /5/ at the measurement point can be calculated from the fluence, Φ, of the neutrons and the fluence to dose equivalent conversion factor, h<sub>Φ</sub>\* (10), i.e.  $H^*(10) = \Phi \cdot h_{\Phi}^*(10)$ . For monoenergetic neutrons, recommended conversion factors may be taken from the literature /6/, but for the case of broad neutron spectra, a neutron energy spectrum averaged conversion factor,  $\bar{h}_{\Phi}^*(10)$ , must be used. If the fluence response of the detector  $R_{\Phi} = M/\Phi$  is introduced, then the calibration factor is given by

$$N = \bar{h}_{\Phi}^*(10)/R_{\Phi} . \quad (1)$$

For the D<sub>2</sub>O-moderated source, it is well known that the neutron leakage spectrum changes with distance from the moderator surface /7/. This occurs because (a) the fluence at any point outside the moderator depends on both the number of neutrons leaving the surface and on their angular distribution, and, (b) moderated neutrons of different energies have different angular distributions. In general, high energy neutrons emerge with directions closer to their original directions than do low energy

neutrons, which have been multiply scattered. Thus, as the distance from the surface increases, the main spectral change is a decrease in the proportion of low energy neutrons, and a consequent hardening of the neutron spectrum. It was also shown that the calculated ratio of the fluence rates due to the moderated and the bare source decreases to an asymptotic value as the separation distance increases /7/.

A computer program was used to determine the spectrum averaged conversion factor,  $\bar{h}_\phi^*(10)$ , as a function of distance from the centre of the source, taking into account the properties of the PTB moderator assembly; i.e., the radius of the moderator, the thickness of the cadmium liner (Cd) and the composition of the  $^{252}\text{Cf}$  source /8/. The energy spectrum of the neutrons and the ratio of the fluence rates produced by the moderated and the bare  $^{252}\text{Cf}$  source can be calculated at any distance from the centre of the moderating sphere. The transport of source neutrons through the moderating sphere filled with  $\text{D}_2\text{O}$  is simulated using a Monte Carlo program. The program includes corrections for neutron attenuation by the Cd liner, and at greater distances, by the air between the source assembly and the measurement position. Normalization is to one  $^{252}\text{Cf}$  fission neutron.

The corresponding  $\bar{h}_\phi^*(10)$  values were calculated for each distance by averaging the fluence to dose equivalent conversion factors for monoenergetic neutrons /6/ over the calculated energy spectrum of the neutrons at that point.

For the PTB moderator assembly, the final computed values of the averaged conversion factor,  $\bar{h}_\phi^*(10)$ , and the ratio of the neutron fluence rates  $\varphi$  due to the moderated (mod) and bare sources,  $\alpha$ , at large distances from the source, are  $\bar{h}_\phi^*(10) = 99.8 \text{ pSv.cm}^2$  and  $\alpha = \varphi(\text{mod})/\varphi(\text{bare}) = 0.898$ , respectively.

## 2.1 Establishment of the fluence response $R_\phi$

According to Hunt /3/, the count rate,  $\dot{C}$ , measured by a spherical detector at a distance  $D_0$  is described by the relationship

$$\dot{C}(D_0) = (K/D_0^2)F_1(D_0)F_2(D_0) \quad (2)$$

where

$$K = R_\phi B F_I / 4\pi \quad (3)$$

$B$  is the source strength of the  $^{252}\text{Cf}$  source,  $F_I$  is a correction factor for anisotropic emission of the source which depends on the direction of neutron emission, and  $D_0$  is the distance between the centre of the source and the centre of the detector. In the case of the  $\text{D}_2\text{O}$ -moderated  $^{252}\text{Cf}$  source, the fluence rate  $\varphi(\text{mod})$  produced by the neutrons at a distance  $D_0$  is determined by

$$\varphi(\text{mod}) = \alpha \varphi(\text{bare}) \quad (4)$$

with

$$\varphi(\text{bare}) = B/4\pi D_0^2 \quad (5)$$

As a result of symmetry arising from the moderation of neutrons in the spherical heavy water volume, the factor  $F_1$  can be set equal to unity. Thus, for calibrations carried out using the  $D_2O$ -moderated  $^{252}\text{Cf}$  source, the fluence response of the instrument is related to the characteristic constant,  $K$ , of Eq. (3) by

$$R_\phi = 4\pi K/B\alpha . \quad (6)$$

The function  $F_1(D_0)$  is the geometric correction, discussed later in Section 2.2. The additional contribution from scattered neutrons is described by the correction function  $F_2(D_0)$  /3/:

$$F_2(D_0) = 1 + A.D_0 + S.D_0^2 . \quad (7)$$

For isotropically emitting sources, the contribution to the instrument reading due to scattering by the walls is assumed to be constant in the vicinity of the source, and the contribution due to scattering of neutrons in the air and by the supporting structures is assumed to be inversely proportional to the distance  $D_0$ .

Eq. (2) is an approximation. For physical reasons, the geometric correction function  $F_1$  should be multiplied with the unity term of  $F_2$  only, and not with the  $D_0$ -dependent scattering terms. The resulting improved relationship

$$\dot{C}(D_0) = (K/D_0^2)(F_1(D_0) + F_2(D_0) - 1) \quad (8)$$

was used in this work instead of Eq. (2).

## 2.2 Geometric correction function

As the detector is brought closer to the neutron source, it begins to overread when compared with that expected on the basis of the inverse square law. The overread increases to a maximum when the detector and the neutron source are touching. The function  $F_1(D_0)$  is intended to correct for this effect. For a point source and a spherical detector, Hunt /3/ proposed the following correction function

$$F_1(D_0) = 1 + \delta[2(D_0/R_D)^2(1 - \sqrt{1-(R_D/D_0)^2}) - 1] \quad (9)$$

where  $R_D$  is the radius of the detector. The square bracketed term, derived purely geometrically /3,4/, represents the additional fractional number of neutrons entering the detector volume due to non-parallel incidence of the neutrons upon the detector, and the free parameter,  $\delta$ , accounts for their relative effectiveness in producing a response in the detector. For the case of a spherical source and a spherical detector, Eisenhauer et al /9/ suggested that a reasonable estimate of the correction factor could be obtained from the product of two factors of the type given in Eq. (9) using the source radius,  $R_S$ , in one factor, and the detector radius,  $R_D$ , in the other factor,

$$F_1(D_0) = F_1(D_0, R_S)F_1(D_0, R_D) . \quad (10)$$

However, the situation is more complicated in the case of the  $D_2O$ -moderated  $^{252}\text{Cf}$  source. Not only is the source physically large,

but both the fluence rate ratio  $\alpha$  and the neutron energy spectrum are known to be distance dependent. Both these effects will lead to departures from the inverse square law at close distances.

### 3 Measurements

Measurements were performed with two spherical devices as transfer devices, a 20.8 cm diameter, commercially available survey meter of the Leake-type /10/, and a 11 cm diameter sphere designed to be used with the central  $^3\text{He}$  proportional counter from the survey meter. The survey meter is more sensitive to the high energy neutrons in the leakage spectrum, whereas the small sphere has an increased response for the low energy neutrons. As the leakage spectrum changes with distance, departures from the inverse-square law for both these instruments will depend upon the differing shapes of the fluence responses as a function of neutron energy as well as upon the different geometries of the source-detector combinations. In order to try and separate out these two effects, a third transfer device was derived from the survey meter by removing the inner perforated cadmium liner, creating a device with the same source-detector geometry as the survey meter but with a different relationship between its response and the incident neutron energy.

The influence of the scattering effects was investigated by performing the measurements in two different sized rooms; the "Bunker"-room at PTB (dimensions 7 m x 7 m x 6.5 m) and the "scatter-free area" at NPL (dimensions 24 m x 30 m x 18 m). If the scatter-dependent effects are taken properly into account, then the measured fluence responses determined solely from data obtained at large separation distances should be the same, within the experimental uncertainties /2/.

All measurements were made with discrimination levels set at the same position in relation to the pulse height distributions, and the count rates obtained were corrected for dead time losses. The distance between the centres of the source and the detector,  $D_0$ , ranged from the minimum possible, direct contact between the surfaces of the  $\text{D}_2\text{O}$ -moderator and the detector, (i.e.,  $D_0(\text{min}) = R_p + R_s$ ), up to 195 cm at PTB, and 250 cm at NPL. Incremental steps varied from 0.1 cm close to the source to a maximum of 10 cm at PTB, and a maximum of 50 cm at NPL for the largest distances. Data were obtained at a minimum of 30 different distances for all three devices, at both laboratories.

### 4 Results

The data sets were fitted to Eq. (8), using Eqs. (9) and (10). The parameters and their uncertainties were calculated from the measured values, and their uncertainties, using weighted least squares techniques, and taking all the correlations into account. However, all attempts to explain the observed dependence of the detector readings with distance, at small separation distances, failed for two reasons. Firstly, as  $D_0 \rightarrow D_0(\text{min})$ , the measured  $dF_1/dD_0$  did not increase as rapidly as predicted using Eqs. (9) and (10), and, secondly, the variation of  $dF_1/dD_0$  as  $D_0$  increased could not be explained using this formulism, irrespective of the values

of the free parameters,  $\delta_s$  and  $\delta_D$ .

#### 4.1 Alternative formulism

The exact form of Eq. (8) can be written as

$$\dot{C}(D_O) = (K/D_O^2)F_3(D_O) \quad (11)$$

were

$$F_3(D_O) = F_1(D_O)\exp(-\Sigma D_O) + F_2'(D_O) - 1 \quad (12)$$

The exponential factor takes into account the attenuation of the 'direct' incident neutrons by the air;  $\Sigma$  is the linear attenuation coefficient of air obtained by averaging the total neutron cross sections of nitrogen and oxygen over the neutron energy distribution of the source. The calculated value of this coefficient for a  $D_2O$ -moderated  $^{252}\text{Cf}$  source is  $2.96 \cdot 10^{-4} \text{ cm}^{-1}$ . The modified scattering correction is

$$F_2'(D_O) = 1 + A'D_O + \Sigma D_O^2 \quad (13)$$

where  $A'$  includes all  $1/D_O$ -dependent effects by inscattered neutrons except outscattering by the air, which is now taken into account by the exponential factor. The relationship between  $A'$  and the total  $1/D_O$ -coefficient  $A$  of Eq. (7) is given by

$$A' = A + \Sigma \quad (14)$$

Another formulation for the geometric correction proved to be considerably more compatible with the measured data:

$$F_1(D_O) = 1 + a_4/(1 + a_5L)^2 \quad (15)$$

where  $L$  is given by

$$L = (D_O - R_S - R_D)/R_D \quad (16)$$

The parameter  $a_4$  corresponds to  $\delta$  in Eq. (9), and the parameter  $a_5$  determines the value of the derivative of  $F_1$  with respect to  $D_O$  for the situation where the spheres are touching, i.e.  $L = 0$ . This finite value of the derivative of  $F_1$  arises because the neutrons which contribute to the overread are mainly emitted from parts of the surface of the spherical moderator which are not directly adjacent to the spherical detector, and thus, apparently from a slightly more distant source.

The expression  $a_4/(1 + a_5L)^2$  is proportional to  $L^{-2}$ , and hence, proportional to  $D_O^{-2}$ , for large values of  $L$ . The conventional geometric correction, given by Eq. (9), also behaves in this way. Furthermore, if one relates the changes in the fluence response  $R_\phi$  of the detector, and the fluence rate ratio  $\alpha$  to the corresponding values  $R_{\phi,O}$  and  $\alpha_O$  applicable at large distances, then the following correction factors can be defined:

$$K_1 = R_\phi/R_{\phi,O} \quad \text{and} \quad K_2 = \alpha/\alpha_O \quad (17)$$

Calculations /8/ for the detectors used in this work showed that

the combined correction factor,  $K_1K_2$ , is given by

$$K_1K_2 = 1 + aD_0^{-2.1} . \quad (18)$$

Hence all the effects discussed are proportional to  $D_0^{-2}$  at large distances. Thus, the parameter  $a_5$  describes the combined influence of all these effects. Attempts to fit the data sets to a more sophisticated relationship based upon two different parameters, one to fix the derivative of  $F_1$  with respect to  $L$  when the two spheres are nearly touching, and the other as the coefficient of the asymptotic  $D_0^{-2}$ -term, failed. Calculated values for chi-square were too small, and the covariance matrix of the parameters became singular. In order to extract additional parameters, the uncertainty associated with the measurements carried out at small separation distances must be reduced considerably.

## 4.2 Final data analysis

The measurements were fitted to Eq. (11), using Eqs. (12), (13), (15) and (16). The parameters and their associated uncertainties were again calculated using least squares techniques as specified in /11/. In all cases, compliance with the chi-square criterion demonstrated that the data were in excellent agreement with the model.

As a comparison, the parameters  $K$ ,  $A$ , and  $S$  of Eqs. (2) and (7) were determined from the measured values at greater distances ( $D_0 > \approx 70$  cm), using the polynomial model described by Hunt /3/, where the geometric correction function  $F_1$  was set equal to unity. The parameter  $A'$  was derived from the computed value of  $A$  using Eq. (14), and  $\Sigma = 2.96 \cdot 10^4 \text{ cm}^{-1}$ , as stated earlier.

Table 1 shows the resulting values for the various parameters. The coefficients  $A'$  and  $S$  reflect the different scattering conditions in both irradiation rooms. The parameters  $a_4$  and  $a_5$  are, within the uncertainties, equal for both the large detectors showing that they are mainly dominated by the geometric dimensions of the detectors. Table 2 shows the values obtained for the fluence responses,  $R_\phi$ , calculated using Eq. (6) with  $\alpha = 0.898$ . The uncertainties given are standard deviations, and contain a contribution associated with the determination of the neutron source strength; 0.5 % in the case of the NPL measurements and 1.3 % in the case of the PTB measurements. The fluence responses determined from the measurements at PTB and NPL differ by less than twice of the associated standard deviations.

The combined function  $F_3(D_0)$  which corrects for the geometric effects as well as for the scattering of neutrons from the air and from the walls, shows a characteristic minimum at  $D_0 \approx 2R_0 + R_D$  for all the measurements. The position of this minimum is determined both by  $F_1(D_0)$  and by  $F_2'(D_0)$ . However, the value of  $F_2'(D_0)$  at, or near, this characteristic minimum was predominantly due to the  $1/D_0$ -dependent scattering effects in the large NPL 'scatter-free area', whereas in the comparatively small PTB 'Bunker'-room, it was strongly influenced by the room-return effects. Fig. 1 shows the variation of the function  $F_3(D_0)$  with distance  $D_0$  for the instruments investigated in this work. For the calibration of the area survey meter, of practical interest in radiation protection, the minimum value lies between  $1.038 \pm 0.017$  (NPL) and  $1.041 \pm 0.007$

(PTB) for both calibration rooms, even though they are very different in size.

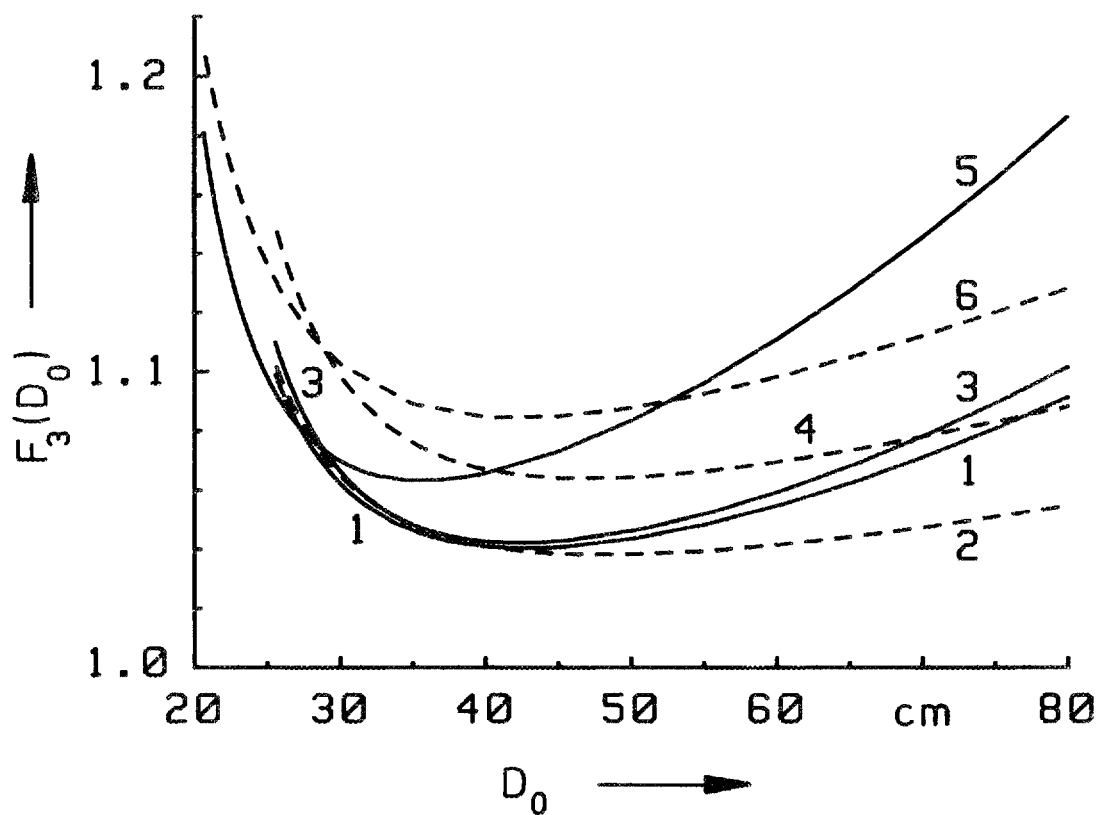
For other spherical dose equivalent measuring instruments, the parameters can be determined from similar measurements carried out once. Routine calibration can then be carried out at any distance, within the measurement range, to produce the necessary dose equivalent rates required for the calibration or at distances where the effects to be corrected are minimum.

Acknowledgement: This work was supported by the Commission of the European Communities under contracts 86E1-027-A and 86E1-027-B.

### References

- /1/ Schwartz R B and Eisenhauer C M. The Design and Construction of a D<sub>2</sub>O-Moderated <sup>252</sup>Cf Source for Calibrating Neutron Personnel Dosimeters Used at Nuclear Power Reactors. NUREG/CR-1204, January, 1980.
- /2/ Kluge H, Rasp W and Hunt J B. An intercomparison of the D<sub>2</sub>O-moderated <sup>252</sup>Cf reference neutron sources at PTB and NPL. Radiat. Prot. Dosim. 11, 61-63 (1985).
- /3/ Hunt J B. The calibration of neutron sensitive spherical devices. Radiat. Prot. Dosim. 8, 239-251 (1984).
- /4/ Axton E J. The effective centre of a moderating sphere when used as an instrument for fast neutron flux measurement. J. Nuclear Energy 26, 581-583 (1972).
- /5/ ICRU, International Commission on Radiation Units and Measurements. Determination of Dose Equivalents Resulting from External Radiation Sources. ICRU Report 39 (1985).
- /6/ Wagner S R, Grosswendt B, Harvey J R, Mill A J, Selbach H J and Siebert B R L. Unified Conversion Functions for the New Operational Radiation Protection Quantities. Radiat. Prot. Dosim. 12, 231-235 (1985).
- /7/ Ing H and Cross W G. Spectra and dosimetric characteristics of a D<sub>2</sub>O-moderated <sup>252</sup>Cf calibration facility. Health Physics 46, 97-106 (1984).
- /8/ Siebert B R L, Hollnagel R and Kluge H. Calculation of Fluence and Dose in the Neutron Field of the D<sub>2</sub>O-Moderated <sup>252</sup>Cf Source of the PTB. Radiat. Prot. Dosim. (to be published).
- /9/ Eisenhauer C M, Hunt J B and Schwartz R B. Calibration Techniques for Neutron Personal Dosimetry. Radiat. Prot. Dosim. 10, 43-57 (1985).
- /10/ Leake J. An Improved Spherical Dose-Equivalent Neutron Monitor. Nucl. Instr. Meth. 63, 329-332 (1968).
- /11/ DIN 1319 Teil 4, Grundbegriffe der Meßtechnik, Behandlung von Unsicherheiten bei der Auswertung von Messungen. Beuth-Verlag, Berlin 1985.

Fig. 1 Combined geometric and scatter correction function  $F_3(D_0)$ , given in Eq. (12) with Eqs. (13), (15), and (16) as a function of the separation distance  $D_0$  of the centres of the neutron source and the detector. Legend (see also Table 1): 1: RC (PTB), 2: RC (NPL), 3: RC without Cd (PTB), 4: RC without Cd (NPL), 5: 11 cm-sphere (PTB), 6: 11 cm-sphere (NPL)



Detector	Establishment	Model	$K \cdot 10^{-5}$ ( $\text{cm}^2\text{s}^{-1}$ )	$A' \cdot 10^4$ ( $\text{cm}^{-1}$ )	$S \cdot 10^5$ ( $\text{cm}^{-2}$ )	$a_4 \cdot 10^1$	$a_5$
RC	PTB	5-Param.	$3.293 \pm 0.021$	$1.7 \pm 1.0$	$1.53 \pm 0.03$	$0.93 \pm 0.04$	$0.76 \pm 0.07$
RC	PTB	Polynomial	$3.228 \pm 0.094$	$4.7 \pm 4.6$	$1.46 \pm 0.20$	-	-
RC	NPL	5-Param.	$5.971 \pm 0.088$	$6.8 \pm 2.2$	$0.32 \pm 0.07$	$0.90 \pm 0.12$	$0.78 \pm 0.22$
RC	NPL	Polynomial	$5.953 \pm 0.086$	$7.6 \pm 2.2$	$0.30 \pm 0.08$	-	-
RC without Cd	PTB	5-Param.	$39.01 \pm 0.20$	$0.94 \pm 0.84$	$1.78 \pm 0.03$	$1.04 \pm 0.04$	$0.82 \pm 0.05$
RC without Cd	PTB	Polynomial	$38.94 \pm 0.29$	$1.95 \pm 1.34$	$1.73 \pm 0.06$	-	-
RC without Cd	NPL	5-Param.	$68.58 \pm 0.83$	$11.6 \pm 1.8$	$0.23 \pm 0.05$	$1.24 \pm 0.11$	$0.77 \pm 0.14$
RC without Cd	NPL	Polynomial	$68.73 \pm 0.71$	$11.7 \pm 1.6$	$0.22 \pm 0.06$	-	-
11 cm-sphere	PTB	5-Param.	$58.81 \pm 0.29$	$3.98 \pm 0.91$	$2.73 \pm 0.03$	$1.68 \pm 0.04$	$0.58 \pm 0.04$
11 cm-sphere	PTB	Polynomial	$58.26 \pm 0.63$	$6.5 \pm 2.0$	$2.64 \pm 0.11$	-	-
11 cm-sphere	NPL	5-Param.	$105.6 \pm 0.9$	$14.9 \pm 1.4$	$0.41 \pm 0.04$	$1.80 \pm 0.10$	$0.41 \pm 0.05$
11 cm-sphere	NPL	Polynomial	$103.5 \pm 1.3$	$18.7 \pm 1.7$	$0.31 \pm 0.06$	-	-

**Table 1** Intercomparison of the computed parameters for the dose equivalent rate meter (RC), the same instrument without its cadmium liner, and for an 11 cm diameter polyethylene sphere. 5-Param.: Evaluation with the suggested correction function given in Eq. (11), with Eqs. (12), (13), (15), and (16). Polynomial: Evaluation at distances greater than 70 cm using a second-order polynomial for adjustment /3/. According to Eq. (14), a value of  $\Sigma = 2.96 \cdot 10^4 \text{ cm}^{-1}$  was added to the parameter A for intercomparison. Distance uncertainties were assumed to be 0.2 mm at PTB, and 0.5 mm at NPL.

		$R_\phi$ ( $\text{cm}^2$ )		
		RC	RC without Cd	11cm-sphere
PTB	5-Param.	$0.1170 \pm 0.0017$	$1.388 \pm 0.019$	$2.092 \pm 0.029$
	Polynomial	$0.1147 \pm 0.0037$	$1.386 \pm 0.021$	$2.073 \pm 0.035$
NPL	5-Param.	$0.1152 \pm 0.0018$	$1.324 \pm 0.017$	$2.039 \pm 0.020$
	Polynomial	$0.1149 \pm 0.0018$	$1.327 \pm 0.015$	$1.999 \pm 0.027$

**Table 2** Intercomparison of the values determined for the fluence response  $R_\phi$ . See caption to Table 1.

HEALTH PHYSICS SOCIETY PROGRAM FOR ACCREDITATION  
OF CALIBRATION LABORATORIES

Leon West  
University of Arkansas

Frank X. Masse  
Massachusetts Institute of Technology

Kenneth L. Swinth  
Battelle Pacific Northwest Laboratory

ABSTRACT

The Health Physics Society has instituted a new program for accreditation of organizations that calibrate radiation survey instruments. The purpose of the program is to provide radiation protection professionals with an expanded means of direct and indirect access to national standards, thus introducing a means for improving the uniformity, accuracy, and quality of ionizing radiation field measurements. Secondary accredited laboratories are expected to provide a regional support basis. Tertiary accredited laboratories are expected to operate on a more local basis and provide readily available expertise to end users. The accreditation process is an effort to provide better measurement assurance for surveys of radiation fields. The status of the accreditation program, general criteria, gamma-ray calibration criteria, and x-ray calibration criteria are reviewed.

INTRODUCTION

In 1986, the Board of Directors of the Health Physics Society approved a plan to establish a standing committee for the purpose of initiating and maintaining an accreditation program for laboratories which calibrate survey instruments. By midyear of 1987, the policy and general criteria for the program were firmly established<sup>1</sup>. Also, specific criteria for gamma-ray and x-ray calibrations were defined<sup>1</sup>, and organizations were invited to submit applications. The purpose of the program, as defined in the policy, is to provide radiation protection professionals with an expanded means of direct and indirect access to the standards maintained by the U.S. National Bureau of Standards, thus introducing a means for improving the uniformity, accuracy, and quality of ionizing radiation field measurements.

This paper reviews the purpose, organization, levels of accreditation, and present status of this new program. Requirements for accreditation in gamma and x-ray categories are presented. The information presented here is a general summary of

the HPS program, and is not binding information. The HPS Secretariat<sup>1</sup> should be consulted for details of the actual program and the binding requirements. Application information may be obtained directly from the Health Physics Society<sup>1</sup>. The authors are the present chair (L.W.) and past chair (F.X.M.) of the HPS standing committee, and chair (K.L.S.) of the operations group.

#### STATUS AND TRENDS

At the present time, a person seeking calibration of a survey instrument will find the best available information in a directory<sup>2</sup> compiled through a joint program between the National Bureau of Standards (NBS) and the Conference of Radiation Control Program Directors, Inc. The directory provides general information concerning institutions and companies which provide calibration services. However, the user of these calibration services has no assurance, other than performing individual audits, of the quality of services rendered by the organizations listed in the directory.

In 1981, the National Bureau of Standards recommended a national program<sup>3</sup> to provide measurement assurance for ionizing radiation measurements. National radiation standards are known in general to within less than  $\pm 3$  percent. Field measurements have a desirable accuracy of  $\pm 20$  percent for radiation survey measurements. Special Publication 603 suggested two intermediate levels (secondary and tertiary) should be considered to achieve the desirable field accuracy<sup>3</sup>.

The Health Physics Society (HPS) has adopted the secondary/tertiary hierarchy. Secondary accredited laboratories are intended to be somewhat regional in scope, requiring instrument interchanges with NBS and requiring the ability to support tertiary laboratories. Tertiary accredited laboratories are intended to provide the bulk of the calibration services to end users, requiring instrument interchanges with secondary laboratories. A standing committee provides primary management of the program. The process of accreditation review and evaluation is assigned to an operations group which is funded entirely from revenues received. An advisory group assists the operations group.

#### GENERAL CRITERIA

The purpose of an accredited laboratory is to support accurate measurements for radiation protection by providing reliable and prompt calibration of survey instruments. Secondary accredited laboratories have the additional responsibility of providing priority services to tertiary accredited laboratories, including calibrations, proficiency tests, consultation, training, and instrument evaluations.

Organizational structure requirements for the Secondary Accredited Laboratory (SAL) require that the laboratory supervisor hold a bachelor's degree in one of several defined disciplines. In the Tertiary Accredited Laboratory (TAL), an associate or bachelor's degree is acceptable for the supervisor. The person in charge of day-to-day operations must have at least three years of experience in instrument calibrations.

Laboratory design is addressed in general terms. Temperature, pressure, and humidity must be monitored at all times.

Calibration equipment must include secondary (or tertiary) radiation measurement standards that cover the range of calibrations performed. Separate working standards are recommended for routine laboratory reference. A high-quality thermometer and barometer must be capable of  $\pm 1$  percent accuracy. Secondary accredited laboratories must also be capable of monitoring relative humidity in the range 15 to 65 percent with an accuracy of  $\pm 5$  percent. All equipment must have been calibrated prior to accreditation and must be subject to continuing quality control.

Operational procedures must be defined in the laboratory protocol. The protocol defines the scope of the calibrations performed, the accuracy goals, the method of tracing the calibration of each supporting piece of equipment used in the radiation calibration, and the uncertainty assessment.

Accuracy and quality assurance are maintained by routine quality control procedures and by proficiency testing. Two sets of barometers and thermometers are required to provide a continuous intercomparison in the SAL. In the TAL, a single barometer and thermometer may be used if they are recalibrated periodically. Recalibration of equipment is required when the need is demonstrated. Proficiency testing of the SAL is to be performed at least annually by the National Bureau of Standards. Proficiency testing of a TAL is to be performed at least annually by a Secondary Accredited Laboratory.

Records must be maintained for the following information:

1. Calibration history of all standards and calibration equipment.
2. Inventory of standards and calibration equipment.
3. Procedures.
4. Permanent records concerning each calibration performed, including details of the instrument and customer.
5. Information to reconstruct a calibration.
6. Record of quality control activities.

7. Copies of all calibration reports issued.
8. Results of all proficiency tests.

Records must be initialed by the person collecting the information and kept at least until the next accreditation renewal is completed.

Calibration reports issued by an accredited laboratory must clearly indicate whether an accredited or non-accredited procedure was utilized for the calibration.

#### GAMMA-RAY CALIBRATIONS

The energy and exposure rate of the radiation field must be appropriate for the type of instrument to be calibrated. Gamma-ray sources listed in the HPS criteria include  $^{241}\text{Am}$  (60 keV),  $^{137}\text{Cs}$  (662 keV),  $^{226}\text{Ra}$  (mean energy of 830 keV), and  $^{60}\text{Co}$  (mean energy of 1.25 MeV). Source activities are not defined, since this is dependent on the range of exposure rates each accredited laboratory will offer.

Beam control is addressed in the HPS criteria with sections concerning shielding, collimation, exposure control and timer equipment.

Laboratory equipment must include two sets of ion chambers and supporting instrumentation; one set serves as an independent backup to verify the results of the secondary (or tertiary) standard ion chamber. Both secondary and tertiary laboratories must have a voltmeter appropriate for the instruments being calibrated. Additional equipment is required for the SAL, including a beam-axis locator, working standard ion chamber, pulser, oscilloscope, current source, and standard capacitors.

Exposure rate must be known as a function of distance from the gamma source. For the SAL, the minimum distance between the source and the detector must be 10 times the largest dimension of the detector. For the TAL, this distance requirement is relaxed to 5 times the largest dimension of the detector. Box-type calibrators may be utilized by a TAL under certain provisions defined in the criteria. Attenuators may be used, provided the effect on the gamma energy spectrum is known. Scattered radiation must not contribute more than 25 percent of the exposure rate response of the instrument; or the effect on accuracy of the scattered radiation must be known.

Accuracy requirements for the SAL are twice as rigorous as the TAL. Exposure rates above 100 mR/h must be known within  $\pm 5$  percent for the SAL and within  $\pm 10$  percent for the TAL. Between 0.5 mR/h and 100 mR/h, the accuracy must be  $\pm 7$  percent for the SAL and  $\pm 15$  percent for the TAL.

## X-RAY CALIBRATIONS

A constant-potential x-ray machine is required for the SAL. Tube potential must range between 30 to 150 kV as a minimum. Ripple must be less than 5 percent. Exposure rate must not vary by more than  $\pm 1$  percent during calibrations. Maximum and minimum exposure rates are not defined by the criteria, but the fields must be appropriate for the instruments to be calibrated.

In the TAL, constant-potential machines are not required, but ripple must be known. If the ripple is greater than 10 percent, the effect on the calibration must be known. Exposure rates must not vary by more than  $\pm 3$  percent.

Requirements for radiation control and supporting laboratory equipment for x-ray calibrations are similar to those for gamma-ray calibrations. Filters must be available in the SAL to permit a variety of x-ray beam qualities.

X-ray beam qualities are defined in Table 1. The SAL is expected to provide calibrations for at least five of the beams of Table 1. The TAL must provide services for at least three of the beams.

TABLE 1  
X-Ray Beam Codes

Beam Code*	Added Filter			First Half-Value Layer		Homogeneity Coefficient	
	Al (mm)	Cu (mm)	Pb (mm)	Al (mm)	Cu (mm)	Al	Cu
M30	0.50			0.36		64	
M50	1.021			1.02	0.032	66	62
H50	4.0		0.10	4.2	0.142	92	90
L80	1.284			1.83		58	
L100	1.978			2.8		59	
M100	5.0			5.0	0.20	72	55
H100	4.0	5.2		13.5	1.14	100	94
M150	5.0	0.25		10.2	0.67	87	62

\*The numerical value indicates the nominal kVp.

Accuracy requirements for the SAL are again twice as rigorous as the TAL. Above 100 mR/h, exposure rates must be known within  $\pm 5$  percent for the SAL and within  $\pm 10$  percent for the TAL. Between 0.5 and 100 mR/h, the requirements are  $\pm 7$  percent for the SAL and  $\pm 15$  percent for the TAL. Scatter contributions are limited to 5 percent (SAL) or 10 percent (TAL).

## ACKNOWLEDGMENTS

The time and effort contributed by Elmer Eisenhower, NBS, in the development of the HPS laboratory accreditation criteria is gratefully acknowledged on behalf of the Health Physics Society. Contributions of members of the HPS Laboratory Accreditation Standing Committee and Operations Committee are also acknowledged.

## REFERENCES

1. Health Physics Society, "Accreditation of Calibration Laboratories for Portable Radiation Protection Instruments by the Health Physics Society", 8000 Westpark Dr., Suite 400, McLean, VA 22102 (1987).
2. H.T. Heaton, "Directory of Calibration Services for Ionizing Radiation Survey Instruments", U.S. National Bureau of Standards, NBS-GCR-88-539 (1988).
3. NBS, "Requirements for an Effective Radiation Measurements Program", U.S. National Bureau of Standards Special Publication 603 (1981).

## A NEW DOSIMETER CALIBRATION LABORATORY AT ORNL

William H. Casson  
C. S. Sims  
Oak Ridge National Laboratory

Introduction. The Dosimetry Applications Research (DOSAR) group at Oak Ridge National Laboratory has established a national and international program for dosimetry testing and intercomparison. Under this program there have been twenty-two nuclear accident dosimeter intercomparisons and thirteen personnel dosimeter intercomparisons conducted with a frequency of about one each a year.<sup>1</sup> The primary tool used in these studies as well as in a wide variety of biological experiments, personnel training programs, and other nuclear and radiation related work has been the Health Physics Research Reactor.<sup>2</sup> Currently the availability of the reactor is uncertain, and it is desirable to have alternate reliable radiation sources to continue an increasing workload.

An important part of the research done at DOSAR involves calibrating several different types of equipment with known sources traceable to the National Bureau of Standards (NBS).<sup>3</sup> These calibrations, although done with sufficient accuracy using available sources, were conducted in a casual manner and often resulted in undesirable exposures to the researchers and posed a general inconvenience to the smooth operation of the facility. Although extensive laboratory space and storage was available at the facility, there were no facilities for a permanent irradiation setup that could house all the neutron, gamma, and beta sources necessary. A permanent facility, the Radiation Calibration Laboratory (RADCAL), was envisioned and plans were formulated that would meet the general needs of the DOSAR group.

The RADCAL facility (Figure 1) consists of three irradiation rooms, a control room, and various storage and utility rooms. These rooms will house various neutron sources, a beta irradiation facility and x-ray source, and a gamma irradiation facility. Each irradiation will be controlled from the control room by a personal computer system. All positioning and placement of equipment will be done manually. When all installation and testing is complete, the facility will allow research level testing of dosimeters, rate meters, and other radiation equipment. The intention is to then start review procedures to obtain approval from NBS to operate as a NBS secondary calibration facility. It is the ultimate goal of the DOSAR group to perform National Voluntary Laboratory Accreditation Program (NVLAP)<sup>4</sup> and Department of Energy Laboratory Accreditation Program (DOELAP)<sup>5</sup> testing of dosimeter systems on a limited scale. The group also intends to make RADCAL available to outside users for research, testing, and training as a user facility.

The Neutron Facility. The neutron room is the largest room which measures 9.1 x 9.1 x 5.5 m. It will house two Cf-252 sources

stored in a 1.2-m diameter by 1.2-m deep well in the center of the room. One source will be used as a bare source of fast neutrons and the second will be housed inside a D<sub>2</sub>O filled 30-cm diameter, cadmium covered, stainless steel sphere to provide irradiations with moderated neutrons. The source to be used bare contains about 800 micrograms of californium which emits approximately  $1.8 \times 10^9$  neutrons/s for a dose of 1.2 mSv/min at 50-cm. The source to be used with the moderator is about 3.0 times larger and, when

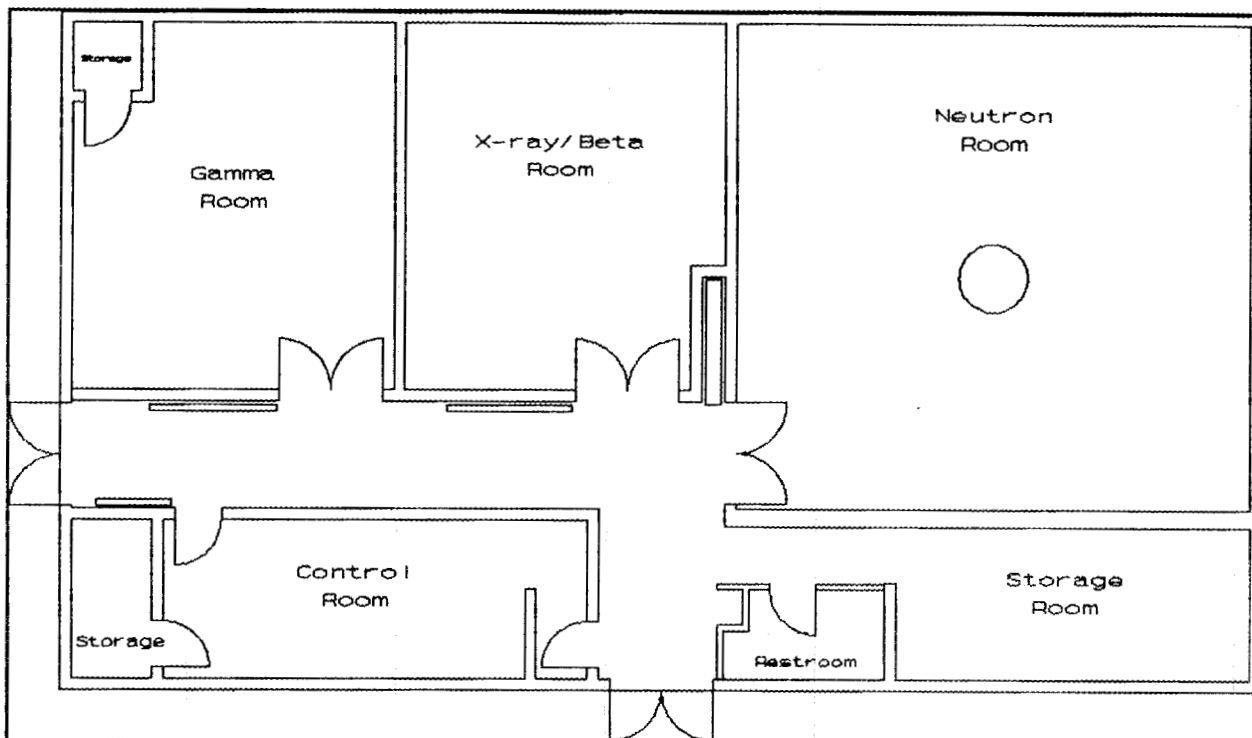


**Figure 1 RADCAL Floor Plan**

moderated and used with the cadmium cover, results in a dose equivalent rate of 0.9 mSv/min at 50-cm. An 8.5 Ci <sup>238</sup>PuBe source is also available at RADCAL. The dose equivalent rate from this source is about 0.02 mSv/min at 50-cm.

X-ray/Beta Facility. The x-ray machine and beta source will share an approximately 6.1 x 7.0 x 4.3 m room. The x-ray source will be a Pantak Model HF320. With the appropriate filters, it will be capable of reproducing all of the new NBS beam codes. The beam will be monitored during exposure by a PTW transmission chamber to ensure constant beam current and reproducible exposures. Calibration at low energies will be done by an extrapolation chamber and at higher energies by ionization chambers. The phantom and calibration detector will be mounted on a movable table such that the beam exposure can be shifted from calibration chamber to phantom without changing the setup or interrupting the x-ray tube operation. A heavy safety shutter will be used to allow personnel to change dosimeters or change the setup in the room with the x-ray tube in full operation, thus significantly reducing delays due

to warmups and improving stability.

The beta source is a  $^{90}\text{Sr}$ - $^{90}\text{Y}$  source manufactured by Isotope Products Lab and has been thoroughly characterized by NBS.<sup>6,7</sup> It will be mounted in one corner of the room with clearances large enough to reduce scattering effects to negligible levels. This source is mounted in an irradiator that rotates the source at 60 rpm during exposures. Three 30 x 30 x 5 cm phantoms can be mounted on a stand at a distance of 35-cm. Six dosimeter positions have been characterized. The delivered absorbed dose rates vary from 1.2 to 1.5 mGy/min at a total depth of 7 mg/cm<sup>2</sup> in mylar. A PTW extrapolation chamber will be mounted between two of the phantoms to monitor the delivered dose during test irradiations.

Gamma Facility. There will be two gamma irradiation sources housed in a 5.8 x 7.0 x 4.3 m room. The first is a Shepard panoramic irradiator with a 1.2 Ci Cs-137 source. It is mounted on a movable platform which can be positioned in the room center. The delivered dose rate at a distance of 50-cm is about 0.25 mGy/min. The second source is an Amersham 10 Ci Cs-137 beam irradiator permanently positioned in a room corner with the beam directed along the diagonal across the room. The delivered dose at 50-cm is about 2.5 mGy/min.

Operations and Safety. To protect against personnel exposure, each source is housed in a remotely operated irradiator. A personal computer in the control room can operate all the sources, check closed doors, shield placement, and safety interlocks. At the beginning of each irradiation, the desired source and dose will be entered into the computer. It will then calculate the exposure time and distance as well as list a checklist of necessary setup procedures. After the setup is completed and all required shields are in place, the computer activates the source and times the exposure. A permanent record is made on disk and a report of irradiation is automatically printed.

The required procedures will be well documented in the RADCAL protocol manual. All personnel operating the sources will be required to review the protocol and undergo a brief training period. During exposures all personnel in the building will be required to be in the control room. Since the building houses no other facilities, this should not be an inconvenience. Personnel in the control room are shielded from each source by at least 45-cm of concrete in the walls, and a combination of concrete and steel in the shield doors. The neutron room shield has an additional 15-cm of polyethylene with 5% boron as a further safety factor.

Conclusions. The RADCAL facility at ORNL was designed to facilitate calibration of instruments and dosimeters in support of work related to the Health Physics Research Reactor. Its role has expanded to include standard dosimeter testing, basic dosimeter research, radiobiology research, and personnel training. The facility is currently operational with two gamma sources, two

neutron sources (polyethylene moderated Cf-252 and a PuBe source), and a Sr-Y beta source. A 320 kV x-ray machine is on order and is due for delivery before the end of the year. Also, two heavy water spheres are under construction to provide a standardized source of moderated fission neutrons. An official dedication ceremony is scheduled early in the second quarter of 1989 and it is hoped all sources will be fully operational at that time. This facility provides a major new tool for research in dosimetry at ORNL and is available as a user facility to qualified participants.

## References

1. C. S. Sims and H. W. Dickson, "Neutron Dosimetry Intercomparison Studies," Radiation Protection Dosimetry, 10, 331-340 (1985).
2. C. S. Sims, "1986 Reference Neutron Dosimetry for the Health Physics Research Reactor," Radiation Protection Dosimetry, 15, 41-44 (1986).
3. R. E. Swaja and C. S. Sims, "Dosimetry Testing and Training Opportunities at Oak Ridge National Laboratory," Radiation Protection Management, 73-77, April 1985.
4. Robert L. Gladhill, Jeffrey Horlich, and Elmer Eisenhower, "The National Personnel Radiation Dosimetry Accreditation Program," NBSIR 86-3350, January 1986.
5. U.S. DOE, Handbook for the Department of Energy Laboratory Accreditation Program for Personnel Dosimetry Systems, DOE/EH-0026, December 1986.
6. M. Ehrlich, J. S. Pruitt, and C. G. Soares, "Standard Beta-Particle and Monoenergetic Electron Sources for the Calibration of Beta-Radiation Protection Instrumentation, NUREG/CR-4266 (August 1985).
7. J. S. Pruitt, C. G. Soares, M. Ehrlich, Calibration of Beta-Particle Radiation Instrumentation and Sources, NBS Special Pub 250-21 (April 1988).

PORTABLE SINGLE CHANNEL ANALYZER INCORPORATED WITH  
A GM COUNTER FOR RADIATION PROTECTION

Cheng-Hsin Mao  
Nuclear Science and Technology Development Center,  
National Tsing Hua University,  
Hsinchu 30043, Taiwan, R.O.C.

ABSTRACT

A compact size of single channel analyzer incorporated with a GM counter has been developed. It measures 8.7 cm (W) × 22.2 cm (L) × 4.4 cm (H) and weighs 0.58 kg excluding the detectors. An adjustable high voltage of 0 - 1000 V is included with an error of ± 0.1% and powered by three mercury batteries of 9 V each. Both the upper and lower level discriminators are set at 0 - 5 V with an error of ± 1%. The timer can be set at either 0 - 99 sec or 0 - 99 min with a buzzer alarm. The resolution of pulse is 5 μs plus the pulse width. The LCD display is either 3 1/2 or 4 digits. The rise time of shaping circuit is 1 μs with a band width of 350 kHz. The voltage indicator for battery is set at 7.5 V. All integrated circuits are of CMOS with low cost OPAMP. Some examples for field applications are given.

## INTRODUCTION

The Geiger-Mueller (GM) counter has long been in widespread use and, although not as versatile as some of the modern counters, it possesses great advantages. It is relatively cheap and the large output pulse which it produces requires very little amplification.<sup>1</sup>

The single channel analyzer (SCA) is an instrument incorporating a pulse height selector in which the channel width is preset and the threshold varied manually to scan the amplitude spectrum of the incoming pulse. The electronic circuit of the pulse height selector permits only the voltage pulses which have amplitudes between predetermined levels to be passed to the succeeding circuits.

The SCA coupled with a NaI(Tl) detector, in contrast to the GM counter, has higher absorption and results in a much higher sensitivity. At the same time, the shorter resolving time also permits the measurement of higher radiation fields.

The disadvantage of NaI(Tl) detector and SCA is the sophisticated electronic requirement, particularly for portable equipment,<sup>2,3</sup> In this article, attempt has been made to incorporate the two counters mentioned above together as a single unit.<sup>4,5</sup>

## THE DESIGN

The newly designed counter itself, excluding the GM tube with its pulse inverter and the NaI(Tl) detector with photomultiplier, preamplifier, and amplifier, weighs 0.58 kg only and its size is shown in Fig.1. It includes a timer, a counter, a high voltage power supply, and a switch selector which can select either GM or SCA.

The block diagram of the counter is illustrated in Fig.2. In addition to the timer, high voltage power supply and display, the NaI(Tl) is connected to a shaping circuit while the GM is connected to a control gate.

The circuitry is depicted in Fig.3. The common power supply for both GM and SCA is two 9 V batteries. The current requirement

is 80 mA. For a stable dc power supply an other driving oscillator coupled to a pulse width modulator is served as a dc-dc converter. The feedback circuit is composed of a voltage divider and a comparator. The feature of this feedback circuit is the voltage control which is by means of the pulse width. The voltage is then raised by a transformer. The comparator makes comparison with a reference voltage, and then amplifies and takes control of the pulse width modulator from 0 to 90%. When the output voltage is too low, the pulse width is broadened. On the other hand, when the output voltage is too high, the pulse width is reduced. The voltage ranges from 0 to 1000 V by a 10-turn potentiometer, and is displayed on a 3 1/2 DVM liquid crystal. The voltage thus obtained can be kept very stable. The power supply is a 9 V battery with a current requirement of 100 mA.

The shaping circuit is a low-pass filter and consists of a quad low-power operational amplifier with a 1  $\mu$ s pulse rise time and 350 kHz band width. This arrangement is to eliminate the high frequency noise. The SCA consists of a window discriminator, a comparator, a one-shot multivibrator, and a control gate. <sup>6,7</sup>

The window discriminator is a quad low-power operational amplifier as mentioned previously. Discrimination is accomplished by using two 10-turn potentiometers with 0 - 5 V each for the upper and lower levels respectively. The input voltage for the window discriminator is limited to 7.5 V. When the input pulse is higher than the lower level, a 5  $\mu$ s pulse is generated after the comparator makes the comparison with reference voltage and triggers the one-shot generator. The signal is transmitted to the control gate and then to the counter. When the input pulse is higher than the upper level, a 100  $\mu$ s pulse is generated after the comparator makes similar comparison as mentioned above. For a SCA, when the input pulse is higher than both the lower and upper levels, no output signal is observed. In this design, the input signal falling edge is used to make comparison with both upper and lower levels. The upper level should have the output signal pulse after making comparison, and the pulse is sufficiently wide so that the output signal above the lower level should occur. At the same time, a reset signal is triggered at the lower-level one-shot generator to make the upper-level one-shot generator back to zero quickly. Through the control gate and logic process, an output pulse is produced only if the input pulse amplitude lies between the two levels. The action of the discriminator is therefore to select a band of amplitudes or window in which the input amplitude must fall in order to produce an output pulse.<sup>8,9</sup> The timing diagram of the SCA is illustrated in Fig.4.

## RESULTS AND DISCUSSION

The newly designed counter combines both functions together : the GM and the SCA. It has all advantages of both counters mentioned above. The disadvantage, however, is the power consumption.

Using a lead shield of 2.54 cm (1 in.) thick with a  $^{60}\text{Co}$ -source to detector distance of 1 cm, the lower limit of detection (LLD) for 1-minute counting time is 1110 Bq (0.03  $\mu$  Ci) for an ORTEC 903 GM tube, and 740 Bq (0.02  $\mu$  Ci) for a Teledyne Isotopes 3.81 cm (1.5 in.)  $\times$  5.08 cm (2 in.) NaI(Tl) detector. The conversion factor from mR/h to counts/min is 1 mR/h=319 counts/min. The  $^{60}\text{Co}$  spectrum thus detected is shown in Fig. 5.

A simple modification can convert this instrument into a GM survey meter. As a matter of fact, this instrument has three functions : (1) GM counter, (2) GM survey meter, and (3) SCA with NaI(Tl) detector.

## ACKNOWLEDGMENTS

The author is indebted to Professor Pao-Shan Weng and Dr. Hwai-Puw Chou for their valuable suggestion and comments throughout this investigation. The author is also indebted to the College of Nuclear Science, National Tsing Hua University for the financial support.

## REFERENCES

1. S. Guldbakke, R. Jahr, H. Lesiecki and H. Scholermann. Health Phys. 39, 963 (1980).
2. L.O. Johnson, J.L. Alvarez, J.M. Hoggan, and R.L. Dickson, IEEE Trans. on Nucl. Sci. NS-30, 543 (1983).
3. B.H. Erkkila, D.A. Waechter, and R.J. Brake, IEEE Trans. on Nucl. Sci. NS-31, 661 (1984).
4. P.E. Fehlauf, IEEE Trans. on Nucl. Sci. NS-31, 664 (1984).
5. M. Yamasita, Nucl. Instrum. Meth. 114, 75 (1974).
6. C.A.B. Correia, C.A.N. Conde and M. Lurdes Dias, IEEE Trans. on Nucl. Sci. NS-25, 59 (1978).
7. R. Bayer, Nucl. Instrum. Meth. 146, 469 (1977).
8. E. Sattler, Nucl. Instrum. Meth. 64, 221 (1968).
9. P. Sperr, H. Spieler and M.R. Maier Nucl. Instrum. Meth. 116, 55 (1974).

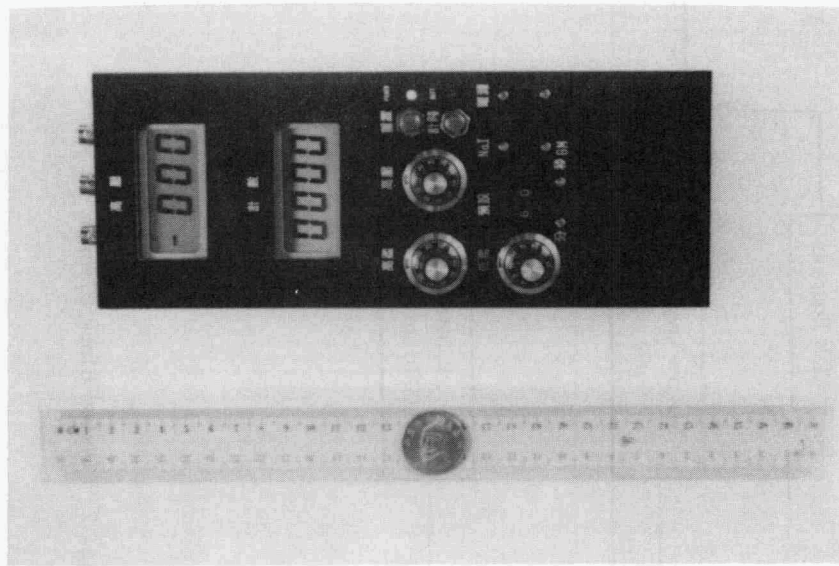


Fig. 1 Dual Purpose Counter for GM and SCA.

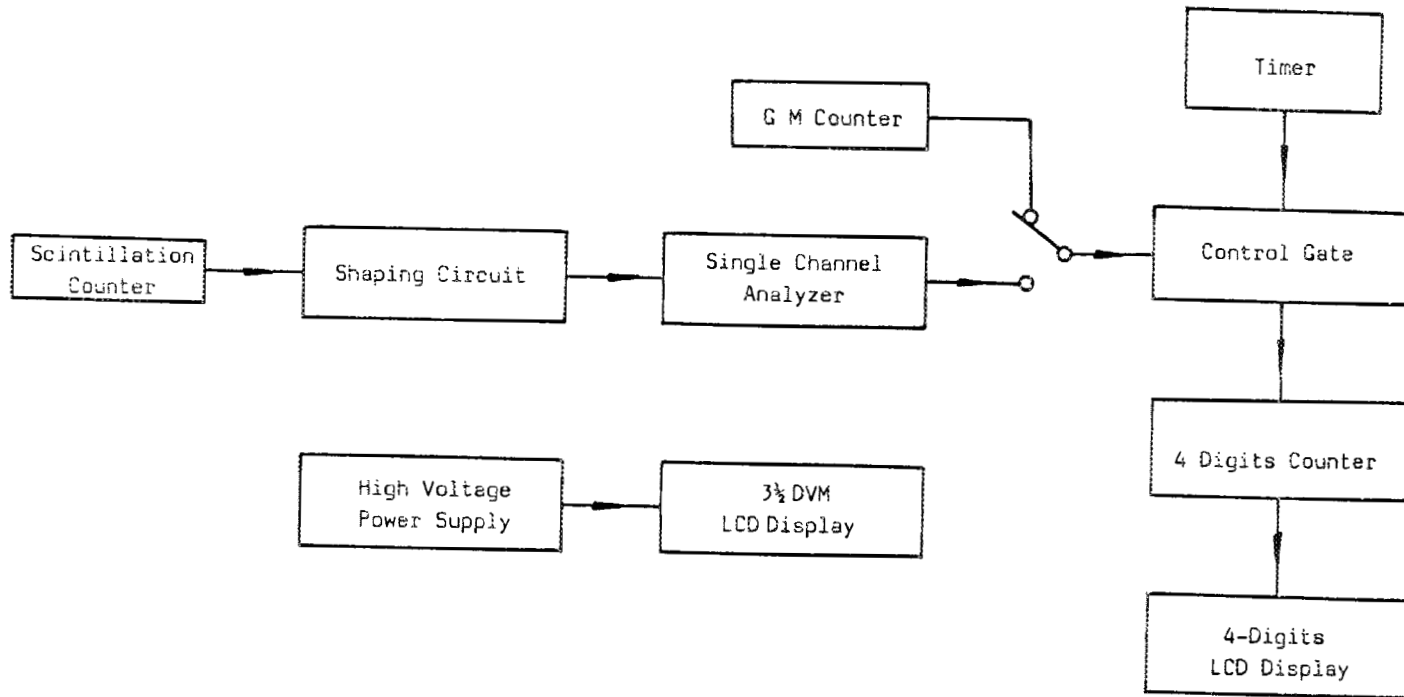


Fig. 2 System Block Diagram

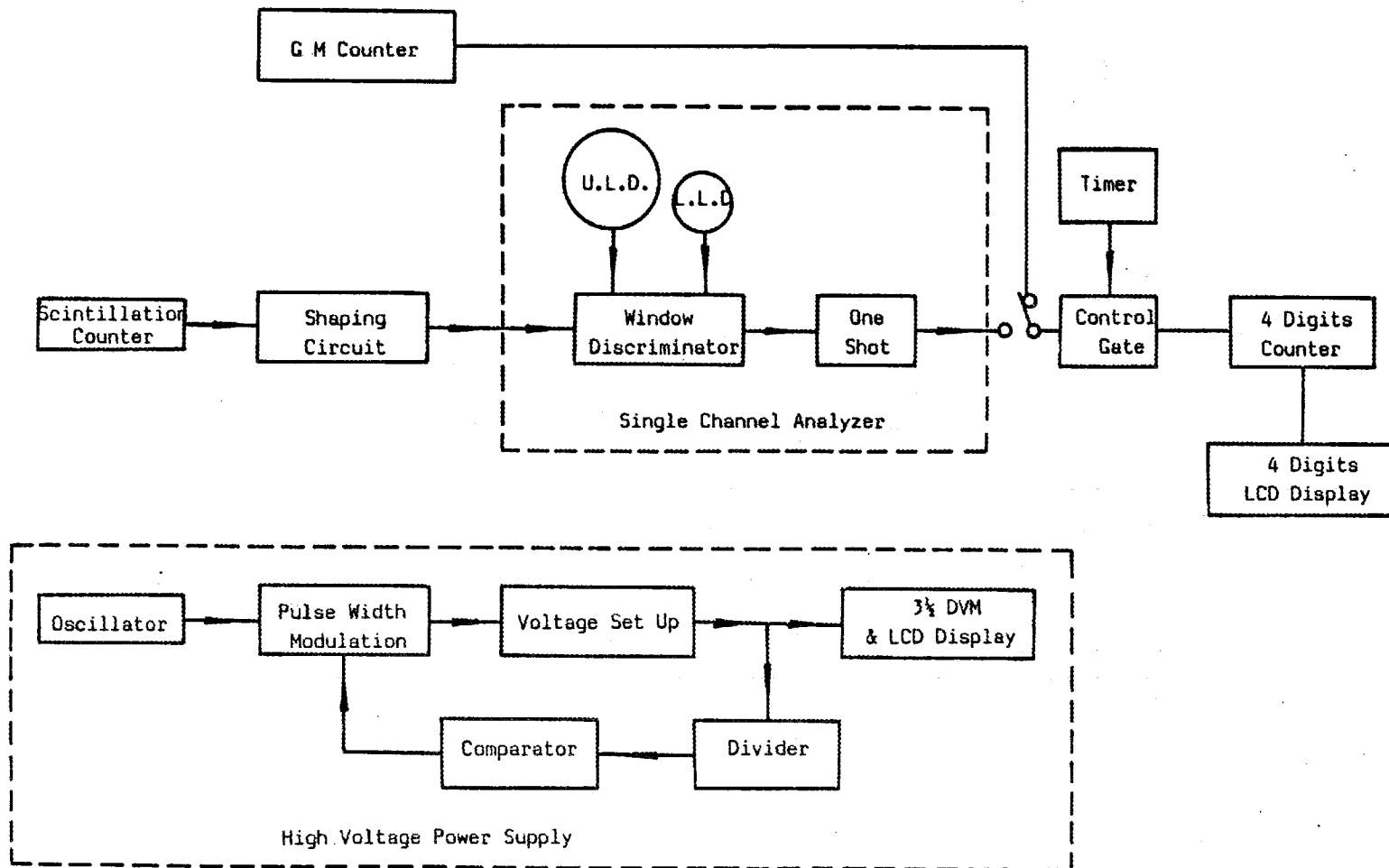


Fig. 3 Circuitry Block Diagram

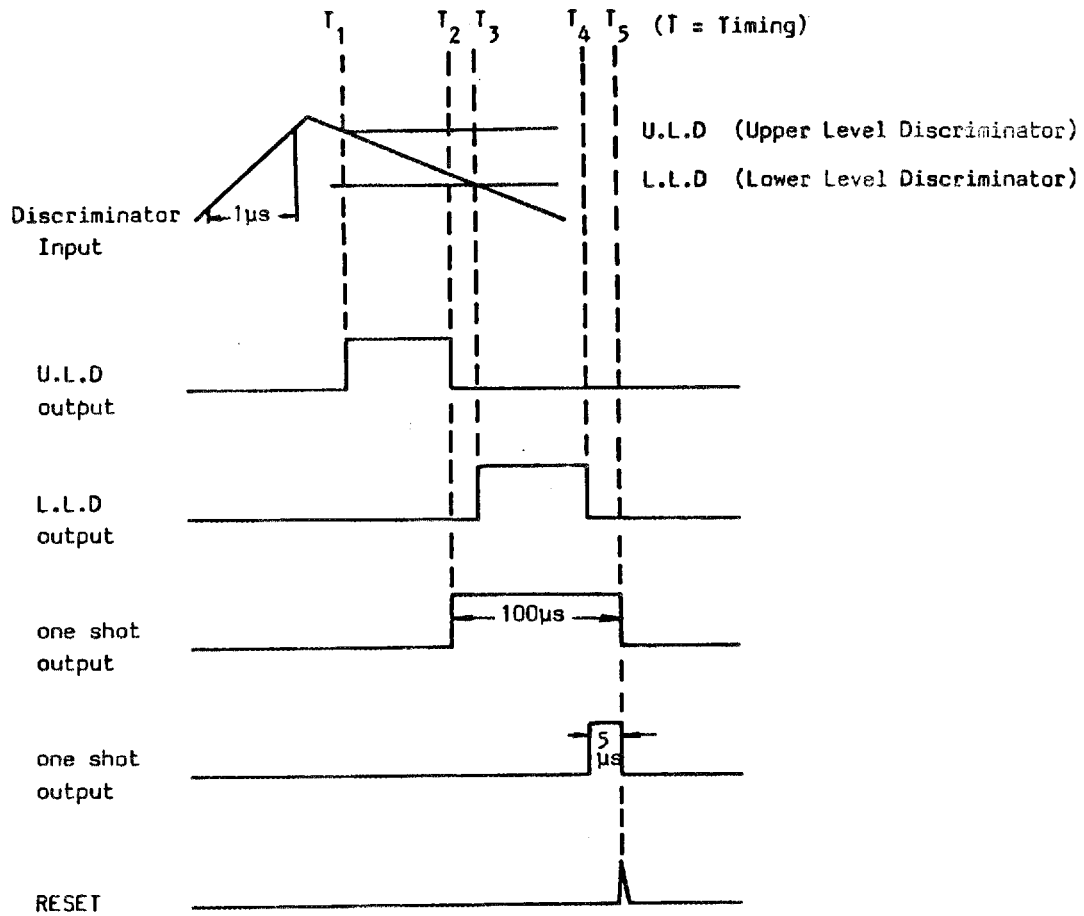


Fig. 4 Single Channel Analyzer Timing Diagram

# REVIEW OF ANSI N13.11: A STATUS REPORT\*

C. S. Sims  
Oak Ridge National Laboratory

In 1983, the American National Standards Institute (ANSI) issued the dosimetry standard titled "Personnel Dosimetry Performance - Criteria for Testing" as ANSI N13.11<sup>1</sup>. This standard forms the basis for the National Voluntary Laboratory Accreditation Program (NVLAP) which has become familiar to dosimeter processors in recent years<sup>2</sup>. This standard is particularly important because the Nuclear Regulatory Commission (NRC) requires that all licensees have personnel dosimetry devices processed by processors that are NVLAP accredited<sup>3</sup>. This standard is currently undergoing review and modifications are going to be made. This paper contains a brief history of the events leading to the development of ANSI N13.11 - 1983, information concerning the present standard and associated performance test results, and the selection of the review group. Following that, the status of the review is presented and statements regarding the future outlook for the standard are made.

## History

Development of ANSI N13.11. In 1973, the Conference of Radiation Control Program Directors appointed a task force to implement its recommendation for establishing a continuing personnel dosimetry performance test program. The task force asked the Health Physics Society Standards Committee (HPSSC) to develop a new standard for personnel dosimeter performance. In 1975, a Health Physics Society (HPS) working group chaired by Margarete Ehrlich of the National Bureau of Standards (NBS) was given the task of writing the standard. In 1976, a draft standard was submitted for comment. In 1978, the draft standard was published for trial use and comment. That version of the standard formed the basis of a pilot test program conducted by the University of Michigan. The present standard was issued in 1983. It is a result of revisions of the draft standard based primarily on modifications made as a consequence of the pilot test program.

The Current Standard. The test categories, irradiation ranges, and tolerance levels associated with the current standard are presented in Table 1. The test requires 15 dosimeters per category. The calculated bias (i.e., accuracy) plus standard deviation (i.e., precision) must be less than or equal to the tolerance level. In equation form, this is

$$|B| + S \leq L.$$

The irradiations are to be performed with the dosimeters mounted on Lucite slab phantoms. The reporting convention requires that the absorbed dose at 1 cm depth be reported for accident cases and that the shallow (0.007 cm) and deep (1 cm) dose equivalent be reported for the others as specified in Table 1.

---

\* Research sponsored by the Office of Health and Environmental Research, U.S. Department of Energy under Contract No. DE-AC05-84OR21400 with Martin Marietta Energy Systems, Inc.

Performance Test Results. The standard is the basis of the performance tests required by the NVLAP administered by the NBS. Certification by the NBS requires passing an on-site assessment as well as the performance test program<sup>4</sup>. Table 2 shows the performance test results obtained during the first four years (1984-1987) since the beginning of the certification program. Since 93% of the tests have been passed, it is concluded that the standard is not very difficult to meet. This is particularly obvious when the values of the accuracy plus precision are considered.

Selection of the Review Group. It is, theoretically, the policy of ANSI and the HPSSC to have their standards reviewed every five years. In September, 1986, the HPSSC issued a call for volunteers to participate as members of the N13.11 review work group<sup>5</sup>. In February, 1987, the review group members were selected by the HPSSC and notified. The review group consists of the nine voting members and four consultants identified in Table 3. The group has a diverse background and is experienced in all areas associated with the standard.

### **Status of the Review**

Activities of the Review Group. The review group issued a call for comments on the existing standard in the HPS Newsletter<sup>6</sup>. At the first meeting, the review group heard formal presentations by several persons interested in the standard. The group has received additional input by mail, telephone, and personal contact. Group members and consultants have also commented on the standard based on their expertise. From all these inputs, the group identified sixteen different issues which need to be resolved prior to revising the standard. The approach chosen by the group is to develop a concensus position on each issue and then make any necessary revisions. This method was chosen because many of the issues are interrelated and changes in one area can affect several others in the standard. The sixteen issues are identified by title in Table 4, but they are actually a series of comments and questions of a technical nature related to each identified area of concern. Working toward the resolution of these issues has been the agenda of the work group meetings. Table 5 is a listing of the meetings to date.

Discussion of the Issues. Each of the issues in Table 4 is considered in this section. The associated discussion reflects the current attitude and thinking of the review group as a whole. The reader should, however, be advised that these currently accepted positions do not necessarily reflect the views of individual group members nor is it certain that they will ultimately find their way into the final version of the revised standard after it has undergone review and approval by the various organizations involved.

1. Philosophy. The review group believes that the existing standard has done a good job toward improving and unifying the practice of dosimetry. It is recognized that every workplace situation cannot be covered in a test standard, but the current one can be broadened somewhat to allow more improved and realistic testing without dramatically increasing the number of dosimeters required. It is not expected that every processor will need or even desire to be accredited in every category, but will select the appropriate ones for his operational situation. The review group also recognizes that algorithms used in the performance tests shouldn't necessarily have to be

the ones used in field monitoring situations if the processor can demonstrate that the ones routinely used in the field lead to superior results. The group believes that operational aspects of the dosimetry program can be as important as specific test results, but they are not properly a portion of this standard.

2. Angular dependence. Testing for angular dependence will be introduced as category IX. The range will be 0.1-10 rem. For the shallow and the deep dose equivalent,  $L=0.5$  and there are no limits on B or S (see item 3 below). The angles of incidence to be used both horizontally and vertically are  $0^\circ$ ,  $\pm 40^\circ$ , and  $\pm 60^\circ$ . The tests will be limited to radiations from categories IIIB and IV (i.e., M100, M150, H150, and Cs-137).
3. Tolerance levels and performance criteria. The performance criterion will be changed from

$$|B| + S \leq L \text{ to } |B| + S - E \leq L$$

where E is the estimated fractional uncertainty in the delivered dose or dose equivalent. The value of E is expected to be  $\leq 0.05$ . The tolerance level, L, is 0.5 in all cases except in categories I and II where it is 0.3. The standard deviation, S, is to be calculated as described in the current standard.

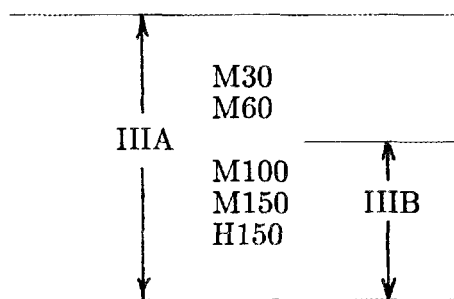
A separate limit for B and for S has been established. That limit is 0.35. This separate limit does not apply for irradiations in categories I, II, VC, and IX.

The lowest dose equivalent allowed in categories III and IV is 30 mrem. The review group is concerned about the disproportionate effect of small absolute errors on the test results at these low levels. In an attempt to be fair to all processors, the test laboratory will modify the dose assignment program to assure that no more than one dosimeter in a test category can receive a dose equivalent between 30-70 mrem.

4. SI units. No changes are planned relative to SI units. The present units are clear, understandable, and familiar to the vast majority of those who are expected to use the standard.
5. Conversion factors and dose equivalent reporting conventions. The review group has not made any decisions regarding this important issue. In recent years there has been a proliferation of dose equivalent quantities and units, many of which are due to the International Commission on Radiological Protection (ICRP) and the International Commission on Radiation Units and Measurements (ICRU). The group is giving serious consideration to the recommendations of these bodies. A particularly close look is being given to the ICRU 39 methodology<sup>7</sup>, but interpretation problems associated with application to angular test applications must be better resolved<sup>8</sup> before intelligent decisions can be made.

Volumes could be written about conversion factors and dose equivalent reporting conventions. For present purposes, however, it should be known that other standards review groups and the NRC are also trying to come to grips with this problem. Any solution must consider the effective dose equivalent concept from ICRP 26<sup>9</sup> and how it relates to the chosen methodology. Recent works such as ICRP 51<sup>10</sup>, soon to be published works such as ICRU 43, additional works in progress by the ICRU, and a large amount of open literature papers on the subject must be reviewed, digested and understood by the group before recommendations are finally made.

6. Unexposed dosimeter category. This issue was studied because most dosimeters processed actually have zero (or below minimum detectable) doses. The issue has also been called the lower limit of detection (LLD). The issue is still open, but the review group will probably suggest that the LLD be calculated from available data and compared with values which constitute good LLDs (e.g., 0.5 of the lower level of the test ranges for each type of radiation specified in the current standard).
7. X-ray category. The new NBS beam codes will replace the ones currently in the standard. Category III will be divided into two subcategories: IIIA and IIIB as shown below.



Subcategory IIIB is added because a large number of facilities do not have a significant number of photons below 50 keV.

There will be a subcategory VIA for participants in IIIA and a subcategory VIB for participants in category IIIB. This will insure that the tests in the x-ray category and the photon mixture category are consistent.

In category I (Accidents, x-ray), the new beam code M150 will replace the currently used MFI.

8. Beta category. Tl-204 will be added to category V. To accomplish this, the category has been restructured to have three subcategories as follows:

VA = Sr-90/Y-90  
 VB = Tl-204  
 VC = Sr-90/Y-90 or Tl-204 (no limit on B,S)

This will introduce a challenge to those who select VC.

Category VII is the photon/beta mixture category and it will be divided into two subcategories as follows:

$$\text{VIIA} = \text{VA} + \text{Cs-137}$$

$$\text{VIIB} = \text{VB} + \text{Cs-137}$$

There will not be a VIIC subcategory at this time.

9. Neutron category. Discussion of this issue is ongoing, but it appears that we will retain the present moderated Cf-252 radiation specified in category VIII and add another neutron source, AmBe, as a subcategory. Questions associated with source to dosimeter distance (50-75 cm), separate reporting of neutron and gamma dose, and filtering of low energy AmBe photons are still under consideration.
10. Photon category. After consideration of various alternatives, it was decided not to make any changes in this category (i.e., IV).
11. Extremity dose category. Extremity dosimetry is not the concern of this standard. The HPSSC is working on a standard for extremity dosimetry. Our group might review that document for consistency with ANSI N13.11, but that will be the extent of our involvement with extremity dosimetry.
12. Phantoms. The Lucite slab phantoms specified in the current standard have proved to be adequate and are widely accepted. No changes are anticipated in this area unless further investigation of the angular dependence question leads us to a different phantom for those tests.
13. Blind test. Blind testing will not be a part of the standard. The review group likes the concept, but no practical method of doing it has been identified.
14. Distance from source. It should be clearly understood that the distance is to be measured from the center of the source to the center of the front face (i.e., the face nearest the source) of the phantom. Although discussion is continuing, it appears that no changes will be made for photon and x-ray distances ( $\geq 100$  cm). Neutron irradiation distances are unsettled, but values of 50-75 cm are under consideration. For betas, the minimum distance will be reduced to 30 cm to allow use of the Physikalisch-Technische Bundesanstalt (PTB) sources. Use of greater distances for betas is still under debate.
15. Category VI photon mixtures. All the concerns associated with this category have been handled with issues 7 and 10.
16. Environmental concerns. No changes will be made in this area. The review group believes that enough changes have been proposed for now. Environmental testing (e.g., heat, cold, humidity, etc.) would require an impractical number of dosimeters and would tax the test lab capabilities and increase the cost of accreditation.

## **Future Outlook**

The review group will meet again in January, 1989 to attempt to resolve the outstanding issues and begin the rewrite of the appropriate sections of the standard. When a rewritten draft is completed, it will be submitted to the HPSSC for their approval.

**Table 1. ANSI N13.11 Test Categories,  
Test Irradiation Ranges, and Tolerance Levels**

Test Category	Test Range	Tolerance Level	
		Deep	Shallow
I. Accidents, x-ray (NBS technique MFI)	10-500 rad	0.3	No test
II. Accidents, Cs-137	10-500 rad	0.3	No test
III. X-rays (NBS techniques LG, LI, LK, MFC, MFI)	0.03-10 rem	0.5	0.5
IV. Cs-137	0.03-10 rem	0.5	No test
V. Betas (Sr-90/Y-90)	0.15-10 rem	No test	0.5
VI. Photon mixtures (III + IV)	0.05-5 rem	0.5	0.5
VII. Photon/beta mixtures (IV + V)	0.20-5 rem	0.5	0.5
VIII. D <sub>2</sub> O moderated Cf-252/Cs-137	0.15-5 rem	0.5	No test

**Table 2. NVLAP Performance Test Results (1984-1987)**

Category	Avg.   B   +S <sup>a</sup>	Attempted/Passed	%Pass
I. Accidents, x-ray	0.15	102/81	79
II. Accidents, Cs-137	0.14	131/126	96
III. X-rays	0.19	116/104	90
IV. Cs-137	0.15	154/153	99
V. Betas	0.20	136/129	95
VI. Photon mixtures	0.19	116/105	91
VII. Photon/beta mixtures	0.18	146/136	93
VIII. Neutron/photon mixtures	0.14	101/99	98
		1002/933	93

<sup>a</sup>Average among those passing tests.

### **Table 3. ANSI 13.11 Review Group**

#### **Members**

1. Doug Carlson, Department of Energy
2. Brian Colby, American Nuclear Insurers
3. Don Jones, Lawrence Livermore National Laboratory
4. Harley Piltingsrud, Public Health Service
5. Sami Sherbini, Nuclear Regulatory Commission
6. Steve Sims, Oak Ridge National Laboratory, Chairman
7. Chris Soares, National Bureau of Standards
8. Stan Waligora, Eberline
9. Gary Zeman, Defense Nuclear Agency

#### **Consultants**

1. Elizabeth Donnelly, Tennessee Valley Authority
2. Bill King, Harshaw
3. Bob Pollock, Siemens Gammasonics
4. Pete Roberson, University of Michigan

**Table 4. Issues for Resolution**

<u>Issue</u>	<u>Subgroup leader</u>
1. Philosophy	Jones
2. Angular dependence	Piltingsrud
3. Tolerance levels and performance criteria	Carlson
4. SI units	-
5. Conversion factors and H reporting conventions	Zeman
6. Unexposed dosimeter category	Sherbini
7. X-ray category	Carlson
8. Beta category	Soares
9. Neutron category	Waligora
10. Photon category	Zeman
11. Extremity dose category	-
12. Phantom	-
13. Blind test	Colby
14. Distance from source	Jones
15. Category VI photon mixtures	Waligora
16. Environmental concerns	Piltingsrud

**Notes:**

Issues 4, 11, and 12 were handled by the entire group.

A voting member has lead responsibility on each subgroup.

No one person has lead responsibility on more than two subgroups.

No one person is a member of more than four subgroups.

### **Table 5. Review Group Meetings**

June 23-24, 1987

September 22-23, 1987

January 20-21, 1988

May 3-4, 1988

August 24-25, 1988

## References

1. American National Standards Institute, Personnel Dosimetry Performance - Criteria for Testing, ANSI 13.11, 1983.
2. Gladhill, R. L. and Horlick, J., The National Personnel Radiation Dosimetry Accreditation Program, NBSIR 86-3350, U.S. Department of Commerce, Washington, D.C., January 1986.
3. U.S. Nuclear Regulatory Commission, "Improved Personnel Dosimetry Processing," Final Rule, Federal Register, Vol. 52, No. 30, 4601-4604, February 13, 1987.
4. Hudson, C. G., "Personnel Dosimetry Accreditation - An Assessor's Perspective," Radiation Protection Management, 37-43, October 1986.
5. Health Physics Society, "N13.11 Standard Review," Health Physics Society Newsletter, XIV(9), 14 (1986).
6. Sims, C. S., "Call for Comment on ANSI 13.11," Health Physics Society Newsletter, XV(6), 19 (1987).
7. International Commission on Radiation Units and Measurements, Determination of Dose Equivalents Resulting from External Radiation Sources, ICRU Report 39, Bethesda, Maryland, 1985.
8. J. A. Dennis, "Celestial Spheres and Mortal Men", Editorial, Radiation Protection Dosimetry, 22, 147 (1988).
9. International Commission on Radiological Protection, Recommendations of the International Commission on Radiological Protection, ICRP Publication 26, Pergamon Press, New York, 1977.
10. International Commission on Radiological Protection, Data for Use in Protection Against External Radiation, ICRP Publication 51, Pergamon Press, New York, 1987.